

This electronic thesis or dissertation has been downloaded from the King's Research Portal at <https://kclpure.kcl.ac.uk/portal/>



Generalised Hydrodynamics and Correlation Functions

Del Vecchio Del Vecchio, Giuseppe

Awarding institution:
King's College London

The copyright of this thesis rests with the author and no quotation from it or information derived from it may be published without proper acknowledgement.

END USER LICENCE AGREEMENT



Unless another licence is stated on the immediately following page this work is licensed

under a Creative Commons Attribution-NonCommercial-NoDerivatives 4.0 International

licence. <https://creativecommons.org/licenses/by-nc-nd/4.0/>

You are free to copy, distribute and transmit the work

Under the following conditions:

- Attribution: You must attribute the work in the manner specified by the author (but not in any way that suggests that they endorse you or your use of the work).
- Non Commercial: You may not use this work for commercial purposes.
- No Derivative Works - You may not alter, transform, or build upon this work.

Any of these conditions can be waived if you receive permission from the author. Your fair dealings and other rights are in no way affected by the above.

Take down policy

If you believe that this document breaches copyright please contact librarypure@kcl.ac.uk providing details, and we will remove access to the work immediately and investigate your claim.

Generalised Hydrodynamics and Correlation Functions



Giuseppe Del Vecchio Del Vecchio

Supervisor: Prof. B. Doyon

Department of Mathematics
King's College London

This dissertation is submitted for the degree of
Doctor of Philosophy

September 2023

To Jasmin, Luisa, Margarita and Vincenzo ...

Declaration

I hereby declare that except where specific reference is made to the work of others, the contents of this dissertation are original and have not been submitted in whole or in part for consideration for any other degree or qualification in this, or any other university. This dissertation is my own work and contains nothing which is the outcome of work done in collaboration with others, except as specified in the text and Acknowledgements. This dissertation contains fewer than 100,000 words including appendices, bibliography, footnotes, tables and equations and has fewer than 150 figures.

Giuseppe Del Vecchio Del Vecchio
September 2023

Acknowledgements

This is probably the most challenging part of all. After 4 intense years spent in one of the most vibrant cities in the world where can I start acknowledging? Of course, being an extremely social individual I met a lot of people along the way. As Londoners say, people come and people go, but in the end everyone goes. And I know now, this is true because I am going to. I cannot name all the faces that gave me advice during these years, some I cannot even remember. What I do remember is people that stayed and that accompanied me, pushed me and comforted me when I was down because they gave me something that will always stay within me. From King's College, these amazing people include Luca, Giorgio, Friederich, Adarsh, Tim, Ned, Andrea, Josph, Gabriele and Michelangelo. Without you, KL4.12 would have been real different and I really wished more time with you. Damian, for making me jealous of your physics trips. From City University, Michele and Fabio, it's like you were at KCL. From outside I want to thank Ginevra and Davide, for accepting being my flatmates and my trusted friends, thank you for your constant support in life. Gioele and Luca for being there for me from my very first day in the UK, I will never forget. There is another Luca, a chemist, with which I shared a lot of good music, science, alcohol and philosophy and Federico, always close to me even from far away. People from 79, I also thank you for spicing up COVID-19 days (and nights). Manuela, for having thought me music. My family, Jasmin, Luisa, Mum and Dad: I lost count of the years I started studying such an intense subject and you never gave up on me, I do not know how you do. This work is for you. Alvis Bastianello and Jacopo De Nardis, you were added mentors along the way. I will have a lot to do to make this fair. Sylvia, thank you for your care and for listening to me when nobody would like to. Olalla, I am so grateful to know you. I hope your art won't leave me. Lastly, Benjamin Doyon, for your kindness, in and out the work and for having shaped my mind to think as a fluid: I hope you will always be the kind of person you are.

Giuseppe

Abstract

This Thesis is devoted to the presentation of recent results of the theory arising from the combination of Generalised Hydrodynamics and Large deviation theory. This theory is termed Ballistic Fluctuation Theory and has been firstly developed in [1, 2]. We will presents more recent developments and applications mainly based on papers [3–5] which were part of the works that I have accomplished during the years spent in my Ph.D. at King’s College London under the supervision of Prof. Benjamin Doyon and are those dedicated to this subject. In particular, we present applications to the correlation functions in spin chains and quantum field theories. In this context we analyse Full counting statistics and cumulants of transported $U(1)$ like quantities. Correlation functions of certain types of fields related to internal symmetries appear also in the context of the calculation of certain measures of entanglement. In this respect we will present the development of a new technique for the application of such theory to the Renyi entropies.

Table of contents

List of figures	vii
List of tables	xi
1 Hydrodynamic approach to correlation functions	1
1.1 Integrable models	1
1.1.1 Prototypes of integrable models	2
1.1.2 Classical integrability	6
1.1.3 Bethe Ansatz	9
1.1.4 Thermodynamic Bethe Ansatz	16
1.1.5 Euler Hydrodynamics	20
1.1.6 GHD: Generalised Hydrodynamics	22
1.2 Probability toolbox	26
1.2.1 Fluctuations	26
1.2.2 Basic probabilistic concepts	26
1.2.3 Correlations in free fermionic systems	29
1.2.4 Large Deviation Theory	32
1.3 Hydrodynamical correlation functions	37
1.3.1 Hydrodynamic projections	38
1.3.2 Ballistic fluctuation theory	44
1.4 Outlook	51
2 Space-time correlation functions	53
2.1 Getting started: XX spin chain	53
2.1.1 Model and correlation functions	54
2.2 Longitudinal correlators from hydrodynamic projections	58
2.2.1 Fluid-cell averages and hydrodynamic projections	58
2.2.2 Wick-theorem from Hydrodynamics and saddle-point	62
2.3 Transverse correlators from ballistic fluctuations	65

Table of contents

2.3.1	Transverse correlators and spin fluctuations	66
2.3.2	Exponential behaviour of transverse correlation function . .	70
2.4	Outlook	73
3	Sine-Gordon Field Theory	77
3.1	Sine-Gordon field theory	78
3.1.1	Classical Sine-Gordon	79
3.1.2	Quantum Sine-Gordon	81
3.2	Thermodynamics	84
3.2.1	Quantum Sine-Gordon	84
3.2.2	Classical Sine-Gordon	88
3.2.3	Low and high temperature quantum thermodynamics . . .	91
3.3	Sachdev-Damle semi-classical theory	91
3.4	Cumulants and Full Counting Statistics	93
3.4.1	Expression for the SCGF: FCS and correlation functions . . .	94
3.4.2	Cumulants	96
3.5	Comparison between semiclassics and BFT at low temperature . . .	103
3.5.1	Semi-classical theory	103
3.5.2	BFT	105
3.5.3	Comment	108
3.6	Outlook	108
4	Renyis and entanglement entropies from hydrodynamic	111
4.1	Model and main results	111
4.1.1	Overview	111
4.1.2	Model and quench protocol	113
4.1.3	Main result	115
4.2	Twist Fields and replicas	117
4.2.1	Replica approach and branch point twist fields	120
4.3	Application to Rényi entropies	123
4.3.1	Entropy of a single interval	123
4.4	Time dependence and long-range correlations	127
4.4.1	Long range correlations and GGE	127
4.4.2	Time evolution of half-system entropy	133
4.5	The case of ballistically growing interval	134
4.5.1	Single-mode and pair-mode twist fields	136
4.5.2	Hydrodynamic derivation of quasi-particle picture	138
4.6	Outlook	140

Appendix A	Jordan-Wigner strings	147
Appendix B	Free fermionic techniques	151
B.1	Diagonalisation of quadratic fermionic Hamiltonians	151
B.2	Fermionic correlation functions	154
B.2.1	Determinants and Pfaffians	154
B.2.2	Correlation functions of quadratic Hamiltonians	156
B.2.3	Application to XY spin chains	159
Appendix C	Asymptotic results	161
C.1	Skellam distribution	161
C.2	Asymptotic of modified Bessel function of infinite order	162
C.3	Fourier transform of Bessel function with respect to its order	164
C.4	Saddle point analysis of (3.97)	165
References		167

List of figures

1.1	Scattering between quasi-particles on a ring causes an additive shift in their wave functions.	15
1.2	Root density distribution in the thermodynamic limit. It measures the density of occupied states.	17
1.3	Caricature of different scales involved in the dynamics of a many-body system. hydrodynamics is expected to emerge at large scales no matter the precise microscopic details.	20
1.4	Local density approximation of the root density in pictures. This corresponds to (1.72).	23
1.5	Correlations and information of conserved densities are transported by Euler sound waves. This is a Onsager-like hypothesis.	40
1.6	Picture taken from [3]. The integral of the two-current on a discrete space. It is defined by integrating over times and summing over positions (discrete space here). The result is independent of the path chosen. In the middle, the case shown is an integral from $(0,0)$ to $(4,t)$ with $t_0 = 0, t_1 = t_2 = t_3 > 0, t = t_5 > t_4 > t_3$, see (1.155).	46
2.1	The leading exponential decay of the two-point function (2.51) is controlled by two effects, as expressed in (2.57): The fermionic JW string eventually modifies the exponential decay, depending on the analytic struture of the dispersion relation and on the phase of the model. Picture from [3].	70
2.2	Exponential decay of the JW string for different values of the magnetic field and different temperatures for fixed large x and $t = 0$. The numerics is done according to the Pfaffian representation derived with the aid of results in Appendix B. The theory is eq. (2.74).	73
2.3	Exponential decay of the two-point function for different rays parametrised by $\tan \varphi = x/t$. The theory is eq. (2.74).	74

List of figures

2.4	Comparison of the generic expression of the SCGF (1.174) controlling the leading exponential decay of the operator $\exp \lambda \Omega(x, t)$ against exact numerical simulations.	75
3.1	For the breathers theoretical value of e^{ϵ_n} as $\beta \rightarrow \infty$ is $\epsilon_n = n(n + 2)$. Parameters as in Table 3.1.	86
3.2	For the breathers theoretical value of e^{ϵ_K} as $\beta \rightarrow \infty$ is $\epsilon_K = n + 1$. Parameters as in Table 3.1.	86
3.3	Filling functions from the numerical solution of the TBA equations (3.39) and (3.40). Same parameters as Table 3.1.	87
3.4	Equal-time probability & cumulants. — We compare analytic predictions (BFT) [black line] in the classical regime of Sine-Gordon model with predictions from the SY picture [red line] and numerical results from Transfer Matrix [blue line and symbols]. The bare mass m is tuned while keeping $\beta = g = c = 1$. (a) The probability of phase differences is reported for a typical mass scale and distance, showing the convergence to the scaling behavior. (b-c) The convergence of cumulants upon increasing the relative distance is shown. (d-f) We scan different values of the bare mass: the vertex operator (d) helps to identify the strongly-interacting regimes away from the massless limit $\langle \cos \phi \rangle \simeq 1$ and the large-mass non-interacting regime $1 - \langle \cos \phi \rangle \simeq (4m)^{-1}$ [6]. (e-f) The large-distance scaling of the 2 nd and 4 th cumulants is shown, clearly non-Gaussian and in perfect agreement with numerics.	95
3.5	Cumulants with space-time separation. — Scaling behavior of the second (a.1) and fourth (b.1) cumulant as function of the ray $x/t = \tan \alpha$ for representative choices of the mass scale m ($\beta = g = 1$) in the classical regime. Numerical values obtained with Monte Carlo (symbols) closely follow the analytic BFT prediction (solid lines). In Figure (a.2) and (b.2) we show the approach of the quantum prediction (dashed lines) to the classical limit (solid line) for the c_2 and c_4 , respectively. We take $m = 0.25$ and increase the number of breathers N , while tuning the quantum soliton mass according to the semiclassical limit [6].	99
3.6	Further details on Monte Carlo data. — (a) Role of periodic boundaries. (b)-(c) linear growth of cumulants along different rays.	100

3.7	(a) Experimental setup. (b-c) Phase-reconstruction protocol from the outcome of a single projective measurement for different pixel resolutions σ (see main text). (d) Statistics built on 100 samples already shows the scaling behavior of the equal-time second cumulant stemming from the center of the trap. The effect of a low resolution σ is to “miss” kinks (see also (c)) and underestimate phase fluctuations. A good quality measurement is already obtained with $\sigma = 1\mu\text{m}$. See main text for discussion of parameters, and the SM of [5] for further details and data. Credits to Dr. Alvise Bastianello for realising this picture.	102
3.8	Caricature of the low temperature breathers cloud (pink) renormalising the kink (blue bump) velocity (arrow). Of course the physics is one dimensional and both kinks and breathers lie on the same line but the analogy with the electron in a solid being renormalised by a photon cloud is powerful.	107
3.9	Difference between Sachdev and Damle semiclassical picture accounting either for trasmission or reflection of quasi-particles and Ballistic Fluctuation Theory accounting for both at the same time. .	109
4.1	Schematic picture of the scenario studied in this chapter. The initial state contains pairs of quasi-particles with opposite momenta that spread in opposite directions. At large time they reach different parts of the system. This quasi-particle picture phenomenological formula is derived from hydrodynamic principles in (4.15).	115
4.2	Evolution of Rényi entropies of half system $A = [0, \infty]$ within BFT. Left: Initial integration path. Because of initially entangled pairs, points along this path at time t will be correlated, which prevents us from applying BFT directly. Right: Deformed integration path. Along this new path points are not correlated anymore. Moreover the only term contributing to the growth in time of entanglement is the vertical path from $(0, t)$ to $(0, 0)$	135
4.3	Evolution of Rényi entropies of finite subsystem $A = [0, x]$ within BFT. The integration path that we need to chose (continuous dark-gray line) in order for BFT to apply is different at short (left) and long (right) times. The choice depends on which points in spacetime get correlated because of initially entangled pairs produced by the initial state.	139

List of tables

- 3.1 In the high temperature limit the fillings are constant. The values are exactly known to be $\varepsilon_n = n(n + 2)$ and here we display the values for the so-called L -functions defined as $L_n(\theta) = \log(1 + \exp(-\varepsilon_n(\theta)))$. See [7] and references therein. The soliton mass is $M = 1$, the inverse temperature $\beta = 0.001$ and the number of breathers is set to $N = 9$. The integral equations are transformed into matrix equations and solved via Newton method. We used 50 points in rapidity space with an error tolerance of 10^{-10} 87

Introduction

Hydrodynamics is a universal theory: it is a condensed description of a physical system capturing large scale properties. Ordinary matter is composed of a virtually infinite number of atoms so that looking at a small piece of it, which is still large enough to contain a macroscopic fraction of elementary constituents, it is possible to describe its behavior in terms of coordinates referring to such small pieces: these pieces are called "fluid cells". This simple concept, the reduction of the degrees of freedom associated with the recognition that at large scales not all degrees of freedom are relevant, is at the heart of every hydrodynamic theory. I say every because in the past years it has been recognised that not all hydrodynamic theories have the same form. The topic of this thesis is a very special type of hydrodynamics, which has similarities and dissimilarities with the conventional one, invented for ordinary matter: this theory is called Generalised Hydrodynamics (GHD).

Conventional hydrodynamics (CHD) (likewise GHD for particle systems) is based on Newton's equations and Einstein's equations (depending on the ratios between typical velocities and the speed of light) and although it has been in the deck of physicists and scientists for two centuries, our complete understanding of it is everything but complete. For instance, turbulence keeps resisting a quantitative description and there are no visible signs at the horizon indicating that the problem is close to a solution. On the mathematical side, existence and uniqueness of Navier-Stokes equations (with appropriate boundary conditions) are listed in the Millennium Prize Problems. This is a short story of course, but it gives meaning to the question: why another hydrodynamic theory?

In the past two decades, nano-technology has made huge advances in most of its sub-fields and we see a clear impact on our everyday lives, no need to give examples. One important recent experimental breakthrough has been the possibility to explore fundamental questions in physics via the realisation of cold atom systems, very close to the quantum regime. One such fundamental question was: how

List of tables

is it possible that a closed macroscopic quantum system can ever reach thermal equilibrium, quantum mechanics being unitary?

This question is fundamental, in the sense that poses serious threats to the very basic principles of a fundamental theory because at first glance it seems to contradict the evident fact that systems do go to thermal equilibrium at some temperature determined by external conditions. It took some time to realise that globally quantum systems do not relax: they do at the level of subsystems. Indeed, when a subsystem is macroscopic, the rest of the system, still macroscopic, acts as an external heat bath. This allows relaxation, and if the dynamics is sufficiently mixing, the system will thermalise at some temperature determined by the total energy. These are the kinds of questions that I will refer to as fundamental.

At the theoretical level, thermalisation, or any equilibration of some sort, has its explanation in the Second Principle of Thermodynamics. This a fundamental principle permeating any branch of physics - and in a sense giving a rule to our lives: time goes forward. As we know, this is equivalent to say that spontaneous processes are irreversible, which said in another way means entropy increases. The equilibrium state is found by maximising the entropy, subject to constraints coming from the microscopic dynamics. In an isolated system, energy is conserved and the distribution maximising the Shannon entropy is the Gibbs distribution of statistical mechanics.

In a breakthrough experiment Kinoshita and collaborators noticed an important difference in the relaxation behavior between a system of bosons in one and two or more dimensions. What they do is a quantum realisation of the famous Newton's cradle, a mechanism which, due to conservation of momentum, is a very good approximation of a perpetual machine, one indeed violating the Second law of thermodynamics. Using a laser they split an initial distribution of bosonic particles into two separate clouds and then leave the system under its own unitary evolution. What was observed was that the one dimensional system was not relaxing to thermal equilibrium in the sense that the Gibbs distribution was not describing the system at long times. This was originally attributed to an approximate form of integrability of the one dimensional system. There is a universal model describing bosonic scalar particles in one dimension: this is the Lieb-Liniger model. Such model at the quantum level is integrable, meaning that, in analogy with classical mechanics, it possess an extensive number of conserved

quantities commuting with each other: signatures of integrability. For the time being suffices to say that integrability will be synonymous with the presence of an extensive number of conservation laws and/or exact understanding of certain micro and macroscopic quantities such as eigenstates, spectrum and other simple thermodynamic quantities.

It was natural then to apply the same entropy maximisation principle to an integrable system: the positive result was that subsystems relax to the so-called Generalised Gibbs Ensemble (GGE). By definition, these are the states that are stationary, homogeneous, and clustering at large distances. I will write its form now as it will be relevant for the rest of the thesis. The density matrix of a subsystem of an integrable system at large times reads

$$\rho = \frac{1}{Z} e^{-\sum_i \beta_i Q_i} \quad , \quad (1)$$

where Z is a normalisation constant (generalised partition function) depending on all the "generalised inverse temperatures" β_i . For each conserved quantity Q_i a lagrange multiplier β_i is introduced in the process of entropy maximisation. These are fixed by the initial expectation values of the conserved quantities, as they cannot change during the evolution. GGEs can explain relatively well situations where systems are isolated and homogeneous.

In a real experiment, all can go wrong, and to any possible extent the system is never really homogeneous. Inhomogeneities can be present in many places, from initial states to the Hamiltonian itself. They can be impurities of the atom system or imperfections of the experimental apparatus or can be purposely introduced. Indeed, we now have another fundamental question: what happens to all such theoretical machinery when we allow a relatively small degree of inhomogeneity? By small here it is meant that *variations* happen on scales that are small compared to the observation scale but generally they do not have to be small in magnitude. This is the fundamental question that the theory of GHD tries to answer. It is the universal large scale theory of integrable models. While one might think that integrable models are rather special and in practice any real system is not exactly integrable, there is now a large set of experiments pointing in the opposite direction. Systems can be engineered to be integrable and exploiting the rich mathematical structure underpinning such models it is possible to make striking predictions on the behavior of many-body systems under complicated

circumstances. GHD is the hydrodynamic theory for all such conserved quantities: local entropy maximisation leads to an infinite set of transport equations for the particles distributions, encapsulating at once all the relevant degrees of freedom needed to describe the system at low energy.

Despite the theory being relatively young, in recent years it has produced a huge amount of results both on the theoretical and on the experimental side. It has been refined to account for diffusion and more recently for dispersive corrections and it has been experimentally verified. In principle one could even consider an infinite order hydrodynamics, something that has been achieved only for free systems. With this last statement we mean that in the gradient expansion, of which the first two terms give standard hydrodynamics as we know it, one is not bound to stop at lowest orders but could in principle resolve arbitrarily small scales. On a practical level, often one is able to relate observable quantities to some sort of correlation function. This thesis is devoted to report recent advances in this direction, which is the result of the combination of GHD with a well established mathematical theory which goes under the name of Large Deviation Theory. The result is Ballistic Fluctuation Theory, a framework capable of capturing relevant fluctuations at the Eulerian scale of the underlying hydrodynamic theory.

Organization of the Thesis

The work can be divided into four main parts. The first part is a gentle and heuristic introduction to the main ideas of the hydrodynamic approach to correlation functions. To do this we introduce the theory of GHD, large deviations, Ballistic Fluctuation Theory (BFT) which constitute the technical tools on which all the results are based. The second part is based on [3] and presents the calculation of correlation function in quantum spin chains, in particular XX spin chain. The third part is of higher complexity and deals with correlation functions in a quantum field theory, the Sine-Gordon model. It is based on [5]. The fourth part, drawing from [4], presents the result that the evolution of the entanglement entropy, and so quantum fluctuations spreading, has a classical hydrodynamic nature.

Chapter 1

Hydrodynamic approach to correlation functions

Goal of the chapter

In this chapter we review the basic hydrodynamic approaches to the calculation of correlation functions, focusing more on the case of two point functions. There are, at present, two main techniques: hydrodynamic projections, whose main idea is to project the late dynamics onto the space spanned by conserved quantities and expand any observable in such a basis. This predicts t^{-1} ballistic decay of correlations in integrable models every time the observable couples to a conserved field. When this does not happen, the decay is faster, generally exponential, and it is a combination of hydrodynamics and large deviation theory that gives the correct description. This theory is termed ballistic fluctuation theory . Here we review the basics of hydrodynamic projections, generalised hydrodynamics and large deviation theory, all of them together forming the basic language and theoretical machinery of all this thesis.

1.1 Integrable models

For experts integrable models are reasonably realistic physical models with exceptionally wonderful mathematical properties. In a sense, while generic interacting many-body systems are difficult to tackle analytically, an integrable model, although very hard, might still be reasonably doable. In this context, reasonably doable means that some non-trivial information can be computed in a very precise way. The kind of information one is interested in depends usually on the domain

of application. It is often the case that the adjective "exactly solvable" is used in place of "integrable". This is not very precise because not everything can be computed in an exact fashion. For non-experts integrable models might seem weird and unusual creatures.

The feeling acquired talking to theorists not working with these models is that most of the people have quite an old perception about them. Indeed, while it is true that in the 70'-80' it might have been very challenging to realise physical systems well described by a certain integrable model in a lab, this is no longer the case: cold atoms experiments offer the perfect playground and the techniques have now become standard in many laboratories.

Here we give an overview of the main topics that comprise what is known as the integrability field to give a taste of the vastness of the subject. We start with classical integrability and after we discuss basics of Bethe Ansatz introducing only the relevant equations needed to introduce Generalised Hydrodynamics.

1.1.1 Prototypes of integrable models

Before introducing the theory of Generalised Hydrodynamics and all the machinery for computing correlation functions derived from it, it is necessary to give some context and motivation to the reason why it was actually born. We have mentioned that this is the large scale hydrodynamical theory of models of a special type: integrable models. In classical mechanics the notion of integrability is bound to that of exact solvability, at least for systems with a finite number of degrees of freedom [8]. In quantum mechanics, while the notion and the signatures of integrability are pretty clear, a mathematical definition is still hard to give. In this thesis, an integrable model will be a model that exhibits an infinite number of conservation laws that we will generically indicate by $Q_i, i = 1, 2, \dots$.

The first example of integrable model can be found in elementary graduate courses when discussing an assembly of N free particles not interacting with one another the Hamiltonian of which is

$$H = \sum_{i=1}^N \frac{p_i^2}{2m} . \quad (1.1)$$

This is a typical model of a dilute quantum or classical gas in solid state physics and it is usually not mentioned that this system's thermodynamics is rather special.

The equations of motion are

$$\begin{cases} \dot{x}_i = p_i \\ \dot{p}_i = 0 \end{cases} . \quad (1.2)$$

The quantities

$$Q_n = \sum_{i=1}^N (p_i)^n \quad (1.3)$$

are conserved for any n and are *local*¹. There is an infinite set of conservation laws. The conserved fields are

$$q_n(x) = \sum_{i=1}^N (p_i)^n \delta(x - x_i) \quad (1.4)$$

$$j_n(x) = \sum_{i=1}^N (p_i)^n \dot{x}_i \delta(x - x_i) = \sum_{i=1}^N (p_i)^{n+1} \delta(x - x_i) = q_{n+1}(x) \quad (1.5)$$

satisfying the continuity equations

$$\partial_t q_n + \partial_x j_n = 0 \quad (1.6)$$

The usual assumption of statistical mechanics is the ergodic theorem [12]. It is the statement that time averages can be replaced by ensemble averages. The ensemble distribution that predicts equilibrium quantities is usually assumed to be the Gibbs distribution

$$P(x_1, \dots, x_N, p_1, \dots, p_N) = \frac{1}{Z} e^{-\beta H(x_1, \dots, x_N, p_1, \dots, p_N)} \quad (1.7)$$

and the argument is usually the one (valid for generic non-integrable systems) starting from the exact Liouville equations for the multi-particle distribution

$$\partial_t f + \{f, H\}_P = 0 \quad (1.8)$$

where $f(x_1, \dots, x_n, p_1, \dots, p_n) d\Gamma$ is the probability to find the system, i.e. the point $(x_1, \dots, x_n, p_1, \dots, p_n)$, in the phase space volume $d\Gamma$. The stationary equilibrium distribution does not depend on time and so it must have zero Poisson bracket with the Hamiltonian. A reasonable choice is that it must be a function of it and the Gibbs distribution (1.7) follows after imposing entropy maximisation. The problem is that all the conservation laws must be taken into account because the

¹Actually, ultra-local see [9–11] and references therein for discussions about locality.

Hydrodynamic approach to correlation functions

dynamics has infinite memory of these. The information is not lost as time goes. The information theoretic principle of maximal entropy "à la de Jaynes" [13, 14] provides an elegant way to find the stationary distribution: it is the distribution that maximises the Shannon entropy defined as

$$S[f] = - \int d\Gamma f \log f \quad . \quad (1.9)$$

Here $S[f]$ is a functional over the space of probability distributions on the phase space. The maximisation procedure constrained by all the conserved quantities Q_i gives the so-called Generalised Gibbs Ensemble already introduced in (1). This way one sees that it is not true that the non-interacting gas thermalises, rather it can sustain non-equilibrium stationary states because GGEs need not be parity invariant and currents might be non-zero.

This discussion can easily be generalised to field theories and quantum many-body situations. The second quantised form of the non-relativistic free particles above is

$$H = \int dx \frac{\hbar^2}{2m} \partial_x \psi^\dagger \partial_x \psi \quad (1.10)$$

where ψ is now a bosonic field satisfying appropriate commutation relations (Poisson brackets in the classical case). The local conserved quantities map to

$$Q_n = (-i\hbar)^n \int dx \psi^\dagger \partial_x^n \psi \quad (1.11)$$

the normalisation of course being arbitrary. The currents and the charges are immediate. The same construction can be done in the Klein-Gordon field theory which is relativistic. The Hamiltonian is

$$H = \frac{1}{2} \int dx \left[\pi^2 + (\partial_x \phi)^2 + m^2 \phi^2 \right] \quad (1.12)$$

where the bosonic field ϕ , as before, satisfies an appropriate algebra depending on whether the model is quantised or not. In this case the construction of the local charges is less straightforward [15]. Changing variables to $\tau_\pm = x \pm t$ and taking derivatives $\partial_\pm \equiv \partial_{\tau_\pm}$ we obtain

$$\partial_+ \partial_-^n \phi = -\frac{m^2}{4} \partial_-^{n-1} \phi \quad , \quad \partial_- \partial_+^n \phi = -\frac{m^2}{4} \partial_+^{n-1} \phi \quad (1.13)$$

so that we can compute

$$\partial_+ [\partial_-^n \phi]^2 = 2\partial_-^n \phi [\partial_+ \partial_-^n \phi]^2 = -\frac{m^2}{2} \partial_-^n \phi [\partial_-^{n-1} \phi] = -\frac{m^2}{4} \partial_- [\partial_-^{n-1} \phi]^2 \quad (1.14)$$

that going back to the original variables gives conservation laws of the form

$$\partial_t q_n^- + \partial_x j_n^- = 0 \quad (1.15)$$

with

$$q_n^- = [\partial_-^n \phi]^2 - \frac{m^2}{4} [\partial_-^{n-1} \phi]^2 \quad , \quad j_n^- = [\partial_-^n \phi]^2 + \frac{m^2}{4} [\partial_-^{n-1} \phi]^2 \quad . \quad (1.16)$$

In the same way one gets another set of the form

$$q_n^+ = [\partial_+^n \phi]^2 - \frac{m^2}{4} [\partial_+^{n-1} \phi]^2 \quad , \quad j_n^+ = [\partial_+^n \phi]^2 + \frac{m^2}{4} [\partial_+^{n-1} \phi]^2 \quad . \quad (1.17)$$

Linear combination of these charges give rise to the Hamiltonian and the momentum for example. In quantum mechanics upon second quantisation one has to construct an Hilbert space. In a free theory this is done simply using field operators. In terms of the modes

$$\psi(x) = \int \frac{dk}{\sqrt{2\pi}} e^{ikx} \psi(k) \quad (1.18)$$

the whole Fock space that is composed by a collection of independent particles labelled by the momentum

$$|k_1, \dots, k_n\rangle = \prod_{i=1}^N \psi^\dagger(k_i) |0\rangle \quad (1.19)$$

where $|0\rangle$ is the vacuum state annihilated by $\psi(k)$ for all k . In this basis the Hamiltonian is diagonal and reads

$$H = \int dk E(k) |\psi(k)|^2 \quad (1.20)$$

with $E(k) = \frac{\hbar^2}{2m} k^2$ being the energy of a single particle. This writing of the Hamiltonian has an action-angle variables form typical of integrable systems with few degrees of freedom [8]. It is clear that the total energy is the sum of the single-particle energies. In the same way local charges can be all written in momentum

space and they read

$$Q_n = \hbar^n \int dk |\psi(k)|^2 h_n(k) \quad , \quad h_n(k) = k^n \quad (1.21)$$

where the function $h_n(k)$ is called one-particle eigenvalue and will be important later. We have

$$Q_n |k_1, \dots, k_n\rangle = \sum_{i=1}^N h_n(k_i) |k_1, \dots, k_n\rangle \quad \forall n \quad (1.22)$$

Not only the total momentum $P = Q_1$ is conserved but each individual particle-momentum is. The scattering between particles is purely elastic. This is of course a triviality in free models but the presence of infinitely many charges makes it happen in integrable models as well. Now we add interactions in such a way the conservation laws are not broken and conserved quantities and currents are, correspondingly, only deformed.

1.1.2 Classical integrability

KAM theory

The first fundamental result is the celebrated Kolmogorov-Arnold-Moser (KAM) theory culminating with the eponymous KAM theorem [16–18]. A good review on this mathematical topic is [19] while a physical and practical approach is followed in [20]. Basically here the question is whether a small non-linear perturbation to an integrable Hamiltonian system can lead to a sustained quasi-periodic orbit in phase space like a system of N harmonic oscillators with different frequencies do. The latter system can indeed be solved using action angle-variables [8]. The theory gives conditions under which quasi-periodic solutions to a perturbed Hamiltonian system persist. These conditions include a non-resonance condition on the frequencies of the quasi-periodic motion and a smallness condition on the size of the perturbation.

In the thermodynamic limit, i.e., when the number of degrees of freedom tends to infinity, both of these conditions become problematic.

1. Non-resonance Condition: The non-resonance condition requires that the frequencies of the quasi-periodic motion are not rationally related. However, as the number of degrees of freedom increases, the chances of finding a resonance (i.e., a rational relationship between frequencies) also increase. In the thermodynamic limit, the space becomes densely filled with resonances,

making the non-resonance condition almost impossible to meet. This is a manifestation of the so-called "small divisor problem", a challenge in mathematical physics concerning the perturbation theory of Hamiltonian systems [21].

2. **Smallness Condition:** The smallness condition requires that the perturbation to the Hamiltonian system is sufficiently small. In a system with a finite number of degrees of freedom, it's possible to adjust the size of the perturbation to satisfy this condition. However, in the thermodynamic limit, even if each individual interaction is weak, the collective effect of an infinite number of such interactions may not be small. Therefore, it becomes increasingly difficult, if not impossible, to ensure the smallness of the perturbation.

These two issues represent significant obstacles to the application of KAM theory in the thermodynamic limit.

Fermi-Pasta-Ulam-Tsingou (FPUT) experiment

The Fermi-Pasta-Ulam-Tsingou (FPUT) problem is a key challenge in the field of nonlinear dynamics and chaos theory, which traces its roots back to a numerical experiment conducted in the 1950s. The original paper is [22] while excellent accounts can be found in [23–25]. This experiment involved a chain of particles connected by nonlinear springs, and it was designed to examine the thermalisation process in this simple system, i.e., whether the energy initially concentrated in one mode would eventually spread out evenly among all modes, which is a prediction of statistical mechanics. In particular they studied the following dynamical system

$$\frac{d^2 x_i}{dt^2} = (x_{i+1} - 2x_i + x_{i-1}) + \beta(x_{i+1} - x_i)^n - \beta_n(x_i - x_{i-1})^n \quad , \quad (1.23)$$

for $n = 2, 3$. Here, β_n is the nonlinear coupling constant. In the original paper [22] $\beta_1 \equiv \alpha$ and $\beta_2 \equiv \beta$. The first term on the right-hand side of each equation corresponds to the standard linear (Hooke's law) interaction between the particles, while the other terms describe the nonlinear interactions.

The surprising discovery was that, instead of reaching a state of thermal equilibrium, with energy distributed equally among all the modes, the system exhibited a quasi-periodic behavior, with the energy oscillating between a few modes, eventually returning near to its initial state. This finding led to a number of significant advances in the understanding of nonlinear dynamics, including soliton theory

Hydrodynamic approach to correlation functions

and chaos theory. The underlying reasons for this behavior, particularly why the FPUT system doesn't thermalize as expected were unclear. An answer to that inexplicable behavior was given by Norman J. Zabusky and Martin D. Kruskal in 1965 [26], where they related the behavior of the Fermi-Pasta-Ulam-Tsingou (FPUT) system to the Korteweg-de Vries (KdV) equation.

In this work, Zabusky and Kruskal discovered that the FPUT system could produce stable, solitary wave packets, which they named "solitons". This was a groundbreaking discovery because, until that time, it was generally believed that nonlinear interactions would inevitably lead to the breakdown of any waveform into simpler waves or result in a chaotic state.

The KdV equation is a third-order partial differential equation that describes the propagation of waves in a one-dimensional shallow water wave channel. It's one of the simplest nonlinear wave equations that permits soliton solutions. What's particularly interesting is that the KdV equation is an integrable system, it has a sufficient number of conserved quantities to allow it to be solved exactly. The equation reads

$$\partial_t u + 6u\partial_x u + \partial_x^3 u = 0 \quad (1.24)$$

where u is related to the velocity field $\frac{dx_i}{dt}$ in an appropriate continuum limit, see [25] for details. By numerically studying the long time evolution of the FPUT system and showing it can be approximated by the KdV equation in the small amplitude limit, they connected the surprising non-thermalizing behavior of the FPUT system to the integrability of the KdV equation. This provided a strong impetus for the development of the Inverse Scattering Transform method, a technique used to solve certain integrable models, including the KdV equation.

Inverse Scattering Method (IST)

The Inverse Scattering Transform (IST) is a mathematical method used to solve certain nonlinear differential equations. The method was developed in the context of soliton theory as a powerful tool for solving integrable partial differential equations. The idea of the IST is to transform the original nonlinear problem into a simpler linear problem through a spectral analysis, solve the simpler problem, and then invert the transformation to obtain the solution to the original problem. See Refs. [27–30] for extensive discussion and Ref. [31] for a modern perspective and application to contemporary issues.

In particular, the IST has been applied to solve equations like the Korteweg-de Vries (KdV) equation and the nonlinear Schrödinger equation, both of which model various physical phenomena and have solutions that describe solitons. The IST consists of three main steps:

1. Direct Scattering Transform: The initial condition of the differential equation is analyzed to find its scattering data. This step involves solving a related linear differential equation known as the scattering problem.
2. Time Evolution of the Scattering Data: Using the integrability of the differential equation, the time evolution of the scattering data is determined.
3. Inverse Scattering Transform: The evolved scattering data is used to reconstruct the solution to the original differential equation at later times.

Solitons

There are many different types of solitons like localised solitons, topological solitons, breathers, magnetic and optical solitons and many others. An account can be found in [32]. The common feature is their scattering properties. The scattering is completely elastic and factorises into two-body processes. This was indeed one of the main findings of Zabusky and Kruskal [26]. They noticed that coherent structures, the solitons, overlapped for a certain time and then re-emerged not having lost their "identity". The only difference is a shift in their relative positions: the emerging solitons are just displaced by a number that, importantly, depends on their velocities. This is a property that is fundamental in quantum mechanical integrable models as well and it is this scattering behavior that allows, to a certain extent, to discuss thermodynamic properties of quantum and classical integrable models on the same footing. Solitons represent the stable excitations out of the vacuum, bumps of energy with well defined dispersion relation: emerging quasi-particles.

1.1.3 Bethe Ansatz

An overview

Bethe Ansatz is basically a method for finding the spectrum of interacting quantum many body systems. It bears the name of its inventor Hans Bethe who actually did not realise that the method would have produced a huge amount of success in

Hydrodynamic approach to correlation functions

later generations of physicists and mathematicians. Bethe used an Ansatz [33] for the wave function of the ferromagnetic XXX spin chain whose Hamiltonian reads

$$H = -J \sum_{i=1}^N \vec{S}_i \cdot \vec{S}_{i+1} \quad (1.25)$$

where $J > 0$ is a ferromagnetic coupling and $\vec{S}_i = (s_1, s_2, s_3)$ is a vector of spin matrices $s_i = \frac{\hbar}{2} \sigma_i$ with σ_i the Pauli matrices.

Although the model was conceived as a spin chain, all integrable theories can be put under the same hood via the Algebraic Bethe Ansatz construction [34]. Spin chains give rise to continuum quantum field theories in appropriate continuum limits [35]. A full discussion of the method would require an entire chapter and there exist a fairly big amount of reviews and lecture notes on the topic [36–39]: these are rather complete and systematic, something which we are not trying to be here for what concerns this particular topic.

The main point behind integrable models is that the spectrum can be organised in terms of stable quasi-particles. In condensed matter physics, especially after the success of Fermi liquid theory [40, 41], the concept of quasi-particle and particle-hole excitations was so important and pervasive that cannot in anyway be underestimated. Landau [42] realised that even though the Coulomb long range interaction is not small compared to the kinetic part of the Hamiltonian, when an electron is excited just above the Fermi surface the phase space available for scattering is very little and suppressed at low energy. The net effect is a renormalisation or "dressing" of single, free, particle states. Doing perturbation theory in the interaction one sees that the energy is shifted due to a superposition of electron-hole pairs. If we stay close to the Fermi surface the typical energy scale will be $\Delta E = E - \epsilon_F \rightarrow 0$ and the life time of excitations diverges. In models solvable by Bethe Ansatz the life time is truly infinite and quasi-particles do not decay. They have sharp energy-momentum dispersion relation and scattering is elastic and factorised. All these properties are in one-to-one correspondence with the behavior of solitons, as we mentioned in the previous section.

Scattering with additional charges

The Bethe Ansatz can be heuristically justified via the concept of scattering states using the assumption that there are infinitely many conserved quantities. To

be precise, in a relativistic theory with Lorentz invariance, only two charges are needed to show factorisability and elasticity of scattering, as long as space-time has dimensions $(1 + 1)$ [43] because otherwise the S -matrix would be trivial (Coleman-Mandula theorem [44]). We instead consider a non-relativistic quantum theory (see [45, 46] for classical particle systems), and we consider then an additional charge Q commuting with the Hamiltonian, the momentum and eventually the number operator. We show that the S -matrix necessarily factorises in a sequence of two-body scatterings. In the same way as the Hamiltonian (which is present in the set of conserved quantities) generates the time evolution, also the other charge generates some flow of some "generalised time" parameter. The unitary transformation is

$$U(s) = e^{isQ} \quad (1.26)$$

and since it is a symmetry it commutes with the S matrix

$$[S, U(s)] = 0 \quad (1.27)$$

which in turn implies that the scattering amplitudes satisfy

$$\langle k'_1, \dots, k'_N | S | k_1, \dots, k_N \rangle = \langle k'_1, \dots, k'_N | U^\dagger(s) S U(s) | k_1, \dots, k_N \rangle \quad (1.28)$$

Particles are labelled in order of increasing momentum from left to right so that $k_i < k_j$ if $i < j$. This is always possible in one spatial dimension.

The parameter s associated to the symmetry Q is the generator of, like the momentum generates translation and the generalised time is space. In a typical scattering experiment, particles in the distant past are well separated. Single particle states are taken centered in (x_i, k_i) in phase space

$$\langle q | k_i \rangle = \left(\frac{1}{2\pi\sigma_i^2} \right)^{1/4} \exp(f(q; k_i, x_i, \sigma_i)) \quad (1.29)$$

where

$$f(q; k_i, x_i, \sigma) = -\frac{(q - k_i)^2}{4\sigma_i^2} - iqx_i \quad (1.30)$$

The multi-particle state in the asymptotic past $t = -t_0 \rightarrow -\infty$ is simply a product state (we consider bosons for definiteness)

$$\langle q_1, \dots, q_N | k_1, \dots, k_N \rangle = \prod_{i=1}^N \left(\frac{1}{2\pi\sigma_i^2} \right)^{1/4} \exp(f(q_i; k_i, x_i, \sigma_i)) \quad (1.31)$$

Hydrodynamic approach to correlation functions

The state is set in motion according the Hamiltonian

$$H = \sum_i \frac{k_i^2}{2} + \lambda(t)V \quad (1.32)$$

where V is the interaction and $\lambda(t)$ is chosen as to switch on the interaction adiabatically in such a way that eigenstates evolve adiabatically as well [42, 47]. A common choice is $\lambda(t) = e^{-\frac{|t|}{\epsilon}}$ with $\epsilon \rightarrow 0^+$. As long as $|t| \gtrsim 2\epsilon^{3/2}$ the interaction is negligible and the time evolution is that of the free Hamiltonian. Its effect is

$$f(q; k_i, x_i, \sigma_i) \rightarrow -\frac{(q - k_i)^2}{4\sigma_i^2} - iqx_i - i\frac{q^2}{2}(t - t_0) \quad (1.33)$$

The average position of a single particle is

$$\langle x_i \rangle (t) = x_i + k_i(t - t_0) \quad (1.34)$$

while the velocity stays constant of course. Since the charge Q commutes with H (the interacting Hamiltonian) and with the momentum operator and thanks to adiabaticity we have that

$$Q |k\rangle = h(k) |k\rangle \quad (1.35)$$

where $h(p)$ is the single-particle eigenvalue specific of the charge Q , analogous to (1.21) in the free theory. The combined effect of the time evolution and the symmetry U is simply

$$f(q; k_i, x_i, \sigma_i) \rightarrow -\frac{(q - k_i)^2}{4\sigma_i^2} - iqx_i - i\frac{q^2}{2}(t - t_0) + ish(q) \quad (1.36)$$

and the average position is now

$$\langle x_i \rangle (t) = x_i + k_i(t - t_0) - s\Delta_i \quad (1.37)$$

where

$$\Delta_i = \left(\frac{1}{2\pi\sigma_i^2} \right)^{1/2} \int dq \exp \left(-\frac{(q - k_i)^2}{2\sigma_i^2} \right) h'(q) \quad (1.38)$$

We see that we can shift the wave packet center arbitrarily. This is much like a gauge freedom we have for the positions of the particles. Note that if Q is the

²The time interval over which the interaction is effective is $\sqrt{\int_{-\infty}^{+\infty} dt e^{-|t|/\epsilon t^2}} = 2\epsilon^{3/2}$.

momentum operator, $h(k) = k$. we obtain a shift in position by s while if Q is the number operator, $h(k) = 1$, no shift occurs, as expected. Assuming Q local³, we can extend this result to the multi-particle scattering states. Indeed, by locality

$$Q |k_1, \dots, k_N\rangle = \sum_{i=1}^N h(k_i) |k_1, \dots, k_N\rangle \quad . \quad (1.39)$$

We consider now the 2-particle scattering process. In a non-relativistic theory the number of particles, the energy and the momentum are conserved

$$\langle k'_1, k'_2 | S | k_1, k_2 \rangle = \delta(k_1 + k_2 - k'_1 - k'_2) \delta \left(\frac{1}{2} (k_1^2 + k_2^2 - (k'_1)^2 - (k'_2)^2) \right) S_{k'_1 k'_2, k_1 k_2} \quad (1.40)$$

which of course sets $k_i = k'_i$ and the scattering is elastic⁴. What happens for 3-body collision? Say we have $k_1 < k_2 < k_3$. After scattering, in the future at time T , we have $k'_1 < k'_2 < k'_3$ and $x_1(T) < x_2(T) < x_3(T)$.

First of all in presence of an additional charge implies that we have an additional constraint

$$\begin{aligned} \langle k'_1, k'_2, k'_3 | S | k_1, k_2, k_3 \rangle &= \delta \left(\sum_i k_i - \sum_i k'_i \right) \delta \left(\frac{1}{2} \sum_i k_i^2 - \sum_i (k'_i)^2 \right) \\ &\times \delta \left(\frac{1}{2} \sum_i h(k_i) - \sum_i h(k'_i) \right) S_{k'_1 k'_2 k'_3, k_1 k_2 k_3} \quad (1.41) \end{aligned}$$

The scattering with the potential has the effect that $x_i(T) = x_i(t_0) + \delta_i$. A solution to the constraints imposed by the δ functions is that $k_i = k'_i$ so the scattering is elastic. If one is not convinced, the case of really integrable model displaying an infinite set of conservation laws Q_i implies that we have to satisfy an infinite number of constraints leading immediately to the elasticity property as the only possible outcome. Next we address the factorisability. Making use of the symmetry U we can shift the final positions $x_i(T)$ by an amount $-s\Delta_i$ such that going back in time along straight line trajectories for the wave packet centers for one of these particles (always $|t| \gtrsim 2\epsilon^{3/2}$) and such that we exactly compensate the shift, say δ_3 of the fastest particle. So one would conclude particle 3 did not scatter at all⁵! But

³In second quantisation, Q local means it is the integral of a local density $q(x)$. Acting on a state it only has effect at x . In a first quantisation language it means it is the sum of single particle operators $Q = \sum_i q_i$.

⁴Recall the labelling of the particles: in an elastic collision 2 particles just exchange their velocities so in the final state the labels are also exchanged.

⁵This assumes T finite so the trajectories are bounded.

Hydrodynamic approach to correlation functions

this is an artificial result coming only from the redundancy we have because of the symmetry Q .

Since particles have to scatter anyways we have to conclude that the collision is independent of the order⁶. Particle 3 has to come out shifted by δ_3 only after collisions with both particles 1 and 2. In this way we have proved that the scattering is factorised. This argument has as a by-product the celebrated Yang-Baxter relations [48, 37]

$$S_{k_1, k_2} S_{k_1, k_3} S_{k_2, k_3} = S_{k_2, k_3} S_{k_1, k_3} S_{k_1, k_2} \quad (1.42)$$

encapsulating elasticity and factorisability of scattering in $(1 + 1)$ dimensions. Adding analyticity and unitarity assumptions of the S -matrix it is possible to try a classification of such integrable S -matrices via the so-called *bootstrap program* but we will not delve into such matters and refer the interested reader to the relevant literature [49–52] and in particular Chapters 17-18 of Ref. [37].

Bethe Equations

It is clear that the shifts accumulated are additive and we can write

$$\delta(k_i) = \sum_{j \neq i} \delta(k_i, k_j) \quad (1.43)$$

where we have used the fact that the only thing they can depend on are the momenta of the incoming particles. By unitarity of the S -matrix we can write its elements as

$$S_{k'_1, \dots, k'_N, k_1, \dots, k_N} = \prod_{(i,j)} \exp(i\Theta(k_i, k_j)) \delta_{k'_i, k_i} \delta_{k'_j, k_j} \quad (1.44)$$

where the sum runs over the $N(N - 1)/2$ particle pairs and $\Theta(k, q)$ is called *phase shift*: it is a characteristic of the potential. Confining the system in the a box of length L and imposing periodic boundary momenta conditions of the particles will be quantised. If we bring a particle with momentum k_i around the circle it will scatter with all the other $N - 1$ particles and the wave function will pick up the phase $\Theta(k_i, k_j)$ for every collision. Taking into account the total kinematic phase accumulated making a round we end up with the consistency equations known as

⁶This heuristically clarifies the statement of the Coleman-Mandula theorem: in higher dimensions higher charges can be used to make the particles not to scatter at all so their S -matrix has to be trivial.

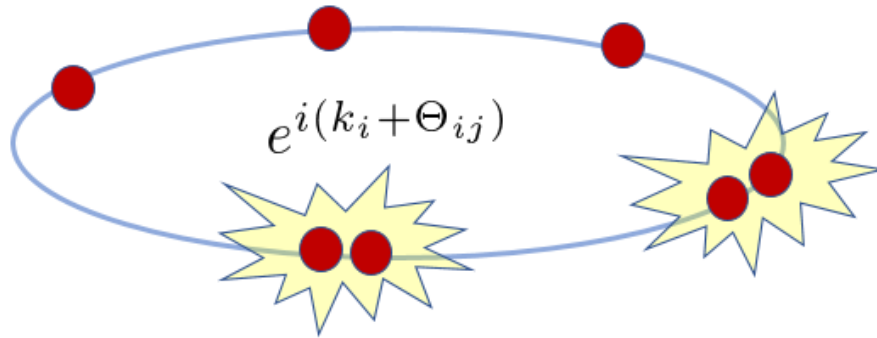


Fig. 1.1 Scattering between quasi-particles on a ring causes an additive shift in their wave functions.

Bethe equations see Fig. 1.1

$$\prod_{i \neq j} e^{i\Theta(k_i, k_j)} = e^{ik_i L} \quad (1.45)$$

which taking the logarithm becomes

$$Lk_i + \sum_{k_i \neq k_j} \Theta(k_i, k_j) = 2\pi I_i \quad (1.46)$$

where I_i is an integer (for every i). For each set of integers I_i there is a state characterised by k_i 's solutions of the above system. The equations (1.46) are highly non-linear coupled for the quasi-momenta of the particles. Note that the quasi-momenta are not eigenvalues of the momentum operator. Only their sum is the eigenvalue of the total momentum. We will call such numbers (Bethe) roots or rapidities (this is what they are in a relativistic theory). Depending on the model at hand, the only thing to be determined under the suspect of integrability is the scattering shift Θ studying two particle scattering. Once this is done the wave function of the system is determined.

There are models, like the Sine-Gordon model that we will introduce in more detail later, with a richer spectrum: there is not only one type of particle and these can scatter non-trivially between them. In this case the treatment becomes significantly more complicated and one has to resort to an Algebraic version of Bethe Ansatz [34, 53] resulting in what is called *nested Bethe Ansatz*. In physical terms this happens because the S -matrix is not diagonal in the space of particle types and one has to diagonalise it. In depth discussion can be found in the books

cited at the beginning of the chapter and an application to the Sine-Gordon model in [54, 55]. By our assumption of adiabaticity, the state is an eigenstate of the interacting Hamiltonian and the spectrum is completely determined once the the Bethe equations are known. The momentum and the energy of the state are the same as (1.39) with charge eigenvalues $h_H(k) = k^2/2$ and $h_P(k) = k$. Of course this is a simplified derivation of the elasticity and factorisation of scattering and the subsequent derivation of the Bethe equations is only an argument. Explicit and rigorous derivations are possible depending on the specific model and have now become standard textbook material, see Refs. [36, 34, 39, 56] and references therein.

1.1.4 Thermodynamic Bethe Ansatz

This subsection serves to the introduction of the relevant ingredients needed for a thermodynamic description of integrable models. These are the total density of "available" Bethe roots ρ_t , the density of "occupied" Bethe roots ρ (commonly known as root density) and the density of "holes" ρ_h . Related quantities are the filling function, which is the fraction of occupied states ϑ , related to the statistic of the particles in the model, the dressing kernel(s) and the dressing operation. These quantities are fundamental for the application of generalised hydrodynamics.

Solving directly the algebraic system of equations (1.46) is a challenging task already for few particles. There exist numerical studies [57–63] and efficient algorithms [64] but our focus is on macroscopic systems. Standard books on the subject are [34, 65, 37, 48] and the original papers of Lieb and Liniger on the exact solution of the Bose gas [66, 67] and for the Thirring model [68] (related to the Sine-Gordon field theory). In this brief part we discuss write down the thermodynamic limit of the Bethe equations both when the S -matrix is diagonal and non-diagonal.

Ingredients of Thermodynamic Bethe Ansatz

Looking at the Bethe equations (1.46) one sees that $k_{i+1} - k_i = O(L^{-1})$ and in the thermodynamic limit $N, L \rightarrow \infty$ with N/L fixed the equations give a finite limit. In this limit the density of particles is finite and so should be the number of roots per unit length. In this limit the roots cover densely the real axis and are described by a distribution function $\rho(k)$ giving the number of roots per unit length (see Fig. 1.2). When there is more than one particle type, in non-diagonal theories, we simply attach an additional index to the root densities specifying the particle type

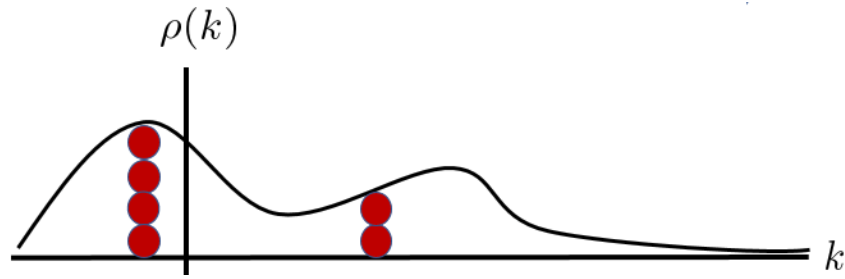


Fig. 1.2 Root density distribution in the thermodynamic limit. It measures the density of occupied states.

so we write

$$\int dk \rho_n(k) dk L = \text{number of occupied roots for particle of species } n \quad (1.47)$$

In an excited state not all the roots are occupied and the unoccupied, still available states form another distribution, the density of "holes" $\rho_n^h(k)$ such the the total density of possible states is

$$\rho_n^t = \rho_n + \rho_n^h \quad (1.48)$$

The ratio

$$\vartheta_n = \frac{\rho_n}{\rho_n^t} \quad (1.49)$$

defines the fraction of occupied states. Note that the spectral space is the doublet (k, n) where k is the quasi-momentum and n the particle type. This description entails the fundamental particle-hole excitation spectrum of integrable models. The pseudo-energies satisfies the non-linear system of Fredholm integral equations of the second kind [69, 70]

$$\varepsilon_n(k) = w_n(k) + \sum_m \int dk' T_{nm}(k - k') F_m(\varepsilon(k')) \quad (1.50)$$

where $F_m(x)$ are the free energy functions and depend on the statistics of the quasi-particles. One has

$$F_m(x) = \begin{cases} -e^{-x} & \text{classical particles} \\ \log(x) & \text{classical radiation} \\ -\log(1 + e^{-x}) & \text{quantum fermion} \\ \log(1 - e^{-x}) & \text{quantum boson} \end{cases} \quad (1.51)$$

Hydrodynamic approach to correlation functions

In the TBA equations (1.50) the scattering kernel is the fundamental object encoding interactions. It is related to the scattering shifts in (1.44) and the S -matrix via

$$T_{nm}(k) = \frac{1}{2\pi} \varphi_{nm}(k) \quad (1.52)$$

with

$$\varphi_{nm}(k) = -i\partial_k \log S_{nm}(k) = \partial_k \Theta_{nm}(k) \quad (1.53)$$

where now Θ_{nm} is the scattering shift in the wave function when particle of type n collides with particle of type m and S_{nm} the matrix element for such scattering process. The function kernel φ is often called differential scattering phase. Note here we are assuming the kernels depend only on the difference of the spectral parameters. In general this might not be true but in most of the models solvable by Bethe Ansatz it is possible to find a transformation to put them in this form.

The free energy function is related to the filling function via

$$\vartheta = \partial_\varepsilon F(\varepsilon) \quad (1.54)$$

The driving term $w(k)$ in (1.50) defines the thermodynamic state. On a homogeneous GGE of the form (1) specified by Lagrange parameters β_i associated to charges Q_i one has

$$w_n(k) = \sum_i \beta_i h_{i,n}(k) \quad (1.55)$$

where $h_{i,n}(k)$ is the one-particle eigenvalue specific of the charge as introduced in (1.39) in Section 1.1.3 and associated to particle of type n . In principle the functions $w_n(k)$ are arbitrary. Conventionally h_0 is often associated to the conservation of some internal charge: in the Lieb-Liniger model there is conservation of particles associated to $U(1)$ symmetry; in the Sine-Gordon model there is an $O(2)$ symmetry inherited by the massive fermion of the Thirring model and it is thus a topological charge. h_1 usually refers to the momentum and h_2 to the energy: quite generally $p(k) = h_1(k) = M \sinh(k)$, $E(k) = h_2(k) = M \cosh(k)$ and $h_1(k) = Mk$, $h_2(k) = M \frac{k^2}{2}$ in relativistic and non-relativistic models respectively where M is a mass scale and k is interpreted as rapidity or quasi-momentum.

The total densities of state ρ_n^t satisfy analogous non-linear integral equations to the pseudo-energy. Quite generically we could write

$$\rho_n^t(k) = \bar{h}_n(k) + \sum_m \int dk' T_{nm}(k - k') \rho_m(k') \quad (1.56)$$

where the driving terms \bar{h}_{nm} depend on the specific model but are often related to the one-particle eigenvalues in a simple way, see [71].

Thermodynamic potentials and dressing operation

To get thermodynamic observables one needs thermodynamic potentials. The free energy functions are related to the thermodynamic free energy (density)

$$f = - \lim_{L \rightarrow \infty} \frac{1}{L} \log Z = \sum_k \int dk F_m(\varepsilon_m(k)) \quad (1.57)$$

where Z is the partition function, for example the normalisation factor in (1), from which we can obtain various response functions in the state of interest by differentiation. Note the similarity with free systems. The whole effect of interactions is encoded in the scattering kernel (1.53) otherwise the form of thermodynamic functions simple. The expectation values of conserved charges of the thermodynamic state specified by the driving terms $w_m(k)$ have simple expressions in terms of the root densities

$$\langle Q_i \rangle = \sum_m \int dk h_{i,m}(k) \rho_m(K) \quad (1.58)$$

from which using the standard thermodynamic relation $\mathcal{F} = \mathcal{U} - T\mathcal{S}$ where $\mathcal{U} = Q_2$ is the total energy and \mathcal{S} is the entropy one derives the thermodynamic entropy. The entropy can also be expressed in terms of purely macrovariables. For example for fermionic systems this is the Yang-Yang (specific) entropy [72]

$$s = \sum_m \int dk \rho_m^t(k) [\vartheta_m(k) \log(\vartheta_m(k) + (1 - \vartheta_m(k)) \log(1 - \vartheta_m(k)))] \quad (1.59)$$

A recurrent operation recurring in studying thermodynamics of integrable models is that of dressing. It a linear operations mapping the space of functions of the spectral variable k and particle type n into itself. It is defined as

$$h_n^{\text{dr}}(k) = h_n(k) + \sum_m \int dk' T_{nm}(k - k') h_m^{\text{dr}}(k') \quad (1.60)$$

With this definition it is very easy to see that expectation values can be rewritten as

$$\langle Q_i \rangle = \sum_m \int \frac{dk}{2\pi} h_{i,m}^{\text{dr}}(k) \vartheta_m(k) \quad (1.61)$$

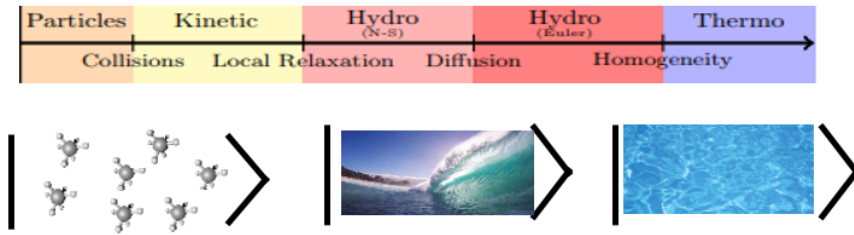


Fig. 1.3 Caricature of different scales involved in the dynamics of a many-body system. hydrodynamics is expected to emerge at large scales no matter the precise microscopic details.

and we see that a completely equivalent way to characterise the state is via the occupation functions ϑ_n . We will see more of this later discussing Generalised Hydrodynamics.

1.1.5 Euler Hydrodynamics

Generalised Hydrodynamics describes quantum and classical integrable models at large scale and it has been developed in the seminal works [71, 73]. The precise meaning of scale is dependent upon the microscopic details of a model in the sense that what might be the relevant scale in a model does not need to be in another. Despite the dependence of the overall scale on the microscopic details, the hydrodynamic equations are universal and apply equally to any system because of the phenomenon of *separation of scales* illustrate in Fig. 1.3. Systems that will be considered in this thesis have a special structure: they admit an infinite number of conservation laws. One might wonder how this can be possible. There are two answers: a not satisfactory one is that mathematically this is what comes out; the good answer is that experimentally, it turns out that systems can be exhibit more than one conservation law with a very good degree of approximation on the relevant time scales one is interested in [74].

Let us start simple and consider a generic system having a certain number M of conservations laws $\dot{Q}_i = 0$ (with the dot being the time derivative). For continuous symmetries, Noether theorem [47] tells us that we have M transport equations of the form

$$\partial_t q_i(x, t) + \partial_x j_i(x, t) = 0 \quad i = 1, \dots, M \quad (1.62)$$

where $q_i(x, t)$ are local charge densities and $j_i(x, t)$ are local current densities and the total charge is just

$$Q_i = \int dx q_i(x, t) \quad (1.63)$$

with the integral extending over the available space. Notice that we are not specifying at all whether the system be quantum or classical. For the most part of this chapter it won't matter and we will explicitly say when it does. It is important to realise that (1.62) refers to microscopic degrees of freedom: in a quantum field theory the q_i 's will be functionals of the field operators while in a spin 1/2 chain they will be combinations of Pauli matrices. Suppose now we want to describe the system at a large scale and call it λ . If $\mathcal{A}_\lambda = [\lambda x_1, \lambda x_2] \times [\lambda t_1, \lambda t_2]$ is a space-time fluid cell with volume $|\mathcal{A}_\lambda| \propto \lambda$, it will contain a lot of microscopic degrees of freedom as $\lambda \rightarrow \infty$. Integrating (1.62) over a fluid cell we have

$$\int_{\lambda x_1}^{\lambda x_2} dx [q_i(x, \lambda t_2) - q_i(x, \lambda t_1)] + \int_{\lambda t_1}^{\lambda t_2} dt [j_i(\lambda x_2, t) - j_i(\lambda x_1, t)] = 0 \quad i = 1, \dots, M \quad . \quad (1.64)$$

Both in quantum and in classical mechanics there are fluctuations at the microscopic level: in a quantum theory this is true even at zero temperature $T = 0$ because the state of the system $|\psi\rangle$ induces fluctuations in observables. Without loss of generality we indicate with $\langle \bullet \rangle$ the average over the state irrespectively of the theory being quantum or classical. It is important to stress that such state can contain inhomogeneities: for example in a spin chain, the state $|\uparrow\uparrow\downarrow \dots \downarrow\rangle$ is clearly not translation invariant. In classical mechanics we might have a space dependent inverse temperature $\beta(x)$ breaking homogeneity. If we now assume that the microscopic space-time variations of q_i and j_i are small, meaning that their space-time gradients happen on scales λ in the large λ limit we can average further (1.64) and we obtain a transport equation for the macroscopic densities⁷

$$\mathbf{q}_i = \langle q_i \rangle \quad \mathbf{j}_i = \langle j_i \rangle \quad . \quad (1.65)$$

The space-time dependence of these macroscopic quantities comes either from the initial state or from the integration over a fluid cell. Indeed, as we will shortly discuss, hydrodynamics is capable of making predictions about homogeneous scenarios. We have found

$$\partial_t \mathbf{q}_i + \partial_x \mathbf{j}_i = 0 \quad i = 1, \dots, M \quad (1.66)$$

⁷Whenever one argument is suppressed we mean it is evaluated at zero. For example $q(x)$ stands for $q(x, t = 0)$. If we suppress both arguments, it means $q(x, t)$ and when there is translation invariance this is equivalent to $q(0, 0)$.

Hydrodynamic approach to correlation functions

which are the sought hydrodynamic equations valid for macroscopic variables at macroscopic space-time scale set by λ . As mentioned in the introduction, λ depends on the system but the equations are completely universal. To close the equations one has to specify the functional

$$\mathbf{j}_i = \mathbf{j}_i(\vec{\mathbf{q}}) \quad (1.67)$$

which goes under the name of "equation of state". Performing a gradient expansion of the equation of state we see that higher order derivatives appear: these will be Navier-Stokes diffusive corrections, dispersive corrections and so on. For the moment we do not specify the equation of state. An important quantity is the flux jacobian defined as

$$\mathcal{A}_i^j = \frac{\partial \mathbf{j}_i}{\partial \mathbf{q}_j} \quad (1.68)$$

as it appears in the convective form of the hydrodynamic equations

$$\partial_t \mathbf{q}_i + \mathcal{A}_i^j \partial_x \mathbf{q}_j = 0 \quad (1.69)$$

where the sum over repeated up and down indices is implied. The flux jacobian is one of the hydrodynamic matrices that we are going to introduce and that will enter expressions for correlation functions at hydrodynamic scale. Generalised Hydrodynamics (GHD) makes use of the integrability structure of a given model to rewrite this coupled system of equations as single equation parametrised by a single spectral parameter that we will call rapidity and we will indicate by θ or k both $\in A \times T \subset \mathbb{R} \times \mathbb{N}$ where T is a discrete set of quasi-particle types. The flux Jacobian can be shown to be diagonalisable and to have a real spectrum [45]. As it is clear from (1.69) the eigenvalues of the \mathcal{A} are the velocities of the sound waves, the ballistically propagating modes.

1.1.6 GHD: Generalised Hydrodynamics

Euler GHD

We have all the ingredients to introduce Generalised Hydrodynamics equations. We have seen in the 1.1.4 that the thermodynamics of integrable models is completely specified once we know the scattering kernel (1.53) and the free energy encoding the statistics of the particles (1.51). In the spirit of the previous discussion and in the Local Density Approximation [75–77] one divides space-time

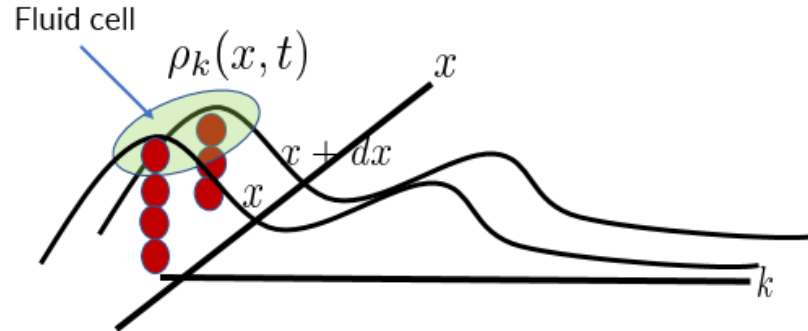


Fig. 1.4 Local density approximation of the root density in pictures. This corresponds to (1.72).

in independent fluid cells and write an equation for the macroscopic densities and currents (1.62). We have seen that in TBA solvable models an expression for the expectation values of the charge is known and given by (1.58) and (1.61) in terms of the root density or in terms of the filling. Let us simplify the writing and consider a model with a single quasi-particle type. Examples are the Lieb-Liniger model and the Sinh-Gordon model. The only bit missing is the equation of state which gives the current expectation value. This was found in the original papers [71, 73] and reads

$$\begin{aligned} \langle \mathbf{j}_i \rangle &= \int dk v^{\text{eff}}(k) h_i(k) \rho(k) \\ &= \int \frac{dk}{2\pi} E'(k) h_i^{dr}(k) \vartheta(k) \end{aligned} \quad (1.70)$$

where the function v^{eff} is a non-trivial functional of the state (i.e. depending on ρ and $E(k)$ is the bare energy of the excitation. Invoking local entropy maximisation [78] one writes at once the infinite set of continuity equations parametrised by the spectral parameters

$$\partial_t \rho + \partial_x (v^{\text{eff}}[\rho] \rho) = 0 \quad (1.71)$$

which are the celebrated GHD equations. The notation $v[\rho]$ is the functional notation, meaning that the v depends of ρ via some operator (linear or not). Basically one has promoted the state to a weakly space-time dependent one

$$\rho(k) \rightarrow \rho_{x,t}(k) \quad . \quad (1.72)$$

We will often suppress the space-time dependence when it is clear from the

Hydrodynamic approach to correlation functions

context. Such replacement corresponds to the Fig. 1.4. GHD are highly non-linear equations due to the presence of $v^{\text{eff}}[\rho]$, the *effective velocity*. This last quantity can be shown to satisfy the integral equation

$$v^{\text{eff}}(k) = E'(k) + \int dk' \varphi(k - k') \rho(k') [v^{\text{eff}}(k') - v^{\text{eff}}(k)] \quad (1.73)$$

where $E(k) = h_2(k)$ is the one-particle eigenvalue associated to the energy (bare energy). The effective velocity has a suggestive semi-classical interpretation: it can be seen as the resulting dressed velocity of a quasi-particle due to scattering with all the others. It should be said the GHD equations (1.71) appeared for the first time in a paper of solitons gases [79] and was proven rigorously for the hard rods gas in an old paper [80]. This was stressed in the paper [81] where the similarity to the Boltzmann equation [82] was underlined. The GHD equations (1.71) are transport equations analogous the equations for the density in conventional hydrodynamics (CHD)

$$\partial_t \rho + \partial_x (v \rho) = 0 \quad (1.74)$$

where ρ is the fluid density. As they are written they are in a conservation law form. To write explicitly the equation in a form that resembles a quasi-linear form one can use the filling function for which it is possible to show that

$$\partial_t \vartheta + v^{\text{eff}}[\vartheta] \partial_x \vartheta = 0 \quad . \quad (1.75)$$

This non-linear equation in quasi-linear form was solved in [83] by "the method of characteristics" which provided an efficient algorithm to its numerical solution as well [84]. Note that by virtue of the relationship between the filling and the root density (1.49), the effective velocity is can be see as a functional of ϑ also. GHD is a cornerstone in the modern undstanding of large-scale behavior of quantum many-body systems. CHD has been widely used to study such models in these regimes over the years but it was finally shown that it is not valid on arbitrary long time scales [85]: it eventually breaks down where it predicts the appearance of shocks which cannot exist in GHD due to the presence of a continuum of modes [45].

It has to be stressed that Euler GHD is a classical theory where no \hbar appears explicitly [86] and quantumness is only present in the initial conditions provided by a local densiy approximation [75–77, 87] and one wonders what happens accounting for further derivative corrections [88]. The fluctuations on top of the sound waves sustained by Euler GHD have been recently quantised [89] and a

number of succesful applications that account for correct reconstruction of the quantum fluctuations have been obtained [90–92].

An easy example: free field

As an elementary example of emerging hydrodynamics where it can be "derived" rigorously and that illustrates the ideas we consider a free field theory defined by the Hamiltonian

$$H = \frac{\hbar^2}{2m} \int dx \partial_x \psi^\dagger(x) \partial_x \psi(x) \quad (1.76)$$

where it does not actually matter whether the field is fermionic or bosonic, quantum or classical. The equations of motion are simple, they are the Schrödinger equation

$$i\partial_t \psi = -\frac{\hbar^2}{2m} \partial_x^2 \psi \quad (1.77)$$

Consider the Wigner-Weyl transform [93, 94] of the two-point correlation function (see also Section 1.2)

$$\vartheta_{x,t}(p) = \frac{1}{\hbar} \int \frac{dy}{2\pi} e^{-i\frac{p}{\hbar}y} \langle \psi^\dagger(x+y/2) \psi(x-y/2) \rangle \quad (1.78)$$

We can compute easily

$$\begin{aligned} \partial_t \vartheta_{x,t}(p) &= \frac{i\hbar}{2m} \int \frac{dy}{2\pi} e^{-i\frac{p}{\hbar}y} \left[\partial_{x-y/2} \langle \psi^\dagger(x+y/2) \psi(x-y/2) \rangle \right. \\ &\quad \left. - \partial_{x+y/2} \langle \psi^\dagger(x+y/2) \psi(x-y/2) \rangle \right] \\ &= -\frac{p}{m} \vartheta_{x,t}(p) \quad (1.79) \end{aligned}$$

This is the simplest instance of Generalised Hydrodynamics. $\vartheta_{x,t}(p)$ in this context is just the Wigner function and it follows an Euler equation: Euler hydrodynamics is exact in this case. The solution of the initial value problem is extremely simple

$$\vartheta_{x,t}(p) = \vartheta_{x-\frac{p}{m}t,0}^0 \quad (1.80)$$

where $\vartheta_x^0(p)$ is the initial condition, saying that the initial information is just transported along straight lines (the characteristics [95]) without dissipation. The Wigner function has been extensively used in the context of cold atoms and (quantum) GHD, see [89, 90, 96–99]. A complete hydrodynamic expansion valid

to all orders in the gradients for the Wigner function has been written in Ref. [100] and later corrected by the same author in Ref. [86].

1.2 Probability toolbox

1.2.1 Fluctuations

The birth of statistical mechanics and consequently all its children, condensed matter, solid state and now even high energy physics [101] is rooted in the acknowledgment that a key role in the weird and different [102] behavior of assemblies of a large amount of elementary constituents is played by *fluctuations*. This is a concept that is so often named and so central in modern science that any chapter dedicated to it will be a total reduction. What is a fluctuation after all and why does it happen? Cambridge dictionary says [103]

...a change, or the process of changing, especially continuously between one level or thing and another.

When we observe a graph of some measured quantity from real life we do not get a smooth curve, rather only a particular realisation: with this we mean that if we perform the experiment in a different moment, the conditions might have slightly changed and we would collect slightly different data. If these changes are quite big, we need to manipulate such data in some way in order to extract some meaningful and predictable information. One of the usual things is to perform an average. But what is the average saying? There is not a single notion of average.

1.2.2 Basic probabilistic concepts

If we measure a quantity X , the *empirical* average of the measured values $\{x_i\}_{i=1}^N$ assigns to this set another number in the following way

$$\langle X \rangle = \frac{1}{N} \sum_{i=1}^N x_i \rightarrow \int_A dx \rho(x) x \quad n \rightarrow \infty \quad (1.81)$$

where we are assuming that the number of measurements N is large and the empirical measure concentrates, something typical in statistical physics. A is the region over which we measure the data. The function $\rho(x)$ is the measure taking into account that the data is not uniformly distributed but there is more in some places and less in others: it is the probability density distribution. Such probability

density defines the dataset itself and viceversa⁸. In general, it is non-negative and sums to 1. A second quantity, and this is the important one, associated to a dataset is the variance

$$\sigma_X^2 = \text{Var}(X) = \langle (X - \langle X \rangle)^2 \rangle \quad (1.82)$$

which measures how much *on average* the data points deviate from the average. The square root of variance, the standard deviation, is a measure of the *fluctuations*. It tells how spread the data points are.

One also defines the *moments* as

$$m_n = \langle X^n \rangle \quad (1.83)$$

Associated to a probability distribution, or to the given random variable X (which is equivalent) there are two useful quantities, which basically contain equivalent information. These are the moment generating (characteristic) function

$$\phi_X(\lambda) = \langle e^{\lambda X} \rangle \quad (1.84)$$

and the cumulant generating function

$$\psi_X(\lambda) = \log \phi_X(\lambda) \quad . \quad (1.85)$$

The first has the property that the moments can be obtained as

$$\partial_\lambda^n \phi_X(\lambda)|_{\lambda=0} = m_n \quad . \quad (1.86)$$

Taking the derivatives of ψ generates the *cumulants* (which will be important later)

$$\partial_\lambda^n \psi_X(\lambda)|_{\lambda=0} = c_n \quad (1.87)$$

and knowing one of these functions gives access to all the information contained in the probability distribution ρ . When we have more than one random variable the situation becomes more interesting. This is because there might be some sort of dependence between them.

An easy example is when one is a function of the other, say $Y = g(X)$. In this

⁸We will follow this empirical point of view but for an interesting discussions about a change of perspective see Ref. [104]

Hydrodynamic approach to correlation functions

case, it is a textbook exercise to derive the probability distribution of Y . In other cases, there is no explicit functional dependence between the variables and all the information is encoded in a joint distribution $\rho_{X,Y}(x, y)$. To know how much one influences the other one computes the correlation as

$$\text{Cov}(XY) = \langle XY \rangle - \langle X \rangle \langle Y \rangle \quad (1.88)$$

where the average is now taken integrating with respect of the density $\rho_{X,Y}$ summing over all possible values. The covariance tells about the linear relationship between the variables. It grows positive whenever both $\Delta X = X - \langle X \rangle$ and $\Delta Y = Y - \langle Y \rangle$ are positive while it receives negative contributions whenever the variables are going in opposite directions. One interprets this thinking the variables influence each other although it must be remarked that *correlation does not imply causation*. This is important. Independence means probability of events multiply and don't affect each other, resulting in a factorisation of the joint distribution. For N variables this means

$$\rho_{\vec{X}}(x_1, \dots, x_N) = \prod_{i=1}^N \rho_{X_i}(x_i) \quad . \quad (1.89)$$

This implies the vanishing of all covariances while the opposite is easily seen not to be true. Indeed just take $Y = g(X)$ with g an odd function and $\rho_X(x)$ defined on a compact symmetric interval and even. This will give straight away $\text{Cov}(XY) = 0$ and although the variables are dependent the correlation function is unable to probe such dependence. More general correlation functions between arbitrary functions of an arbitrary number of variables can be defined.

A note on Stochastic Processes and Random Fields

What we have said before is generalised to stochastic processes. We will not give precise mathematical definitions of what a stochastic process is for reasons of space and because it is not in the spirit of this thesis much like in Ref. [105]. We will stick to an intuitive definition and this will be enough for our purposes. A stochastic process is just a random function. If coordinates are space and time such a function $\phi(x, t)$ is commonly called random field. This simply means that the value of the field at each point of space-time is random and determined by some probability distribution over the space of fields, often some Banach or Hilber space, see [106] for rigorous definitions. Equivalently, for each $\vec{x} = (x, t)$ the field is a random variable specified by the space-time dependent probability distribution $P(\phi; x, t)$

which can be empirically defined as

$$P(\phi = \tilde{\phi}; x, t) = \lim_{N \rightarrow \infty} \frac{1}{N} \sum_{i=1}^N \delta(\phi(x_i, t_i) - \tilde{\phi}) \quad (1.90)$$

where δ is the Dirac delta function and N is the number of empirical observations. One is interested in computing N -point correlation functions defined as

$$G(\vec{x}_1, \dots, \vec{x}_N) = \langle \phi(\vec{x}_1), \dots, \phi(\vec{x}_N) \rangle \quad (1.91)$$

and naturally extends the definitions of characteristic function to functionals of random fields. In statistical theories of fields like in quantum field theory and statistical mechanics this is the correct point of view.

1.2.3 Correlations in free fermionic systems

The Gibbs distribution over the phase space (1.7) is the probability distribution that describes classical particles at thermal equilibrium with temperature T and it is a distribution in a very high dimensional space depending on all the variables. The dynamical variables are fluctuating in the statistical mechanics description. In quantum mechanics probability distributions are replaced by density matrices and the notion of probability on the phase space loses meaning although Wigner functions and Weyl transforms can be employed to give an alternative formulation in terms of quasi-probabilities (they can be negative) [107, 93]. Nevertheless, nature being quantum mechanical, we cannot escape a probabilistic description of reality⁹ and probability is built in even at $T = 0$. Take a quantum many-body system of N spinless non interacting fermions described by the Hamiltonian

$$H = \sum_{i=1}^N \frac{p_i^2}{2m} + V(x_i) \quad , \quad (1.92)$$

confined on the line by the potential $V(x)$. The Pauli principle acts as a repulsive force not allowing the particles to be in the same state (for example same position) and although the particles are only confined and not interacting they exhibit strong correlations. The eigenfunctions of the Schrödinger equation $\phi_{k_j}(x_i)$ are normalisable if the potential is sufficiently confining and the many-body wave

⁹There are famous objections [108, 109]

Hydrodynamic approach to correlation functions

function is the normalised Slater determinant

$$\Phi(x_1, \dots, x_N) = \frac{1}{\sqrt{N!}} \det \left[\phi_{k_j}(x_i) \right]_{i,j=1}^N \quad (1.93)$$

which ensures anti-symmetry. One sees that already this simple system exhibits correlations due to quantum statistics. In second quantised form this simple system is described by the following Hamiltonian

$$H = \int dx \left[\frac{\hbar^2}{2m} \partial_x \psi^\dagger(x) \partial_x \psi(x) + (V(x) - \mu) \psi^\dagger(x) \psi(x) \right] \quad (1.94)$$

where $\{\psi(x), \psi^\dagger(y)\} = \delta(x - y)$ are standard fermionic field operators and where we are allowing the number of particles to fluctuate introducing a chemical potential μ fixed by the average number of particles

$$\bar{N} = \langle N \rangle = \int dx \langle \psi^\dagger(x) \psi(x) \rangle \quad (1.95)$$

with the expectation value, for concreteness an arbitrary GGE. The non-relativistic Hamiltonian (1.94) describes not only free fermions but also hard core bosons as the spectrum of the two systems is completely equivalent [110]. Due to the $U(1)$ symmetry there is a basic conservation law of the form (1.62) with charge density

$$\rho(x, t) = \psi^\dagger(x, t) \psi(x, t) \quad (1.96)$$

and associated current ¹⁰ (via Noether's theorem [47])

$$j(x, t) = \frac{\hbar}{2m} \left(\psi^\dagger(x, t) \partial_x \psi(x, t) - \partial_x \psi^\dagger(x, t) \psi(x, t) \right) \quad (1.97)$$

By definition, a gaussian state is a state (or a probability distribution) in which all correlation functions are characterised by the basic two-point function (propagator)

$$G(x, t; x', t') = \langle \psi^\dagger(x, t) \psi(x', t') \rangle \quad (1.98)$$

which is nothing but the elementary Wick contraction. Gaussian states are states for which Wick's theorem holds. Ground states and GGEs of quadratic Hamiltonians fall within this category [112]. In particular this is true even in presence of

¹⁰Note that in the quantum field theory the current operator is quadratic in the fields and one has to give a prescription of ordering. The way we have written the current is normally ordered [111, 47].

a confining potential without two-body interactions because the Hamiltonian remains quadratic. The propagator can be interpreted in two ways. In a quantum field theoretic perspective, it characterises a certain "scattering" process in that it gives the probability amplitude for a particle to be destroyed at (x', t') and later created at (x, t) . On the other hand, a probabilistic interpretation is that it tells how the field at two different space-time points correlates with itself meaning that what happens at some location will "feel" what happened at another location.

Invoking locality we can argue that the basic *connected*¹¹ two-point function has to go to zero when points are sufficiently far away from each other

$$\lim_{\|(x,t)-(x',t')\| \rightarrow \infty} \langle \psi^\dagger(x,t)\psi(x',t') \rangle^c \rightarrow 0 \quad . \quad (1.99)$$

This property, the factorisation of correlation functions is known as *clustering*. Let us do an example. Let us take a homogeneous thermal state for the free fermion Hamiltonian (1.94) with $V(x) = 0$

$$\rho = \frac{1}{Z} e^{-\beta \int dk E(k) \psi^\dagger(k) \psi(k)} \quad (1.100)$$

where $E(k) = \frac{\hbar^2 k^2}{2m} - \mu$ is the dispersion relation obtained writing the field in Fourier space¹²

$$\psi(x) = \frac{1}{\sqrt{2\pi}} \int dk e^{ikx} \psi(k) \quad . \quad (1.101)$$

The basic two point function is easy to compute¹³

$$\langle \psi^\dagger(x,t)\psi(x',t) \rangle^c = \int \frac{dk}{2\pi} \frac{e^{-ik(x-x') + iE(k)(t-t')}}{e^{\beta E(k)} + 1} \quad (1.102)$$

where we used that the equilibrium occupation function is

$$\langle \psi^\dagger(k)\psi(k') \rangle = \frac{1}{e^{\beta E(k)} + 1} \delta(k - k') \equiv \delta(k - k') \vartheta(k) \quad . \quad (1.103)$$

It is easy to see that the Fourier transform of an analytic function decays faster than any polynomial so that clustering is exponential *in space* ($t = t'$). Setting

¹¹Notice that $\langle AB \rangle^c = \text{Cov}(AB)$ in probabilistic notation.

¹²With standard abuse of notation we distinguish the Fourier transform of the field by the field by its argument only.

¹³Note here $\langle \psi \rangle = 0$.

Hydrodynamic approach to correlation functions

$x = x'$ we apply the saddle point method that gives

$$\langle \psi^\dagger(x, t) \psi(x, t) \rangle^c = \mathcal{O}(t^{-\frac{1}{2}}) \quad (1.104)$$

and clustering in time holds but it is not exponential rather algebraic. Above, \mathcal{O} is the standard "Big-O" symbol. At the Euler scale, the behavior of the two point function can be complicated depending on the specific analytic structure of the dispersion relation. If we fix

$$\xi = x/t \quad (1.105)$$

it is easy to see that in the limit $x, t \rightarrow \infty$ the asymptotic behavior is determined by the solutions to the equation

$$v(k) = \xi \quad (1.106)$$

with $v(k) = E'(k)$ being the velocity of excitations. The existence of non trivial solutions to this equation tells whether we transition from exponential to algebraic decay. In lattice models the dispersion relation is bounded meaning there is a maximal velocity [113] and so that there is a ray ξ^* that marks the transition. This is the edge of the lightcone. In the case at hand the model is continuous and there is no maximal velocity and there is always a solution to the saddle point equation and the decay is always algebraic. Consider the density operator in (1.96). Its correlation functions on the same thermal state can be obtained from Wick's theorem, for instance,

$$\langle \rho(x, t) \rho(x', t') \rangle^c = \langle \psi^\dagger(x, t) \psi(x', t') \rangle \langle \psi(x, t) \psi^\dagger(x', t') \rangle \quad . \quad (1.107)$$

Using the simple results above we see that at equal times there is exponential clustering while in any other region of space-time only algebraic clustering with a power t^{-1} . We will see later that this exponent is not specific of this system but it is a rather generic feature of correlation functions at Euler scale in integrable models for operators that couple to conserved densities.

1.2.4 Large Deviation Theory

Typical and rare events

Large deviation theory (LDT) is now a well established and fascinating piece of mathematics, see Ref. [114] for an almost exhaustive account of the literature with

emphasis on statistical mechanics applications. It is a powerful theory and we think it is fair to say that, to be descriptive, it is nothing but the generalisation of the central limit theorem.

There are many specific forms of the central limit theorem: a classical CLT [115], Lindeberg–Lévy CLT [116], Lyapunov CLT [117], Martingale CLT [118] and Ibragimov–Linnik CLT [119] but the main idea behind remains the same. If we have a collection of weakly correlated random variables such that the first two moments are finite, say they are μ and σ^2 , then their sum is distributed as a gaussian variable¹⁴

$$\lim_{N \rightarrow \infty} P \left(\frac{\sum_{i=1}^N X_i - \mu}{\sqrt{N}\sigma} < x \right) = \int_{-\infty}^x \exp \left[-\frac{x^2}{2} \right] . \quad (1.108)$$

The above statement characterises the limit distribution of a sum of random variables under relatively mild assumptions in the sense that it describes the *typical* values and the fluctuations around the mean. The most common formulation is that of Lindberg-Levy and assumes independent and identically distributed (i.i.d.) random variables with finite mean and variance [116].

Indeed, we might want to know what happens away from the mean, when a so-called *large deviation* occurs. How rare is really this rare event? To answer this question one wants to give an estimate of the probability of such large fluctuations and in turn, to do this, one has to know about the tails of the distribution. Consider for instance a set of random variables X_n and consider a function of them of the form $J_n = J(X_1, \dots, X_n)$. Informally, we say that J_n satisfies a large deviation principle (LDP) with linear velocity¹⁵ if

Definition 1.2.1 (Large deviation principle, informal).

$$P(J_n = nj) \propto \exp(-nI(j)) \quad n \rightarrow \infty \quad (1.109)$$

where the function $I(j)$ is the *rate function* or *large deviation* function and characterises the tails of the distribution and the rate of decay to zero. Note that it is independent of n . In physics jargon, this means that the observable is *extensive* in n . Most rate functions have the important properties

- $I(j) \geq 0$ for all j

¹⁴This is called convergence in distribution.

¹⁵In principle one can consider other scalings with n : any increasing function of n , say v_n is good. In the context of LDT v_n is called velocity.

Hydrodynamic approach to correlation functions

- $I(\langle X_1 \rangle) = 0$
- $I''(j) > 0$.

Knowing this asymptotic form of the distribution we have a way to estimate large deviations. An easy example is from statistics, where we have the sample mean $S_n = \frac{1}{n} \sum_{i=1}^n X_i$. We know that under mild assumptions of weak independence and finiteness of moments, this variable is gaussian but we might want to know its large deviations from the mean. To do so we must compute the rate function.

Let us take a sequence of random bits b_i taking values in a binary alphabet $\{0, 1\}$. These are of the form $\vec{b}_n = (b_1, \dots, b_n)$. If the bits are independent and happen with the same uniform probability $1/2$ the probability of a given sequence of length n is just $P(\vec{b}_n) = 2^{-n}$ and we have

$$P(S_n = s) = \langle \delta(S_n - s) \rangle = \sum_{\vec{b}: S_n=s} P(\vec{b}) = \frac{1}{2^n} \frac{n!}{(n - sn)!(sn)!} \quad (1.110)$$

that applying the Stirling approximation [120], gives

$$P(S_n = s) \propto \exp(-nI(s)) \quad (1.111)$$

with

$$I(s) = \log(2) + s \log(s) + (1 - s) \log(1 - s) \quad (1.112)$$

which we recognise to be the binary Shannon entropy [121] from classical information theory. Also, compare this expression with (1.59) for the entropy of fermionic Bethe Ansatz integrable model. We can see from the picture it has all the properties stated above. Before turning to the discussion of the practical way to compute rate functions and to a more formal statement of the large deviation principle we give an example from physics which will be relevant in the rest of the thesis. Consider a model, a field theory for example, with a $U(1)$ symmetry. Let us think of the $U(1)$ conserved field as number of particles. In the free non-relativistic theory example in (1.94) this is the density operator $\rho(x) = \psi^\dagger(x)\psi(x)$. One might want to know the distribution of the number of particles within a given interval. If that interval grows, then one might look for a LDP analysis.

Garthner-Ellis and Varadhan's theorems

In probability theory and statistical physics [114, 122], large deviation theory provides a framework for understanding the rare fluctuations in stochastic systems. The Gartner-Ellis Theorem is a cornerstone of this theory, giving conditions under which the logarithm of the moment generating function of a random process exhibits a particular variational structure, which in turn characterizes the large deviation rate function. We will only give a statistical physics argument for its plausibility and refer to specialised mathematical literature for a full proof and precise statement. Varadhan's theorem is the generalisation to functions of the random variable satisfying a large deviation principle [114, 123].

The problem is to calculate the large deviation function $I(x)$ in (1.109). The basic quantity to compute is the so-called *scaled cumulant generating function* (SCGF)

$$f(\lambda) = \lim_{n \rightarrow \infty} \frac{1}{n} \log \langle e^{\lambda n S_n} \rangle \quad (1.113)$$

where note that this can be interpreted as a non-equilibrium generalisation of the specific free energy of equilibrium statistical mechanics (see (1.57)). Consider a sequence of random variables X_i and an observable of them which has a finite limit as $n \rightarrow \infty$, call it S_n . We have¹⁶

$$\langle e^{n\lambda S_n} \rangle = \int ds P(S_n = s) e^{n\lambda s} \asymp \int ds e^{n(\lambda s - I(s))} \asymp e^{\sup_s (n(\lambda s - I(s)))} \quad (1.114)$$

where in we have used the assumption that S_n satisfies a large deviation principle (1.109) and a saddle point approximation. We thus obtain an argument for which

$$f(\lambda) = \sup_s (\lambda s - I(s)) \quad (1.115)$$

which we recognise to be the Legendre-Fenchel transform of the rate function. Whenever the function $I(s)$ is everywhere differentiable in the given domain of definition of s the Legendre-Fenchel transform is involutive [124, 125] and we have

$$I(s) = \sup_{\lambda} (\lambda s - f(\lambda)) \quad (1.116)$$

¹⁶ $f \asymp g$ means $\lim_{n \rightarrow \infty} \log f / \log g = 1$.

Hydrodynamic approach to correlation functions

Let us do the simple example of a sequence of i.i.d. random variables and their sample mean

$$S_n = \frac{1}{n} \sum_{i=1}^n X_i \quad (1.117)$$

The result for its asymptotic behavior as $n \rightarrow \infty$ is known as Cramer's theorem [126] and we obtain

$$f(\lambda) = \log \langle e^{\lambda X_1} \rangle \quad (1.118)$$

Since the characteristic function, whenever it exists, is real analytic [127], it is differentiable and the Legendre-Fenchel transform can be inverted giving access to a full range of large deviation functions. We can check that when X_i are binary random variables we recover the result (1.112). Here the probability distribution is

$$P(X_i = x) = \frac{1}{2} (\delta(x) + \delta(x - 1)) \quad (1.119)$$

and according to Cramer's theorem the SCGF

$$f(\lambda) = \log \left[\frac{1}{2} (1 + e^\lambda) \right] \quad (1.120)$$

from which, using the fact that $\partial_\lambda (\lambda s - f(\lambda)) = 0$ has solution $\lambda^* = \log \left(\frac{s}{1-s} \right)$

$$I(s) = \lambda^* s - f(\lambda^*) = \log(2) + s \log(s) + (1 - s) \log(1 - s) \quad (1.121)$$

in agreement with (1.112). The important message is : the Gartner-Ellis theorem provides a powerful tool to derive the large deviation rate function of random variables under quite general conditions. The rate function, $I(x)$, gives insight into the exponential rate at which the probability of a rare event decays as the system size increases. In essence, this theorem is central to understanding the tail behavior of probability distributions.

So as long as variables are uncorrelated, Cramers theorem gives he full answer. The most interesting situation occurs in presence of long range correlations where also the central limit theorem breaks down.

Varadhan's theorem [123] is the generalisation obtained substituting λS_n in (1.113) with a function of $g(S_n)$ so that the SCGF becomes a non-linear functional of g . In this case

$$f[g] = \lim_{n \rightarrow \infty} \frac{1}{n} \langle e^{n g(S_n)} \rangle = \sup_s (g(s) - I(s)) \quad (1.122)$$

and we have a generalisation to stochastic processes.

Breaking gaussianity

An illuminating discussion about possible ways to break the CLT is given in [128] and it is a somewhat intuitive way of explaining the ideas behind the Ibragimov-Linnik CLT [119] (also known as functional central limit theorem): either we break the not too broad distribution condition, that means that random variables might not have finite variance or mean, or we relax independence condition. The latter means having to deal with a correlated stochastic process either in time or in space to allow for such correlations between the variables. These are the ways to avoid CLT and break gaussianity. We can interpret the fact that so many distributions "flow" - in a renormalisation group language - to the gaussian distribution saying that they form a basin of attraction towards the gaussian fixed point. That is we can interpret this behavior of distributions in the large N limit as a critical phenomenon [128].

1.3 Hydrodynamical correlation functions

Correlation functions represent the fundamental quantities that one might want to compute in any physical theory. There are of course others, but it is often the case that correlations are *what we can actually probe*. Indeed, given a system described by a Hamiltonian H , a simple calculation shows that the specific heat is related to the energy fluctuations by the following formula

$$c_V = \frac{\partial \langle H \rangle}{\partial T} = \frac{\langle H^2 \rangle - \langle H \rangle^2}{T^2} = \frac{\text{var } H}{T^2} \quad (1.123)$$

where the expectation value is taken with respect to the canonical Gibbs distribution $\rho \propto \exp(-H/T)$. Measuring the fluctuations of the energy gives an estimate of the specific heat of the system and vice-versa. The same is easily proven for the fluctuations of the number of particles. Estimating such deviations will give an estimate of the chemical potential of the system i.e. the energy needed to change the number of particles by a unit. This simple observations are generalised to the point that in field theories measurable quantities are synonyms of correlation functions. For example, in the case of elementary particles, the S -matrix elements involved in a scattering process are related to the connected multi-point correlation functions of the field operators by the celebrated LSZ reduction formula [129].

Having this simple observations in mind, our point of view will be at points rather abstract, focusing at all times on the computation of fundamental correlators in a given theory.

1.3.1 Hydrodynamic projections

Sound waves

Consider the following situation: a stationary fluid background has constant macroscopic densities \mathbf{q}_i^0 and we are interested in understanding how correlations among different densities are propagated after an initial perturbation, a spike for example. It is like when one touches the flat surface of a pool and waves start to travel from the point of contact with the finger. If $\delta\mathbf{q}_i(x, t) = \mathbf{q}_i(x, t) - \mathbf{q}_i^0$ is the variation of a density at a macroscopic scale, we are interested in how the spreading of microscopic correlations look at large scales. Clearly

$$\partial_t \delta\mathbf{q}_i + \partial_x \left[\mathcal{A}_i^j(\vec{\mathbf{q}}) \delta\mathbf{q}_j \right] = 0 \quad (1.124)$$

where \mathcal{A} is the flux jacobian defined in (1.68). Assuming the background to be stationary and homogeneous, we can linearise around \mathbf{q}_i^0 and write

$$\partial_t \delta\mathbf{q}_i + \mathcal{A}_i^j(\vec{\mathbf{q}}^0) \partial_x \delta\mathbf{q}_j = 0 \quad . \quad (1.125)$$

Onsager regression hypothesis [130, 131] tells us that fluctuations relaxation will follow the same rule as the macroscopic variables. Noticing that¹⁷ $\langle \delta q_i(x, t) \delta q_i \rangle = \langle q_i(x, t) q_i \rangle^c$

$$\partial_t \langle q_i(x, t) q_j \rangle^c + \mathcal{A}_i^k(\vec{\mathbf{q}}^0) \partial_x \langle q_k(x, t) q_j \rangle^c = 0 \quad . \quad (1.126)$$

This equation is valid at *large scales* and this remark is very important. In particular, this regime is called Euler scale, or ballistic scale. This name has its roots in the analogy with a particle moving according to Newton's equations without the action of an external force whose position grows linearly with time, $x(t) = vt$, the proportionality constant being the velocity. In particular the ballistic scaling limit is one in which both space and time go to infinity with a fixed ratio

$$\lim_{x, t \rightarrow \infty} x/t = \zeta < \infty \quad . \quad (1.127)$$

¹⁷ $\langle AB \rangle^c = \langle AB \rangle - \langle A \rangle \langle B \rangle$.

1.3 Hydrodynamical correlation functions

The solution to (1.126) is easy in Fourier space, possible due to the homogeneous background \vec{q}^0 . If

$$\mathcal{S}_{ij}(k, t) = \int dx e^{ikx} \langle q_i(x, t) q_j \rangle^c \quad (1.128)$$

then in matrix form

$$\mathcal{S}(k, t) = e^{i\mathcal{A}t} \mathcal{S}(k) \quad (1.129)$$

and inverting¹⁸

$$\langle q_i(x, t) q_j \rangle^c = (\delta(x - \mathcal{A}t) \mathcal{C})_{ij} \quad (1.130)$$

where we have introduced another hydrodynamic matrix, the static correlation matrix

$$\mathcal{C}_{ij} = (q_i, q_j) \equiv \int dx \langle q_i(x, 0) q_j \rangle^c \quad (1.131)$$

where we have introduced the inner product between two observables

$$(O_1, O_2) = \int dx \langle O_1(x, 0) O_2 \rangle^c \quad (1.132)$$

The picture behind equation (1.130) is very neat and appealing: a disturbance at time $t = 0$ propagates ballistically only along certain directions where the δ function is non-zero. This happens when the flux jacobian has an eigenvalue. The spectrum of the flux jacobian is made of the linear wave propagation velocities (sound velocities) with which correlations travel over a stationary fluid background. In ordinary fluids [132], there are few conservation laws and the typical correlation spreading will look like We can see there are only three rays along which the correlations can travel and the central peak is called heat peak. In integrable models, that are our main concern, there infinitely many conserved quantities, causing correlations spread inside a light cone instead on discrete rays and we will see later that this has remarkable consequences for the decay of correlation functions.

The use of the Onsager hypothesis is not limited to correlation functions of conserved densities but it is general, see Fig. 1.5.

This is the modern perspective on Euler scale correlation functions and it is realised through a very practical technical tool going under the name of Hydrodynamic Projections [78]. This is a precise mathematical statement on the relaxation of correlation functions at Euler scale rooted in a very simple physical picture.

¹⁸The delta function of a matrix is interpreted in terms of its eigenvalues: $\delta(A)v = \delta(\lambda)v$ with $Av = \lambda v$.

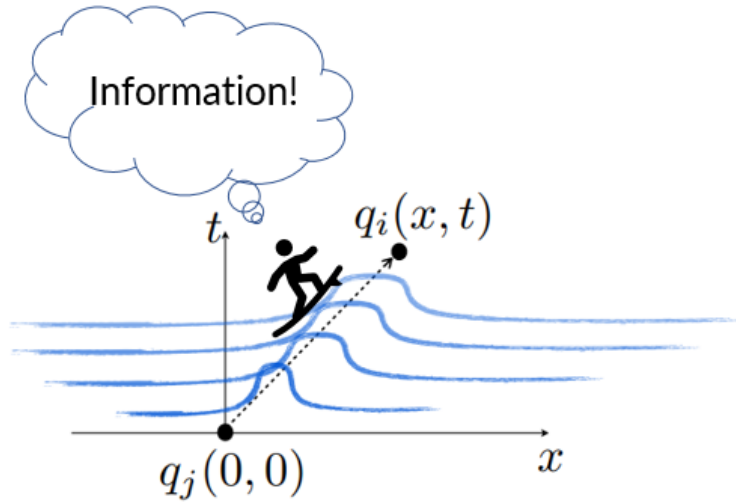


Fig. 1.5 Correlations and information of conserved densities are transported by Euler sound waves. This is a Onsager-like hypothesis.

Indeed, at large time, the relevant part of the dynamics is expected to happen in a subspace of observables spanned by the conserved quantities. This is pretty reasonable as long as any observable can be written as a combination of conserved quantities, so they are "complete". What is the precise meaning of "subspace" and "complete" here is not important and we refer to Ref. [133] for proper mathematical treatment but a good intuition is that of completeness of operators in quantum mechanics. Our focus wants to be more on the physical understanding and on explaining why equations look what they look on concrete grounds.

If, for any two observables O_1, O_2 , we define

$$\mathcal{S}_{O_1, O_2}(k, t) = \int dx e^{ikx} \langle O_1(x, t) O_2 \rangle^c \quad (1.133)$$

we can formalise the idea just explained. The hydrodynamic projection principle states that [45]

$$\lim_{k \rightarrow 0, t \rightarrow \infty} \mathcal{S}_{O_1, O_2}(k, t) = \mathcal{S}_{\mathbb{P}O_1, \mathbb{P}O_2}(k, t) \quad kt < \infty \quad (1.134)$$

where \mathbb{P} is the operator projecting an observable on the subspace of conserved charges acting in the following way

$$\mathcal{S}_{\mathbb{P}O_1, \mathbb{P}O_2}(k, t) = \sum_{ij, mn} (O_1, q_i) \mathcal{C}^{ij} \mathcal{S}_{jm}(k, t) \mathcal{C}^{mn} (q_n, O_2) \quad (1.135)$$

1.3 Hydrodynamical correlation functions

where C_{ij} and C^{ij} its inverse (Einstein convention) is the static covariance matrix defined in (1.131) playing the role of normalisation factor and S_{ij} is the Fourier transform of the two point function of conserved densities defined in (1.128). The projection is explicitly given as [134]

$$\mathbb{P}O = \sum_{ij} q_i C^{ij}(O, q_j) \quad (1.136)$$

As we can see, the evolution of the Fourier transformed two-point function between two generic observables is expanded in terms of that between conserved densities for which we know the solution in (1.130). It follows that introducing a short-hand notation for the overlap between a local observable O and a local conserved density q_i as

$$\mathcal{V}_i^O = (O, q_i) \quad (1.137)$$

we can write the hydrodynamic projection formula in a general matrix form

$$\lim_{\substack{x, t \rightarrow \infty \\ x/t = \zeta}} \langle O_1(x, t) O_2 \rangle = \mathcal{V}^{O_1} C^{-1} \delta(x - \mathcal{A}t) \mathcal{V}^{O_2} \quad (1.138)$$

We read an important lesson applicable to *integrable* models from this: whenever the observable couples to a local density, the two-point function, due to the δ function in (1.130) and the fact that the summation becomes infinite, decays ballistically as t^{-1} . This is not true if there are finitely many conservation laws. If coupling between the observable and the conserved density does not occur, the decay is faster, typically exponential. Thus, at this level, hydrodynamics seems unable to predict exponential decays of correlation functions. Let us now discuss more formally hydrodynamic projections.

Fluid cell averaging and macroscopic observables: Euler scale

We admit that in the paragraph above we have not been very precise. For example, in using the Onsager hypothesis we have replaced the microscopic position x with the macroscopic position of the fluid cell and we called it x as well! How can we compare microscopic theories and hydrodynamic predictions? This is a fundamental question, especially in an era where theoretical physics has at disposal huge computational resources that allow simulation of microscopic dynamics. In order to answer this question, we must not forget the fundamental coarse-graining procedure behind hydrodynamics equations, also called fluid-cell averaging [3, 135].

Hydrodynamic approach to correlation functions

This is a simple concept but it must be born in mind if one wants to be successful in making comparisons at Euler scale. In particular, there are many average procedures that can be defined. For example, if we call a subset of the space-time Ω we can divide it in rectangles centered at positions and times \bar{x}, \bar{t} respectively, the fluid-cells, of the type $F_{\bar{x}, \bar{t}} = [\bar{x} - \delta/2, \bar{x} + \delta/2] \times [\bar{t} - \tau/2, \bar{t} + \tau/2]$ in such a way that $\Omega = \cup_{\bar{x}, \bar{t}} F_{\bar{x}, \bar{t}}$. These cells have volume $|F_{\bar{x}, \bar{t}}| = \delta \cdot \tau$. With this we can define the fluid-cell average of a single point observable as

$$\bar{A}(\bar{x}, \bar{t}) = \overline{A(x, t)} = \frac{1}{|F_{\bar{x}, \bar{t}}|} \int_{F_{\bar{x}, \bar{t}}} dx dt A(x, t) \quad (1.139)$$

If ℓ is a typical scale, say of lengths, and we want to probe the physics at that scale we can average out microscopic degrees of freedom at scales smaller than ℓ . To do this we can choose the fluid cell size monotonically increasing with ℓ , that is

$$\delta = \delta(\ell) \quad , \quad \tau = \tau(\ell) \quad (1.140)$$

with

$$\delta(\ell_1) \leq \delta(\ell_2) \quad , \quad \tau(\ell_1) \leq \tau(\ell_2) \quad , \quad \ell_1 \leq \ell_2 \quad (1.141)$$

but at the same time

$$\frac{\delta(\ell)}{\ell} \rightarrow 0 \quad , \quad \frac{\tau(\ell)}{\ell} \rightarrow 0 \quad , \quad \ell \rightarrow \infty \quad . \quad (1.142)$$

Different space-time regions are correlated in different ways meaning correlations have a different behavior. Thus, we must specify how x and t scale with respect to one another in order to describe specific space-time regions. One choses $x = f_x(\ell)\bar{x}$ and $t = f_t(\ell)\bar{t}$. In this way, the result of a fluid cell averaging is parametrically dependent on the observation scale ℓ . In hydrodynamics we have two common scales. The following

$$x \sim t \sim \ell \quad (1.143)$$

is called Euler scaling while

$$x \sim \sqrt{t} \sim \ell \quad (1.144)$$

is called diffusive or Navier-Stokes scaling. The fluid average described in (1.139) is the most generic one but depending on the system at hand it might be possible to simplify the average prescription [134]. For example, the Euler scale averaged

observable O would be

$$\begin{aligned}\bar{A}^{\text{Eul}}(\bar{x}, \bar{t}) &= \lim_{\ell \rightarrow \infty} \frac{1}{|F_{\ell\bar{x}, \ell\bar{t}}|} \int_{F_{\ell\bar{x}, \ell\bar{t}}} dx dt A(x, t) \\ &= \lim_{\ell \rightarrow \infty} \frac{1}{\delta(\ell)\tau(\ell)} \int_{-\delta(\ell)/2}^{\delta(\ell)/2} dx' \int_{-\tau(\ell)/2}^{\tau(\ell)/2} dt' A(\ell\bar{x} + x', \ell\bar{t} + t') \quad . \quad (1.145)\end{aligned}$$

We see immediately that this definition makes sense only if we specify what an observable is. It is very important at this point to make a distinction between deterministic systems and non-deterministic ones. In real systems there is always some sort of fluctuation present: in classical systems there is uncertainty in the initial conditions, resulting in the description of the stationary state in terms of some probability measure. This probability measure can be largely independent on the initial conditions (generic systems) like thermal Gibbs states or memory conserving of all conserved quantities (integrable systems) like (1); in quantum systems at zero temperature $T = 0$ fluctuations are encoded in the initial state of the system and in quantum statistical mechanics the state generically contains both quantum and classical fluctuations. Let us take as an example a non-relativistic free field theory with a complex scalar field $\psi(x, t)$ where the density of particles is an operator

$$\hat{\rho}(x, t) = \hat{\psi}^\dagger(x, t)\hat{\psi}(x, t) \quad . \quad (1.146)$$

This would be called a *microscopic* observable but in the presence of fluctuations one must be careful. It has to be remembered that in all experimentally relevant situations, we never measure exactly a microscopic observable, but rather its mean, or if we want, just a single eigenvalue. This is a question of nomenclature of course and overall what matters is the value that we read out from a meter or any other experimental tool. What we want to emphasize is that a definition like (1.139) must be applied after average over fluctuations has been already performed and that the two kinds of averages do not commute in general. In a more general scenario, more appropriately, a *macroscopic* observable is a multi-point correlation function *averaged over a fluid cell*. For example, what we measure is the average microscopic density

$$\rho(x, t) = \langle \hat{\psi}^\dagger(x, t)\hat{\psi}(x, t) \rangle \quad (1.147)$$

and the macroscopic fluid density at Euler scale will be

$$\bar{\rho}^{\text{Eul}}(\bar{x}, \bar{t}) = \lim_{\ell \rightarrow \infty} \frac{1}{\delta(\ell)\tau(\ell)} \int_{-\delta(\ell)/2}^{\delta(\ell)/2} dx' \int_{-\tau(\ell)/2}^{\tau(\ell)/2} dt' \rho(\ell\bar{x} + x', \ell\bar{t} + t') \quad (1.148)$$

Hydrodynamic approach to correlation functions

where the x dependence of the integrand can come also from inhomogeneities in the state. A two-point function, averaged over fluid cells, will be

$$\overline{\langle O_1(x_1, t_1) O_2(x_2, t_2) \rangle} = \int_{F_{\bar{x}_1, \bar{t}_1}} \frac{dx_1 dt_1}{|F_{\bar{x}_1, \bar{t}_1}|} \int_{F_{\bar{x}_2, \bar{t}_2}} \frac{dx_2 dt_2}{|F_{\bar{x}_2, \bar{t}_2}|} \langle O_1(x_1, t_1) O_2(x_2, t_2) \rangle \quad (1.149)$$

and it is clear how to generalise this to multi-point correlation functions. At Euler scale, in inhomogeneous states, no modifications are needed with respect to (1.148)

$$\langle O_1(\bar{x}, \bar{t}) O_2 \rangle_{\text{Hom}}^{\text{Eul}} \equiv \lim_{\ell \rightarrow \infty} \frac{1}{\delta(\ell) \tau(\ell)} \int_{-\delta(\ell)/2}^{\delta(\ell)/2} dx' \int_{-\tau(\ell)/2}^{\tau(\ell)/2} dt' \langle O_1(\ell \bar{x} + x', \ell \bar{t} + t') O_2 \rangle \quad (1.150)$$

and this will serve to our purposes when we will compute two-point function of the magnetisation in spin chains. It is not difficult to take into account inhomogeneities in the initial state as done in [136] and numerically in [137] but we will not delve into this scenarios in the present manuscript. With Euler scale two-point functions defined the correct statement of hydrodynamic projections is

$$\langle O_1(x, t) O_2 \rangle_{\text{Hom}}^{\text{Eul}} = \mathcal{V}^{O_1} \mathcal{C}^{-1} \delta(x - \mathcal{A}t) \mathcal{V}^{O_2} \quad , \quad \frac{x}{t} = \zeta < \infty \quad (1.151)$$

meaning that the prediction is for fluid-cell averaged two point correlation functions. Generalisation to multi-point functions can be found in [138]. Expression (1.151) is a hydrodynamic projection formula, where \mathcal{V}^{O_1} and \mathcal{V}^{O_2} represent the projection of O_1 and O_2 onto conserved quantities, and $\mathcal{C}^{-1} \delta(\bar{x} - \mathcal{A}\bar{t})$ represents the propagation of hydrodynamic modes. The limit in (2.25) is a generalised function of the scaled space-time coordinates \bar{x} , \bar{t} , concentrated on the space-time rays of velocities equal to the eigenvalues v_i^{eff} of \mathcal{A} . These eigenvalues are therefore interpreted as the velocities of propagation of linear disturbances on top of the fluid, which give rise to the leading (Euler-scale) correlations.

1.3.2 Ballistic fluctuation theory

General setup

We now explain the basics of the ballistic fluctuation theory [139]. This framework generalizes the ideas originally introduced in the context of large deviations in conformal field theory [140]. Whenever an observable does not couple to at least one of the conserved charges, the hydrodynamic projection principle (1.151) is not predictive as it gives simply zero, meaning that the correlation function decays

1.3 Hydrodynamical correlation functions

faster the t^{-1} , usually exponentially. Examples are correlation functions of vertex operators in the Sine-Gordon field theory and of the order parameter in spin chains, as we will see in detail later.

Consider the general hydrodynamic setup of section 1.1.5. Let us focus on a particular charge $Q_{i^*} \equiv Q$ with its associated density and current $q_{i^*} \equiv q$ and $j_{i^*} \equiv j$ respectively and for simplicity let us assume that the charge corresponds to a *continuous* symmetry. Let us agree that space-time points are labeled as $\vec{l} = (x, t) \in \mathbb{R}^2$, in this order. In a relativistic notation, we can define a 2-component current in the following way

$$\vec{j} = (j, q) \tag{1.152}$$

so that the conservation law can be written as

$$\partial_\mu j^\mu = \partial_t q + \partial_x j = 0 \tag{1.153}$$

where it is understood that $\partial_0 = \partial_x$ and $\partial_1 = \partial_t$. A generalised current in space-time can then be defined as

$$d\omega(x, t) = \vec{j}(x, t) \times d\vec{l} = j(x, t)dt - q(x, t)dx \quad . \tag{1.154}$$

The remarkable fact about such current is that it is an exact differential [141] thanks to the conservation law (1.153) (just take the mixed derivatives). This implies that its line integral in space-time only depends on the end points, see Fig. 1.6. In this way, given a space-time path $\gamma(s) = (x(s), t(s))$ with $\gamma(s^*) = (x, t)$ for some s^* (which is not important) we can define a function of the end point¹⁹

$$\Omega(x, t) = \int_\gamma d\omega = \int^{(x,t)} j(x, t)dt - q(x, t)dx \tag{1.155}$$

since the lower integration extremum only contributes a constant. This is a potential coming from a conservative force ω directed along the axis exiting the paper according to the standard right hand rule. The BFT is concerned with the evaluation of the average

$$g_\lambda(\ell; \bar{x}, \bar{t}) = \langle \exp(\lambda \Omega(\ell \bar{x}, \ell \bar{t})) \rangle \tag{1.156}$$

¹⁹Here we are using a continuous space notation. In later sections the space will be also discrete and it will be enough to replace integrals with discrete sums.

Hydrodynamic approach to correlation functions

for $\lambda \in \mathbb{C}$. In particular we can define

$$\mathcal{T}_\lambda(x, t) = \exp(\lambda \Omega(x, t)) \quad (1.157)$$

which is an example of what is known as *twist fields*²⁰. The state is taken to be some maximal entropy state of the Gibbs form (1), with Lagrange parameters β^i . Then, $g_\lambda(\ell; \bar{x}, \bar{t})$ is recognised to be the characteristic function for the random process $\Omega(x, t)$ according to (1.84).

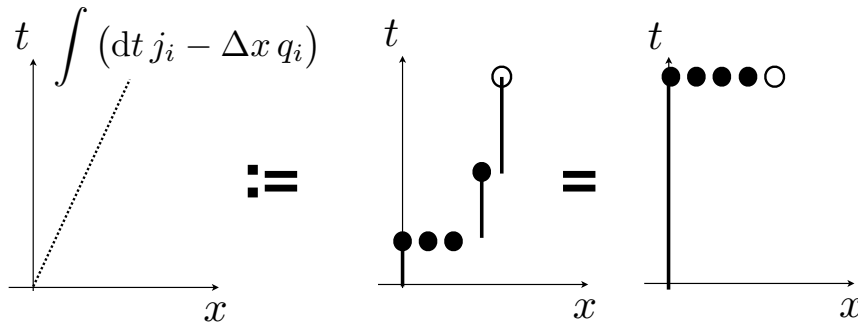


Fig. 1.6 Picture taken from [3]. The integral of the two-current on a discrete space. It is defined by integrating over times and summing over positions (discrete space here). The result is independent of the path chosen. In the middle, the case shown is an integral from $(0, 0)$ to $(4, t)$ with $t_0 = 0, t_1 = t_2 = t_3 > 0, t = t_5 > t_4 > t_3$, see (1.155).

We are interested in the asymptotic regime (2.22), and in particular in the exponential behaviour (renaming $\bar{x}, \bar{t} \rightarrow x, t$)

$$g_\lambda(\ell; x, t) \asymp e^{\ell f_{\lambda, x, t}[\boldsymbol{\beta}]} \quad (\ell \rightarrow \infty). \quad (1.158)$$

The function in the exponent may be complex, and thus this includes oscillatory terms. On the right-hand side, we explicitly write the dependence on the state specified by the Lagrange parameters $\boldsymbol{\beta}$. The precise limit to be evaluated is

$$f_{\lambda; x, t}[\boldsymbol{\beta}] = \lim_{\ell \rightarrow \infty} \ell^{-1} \log g(\lambda, \ell; x, t). \quad (1.159)$$

which is the SCGF in accordance with (1.113).

A typical physical scenario where BFT is most naturally formulated is the so-

²⁰See Section 4.2

called *partitioning protocol*²¹. Basically one divides the system into two halves with different constant value of one (or more) of the conserved densities. Then one quenches the system connecting the two pieces and observing the evolution. In integrable models for example, at large times, a sustained current appears breaking time reversal symmetry and making the state out-of-equilibrium. Such current fluctuates (the theory being classical or quantum does not matter) and the goal is to characterise such fluctuations. The total charge passed through the junction in time t

$$\Delta Q(t) = \int_0^t j(0, t) dt \quad (1.160)$$

is extensive in t and falls within observables amenable of large deviation analysis as explained in 1.2.4 (compare with (1.117)).

Prediction and flow equation

The BFT predicts that

$$f_{\lambda; x, t}[\boldsymbol{\beta}] = \int_0^\lambda d\lambda' (t \mathbf{j}_i(\lambda'; \xi) - x \mathbf{q}_i(\lambda'; \xi)) \quad (1.161)$$

where $\mathbf{j}(\lambda; \xi)$ and $\mathbf{q}(\lambda; \xi)$ are (G)GE averages of the current and density evaluated in a λ -dependent state described by $\beta^j(\lambda; \xi)$, which depends on the ray $\xi = x/t$ and obey the BFT flow equation

$$\partial_\lambda \beta^j(\lambda; \xi) = \text{sgn}(x \mathbf{1} - t \mathcal{A}(\lambda; \xi))_{i_*}^j, \quad \beta^j(0; \xi) = \beta^j, \quad \xi = x/t \quad (1.162)$$

where i_* is the index associated of the chosen conserved charge (cf. the beginning of this subsection). The sign of the matrix is understood by diagonalisation as usual, and makes sense as \mathcal{A} , the flux jacobian (1.68), has real spectrum. The last two equations represent the central objects and the constitutive equations of BFT. The flow equation is derived under certain assumptions; it is expected to hold if the spectrum of \mathcal{A} does not contain x/t , and also for (a large class of) integrable models, which possess a continuous spectrum.

The function $f_{\lambda; x, t}[\boldsymbol{\beta}]$ has an interpretation in terms of large-deviation theory. In the classical context, for instance at $x = 0$ (where it is sufficient to consider $t = 1$), it encodes the large deviations of the total current $J^{(\ell)} = \int_0^\ell ds j(0, s)$ in the time interval $[0, \ell]$: it is the “full counting statistics”, or scaled cumulant generat-

²¹also known in hydrodynamics as *Riemann problem*.

Hydrodynamic approach to correlation functions

ing function, for the total amount of charge Q that has crossed the point $x = 0$, between times 0 and ℓ and it is a random process. By large-deviation principle (1.109), the probability that $J^{(\ell)}$ takes the large value ℓj is generically exponentially decaying with ℓ as

$$P(J^{(\ell)} = \ell j) \asymp e^{-\ell I(j)} \quad (1.163)$$

for some large-deviation function $I(j)$ (with $I(\mathbf{j}) = 0$ and $I(j) > 0$ if $j \neq \mathbf{j}$, where $\mathbf{j} = \langle j \rangle$). The function $f_{\lambda;0,1}[\boldsymbol{\beta}]$, as a function of λ , is the Legendre-Fenchel transform of $I(j)$. The BFT gives a nontrivial prediction for this Legendre-Fenchel transform.

Likewise, at $x = 1$ and $t = 0$, a similar analysis applies where $\Delta Q_{i_*}(t)$ is replaced by the random variable $\Omega(\ell, 0) = Q_{i_*}|_0^\ell = \int_{s=0}^\ell dx q_{i_*}(x, 0)$, the total charge on the spatial interval $[0, \ell]$. In this case, the BFT formulae above imply that $f_{\lambda;1,0}[\boldsymbol{\beta}]$ is the difference of specific free energies $f[\boldsymbol{\beta}]$ defined in (1.57) at different states as follows:

$$f_{\lambda;1,0}[\boldsymbol{\beta}] = \lim_{\ell \rightarrow \infty} \ell^{-1} \log \langle \exp -\lambda \int_0^\ell ds q_{i_*}(s, 0) \rangle = f[\boldsymbol{\beta} + \lambda \delta_{i_*}] - f[\boldsymbol{\beta}] \quad (1.164)$$

where $(\delta_j)^i = \delta_j^i$. As a consequence, the corresponding large-deviation function $I(q)$ is simply related to the thermodynamic entropy density as a function of the charge q .

The BFT thus gives predictions for the full counting statistics of total transported charges at large times, and total charges on large intervals, purely in terms of hydrodynamic and thermodynamic quantities, in any maximal entropy state²² as we will see later.

General expression in integrable models

In integrable models, using GHD, the above has been translated into an expression in terms of the thermodynamic Bethe ansatz when considering current fluctuations only in Ref. [1]. To write a generalisation valid along arbitrary rays it is more convenient to parametrise

$$(x, t) = \ell(\sin \alpha, \cos \alpha) \quad , \quad (1.165)$$

²²The BFT is based on an assumed fast enough decay of correlation functions at large distances, and thus it applies in finite-entropy states; ground states may need further analysis.

with

$$\ell = \sqrt{t^2 + x^2} \quad , \quad x/t = \zeta = \tan \alpha \quad . \quad (1.166)$$

In this way the expression for the scaled cumulant generating function is

$$\begin{aligned} f_{\lambda, \alpha} = & \sum_j \int \frac{d\theta}{2\pi} \left\{ -(\partial_\theta p_j(\theta) \sin \alpha - \partial_\theta E_j(\theta) \cos \alpha) \operatorname{sign}(\sin \alpha - \cos \alpha v_j^{\text{eff}}(\theta, \lambda)) \right. \\ & \times (F(\vartheta_j(\theta, \lambda)) - F(\vartheta_j(\theta, 0))) \\ & \left. + 2 \sum_{\kappa \in \{\pm\}} \sum_{v_j^{\text{eff}}(\theta, \bar{\lambda}) = \tan \alpha} \kappa (F(\vartheta_j(\theta, \bar{\lambda})) - F(\vartheta_j(\theta, 0))) \right\} \end{aligned} \quad (1.167)$$

where κ is the sign of $\partial_\lambda v_j^{\text{eff}}(\theta, \lambda)|_{\lambda=\bar{\lambda}}$ and where the inner sum of the last term is over $\bar{\lambda}$ belonging to the set

$$\left\{ \lambda \in \mathbb{R} : v_j^{\text{eff}}(\theta, \lambda) = \tan \alpha \right\} \quad (1.168)$$

Although the derivation of this formula is very simple and follows the same argument of Ref. [2] used to derive the current fluctuations it was never written before and it is new. The latter case is recovered for $\alpha = 0$. Note the factor of 2 which corrects a typo in the same Ref. [2] (eq. (25) in that paper).

The function F is the free energy function (1.51) and ϑ_j the filling functions (1.54). Recall that in fermionic models they have explicit expression

$$\vartheta_j(\theta) = \frac{1}{1 + e^{\varepsilon_j(\theta)}} \quad (1.169)$$

in terms of the pseudo-energies satisfying the TBA equations (1.50). The flow equations for the pseudo-energies are simple to derive and are

$$\partial_\lambda \varepsilon_j(\theta; \alpha) = \operatorname{sign}(\sin \alpha - v_j^{\text{eff}}(\theta; \alpha) \cos \alpha) h_j^{\text{dr}}(\theta; \alpha) \quad (1.170)$$

or equivalently in terms of the filling

$$\partial_\lambda \vartheta_j(\theta; \alpha) = \operatorname{sign}(\cos \alpha v_j^{\text{eff}}(\theta; \alpha) - \sin \alpha) h_j^{\text{dr}}(\theta; \alpha) \vartheta_j(\theta; \alpha) g_j(\theta; \alpha) \quad . \quad (1.171)$$

where here g_j is a statistical factor. It is related to the filling function as

$$g = -\partial_\varepsilon \log \vartheta(\varepsilon) \quad . \quad (1.172)$$

Free theories

In a free theory, where the Bethe Ansatz structure is trivial, this simplifies because $\varepsilon = w$ i.e. the pseudo-energy equals the driving term in the TBA equations. With the GHD description as given in section 2.2.1, and further using the free-energy function $F(k) = -\log(1 + e^{-w(k)})$, the results of the BFT specialise as follows. The GGE along the flow is described by the function

$$w(\lambda; \xi; k) = w(k) + \lambda \operatorname{sgn}(x - v(k)t) h_{i_*}(k) \quad (1.173)$$

where $v(k) = E'(k)$ is the group velocity with $E(k)$ the dispersion relation (see (2.32) for the XX spin chain), and the scaled cumulant generating function is

$$f_{\lambda; x, t}[w] = \int_{-\pi}^{\pi} \frac{dk}{2\pi} |x - t v(k)| \log \left(\frac{1 + e^{-w(\lambda; \xi; k)}}{1 + e^{-w(k)}} \right) \quad (1.174)$$

where we use w instead of the Lagrange parameters β to specify the state²³. In a generic interacting theory, it is not possible to solve the flow equation (1.162) and one must either solve it numerically or resort to some approximation. We will pursue both approaches in the next chapters.

Long range correlations

It is very important for the subsequent discussions to say a little bit more about the large deviation principle validity and in particular to discuss its possible breakings. We have already mentioned that the large deviation principle represents an extension of the central limit theorem. It gives access to the large deviations compared to the mean. Small fluctuations are gaussian in this context. When this does not hold, the large deviation principle breaks down. In this case the fluctuation spectrum changes. For example, when the SCGF diverges the fluctuations are power law and long ranged. This happens when

$$\log \langle e^{\lambda \Omega(x, t)} \rangle \neq \mathcal{O}(t) \quad t \rightarrow \infty \quad . \quad (1.175)$$

²³In a free theory a GGE has the form $\rho \propto \exp - \sum_k W_k n_k$ where n_k are the occupation numbers and W_k is function (and $w(k)$ is its continuous interpolation) since we use continuum notation here), see also sections below.

Consider for the moment the current fluctuations. Expanding in powers the exponential implies that

$$\int_0^t dt_1 \cdots \int_0^t dt_n \langle j(t_1) \dots j(t_n) \rangle^c \neq \mathcal{O}(t) \quad (1.176)$$

that is time-integrated multi-point generating functions do not have the correct scaling. Of course, in the case all cumulants scale with the same power t^α , this can be remedied dividing by t^α with an appropriate exponent, but generically it will happen that they all scale with a different power. In this case there is no large deviation principle as cumulants do not scale correctly and the series defining the SCGF cannot be resummed.

1.4 Outlook

In this first introductory part we have mainly reviewed known things with the hope to set up a good notation for actually implementations and to give the reader a general idea of the concepts and the tools used to approach complex questions such as those related to the out-of-equilibrium dynamics of many-body systems, especially quantum ones. It should have emerged a certain degree of "classicality" : Euler equations are classical equations are the result of coherent, ballistic, dissipationless motion of the elementary excitations of the system. Now we are in a position to start the actual journey into the application of these hydrodynamic concepts to correlation functions in many-body systems, the building blocks being the hydrodynamic projections and ballistic fluctuation theory.

Chapter 2

Space-time correlation functions

2.1 Getting started: XX spin chain

Goal of the chapter

In this chapter we present results of the application of ballistic fluctuation theory (BFT) to dynamical spin-spin correlation functions in the XX spin chain. We show that hydrodynamic projections reproduce known asymptotic coming from exact Wick's theorem in the case of the magnetisation correlation function. The longitudinal correlator has a long history and the first asymptotic expressions were given in [142] in the gapped regime. The full asymptotic behavior was settled in [3] providing expressions valid for any value of the magnetic field and all regions of space-time. We start simple with the XX spin-chain, introducing its main features and the correlators of interest. Only at the end we move to the more complicated Ising model in transverse field. We benchmark our analytical predictions against exact numerical calculations.

Generalities of the problem

Understanding the dynamic behaviors of many-body systems on large spatial and temporal scales presents a significant challenge in the field of many-body physics. According to the fundamental principles of hydrodynamics, in stationary and homogeneous states, such as thermal or generalized Gibbs ensembles (GGE), the propagation of "linear waves" provides straightforward predictions for the algebraic decay of dynamic two-point connected correlation functions [143–145]. Linear waves correspond to small perturbations of the GGE in space-time, de-

scribed effectively by linear response theory. They propagate following the laws of Euler hydrodynamics and mathematically reside in the tangent space of the state manifold, which represents the space of extensive conserved quantities associated with that state. Consequently, dynamic correlation functions are expected to exhibit exponential decay in space-time, except at certain hydrodynamic velocities known as elements of the flux Jacobian spectrum, where algebraic decay is observed. This phenomenon arises from the projection of observables onto the conserved quantities carried by the linear waves, a principle known as the Boltzmann-Gibbs principle [78, 146].

We have already seen that hydrodynamic algebraic decay occurs whenever observables "couple" to at least one linear wave, meaning that their expectation values vary along the state manifold, resulting in nonzero susceptibilities. However, certain observables do not exhibit variation along any direction on the manifold and therefore do not couple to linear waves. These observables may display exponential decay throughout space-time, and the Boltzmann-Gibbs principle is not applicable in these cases. This situation often occurs for order parameters or twist fields (both highest-weight and descendants under the local observable algebra) in thermal states and other GGEs, as order is typically destroyed at nonzero entropy. We refer to these fields collectively as order parameters, and they possess zero expectation values (at least in the vicinity of the GGE) and hence zero susceptibility.

2.1.1 Model and correlation functions

XX spin chain

Here we employ the XX quantum spin chain as an example, described by the Hamiltonian :

$$H = - \sum_{x \in \Lambda} \left[\sigma_x^1 \sigma_{x+1}^1 + \sigma_x^2 \sigma_{x+1}^2 - h \sigma_x^3 \right] \quad (2.1)$$

where $\sigma_x^{1,2,3}$ represent the Pauli matrices at site $x \in \mathbb{Z}$. We present results for infinite volumes, with $\Lambda = \mathbb{Z}$. Hydrodynamic linear response theory is applied to correlation functions involving σ_x^3 (referred to as "longitudinal"), while the new theory is applied to correlation functions of order parameters, which can be chosen as σ_x^1 or σ_x^2 (referred to as "transverse"). This model offers a balance between simplicity, as it possesses a free-fermionic description, and complexity,

as it highlights crucial aspects of the problem. Both the hydrodynamic principles and the proposed theory can be extended to truly interacting models, regardless of whether they are integrable.

The XX spin chain (2.1) is one of the simplest examples of exactly solvable one-dimensional models, a special case of the more general XY spin model introduced and solved in [147]. We consider the system on a finite periodic lattice $\Lambda = \{0, 1, \dots, N-1\}$. The Hamiltonian is diagonalisable by means of the Jordan-Wigner transformation and Fourier transform. The relevant spin matrices are written as

$$\sigma_x^+ = \frac{1}{2}(\sigma_x^1 + i\sigma_x^2) = \exp\left(i\pi \sum_{y=0}^{x-1} a_y^\dagger a_y\right) a_x^\dagger \quad (2.2)$$

$$\sigma_x^- = (\sigma_x^+)^{\dagger} \quad (2.3)$$

$$\sigma_x^3 = 2a_x^\dagger a_x - 1 \quad (2.4)$$

in terms of canonical complex fermions a_x , with $\{a_x^\dagger, a_y\} = \delta_{x,y}$, $\{a_x, a_y\} = 0$. This transformation preserves the $su(2)$ algebra in the sense of commutation relations and structure of its spin-1/2 representation. The Hamiltonian is made quadratic, taking a different form on the sectors with even and odd fermion numbers,

$$H = P_+ H_+ + P_- H_-, \quad P_{\pm} = \frac{1}{2} \left(1 \pm (-1)^{\Omega}\right) \quad (2.5)$$

where the projectors are expressed in terms of the fermion number $\Omega = \sum_{x=0}^{N-1} a_x^\dagger a_x$. The even and odd Hamiltonians are

$$H_{\pm} = -2 \sum_{x=0}^{N-1} \left[a_x^\dagger a_{x+1} + a_{x+1}^\dagger a_x + h a_x^\dagger a_x \right] + hN \quad (2.6)$$

where, implicitly, the boundary condition is anti-periodic (even sector, +) or periodic (odd sector, -), $a_{x+N} = (-1)^{\Omega+1} a_x$. The difference between H_+ and H_- is a boundary term

$$H_- - H_+ = -4(a_{N-1}^\dagger a_0 + a_0^\dagger a_{N-1}) \quad (2.7)$$

which on average decays exponentially and thermodynamic quantities are not affected by the choice of the boundary condition. A Fourier transform diagonalises

Space-time correlation functions

the Hamiltonian,

$$a_x = \frac{1}{\sqrt{N}} \sum_{k \in \Gamma_{\pm}} e^{ikx} \eta_k, \quad \{\eta_k^{\dagger}, \eta_l\} = \delta_{k,l}, \quad \{\eta_k, \eta_l\} = 0 \quad (2.8)$$

where the momentum sets are such that the (anti-)periodicity condition is satisfied, $\Gamma_+ = \{j\Delta k : j = \lfloor -N/2 \rfloor, \dots, \lfloor N/2 \rfloor - 1\}$ and $\Gamma_- = \{j\Delta k : j = \lfloor -N/2 \rfloor + 1/2, \dots, \lfloor N/2 \rfloor - 1/2\}$ for $\Delta k = \frac{2\pi}{N}$ (with $|\Gamma_{\pm}| = N$). This gives the dispersion relation $E(k)$:

$$H_{\pm} = \sum_{k \in \Gamma_{\pm}} E(k) \eta_k^{\dagger} \eta_k, \quad E(k) = 2(h - 2 \cos(k)). \quad (2.9)$$

In each sector, the Fourier modes evolve simply as

$$\eta_k(t) \equiv e^{iH_{\pm}t} \eta_k e^{-iH_{\pm}t} = e^{-iE_k t} \eta_k \quad (2.10a)$$

$$\eta_k^{\dagger}(t) \equiv e^{iH_{\pm}t} \eta_k^{\dagger} e^{-iH_{\pm}t} = e^{iE_k t} \eta_k^{\dagger} \quad (k \in \Gamma_{\pm}) \quad (2.10b)$$

The states of interest are the generalised Gibbs ensembles (1) for which in free theories, with the density matrix fully fixed by a function $W : \Gamma_{\pm} \ni k \rightarrow W_k \in \mathbb{R}$,

$$\rho = \frac{1}{Z} \left(P_+ e^{-\sum_{k \in \Gamma_+} W_k \eta_k^{\dagger} \eta_k} + P_- e^{-\sum_{k \in \Gamma_-} W_k \eta_k^{\dagger} \eta_k} \right) \quad (2.11)$$

where Z is such that $\text{Tr} \rho = 1$. The case

$$W_k = \beta E(k) \quad (2.12)$$

is the thermal state at temperature β^{-1} .

We are interested in the infinite-length limit $N \rightarrow \infty$, where we have, in both sectors,

$$a_x = \int_{-\pi}^{\pi} \frac{dk}{\sqrt{2\pi}} e^{ikx} \eta(k) \quad (2.13)$$

with usual anti-commutation relations

$$\{\eta^{\dagger}(k), \eta(l)\} = \delta(k-l), \quad \{\eta(k), \eta(l)\} = 0, \quad x \in \mathbb{Z} \quad (2.14)$$

Assuming that there is a function $w(k)$ that is continuous or continuous by part, and such that $w(k) = W_k \forall k \in \Gamma_{\pm}, \forall N$, this simplifies the density matrix to

$$\rho = \frac{1}{Z} \exp \left[- \int_{-\pi}^{\pi} dk w_k \eta^{\dagger}(k) \eta(k) \right]. \quad (2.15)$$

Correlation functions

Correlation functions in many-body quantum and classical systems can be analysed at the Euler scale using the hydrodynamic description of the system. The Euler scale is that in which space and time are taken to be large, simultaneously. The hydrodynamic theory gives predictions for correlation functions of local (or quasi-local) observables at the Euler scale in stationary, homogeneous, clustering states like those described in (2.15) for free theories. The latter are states which are invariant under time and space translations, and in which averages of observables factorise in the limit where they are placed at large spatial separation. Here we assume that clustering is fast enough, but we will not give a detailed description of the requirements on the state, see for instance [148] for a rigorous treatment of Euler-scale correlation functions, [136] for extension to inhomogeneous settings and [143] for a review of the theory of correlation functions in GHD, of which the discussion below is a special case.

The prediction from hydrodynamics is based on the available conservation laws admitted by the system. Consider a quantum chain on \mathbb{Z} admitting N conservation laws

$$\partial_t q_i(x, t) + j_i(x + 1, t) - j_i(x, t) = 0, \quad (2.16)$$

where q_i and j_i are the conserved densities and currents, respectively. We assume for simplicity that the state is invariant under the action of all total charges $Q_i = \sum_{x \in \mathbb{Z}} q_i(x)$, that is $\langle [Q_i, \dots] \rangle = 0$, although this is not a necessary condition for the hydrodynamic theory to apply. Consider the following covariance matrices:

$$\mathcal{C}_{ij} = \sum_{x \in \mathbb{Z}} \langle q_i(x) q_j(0) \rangle^c, \quad \mathcal{B}_{ij} = \sum_{x \in \mathbb{Z}} \langle j_i(x) q_j(0) \rangle^c. \quad (2.17)$$

Both matrices are symmetric; this is evident for \mathcal{C} , less so for \mathcal{B} but a proof can be found in [133, 45] for instance. Consider also the flux Jacobian

$$\mathcal{A}_i^j = \sum_k \mathcal{B}_{ik} \mathcal{C}^{kj} \quad (2.18)$$

Space-time correlation functions

where we denote the inverse matrix with upper indices, $\sum_k C^{ik} C_{kj} = \delta_j^i$ as in 1.138. For any local observable O recall the overlap with a conserved charge (1.137) which in this case reads

$$\mathcal{V}_i^O = \sum_{x \in \mathbb{Z}} \langle q_i(x) O(0) \rangle^c. \quad (2.19)$$

In particular, for conserved densities and currents we have $\mathcal{V}_k^{q_i} = C_{ik}$ and $\mathcal{V}_k^{j_i} = \mathcal{B}_{ik}$.

The correlation functions whose asymptotics we are looking to evaluate are

$$\text{(longitudinal)} \quad \langle \sigma_x^3(t) \sigma_0^3(0) \rangle^c = \text{Tr}(\rho \sigma_x^3(t) \sigma_0^3(0)) - \left(\text{Tr}(\rho \sigma_0^3) \right)^2 \quad (2.20)$$

$$\text{(transverse)} \quad \langle \sigma_x^+(t) \sigma_0^-(0) \rangle = \text{Tr}(\rho \sigma_x^+(t) \sigma_0^-(0)) \quad (2.21)$$

where the nomenclature refers to the direction of the spin component with respect to the magnetic field (σ^\pm are linear combinations of $\sigma^{1,2}$). We are looking for the asymptotic regime

$$x = \lfloor \ell \bar{x} \rfloor, \quad t = \ell \bar{t}, \quad \ell \rightarrow \infty. \quad (2.22)$$

Below, for simplicity we assume that $w(k)$ is a continuous and periodic function on the interval $k \in [-\pi, \pi]$ – that is, continuous on the interval seen as a topological circle.

2.2 Longitudinal correlators from hydrodynamic projections

The leading asymptotics of the longitudinal correlation function $\langle \sigma_x^3(t) \sigma_0^3(0) \rangle^c$ in space-time can be predicted by the standard hydrodynamic linear response theory. In this section we explain how this is done, and we compare with the result of the elementary computation using Wick's theorem, confirming the hydrodynamic theory of projections after suitable averages.

2.2.1 Fluid-cell averages and hydrodynamic projections

The hydrodynamic prediction is for the correlation function of fluid-cell means $\overline{O}_{1,2}(x, t)$ of local observables $O_1(x, t)$ and $O_2(x, t)$. For our purpose, consider a family of closed time intervals $I_x \subset \mathbb{R}$ (which may be single points), one for each position $x \in \mathbb{Z}$ on the chain. Then a fluid cell is a set $Y = \cup_{x=-\ell_1}^{\ell_2} (x, I_x) \subset \mathbb{Z} \times \mathbb{R}$ in space-time, with $\ell_1, \ell_2 \geq 0$, and the fluid-cell mean is the average over the fluid

2.2 Longitudinal correlators from hydrodynamic projections

cell $Y + (x, t)$:

$$\bar{O}(x, t) = \frac{1}{\ell_2 + \ell_1 + 1} \sum_{y=-\ell_1}^{\ell_2} \frac{1}{|I_y|} \int_{I_y} ds O(x + y, t + s). \quad (2.23)$$

The fluid cell is taken to be mesoscopic. Here in the notations of 1.3.1 we are taking

$$\delta(\ell) = \ell_1 + \ell_2 + 1 \quad , \quad \tau(\ell) = |I_y| \quad (2.24)$$

That is, the parameters ℓ_1 , ℓ_2 and I_x are taken to be dependent on an “observation scale” ℓ , such that the linear extent ℓ_0 of the fluid cell, say $\ell_0 = \max\{\ell_1, \ell_2, |t| : t \in \cup_{x \in [-\ell_1, \ell_2]} I_x\}$, is monotonically increasing with ℓ but much smaller, $\lim_{\ell \rightarrow \infty} \ell_0/\ell = 0$. The hydrodynamic prediction is that for ℓ_1 , ℓ_2 and the intervals I_x growing fast enough with ℓ (typically $\ell_0 \rightarrow +\infty$ fast enough, but within the mesoscopic constraint), the correlation function of fluid-cell means, times the scale ℓ of the space-time positions, has a limit expressible solely in terms of the hydrodynamic matrices \mathcal{C} , \mathcal{A} and the vectors \mathcal{V}^{O_1} , \mathcal{V}^{O_2} , as follows:

$$S_{O_1 O_2}(\bar{x}, \bar{t}) := \lim_{\ell \rightarrow \infty} \ell \langle \bar{O}_1(\ell \bar{x}, \ell \bar{t}) O_2(0, 0) \rangle^c = \mathcal{V}^{O_1} \cdot \mathcal{C}^{-1} \delta(\bar{x} - \mathcal{A} \bar{t}) \mathcal{V}^{O_2}. \quad (2.25)$$

Note that it is sufficient, by space-time translation invariance, to average over the positions of a single observable. The application of these general principles to GHD was done in [144], see the review [143] and references therein. In particular we consider two types of averages:

Definition 2.2.1 (Time mean).

$$\bar{\sigma}_{\ell \bar{x}}^3(\ell \bar{t}) = \frac{1}{2\ell_0} \int_{-\ell_0}^{\ell_0} \sigma_{\ell \bar{t}}^3(\ell \bar{t} + s) \quad , \quad (2.26)$$

Definition 2.2.2 (Ray mean).

$$\bar{\sigma}_{\ell \bar{x}}^3(\ell \bar{t}) = \frac{1}{2\ell_0} \sum_{y=-\ell_0+1}^{\ell_0} \sigma_{\ell \bar{x}+y}^3(\ell \bar{t} + y/\xi) \quad (2.27)$$

and show that they reproduce exact calculation from Wick’s theorem reported below. The fluid-cell mean (2.26) is a specialisation of the general form (2.23), with $\ell_1 = \ell_2 = 0$ and $I_0 = [-\ell_0, \ell_0]$. The value of ℓ_0 (for both averages) does not have to be taken “large enough”, and any $0 \ll \ell_0 \ll \ell$ will work. For $\xi \in \Xi$ (see below for the definition of Ξ), the ray mean (2.28) *does not give the hydrodynamic prediction*,

but with an additional minimal averaging over rays

$$\frac{1}{2\epsilon} \int_{\tilde{\zeta}_* - \epsilon}^{\tilde{\zeta}_* + \epsilon} d\tilde{\zeta} \quad (2.28)$$

the prediction is reproduced (again this can be recast into a specialisation of the general fluid-cell mean (2.23)). The case (2.27) is a specialisation to the choice $\ell_1 = -\ell_0 + 1$, $\ell_2 = \ell_0$ and the minimal choice of one-point time intervals $I_x = \{x/\tilde{\zeta}\}$. Both averages are therefore minimal expressions of the fluid-cell mean, in some way with a fluid cell that is the “least extended possible”. However, we will see that the average (2.28) is a valid mean for all rays in a certain set, $\tilde{\zeta} \in (-4, 4) \setminus \Xi$ with

$$\Xi = \{0\} \cup \{\tilde{\zeta}_* \in (-4, 4) \setminus \{0\} : 2 \arcsin(\tilde{\zeta}_*/4) + 2\sqrt{16\tilde{\zeta}_*^{-2} - 1} \in 2\pi\mathbb{Z} + \pi\} \quad (2.29)$$

(where $\arcsin(\tilde{\zeta}_*/4) \in (-\pi/2, \pi/2)$). This is the interval $(-4, 4)$, but excluding a countable set, of measure zero.

Hydrodynamic projection

As the XX model has a free fermion structure, GHD simplifies drastically, see [100]. The state (2.15) is stationary and homogeneous, and one can show that it is clustering as long as $w(k)$ has appropriate analytic properties; in particular, if $w(k)$ is analytic on the real line, then the two-point functions of fermions are exponentially decaying. The states (2.15) are in fact the generalised Gibbs ensembles, and on these states one may apply the hydrodynamic theory of correlation functions.

Given the state (2.15), one may construct the occupation function

$$\vartheta(k) = \frac{1}{1 + e^{w(k)}}. \quad (2.30)$$

All local conserved quantities, such as the Hamiltonian, have the form

$$Q_i = \int_{-\pi}^{\pi} dk h_i(k) c^\dagger(k) c(k) \quad (2.31)$$

where the function $h_i(k)$ is the one-particle eigenvalue of Q_i introduced in 1.1.4. The index i indexes any chosen (discrete, say) basis of the set of conserved quantities. The average densities may be evaluated by going back to a finite system, with discrete values of k , density matrix (2.15) and $Q_i = \sum_{k \in \Gamma_+ \cup \Gamma_-} h_i(k) \eta_k^\dagger \eta_k$, and

2.2 Longitudinal correlators from hydrodynamic projections

by evaluating $\lim_{N \rightarrow \infty} \langle Q_i \rangle / N$. The currents also take the universal form of (1.70)[100, 86]. The result is the standard one of GHD (see e.g. [73, 149] as well as [150–154] for other derivations), and are (1.61) for the charge and (1.70) for the current. The group velocity is

$$v(k) = E'(k) = 4 \sin(k). \quad (2.32)$$

The covariance matrices are evaluated by standard statistical mechanics methods, for instance

$$C_{ij} = \int_{-\pi}^{\pi} \frac{dk}{2\pi} \vartheta(k)(1 - \vartheta(k))h_i(k)h_j(k). \quad (2.33)$$

The flux Jacobian is diagonalised by passing to the continuous basis of the Fourier modes, and one has

$$\sum_j \mathcal{A}_i^j h_j(k) = v(k)h_i(k). \quad (2.34)$$

Thus the spectrum of \mathcal{A} is the interval $[-4, 4]$. Using the continuous diagonal basis, one can simplify the expression (2.25) into a single integral:

$$\begin{aligned} S_{q_i, q_j}(x, t) &= \int_{-\pi}^{\pi} \frac{dk}{2\pi} \delta(x - v(k)t) \vartheta(k)(1 - \vartheta(k))h_i(k)h_j(k) & (2.35) \\ &= \begin{cases} \frac{1}{2\pi\sqrt{16t^2 - x^2}} \sum_{\substack{\sin(k_{\pm}) = \bar{x}/4 \\ k_{\pm} \in [-\pi, \pi]}} \vartheta(k_{\pm})(1 - \vartheta(k_{\pm}))h_i(k_{\pm})h_j(k_{\pm}) & (|x/t| \leq 4) \\ 0 & (|x/t| > 4). \end{cases} & (2.36) \end{aligned}$$

For $|x/t| < 4$, as the result is a finite ordinary function, and not a generalised function, the hydrodynamic prediction is therefore that the mean-observable correlation function decays as $1/\ell$,

$$\langle \bar{q}_i(\ell \bar{x}, \ell \bar{t}) q_j(0, 0) \rangle \sim \ell^{-1} S_{q_i, q_j}(\bar{x}, \bar{t}) \quad (\ell \rightarrow \infty, |x/t| < 4). \quad (2.37)$$

For $|x/t| > 4$, the result for $S_{q_i, q_j}(x, t)$ vanishes, meaning that the decay is faster than ℓ^{-1} . For $|x/t| = 4$, the result diverges, meaning that the decay is slower than ℓ^{-1} .

2.2.2 Wick-theorem from Hydrodynamics and saddle-point

As the total spin shifted by a constant is twice the total number of fermions,

$$Q_0 := \frac{1}{2} \sum_{x=0}^{N-1} (\sigma_x^3 + \mathbf{1}) = \Omega, \quad q_0(x) \equiv q(x) = \frac{1}{2} (\sigma_x^3 + 1) = a_x^\dagger a_x \quad (2.38)$$

and thus a conserved quantity, we may use the above theory in order to predict the asymptotics of the correlation function of its density $\langle q(x, t)q(0, 0) \rangle$ at the Euler scale. The constant shift does not affect connected correlation functions, which then boils down to $\frac{1}{4} \langle \sigma_x^3(t) \sigma_0^3(0) \rangle^c$. In the general result (2.36), the required ingredients, besides the occupation function, is the one-particle eigenvalue $h_0(k) \equiv h(k)$ corresponding to this conserved quantity.

The longitudinal correlation function, as given in (2.20), can also be evaluated by a direct microscopic calculation using Wick's theorem. The last formula in (2.4) and space-time translation invariance give the connected longitudinal correlation function

$$\langle \sigma_x^3(t) \sigma_0^3(0) \rangle^c = 4 \langle a_x^\dagger(t) a_x(t) a_0^\dagger(0) a_0(0) \rangle - 4 \langle a_0^\dagger(0) a_0(0) \rangle^2 \quad (2.39)$$

which gives by Wick's theorem

$$\langle \sigma_x^3(t) \sigma_0^3(0) \rangle^c = 4 \langle a_x^\dagger(t) a_0(0) \rangle \langle a_x(t) a_0^\dagger(0) \rangle. \quad (2.40)$$

We work directly in the thermodynamic limit as prescribed in Eq. (2.13). Using $\langle c^\dagger(k) c(l) \rangle = \delta(k-l) \vartheta(k)$ and $\langle c(k) c^\dagger(l) \rangle = \delta(k-l) (1 - \vartheta(k))$, we obtain

$$\langle \sigma_x^3(t) \sigma_0^3(0) \rangle^c = 4 \int_{-\pi}^{\pi} \int_{-\pi}^{\pi} \frac{dk dl}{(2\pi)^2} e^{-i(k-l)x + i(E(k) - E(l))t} \vartheta(k) (1 - \vartheta(l)). \quad (2.41)$$

We consider $t > 0$ for simplicity.

Inside the light-cone, that is when $\xi = \bar{x}/\bar{t} \in (-4, 4)$, the asymptotic regime (2.22) is obtained by a stationary phase analysis taking x and t both of order $\ell \gg 1$.

The result, derived below, is a power law decay with power -1 , in agreement with (1.151) and (2.25). Away from the light-cone, $|\xi| > 4$, as the stationary phases do not lie on the integration region, the vanishing is faster, thus the second line of (2.36) holds. Its precise form depends on the analytic structure of $\vartheta(k)$. For instance, if $\vartheta(k)$ is analytic on $[-\pi, \pi]$, the asymptotic is obtained by contour deformation and the vanishing is at least exponential; this is because everywhere

2.2 Longitudinal correlators from hydrodynamic projections

on $[-\pi, \pi]$, the phase derivative is either positive or negative (since it is never zero), and hence there is a purely imaginary direction in which an infinitesimal displacement gives a real decaying exponential. We omit the general analysis of the case $|\zeta| > 4$ here for simplicity. At $|\zeta| = 4$, the stationary phase analysis must be modified, leading to a slower decay, as we explain below.

Case $|\zeta| < 4$

In the asymptotic regime (2.22), no matter the specific fluid-cell mean, we may perform a saddle point analysis. The exponential in (2.41) admits, for both the k and l integration, a set of two stationary points $k_{\pm} = k_{\pm}(\zeta)$ on the integration intervals, given by $k_+(\zeta) = \arcsin(\zeta/4) \in (-\pi/2, \pi/2)$ and $k_- = \text{sgn}(k_+)\pi - k_+$, which solve the saddle-point equation $E'(k_{\pm}) = \zeta$. Using the fact that $E''(k_{\pm}) = \pm\sqrt{16 - \zeta^2}$ and $E(k_+) - E(k_-) = -2\sqrt{16 - \zeta^2}$, the result may be written, with $x = \zeta t$, as

$$\begin{aligned} \langle \sigma_x^3(t+s)\sigma_0^3(0) \rangle^c &= \frac{2}{\pi\sqrt{16t^2 - x^2}} \\ &\times \sum_{a=\pm} n_a \left(1 - \vartheta_a + ai(1 - \vartheta_{-a})(-1)^x \right) \\ &\times e^{-2ai(k_+x + (t+s)\sqrt{16 - \zeta^2})} + O\left(t^{-1}\right) \end{aligned} \quad (2.42)$$

where $\vartheta_{\pm} = \vartheta(k_{\pm})$.

Below we show that after fluid-cell averaging this reproduces (2.36).

Time average

In (2.42) we separate the ℓ -scaling variables $x = \zeta t = \ell\bar{x}$, which stay on the ray ζ , from the ℓ_0 -scaling variable s , the addition to the time variable, which goes away from it, and use ℓ as the large parameter for the stationary point analysis. We choose a ray $\zeta \in (-4, 4)$ and set $x = \ell\bar{x}$, $t = \ell\bar{t}$, and perform the average over s . The non-oscillating term is independent of s and gives

$$\frac{2}{\pi\sqrt{16t^2 - x^2}} \sum_{a=\pm} \vartheta_a(1 - \vartheta_a) + O(\ell^{-1}). \quad (2.43)$$

Space-time correlation functions

In order to evaluate the oscillating term, we perform the fluid cell averaging, which gives the vanishing

$$\lim_{\ell_0 \rightarrow \infty} \frac{1}{2\ell_0} \int_{-\ell_0}^{\ell_0} ds \exp(-ai(2k_+x + 2(t+s)\sqrt{16-\zeta^2})) = 0 \quad (2.44)$$

uniformly on x, t , using the fact that $|\zeta| < 4$. This correctly reproduces (2.36) in accordance with the hydrodynamic prediction.

Ray average

Everywhere within the fluid cell, both x and t are large and stay on the ray ζ , with $x = \zeta t = \ell\bar{x}(1 + \mathcal{O}(\ell_0/\ell))$. In this case, we may do the stationary phase analysis uniformly everywhere within the cell, the scale $O(\ell) = O(x) = O(t)$ being the large parameter. We choose a ray $\zeta \in (-4, 4) \setminus \{0\}$, set $x = \ell\bar{x} + y$, $t = \ell\bar{t} + y/\zeta$, and consider the fluid-cell averaging (2.27) with $\ell_0 \ll \ell$. In this limit, the non-oscillating terms in (2.42) may be evaluated by using

$$\frac{1}{2\ell_0} \sum_{y=-\ell_0+1}^{\ell_0} \frac{1}{\ell\bar{t} + y/\zeta} \frac{1}{\sqrt{16-\zeta^2}} = \frac{1}{\ell} \frac{1}{\sqrt{16\bar{t}^2 - \bar{x}^2}} (1 + \mathcal{O}(\ell_0/\ell)).$$

This immediately reproduces (2.36), and we must show that the fluid-cell averaging vanishes on the oscillating terms. In order to do so, consider

$$(-1)^{\ell\bar{x}+y} \exp(-ai(2k_+ + 2\sqrt{16\zeta^{-2} - 1})(\ell\bar{x} + y)). \quad (2.45)$$

The fluid-cell sum over y vanishes if, and only if,

$$\zeta \notin \Xi \quad (2.46)$$

where Ξ is given in (2.29): if $\zeta \in \Xi$, the terms are in fact not oscillating for $y \in \mathbb{Z}$, and add up to a finite contribution. There are infinitely many rays $\zeta \in (-4, 0)$, and $\zeta \in (0, 4)$, which break the condition. For instance, as ζ increases from -4 to 0 , k_+ increases from $-\pi/2$ to 0 , while $\sqrt{16\zeta^{-2} - 1}$ increases from 0 to ∞ ; therefore, all values $2\pi n + \pi$ for $n = 1, 2, \dots$ will be crossed. However, as this is a set of isolated values ζ_* of ζ , of measure zero, under additional averaging (2.28) the oscillatory terms contribution vanishes. As the sum over y can be uniformly bounded for all rays, it can be evaluated on the integrand in (2.28) by the dominated convergence

theorem, giving a result that is zero except for a set of measure zero (which is the single-point set $\{\tilde{\zeta}_*\}$ as $\epsilon \rightarrow 0$).

Case $|\tilde{\zeta}| = 4$

In this case the precise asymptotics is not predicted by Euler hydrodynamics (it should be by higher order hydrodynamics [86]), but the Wick-theorem result allows us to evaluate it. We look for the leading asymptotics in the region $x = \ell\bar{x}$, $t = \ell\bar{t}$, $\ell \rightarrow \infty$. In this case $E''(k_{\pm}) = 0$ and therefore in the exponent in (2.41) we must expand to 3rd order. Using $k_{\pm} = k_+ = \text{sgn}(\tilde{\zeta}) \pi/2$ (there is a single stationary point), $E'''(k_+) = -4 \text{sgn}(\tilde{\zeta})$ and $x = 4 \text{sgn}(\tilde{\zeta})t$, we evaluate

$$\begin{aligned} \int_{-\pi}^{\pi} \frac{dk}{2\pi} e^{-ikx+iE(k)t} f(k) &\sim e^{-2i\pi t+iE(\pi/2)t} \int_{-\pi}^{\pi} \frac{dk}{2\pi} e^{-4i \text{sgn}(\tilde{\zeta}) tk^3/3!} f(k_+ + k) \\ &\sim t^{-1/3} e^{-2i\pi t+iE(\pi/2)t} \int_0^{\infty} \frac{dk}{2\pi} e^{-k^3} (1/u + 1/u^*) f(k_+) \\ &\sim t^{-1/3} e^{-2i\pi t+iE(\pi/2)t} \frac{\Gamma(4/3)}{2\pi} 2 \text{Re}(1/u) f(k_+) \end{aligned} \quad (2.47)$$

where $u = (4i \text{sgn}(\tilde{\zeta})/3!)^{1/3}$, and the integral contour has been deformed into a wedge in the complex plane around $k = 0$ in order to have a sum of two convergent real integrals. The result is therefore

$$\langle \sigma_x^3(t) \sigma_0^3(0) \rangle^c \sim t^{-2/3} \left(\frac{\Gamma(4/3)}{\pi} 3^{5/6} 2^{-4/3} \right)^2 \vartheta_+(1 - \vartheta_+) \quad (x = \pm 4t). \quad (2.48)$$

This agrees with the hydrodynamic prediction (2.37): the decay $t^{-2/3}$ is slower than t^{-1} .

2.3 Transverse correlators from ballistic fluctuations

The prediction from the hydrodynamic linear response theory for the transverse correlation function $\langle \sigma_x^+(t) \sigma_0^-(0) \rangle$, see section 2.2.1, is a vanishing Euler-scale asymptotics. Indeed, according to formula (2.25), the correlation function is proportional to the integrated correlator $\mathcal{V}_i^{\sigma^{\pm}} = \sum_{x \in \mathbb{Z}} \langle q_i(x) \sigma_0^{\pm} \rangle^c$, Eq. (2.19), involving the operator σ_0^{\pm} at position 0, and the conserved densities $q_i(x)$. But all conserved charges (2.31) preserve the total 3-component of the spin, as does the GGE (2.15), and thus $\mathcal{V}_i^{\sigma^{\pm}} = 0$; formula (2.25) gives zero. This means that the decay of the fluid-cell average of the correlator must be faster than $1/t$.

In fact, it is known [142, 155] that the decay is exponential along any ray in space-time. Such exponential decays are not predicted by current hydrodynamic theories. However, recently [139] it was proposed that the leading exponent for the decay of correlation functions of certain types of observables, referred to as twist fields, may be predicted by Euler hydrodynamics, via the *ballistic fluctuation theory* (BFT).

2.3.1 Transverse correlators and spin fluctuations

Fermion number and current fluctuations

The basis for the hydrodynamic theory of the correlation function $\langle \sigma_x^+(t) \sigma_0^-(0) \rangle$ is the realisation that it is related to large deviations of the fermion number 2-current along the ray $(0, 0) \rightarrow (x, t)$.

The first step is the extension of the usual Jordan-Wigner (JW) strings to “space-time JW strings”. By the JW transformation (2.4),

$$\langle \sigma_x^+(0) \sigma_0^-(0) \rangle = \langle a_x^\dagger e^{i\pi\Omega_0(x,0)} a_0 \rangle \quad (2.49)$$

as per the definition in (1.156). Here we identify the total fermion number with the $i = 0$ charge (2.38), and use

$$\sum_{y=0}^{x-1} a_y^\dagger a_y = -\Omega_0(x, 0) \quad (2.50)$$

(the sign is unimportant in the exponential in (2.49), as the fermion number is an integer). It turns out that a similar formula holds for the large-scale exponential decay of the time-dependent correlator,

$$\langle \sigma_x^+(t) \sigma_0^-(0) \rangle \asymp \langle a_x^\dagger(t) e^{i\pi\Omega_0(x,t)} a_0(0) \rangle \quad (x = \lfloor \ell \bar{x} \rfloor, t = \ell \bar{t}, \ell \rightarrow \infty), \quad (2.51)$$

where, on the right-hand side, $\Omega_0(x, t)$ is defined in (1.155), and the time evolution in $a_x^\dagger(t)$ is under the sector-specific free-fermion Hamiltonian, as per (2.10); as the limit of infinite chain length has been taken, the choice of sector does not matter. Formula (2.51) is derived below. We also establish that exact, instead of asymptotic, equality holds in (2.51) not only at $t = 0$, but also at $x = 0$. In fact, the

2.3 Transverse correlators from ballistic fluctuations

following expression is exact for all x, t 's (see Appendix A):

$$\sigma_x^+(t)\sigma_0(0) = a_x^\dagger(t) \exp\left(i\pi \sum_{y=0}^{x-1} q(y, t)\right) \exp\left(i\pi \int_0^t ds j(0, s)\right) a_0(0) \quad (2.52)$$

where we recall that $q(x, t)$ is the fermion density (2.38), and $j(x, t) = j_0(x, t)$ is its associated current. An heuristic argument about what controls the asymptotic behavior in the Euler scaling limit $x/t = \xi = \text{const.}$ of transverse correlation function (2.21) is based on the conservation law (2.16): denoting $Q|_0^z = \sum_{x=0}^{z-1} q(x)$ we have

$$Q|_0^z(t) - Q|_0^z + \int_0^t ds [j(z, s) - j(0, s)] = 0 \quad (2.53)$$

and so if we are interested in the Euler scaling limit we want to "move" along a ray $x = \xi t$. Starting at point $(0, 0)$ we move diagonally along such ray up to the point $(\xi t, t)$. This is done summing contributions along the ray as in (1.155). Using (2.53) we have

$$\begin{aligned} \sigma_x^+(t)\sigma_0(0) &= a_x^\dagger(t) \exp\left(i\pi \sum_{y=0}^{x-1} q(y, t)\right) a_0(0) \\ &= a_x^\dagger(t) \exp\left(i\pi \sum_{y=0}^{x-1} q(y, 0) - \int_0^t ds j(x, s) + \int_0^t ds j(0, s)\right) a_0(0) \end{aligned} \quad (2.54)$$

and we have that

$$\int_0^t ds j(0, s) = \int_0^{\xi/x} ds j(0, s) \rightarrow 0 \quad , \quad x, t \rightarrow \infty \quad , \quad \xi = x/t \quad (2.55)$$

while the other two contributions stay finite in the scaling limit. In particular by the Lieb-Robinson bound [113] the operator $j(x, s)$ is supported in a region growing linearly with time $[x - vt, x + vt]$ and this is the reason why

$$\int_0^t ds j(x, s) < \infty \quad (2.56)$$

in the scaling limit. The integration path in (2.54) corresponds to $(0, 0) \rightarrow (x, 0)$ horizontally and $(x, 0) \rightarrow (x, t)$ vertically but by contour deformation this path can be arbitrarily deformed.

We see in (2.51) that the transverse correlation function is related to the two-point function of fermion operators, modified by a counting function for the

integrated fermion number 2-current in (1.154): the number of fermions lying, and the current flowing, between them. This counting function, the space-time JW string $e^{i\pi\Omega_0(x,t)}$, gives a factor -1 for every fermion counted or flowing by. As the fermion number is the number of spins in the direction up, the transverse correlator is a modification of a local fermion correlator by the fluctuation of the total spin and its current between them.

We note that a formula similar to (2.51) is well-known for the classical, two-dimensional Ising model, a statistical model simply related to this XX quantum chain but in Euclidean time [156, 157].

Asymptotic behavior and exact factorisation

In the work [3] we have proposed the asymptotic factorisation property

$$\langle a_x^\dagger(t) e^{\lambda\Omega_0(x,t)} a_0(0) \rangle \asymp \langle a_x^\dagger(t) a_0(0) \rangle_{\lambda;\zeta} \langle e^{\lambda\Omega_0(x,t)} \rangle \quad (2.57)$$

where $\langle \cdot \cdot \rangle_{\lambda;\zeta}$ is the state characterised by $\beta^j(\lambda; \zeta)$ as determined by (1.162). In the same work it was argued that such property is valid asymptotically. In reality such factorisation should be exact. First, recall that $\zeta = x/t$, and that for the free-fermionic model we are considering, one uses the function $w(k)$ instead of the Lagrange parameters β^j , and on the flow this has the explicit solution $w(\lambda; \zeta; k)$ given by (1.173) with $h_{i_*}(k) = h_0(k) = 1$. The factorisation is *exact*, after we have taken the scaling limit as in (2.55) and can be viewed as a simple consequence of a redefinition of the state

$$\begin{aligned} \langle a_x^\dagger(t) e^{\lambda\Omega_0(x,t)} a_0(0) \rangle &= \frac{\langle a_x^\dagger(t) e^{\lambda\Omega_0(x,t)} a_0(0) \rangle}{\langle e^{\lambda\Omega_0(x,t)} \rangle} \langle e^{\lambda\Omega_0(x,t)} \rangle \\ &= \langle a_x^\dagger(t) a_0(0) \rangle_{\lambda;\zeta} \langle e^{\lambda\Omega_0(x,t)} \rangle \quad . \end{aligned} \quad (2.58)$$

Since the algebra of quadratic fermionic operators is closed under commutators [158, 159] the expectation value in the λ -modified state is still a gaussian state coming from some quadratic Hamiltonian. Second, the asymptotic (2.57) is supported by an *exact* factorisation of the correlation function found in the literature. In the XX model case considered here the transverse correlation function is expressed exactly as a product [142]

$$\langle \sigma_x^+(t) \sigma_0^-(0) \rangle = e^{-2iht} b_{++}(x,t) e^{\sigma(x,t)} \quad . \quad (2.59)$$

2.3 Transverse correlators from ballistic fluctuations

Let us explain the various terms here. Let λ and μ be complex spectral parameters on the unit circle $|\lambda| = |\mu| = 1$. Then, $\sigma(x, t)$ is the logarithm of a Fredholm determinant associated with the integrable operator having the following kernel

$$V(\lambda, \mu) = \frac{e_+(\lambda)e_-(\mu) - e_-(\lambda)e_+(\mu)}{\lambda - \mu} \quad (2.60)$$

and it is explicitly written as follows

$$\sigma(x, t) = \log \det (\hat{1} + \hat{V}) \quad . \quad (2.61)$$

The functions e_{\pm} depend on space-time x, t , on (inverse) temperature β , magnetic field h and the spectral parameter λ via the filling ϑ and have the following simple form

$$e_-(\lambda) = \sqrt{\vartheta(\lambda)} \lambda^{x/2} e^{-ith(\lambda+1/\lambda)} \quad (2.62a)$$

$$e_+(\lambda) = e_-(\lambda) E(x, t, \lambda) \quad (2.62b)$$

with (P.V. is the Cauchy principal value)

$$E(x, t, \lambda) = \text{P.V.} \int \frac{d\mu}{\pi} \frac{e^{2ith(\mu+1/\mu)} \mu^x}{\mu - \lambda} \quad . \quad (2.63)$$

Above, $\vartheta(\lambda)$ is the occupation function appearing in all Thermodynamic Bethe Ansatz solvable models that we introduced in (1.49) and (2.30). The difference here is only in the parametrisation of the spectral parameter, here being $\lambda(k) = e^{ik}$, and in the choice of a thermal state corresponding to $w(k) = \beta E(k)$, proportional to the dispersion relation as in (2.12). The ‘‘potential’’ $b_{++}(x, t)$ can be shown to satisfy the discretised non-linear Schrödinger equation [160]. In turn, space-time derivatives of $\sigma(x, t)$ can be written in terms of the $b_{++}(x, t)$. After, rewriting the integrable PDEs system mentioned above as a Riemann-Hilbert matrix factorisation problem one can extract the asymptotic in relevant regimes. It might well be that BFT formalism can have connections with non-linear steepest descent method [161]. A possible one-to-one correspondence of the terms involved is tempting. The physical idea behind it is that the leading exponential behaviour of the correlator on the left-hand side of (2.57) is controlled by two effects. The first is the (eventual) exponential decay due to the interaction between the fermions $a_x^\dagger(t)$ and $a_0(0)$, which occurs in the region ‘‘deep’’ between $(0, 0)$ and (x, t) and is thus in a state modified by the presence of the space-time JW string; the second is the exponential decay due to the change of ‘‘free energy’’ induced by the space-

Space-time correlation functions

time JW string representing the spin fluctuations, as given by the BFT, a classical hydrodynamical effect. This is in agreement with Sachdev's semiclassical theory that we will discuss in more detail later [162, 163]. See Fig. 2.1.

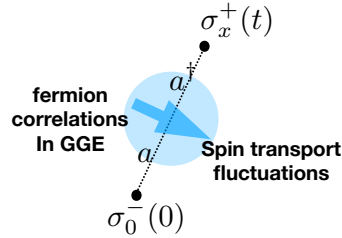


Fig. 2.1 The leading exponential decay of the two-point function (2.51) is controlled by two effects, as expressed in (2.57): The fermionic JW string eventually modifies the exponential decay, depending on the analytic structure of the dispersion relation and on the phase of the model. Picture from [3].

2.3.2 Exponential behaviour of transverse correlation function

We now analyse the leading exponential behaviour as obtained from (2.57). In principle, our methods, including the BFT, provide also certain oscillations on top of the decay. Although this is an interesting subject, we still don't have a full understanding, and thus we focus on the exponentially decaying envelope.

The first contribution to (2.57) comes from the two-point function of fermions. This is obtained by Wick's theorem, and using (1.173) we get

$$\langle a_x^\dagger(t) a_0(0) \rangle_{\lambda; \tilde{\zeta}} = \int_{-\pi}^{\pi} \frac{dk}{2\pi} \frac{e^{iE(k)t - ikx}}{1 + e^{w(k) + \lambda \operatorname{sgn}(x - v(k)t)}}. \quad (2.64)$$

Let us extract the exponential asymptotic behavior of this quantity.

Time-like region

In the time-like region $|\tilde{\zeta}| < 4$ the phase has a stationary point on the integration contour, and the behaviour is algebraic for all values of λ and by a straightforward saddle-point application we get

$$\langle a_x^\dagger(t) a_0(0) \rangle_{\lambda; \tilde{\zeta}} = O(t^{-\frac{1}{2}}) \quad (|\tilde{\zeta}| < 4). \quad (2.65)$$

The same conclusion holds for $|\tilde{\zeta}| = 4$ (although the algebraic decay is slower, like in the case of the longitudinal correlator).

Space-like region

In the space-like region no stationary point exist on the integration contour, and the exponential behaviour is obtained by an application of contour deformations and the steepest descent method. The formula simplifies as in this region, $\text{sgn}(x - v(k)t) = \text{sgn}(x)$. For evaluating (2.51), we need $\lambda = i\pi$, and thus

$$\langle a_x^\dagger(t)a_0(0) \rangle_{i\pi; \xi} = \int_{-\pi}^{\pi} \frac{dk}{2\pi} \frac{e^{iE(k)t - ikx}}{1 - e^{w(k)}} \quad (|\xi| > 4). \quad (2.66)$$

Saddle point analysis gives (see Appendix of [3]):

$$\begin{aligned} \langle a_x^\dagger(t)a_0(0) \rangle_{i\pi; \xi} &\asymp \exp \left(- \cosh^{-1}(\xi/4) |x| + \sqrt{x^2 - 16t^2} - i\pi|x|/2 + 2ih t \right) + \Lambda \\ &= \exp \left(- M_\xi |x| - i\pi|x|/2 + 2ih t \right) + \Lambda \quad (|\xi| > 4) \end{aligned} \quad (2.67)$$

where

$$M_\xi = \cosh^{-1}(\xi/4) - \sqrt{1 - \frac{16}{|\xi|^2}} \quad (2.68)$$

and Λ is the contribution coming from residues of the integrand due to the poles in the denominator. In (2.67), the most slowly decaying exponential amongst the terms on the right-hand side is to be taken.

Deep analysis has been done for the thermal state, for which $w(k) = \beta E(k)$. In the space-like region $|\xi| > 4$, the quantity Λ is obtained from solving $w(z) = 0$. The solution depends on the value of $|h|$.

- If $|h| \leq 2$, the gapless regime, then a zero exists at $z = 0$ and we find $\Lambda = 1$ and therefore

$$\langle a_x^\dagger(t)a_0(0) \rangle_{i\pi; \xi} \asymp 1. \quad (2.69)$$

In the gapless regime, the two-point function of fermions does not give additional exponential decay in (2.51), and the exponential behaviour of the transverse correlator is fully determined by spin fluctuations.

- If $|h| > 2$, there is a nontrivial solution with $\hat{z} = \hat{k} + i\hat{q}$ with $\hat{k} = 0$ ($\hat{k} = \pi$) for $h > 0$ ($h < 0$), and with $\hat{q} = \cosh^{-1}(h/2)$. It is found that this contributes to Λ if and only if $2|h| < |\xi|$, in which case it is the leading contribution to Λ and otherwise $\Lambda = 1$, thus

$$\Lambda = \exp \left(- \cosh^{-1}(h/2) |x| \right) \times \begin{cases} (-1)^x & (h < 0) \\ 1 & (h > 0). \end{cases} \quad (2.70)$$

Hence

$$\langle a_x^\dagger(t)a_0(0) \rangle_{i\pi, \xi} \asymp e^{i\Phi} \exp(-\min(\cosh^{-1}(h/2), M_\xi) |x|) \quad (2.71)$$

with

$$\Phi = \begin{cases} \pi x & \text{(first argument, } h < 0) \\ 0 & \text{(first argument, } h > 0) \\ -\pi|x|/2 + 2ht & \text{(second argument)} \end{cases} \quad (2.72)$$

where ‘‘argument’’ refers to that taken by the min function in (2.71). Thus when there is a gap between the energy of the ground state and that of the lowest excited state, an extra contribution to the exponential decay of the transverse correlator arises from the fermion correlations. It may be surprising that the gap affects the correlation function in a finite-density GGE, far from the ground state; the important point here is that the state is modified by the presence of the JW string. This transforms the distribution into that of bosons instead of fermions, which is strongly affected by the presence or not of a gap.

The second contribution in (2.57) comes from the spin fluctuations and may be evaluated using the BFT results (1.158) with (1.174) and (1.173). This gives precisely the formula (1.174) with the state defined by (1.173). Eq. (1.174) is evaluated at $\lambda = \pm i\pi$ but the sign here does not affect any of the calculations, however the direction in which the analytic continuation of the explicit asymptotic formula is taken affects the result. We believe that this is because the analytic continuation to $\pm i\pi$ does not commute with the evaluation of the asymptotics. However this only gives additional oscillations, which we do not address here and that can be washed out either taking the absolute value or perform a suitable fluid-average. We take the former route for simplicity here. We obtain

$$\left| \langle e^{i\pi\Omega_0(x,t)} \rangle \right| \asymp e^{f_{x,t}[w]} \quad (2.73)$$

where we use the notation $f_{x,t}[w] = f_{i\pi, x,t}[w]$ from (1.174), giving

$$\log |\langle \sigma_x^+(t)\sigma^- \rangle| = \begin{cases} f_{x,t}[\beta E] & (|\xi| \leq 4) \\ |x|f_{1,0}[\beta E] & (|\xi| > 4, |h| \leq 2) \\ -|x| \min(\cosh^{-1}(h/2), M_\xi) + |x|f_{1,0}[\beta E] & (|\xi| > 4, |h| > 2) \end{cases} \quad (2.74)$$

where Λ is defined in (2.70) and M_{ξ} in (2.68). The numerical results are shown in the pictures below and the techniques used to compute such correlation functions are based on Pfaffian techniques reported in Appendix B.

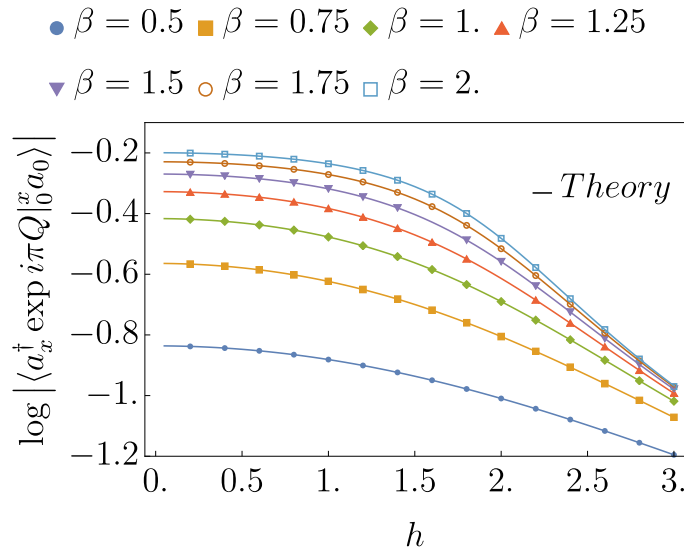


Fig. 2.2 Exponential decay of the JW string for different values of the magnetic field and different temperatures for fixed large x and $t = 0$. The numerics is done according to the Pfaffian representation derived with the aid of results in Appendix B. The theory is eq. (2.74).

2.4 Outlook

In this chapter we have presented a full Euler hydrodynamic theory of dynamical correlation functions in the XX spin chain, the easiest possible model to test our physical ideas. The underlying physical principle underlying the calculations and the results presented above is relatively straightforward: the exponential decay of the correlation function $\langle \sigma_x^+(t) \sigma_0^-(0) \rangle$ is influenced, in part, by the number of domain walls crossing between the two observables and their fluctuations, as initially proposed for the Ising model [162–164]. The large-deviation theory is applied to this extensive, fluctuating variable (the number of domain walls). Due to the free-fermion structure inherent to the XX chain and its Euler hydrodynamics, which is a special case of generalized hydrodynamics, the large-deviation theory takes a simple form. Moreover, the specific form of the observables σ_x^\pm allows them to act as both domain wall counters and sources/sinks of domain walls.

Space-time correlation functions

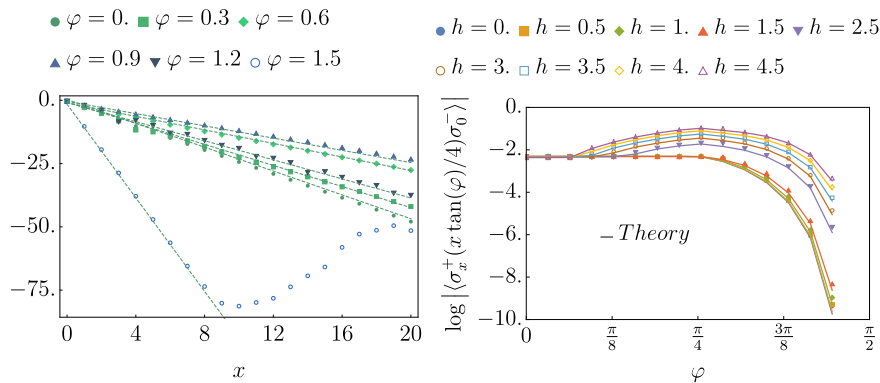


Fig. 2.3 Exponential decay of the two-point function for different rays parametrised by $\tan \varphi = x/t$. The theory is eq. (2.74).

Through the Jordan-Wigner transformation, they can be identified as fermionic descendants of the $U(1)$ twist field of the XX model. We have explained the correct treatment of these observables and demonstrated that they provide an additional contribution to the exponential decay under certain parameter values benchmarking our predictions against accurate numerical simulations.

More correlation functions

Recent studies have also examined the asymptotic behavior of dynamical correlation functions in spin chains. For example, in the transverse field Ising model, a partial resummation of the form factor expansion yields the asymptotic behavior of the order parameter in the low-density regime [165]. Notably, Fredholm determinant techniques continue to yield non-trivial results regarding the large-time behavior [166–168] of correlation functions in spin chains. This provides a connection between hydrodynamic-based techniques and the asymptotic behavior of a specific class of Fredholm determinants, which could be valuable beyond the current scope of applications. Further analysis and explicit connections will be explored in future studies.

Two-point function of 1d impenetrable Bosons

It is known that in the continuum limit the XX spin chain gives the Tonks gas of hard core bosons [110, 35, 169]. Formula (2.74) is equally applicable to the correlation function of Bose fields in the large coupling limit upon fermionisation using a continuum version of the Jordan-Wigner string. The only difference is in

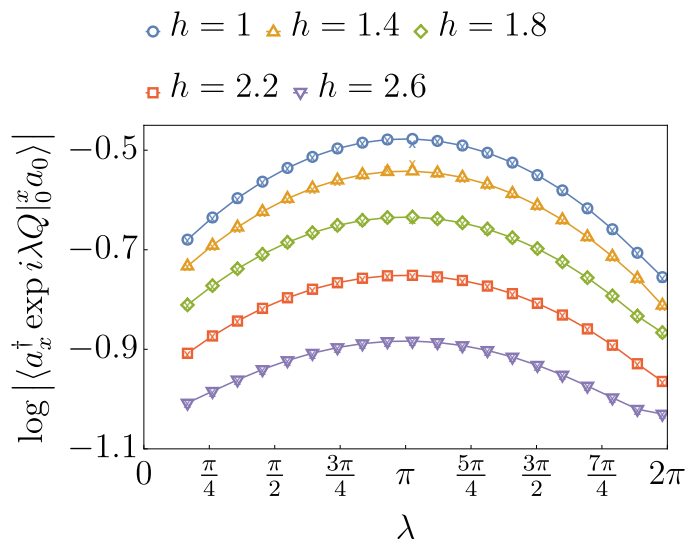


Fig. 2.4 Comparison of the generic expression of the SCGF (1.174) controlling the leading exponential decay of the operator $\exp \lambda \Omega(x, t)$ against exact numerical simulations.

the dispersion relation, in the integration extrema in momentum space and the fact that the fermionic correlator does not contribute to the exponential decay because the saddle-point equation always has a solution.

Full counting statistics

We have seen that the expectation value of λ -dependent the Jordan-Wigner string is nothing but the characteristic functional of fluctuating process

$$\Omega_0(x) = \frac{1}{x} \sum_{z=0}^{x-1} q(z) \quad (2.75)$$

which counts the average number of fermions in the interval $[0, x - 1]$. It is interesting to note that such quantities are not known in explicit form in the literature and there have been several attempts in a number of ways [170–172]. Importantly, the full counting statistics has been proposed as a tool to classify phases of matter [173]. This is a really interesting line of research and we plan to give full exposition in a future publication.

Chapter 3

Sine-Gordon Field Theory

Goal of the chapter

In this third chapter we present results for what concerns correlation functions in the Sine-Gordon field theory and we draw heavily on the paper [5]. The step from a discrete and non-interacting spin-chain to a continuous field theory is motivated by two facts: on one hand, we want to take into account effects of interactions; technically, this is a notoriously difficult problem, and there exist very few methods that are able to exactly account for that when computing dynamical correlation functions, especially in non-equilibrium settings. On the other hand, we want to describe current state-of-art experiments. We will realise these two goals presenting exact results for dynamical correlations functions at finite temperature at Euler scale and we will compare the prediction against parameters of a real experiment of tunnel-coupled quasicondensates [174–178], in particular Fig. 3.7. We are going to provide exact analytic expressions for correlation functions of certain observables of special interest in the Sine-Gordon model: these are called vertex operators and are defined as follows

$$V_\lambda(x, t) = e^{i\lambda\phi(x,t)} \quad . \quad (3.1)$$

The expectation value of the vertex operator is nothing but the characteristic functional of the field (1.84). Correlation functions of vertex operators will be

$$G_\lambda(x, t) = \langle V_\lambda(x, t)V_\lambda(0, 0) \rangle = \langle e^{i\lambda(\phi(x,t) - \phi(0,0))} \rangle \quad (3.2)$$

where the average is taken over some arbitrary homogeneous GGE of the type (1) or thermal state thereof.

We show that the probability distribution of the phase differences obeys a large deviation principle

$$P \left[\frac{\Delta\phi(t, x)}{2\pi} = \delta \right] \asymp e^{-\ell I_\alpha(\delta)} \quad (3.3)$$

where $\ell = \sqrt{x^2 + t^2}$ and the large-deviation function (LDF) I_α is fully determined by hydrodynamic modes and depends only on the "ray" $x/t = \tan \alpha$. As a consequence, cumulants (connected correlators) scale linearly with ℓ and vertex operator correlations decay exponentially. In formulae

$$C_n = \left\langle \left(\frac{\Delta\phi}{2\pi} \right)^n \right\rangle^c \sim \ell c_n \quad , \quad \ell \rightarrow \infty \quad (3.4)$$

We achieve such goals deriving exact expressions for the SCGF in the classical Sine-Gordon field theory, solve it numerically and compare with microscopic numerical simulations of the field equations. We also discuss Sachdev-Damle semiclassical picture to approach correlation functions at low temperature [162, 163], and compare its prediction with BFT. We want to give credit to Dr. Alvisio Bastianello for performing the microscopic Montecarlo simulations of the classical Sine-Gordon equation.

3.1 Sine-Gordon field theory

This is an intriguing model, that offers a solvable and mathematically elegant description of a scalar field in (1+1)-dimensional space-time. It exhibits a remarkable spectrum of particles, including solitons known as kinks and anti-kinks, which possess unique properties.

To quantize the sine-Gordon field, we introduce creation and annihilation operators and formulate the theory in terms of these operators and their commutation relations. The process of quantization enables us to explore the quantum fluctuations of the scalar field, revealing a vast array of intriguing phenomena. The quantised field operators pave the way for studying correlation functions, scattering amplitudes, and other observables of the theory.

A defining feature of the Sine-Gordon field theory is the existence of solitons, specifically kinks and antikinks. These solitons represent topological defects that

possess localized energy and intriguing non-trivial topological properties. Kinks and antikinks are stable solutions of the field equations and exhibit unique dynamics and interaction patterns. The scattering behavior of these solitons provides valuable insights into the underlying theory and its broader implications.

The Sine-Gordon field theory possesses a remarkable attribute—exact solvability. Several powerful solution techniques have been developed to precisely solve this model. These include the bootstrap approach, the quantum inverse scattering method, and the form factor approach. These methodologies allow for the calculation of various physical quantities, such as correlation functions and scattering amplitudes, enabling a detailed understanding of the theory's behavior.

Beyond its intrinsic theoretical appeal, the quantum sine-Gordon field theory finds applications and connections to diverse branches of physics. It emerges in condensed matter physics, statistical mechanics, and integrable systems, offering insights into one-dimensional quantum systems, superconductivity, and quantum impurities. Its connections to these areas enrich our understanding of physical phenomena and pave the way for further exploration.

3.1.1 Classical Sine-Gordon

The Sine-Gordon field theory, despite its apparent simplicity, entails a certain degree of universality. It appears in the most varied contexts, from cold atoms experiments, of main interest to us, to fiber optics physics and geometry. Consider a real scalar field $\phi(x, t)$ in $(1 + 1)$ dimensions. The Sine-Gordon Hamiltonian is

$$H = \int dx \left\{ \frac{1}{2} \pi^2 + \frac{1}{2} (\partial_x \phi)^2 - \frac{m^2}{g^2} \cos(g\phi) \right\} . \quad (3.5)$$

Here g is an interaction parameter and m is a mass scale, the bare mass. The identification of these parameters is easily seen expanding the cosine term

$$H = \int dx \left\{ \frac{1}{2} \pi^2 + \frac{1}{2} (\partial_x \phi)^2 + \frac{m^2}{2} \phi^2 + \frac{m^2 g^4}{4!} \phi^4 + \dots \right\} + const. \quad (3.6)$$

This theory can be seen as a "deformation" of the more traditional Klein-Gordon scalar field theory corresponding to the quadratic approximation of the potential. The very special type of the interaction term, makes this theory special, hard, and

Sine-Gordon Field Theory

rich at the same time. The field classical equations are

$$\partial_t \pi = \{\pi, H\} = \partial_x^2 \phi - \frac{m^2}{g} \sin(g\phi) \quad (3.7)$$

that using $\pi = \partial_t \phi$ becomes

$$\partial_t^2 \phi - \partial_x^2 \phi + \frac{m^2}{g} \sin(g\phi) = 0 \quad . \quad (3.8)$$

The nice feature of this model, which comes from its integrable structure, is that it admits explicit soliton solutions. A soliton is just a wave packet that has elastic scattering properties, it is stable and not dissipative.

Field excitations

First of all, one should specify what kind of field ϕ is, besides the space-time dimensionality it is living in. In the Sine-Gordon model (3.5) the potential is periodic and there are infinitely many vacua at $\phi_n(x) = \frac{2\pi n}{g}$ with $n \in \mathbb{Z}$. This degeneracy makes it possible to have topological excitations interpolating between each vacua, that is solitons that are not localised but extended in space. This is not so for example in the Sinh-Gordon model [179]. The spatial profile of a soliton at rest is easily obtained looking for a stationary solution of (3.8), multiplying by $\partial_x \phi$ and integrating

$$\frac{1}{2}(\partial_x \phi)^2 = -\frac{m^2}{g^2} \cos(g\phi) + c_1 \quad . \quad (3.9)$$

If we want a solution interpolating between vacua we ask

$$\phi(+\infty, t) - \phi(-\infty, t) = \frac{2\pi}{g} \quad (3.10)$$

and we get $c_1 = m^2/g^2$ and the equation can be integrated to give the kink solution

$$\phi_K(x) = \frac{4}{g} \arctan(e^{-mx}) + \frac{2\pi}{g} \quad (3.11)$$

The soliton configuration can be translated and set in motion by using relativistic invariance and boosting the spatial coordinate $\phi_K(x) \rightarrow \phi_{K,\theta}(x - x_0, t) = \phi_K(\cosh \theta(x - x_0) - \sinh \theta t)$, where θ is the rapidity and x_0 the soliton position at $t = 0$. The antikink configuration is simply the reflected profile $\phi_{\bar{K},\theta}(x, t) = -\phi_{K,\theta}(x, t)$. Backlund transformations [180] allow for the construction of multi-

soliton solutions, that is bound states of single solitons. The profile of a bound state is

$$\phi_{K,\bar{K}}(t, x) = -\frac{4}{g} \arctan \left(\frac{\sinh(mt \sinh \theta)}{\tanh \theta \cosh(mx \cosh \theta)} \right) \quad (3.12)$$

and it can be easily seen that as $t \rightarrow \infty$ the solution factors into two travelling solitons with their position shifted [37]: the shift is quantified by the phase shift, the same phenomenology of free single particles scattering. The scattering between these classical solitonic waves in the Sine-Gordon model is only transmissive not reflective. This means that solitons can only pass through each other and will not bounce back. We will see this is a crucial difference with the quantised version of the model. We can write the scattering matrix for the 2-body scattering process in block diagonal form

$$S = \begin{pmatrix} S_0 & 0 & 0 & 0 \\ 0 & S_T & 0 & 0 \\ 0 & 0 & S_T & 0 \\ 0 & 0 & 0 & S_0 \end{pmatrix} \quad (3.13)$$

where the elements on the scattering matrix are functions of the difference of the rapidity variable and will be introduced in 3.2. The matrix above is written in basis where the state $|a_1, a_2\rangle$ with $a_i = \pm$ represent solitons $+$ and anti-solitons $-$. Note that a_i is a topological index and specifies the nature of the soliton because the topological charge is a constant of motion.

3.1.2 Quantum Sine-Gordon

The Sine-Gordon field theory can be quantised posing

$$[\phi(x, t), \pi(x', t)] = i\delta(x - x') \quad . \quad (3.14)$$

Integrability is kept at the quantum level in the sense that the full, infinite, set of conservation laws (available in [28]) is not destroyed, just deformed, although in a complicated way [181, 182] due to UV singularities coming from multiplication of field operators. This means that there exist an infinite number of *independent* conservation laws. This is, as we have already mentioned, at the heart of integrability, both classical and quantum. Quantisation comes with a price: with an elegant variational calculation Coleman [183] shows that the theory has a stable ground state only if

$$g \in [0, \sqrt{8\pi}] \quad . \quad (3.15)$$

Sine-Gordon Field Theory

The nature of interactions determines the spectrum of elementary excitations on top of the vacuum. There are solitons (kink and anti-kinks) and bound states, the breathers. The spectrum is described conveniently by the parameter

$$\zeta = \frac{g^2}{8\pi} \left(1 - \frac{g^2}{8\pi}\right)^{-1} \in [0, +\infty] \quad (3.16)$$

according to the mass law

$$m_n = 2M \sin(\pi n \zeta / 2) \quad , \quad 1 \leq n < \lceil \zeta^{-1} \rceil \quad . \quad (3.17)$$

This is only possible if $0 \leq \zeta \leq 1$ and it is the attractive phase. Conversely, kink and antikink persist uniformly in the spectrum, each possessing a bare mass (at rest)

$$M = 8m/(g^2) \quad (3.18)$$

which is then renormalized upon quantization [184]. Together, kinks, antikinks, and breathers constitute the model's particle content, analogously to the classical model.

A sidde: Sine-gordon and Thirring model

This short subsection can be skipped because it is not relevant to the main discussion and it is included only for curiosity and completeness. Nevertheless, we think it could be of value in understanding the Sine-Gordon model as quantum field theory in general. The Sine-Gordon field theory has intriguing connections with many models of quantum field theory and statistical physics: this is due to its universality. The Thirring model [185] for instance, is a quantum field theory made of a single Dirac fermion in $(1 + 1)$ dimensions $\Psi = \begin{pmatrix} \Psi_1 \\ \Psi_2 \end{pmatrix}$. The lagrangian is the Dirac lagrangian [34]

$$L_{\text{Th}} = \int dx \left[i\bar{\Psi}\gamma^\mu\partial_\mu\Psi - m_{\text{Th}}\bar{\Psi}\Psi - \frac{g_{\text{Th}}}{2} : (\bar{\Psi}\gamma_\mu\Psi)(\bar{\Psi}\gamma^\mu\Psi) : \right] \quad (3.19)$$

where the γ -matrices in this case are $\gamma_0 = \sigma_1$ and $\gamma_1 = i\sigma_2$, Th is a coupling constant and m_{Th} a bare mass parameter. The Hamiltonian can be derived by standard methods

$$H_{\text{Th}} = \int dx \left[i\Psi^\dagger\sigma_3\partial_x\Psi + m_{\text{Th}}\Psi^\dagger\sigma_1\Psi + 2g_{\text{Th}}\Psi_1^\dagger\Psi_2^\dagger(x)\Psi_2(x)\Psi_1(x) \right] \quad . \quad (3.20)$$

There is $U(1)$ symmetry $\Psi \rightarrow e^{i\alpha}\Psi$. The Dirac current

$$j^\mu = \bar{\Psi}\gamma^\mu\Psi \quad (3.21)$$

is conserved

$$\partial_\mu j^\mu = 0 \quad (3.22)$$

and the associated charge is

$$Q = \int dx \Psi^\dagger(x)\Psi(x) \quad . \quad (3.23)$$

The Thirring model in the zero charge sector is equivalent to the Sine-Gordon model via bosonisation as showed by Coleman [183]. In bosonisation the density waves are the bosonic collective excitations. Following Coleman (which is actually standard bosonisation [182]) we put

$$\Psi_1^\dagger\Psi_2 = \frac{1}{2}e^{ig\phi} \quad , \quad m_{\text{Th}} = \frac{m^2}{g^2} \quad (3.24)$$

and we see that the mass term becomes

$$m_{\text{Th}}\Psi^\dagger\sigma_1\Psi = \frac{m^2}{g^2}\cos(g\phi) \quad . \quad (3.25)$$

Further we see that if we put $j^\mu \propto -\epsilon^{\mu\nu}\partial_\nu\phi$ this current is going to be conserved no matter the choice of the coefficient ¹. Coleman identification is

$$j^\mu = -\frac{g}{2\pi}\epsilon^{\mu\nu}\partial_\nu\phi \quad , \quad \frac{1}{1+g_{\text{Th}}/\pi} = \frac{g^2}{4\pi} \quad (3.26)$$

and this corresponds to the Hamiltonians (3.5) and (3.20) . The relation between Sine-Gordon and Thirring bare parameters is universal and independento on the renormalisation scheme. The choice of the fields is quite arbitrary. The constraint (3.15) translates into

$$g_{\text{Th}} \geq -\pi/2 \quad (3.27)$$

which is interesting since it can be shown that in the massless Thirring model ($m = 0$) stability only requires $g \geq -\pi$: no matter how small the mass is, it kills a whole region of the spectrum.

¹This reflects the fact that the kinetic field gets renormalised multiplicatively and the coefficient in from of the kinetic term has not intrinsic meaning, it depends on the renormalisation procedure [183].

3.2 Thermodynamics

3.2.1 Quantum Sine-Gordon

The precise thermodynamics of the sine-Gordon field theory hinges on an understanding of the exact spectrum and scattering matrix, elaborated in Ref. [49]. In this section, we revisit the fundamental concepts of the Thermodynamic Bethe Ansatz and its application to BFT. Given the relativistic nature of the theory, the bare (one-particle eigenvalues) energy and momentum of a soliton with mass M are

$$E(\theta) = M \cosh \theta \quad (3.28)$$

$$p(\theta) = M \sinh \theta \quad (3.29)$$

For the rest of the discussion we normalise the Sine-Gordon topological charge as

$$Q = \int dx \partial_x \phi(x) = \phi(\infty) - \phi(-\infty) \quad (3.30)$$

so that the field jumps by $\frac{2\pi}{g}$ each time we change topological sector although in the semiclassical model we will set $g = 1$ to simplify the calculations. Breathers do not carry topological charge and the one-particle eigenvalue of it for the (anti-)kinks is

$$h_K(\theta) = \frac{2\pi}{g} \quad (3.31)$$

Scattering data

The scattering data do not depend on the values of interaction one considers. During scattering, breathers undergo transmissive scattering characterized by a scattering matrix [37, 6]:

$$S_{n,m}(\theta) = \frac{\sinh(\theta) + i \sin((n+m)\pi\zeta/2)}{\sinh(\theta) - i \sin((n+m)\pi\zeta/2)} \frac{\sinh(\theta) + i \sin(|n-m|\pi\zeta/2)}{\sinh(\theta) - i \sin(|n-m|\pi\zeta/2)} \\ \times \prod_{k=1}^{\min(n,m)-1} \frac{\sin^2((|n-m|+2k)\pi\zeta/4 - i\theta/2) \cos^2((n+m-2k)\pi\zeta/4 + i\theta/2)}{\sin^2((|n-m|+2k)\pi\zeta/4 + i\theta/2) \cos^2((n+m-2k)\pi\zeta/4 - i\theta/2)} \quad (3.32)$$

where θ signifies the difference in rapidities between the scattering particles.

Similarly, (anti-)kinks are transmitted upon scattering with breathers, following a scattering matrix pattern:

$$S_n(\theta) = \frac{\sinh(\theta) + i \cos(n\pi\zeta/2)}{\sinh(\theta) - i \cos(n\pi\zeta/2)} \prod_{k=1}^{n-1} \frac{\sin^2((n-2k)\pi\zeta/4 - \pi/4 + i\theta/2)}{\sin^2((n-2k)\pi\zeta/4 - \pi/4 - i\theta/2)} . \quad (3.33)$$

The scattering kernels entering the TBA equations are derived by differentiation as in (1.53). However, when it comes to the scattering of topological excitations, the scenario is much more intricate, with both transmission and reflection pathways in play. In this context, the scattering matrix takes on the form of an actual 4 matrix, featuring entries as follows:

$$S(\theta) = \begin{pmatrix} S_0(\theta) & 0 & 0 & 0 \\ 0 & S_T(\theta) & S_R(\theta) & 0 \\ 0 & S_R(\theta) & S_T(\theta) & 0 \\ 0 & 0 & 0 & S_0(\theta) \end{pmatrix} \quad (3.34)$$

where the (anti-)kink transmission and reflection amplitude are

$$S_T(\theta) = \frac{\sinh(\zeta^{-1}\theta)}{\sinh((i\pi - \theta)\zeta^{-1})} S_0(\theta) \quad (3.35)$$

$$S_R(\theta) = i \frac{\sin(\pi\zeta^{-1})}{\sinh((i\pi - \theta)\zeta^{-1})} S_0(\theta) \quad (3.36)$$

and they weight the transmission and reflection channel respectively, where

$$S_0(\theta) = - \exp \left[-i \int_0^\infty \frac{dt}{t} \frac{\sinh(\pi t(1 - \zeta)/2)}{\sinh(\pi\zeta t/2) \cosh(\pi t/2)} \sin(\theta t) \right] . \quad (3.37)$$

The matrix structure is again consistent with the choice of the basis $|a_1, a_2\rangle$ with $a_i = \pm$ for kink and anti-kink respectively. For general interaction values of ζ , the thermodynamic solution requires employing the Nested Bethe Ansatz. Here, for simplicity, we focus on specific regimes where simplifications arise, while acknowledging that BFT's predictions extend more broadly.

Reflectionless points

When considering specific interaction values

$$\zeta = 1/(N+1) \quad , \quad N \in \mathbb{N} \quad (3.38)$$

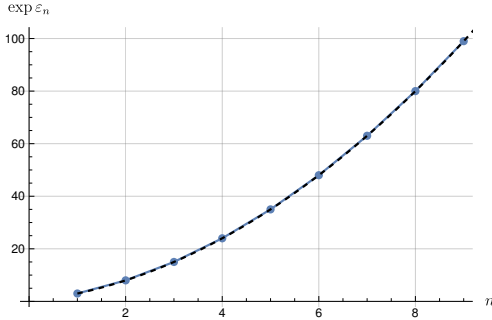


Fig. 3.1 For the breathers theoretical value of e^{ε_n} as $\beta \rightarrow \infty$ is $\varepsilon_n = n(n+2)$. Parameters as in Table 3.1.

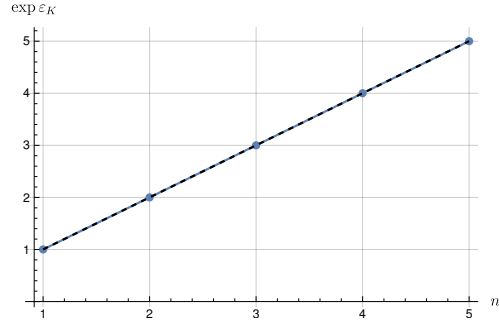


Fig. 3.2 For the breathers theoretical value of e^{ε_K} as $\beta \rightarrow \infty$ is $\varepsilon_K = n+1$. Parameters as in Table 3.1.

the reflection channel for kink-antikink scattering vanishes for any rapidity, leading to $S_R(\theta) = 0$, rendering scattering purely transmissive. In this scenario, thermodynamics is derived via the standard machinery of the Thermodynamic Bethe Ansatz [65]. To facilitate this, the root density describing particle density of kink, antikink, and breathers for any rapidity is supplemented by introducing the filling fraction ϑ to quantify relative mode occupancy. Conveniently, the filling functions can be parametrized through effective energy as $\vartheta(\theta) = \frac{1}{1+e^{\varepsilon(\theta)}}$. Kinks, antikinks, and breathers are each characterized by their own effective energy, determined as the solution to the following integral equations:

$$\varepsilon_K(\theta) = \beta E_K(\theta) + \int \frac{d\theta'}{2\pi} \varphi(\theta - \theta') \left(\log(1 + e^{-\varepsilon_K(\theta')}) + \log(1 + e^{-\varepsilon_{\bar{K}}(\theta')}) \right) \quad (3.39)$$

$$+ \sum_{n=1}^N \int \frac{d\theta'}{2\pi} \varphi_n(\theta - \theta') \log(1 + e^{-\varepsilon_n(\theta')})$$

$$\varepsilon_n(\theta) = \beta E_n(\theta) + \int \frac{d\theta'}{2\pi} \varphi_n(\theta - \theta') \left(\log(1 + e^{-\varepsilon_K(\theta')}) + \log(1 + e^{-\varepsilon_{\bar{K}}(\theta')}) \right)$$

$$+ \sum_{n'=1}^N \int \frac{d\theta'}{2\pi} \varphi_{n,n'}(\theta - \theta') \log(1 + e^{-\varepsilon_n(\theta')}) \quad (3.40)$$

where E_K and E_n are relativistic bare energies for (anti-)kink and breathers with masses M and m_n respectively.

	Numerics	Theory
$L_{\text{kink}}(0)$	0.0953101	0.0953102
$L_1(0)$	0.287682	0.287682
$L_2(0)$	0.117783	0.117783
$L_3(0)$	0.0645385	0.0645385
$L_4(0)$	0.040822	0.040822
$L_5(0)$	0.0281709	0.0281709
$L_6(0)$	0.0206193	0.0206193
$L_7(0)$	0.0157483	0.0157484
$L_8(0)$	0.0124225	0.0124225
$L_9(0)$	0.0100503	0.0100503

Table 3.1 In the high temperature limit the fillings are constant. The values are exactly known to be $\varepsilon_n = n(n + 2)$ and here we display the values for the so-called L -functions defined as $L_n(\theta) = \log(1 + \exp(-\varepsilon_n(\theta)))$. See [7] and references therein. The soliton mass is $M = 1$, the inverse temperature $\beta = 0.001$ and the number of breathers is set to $N = 9$. The integral equations are transformed into matrix equations and solved via Newton method. We used 50 points in rapidity space with an error tolerance of 10^{-10} .

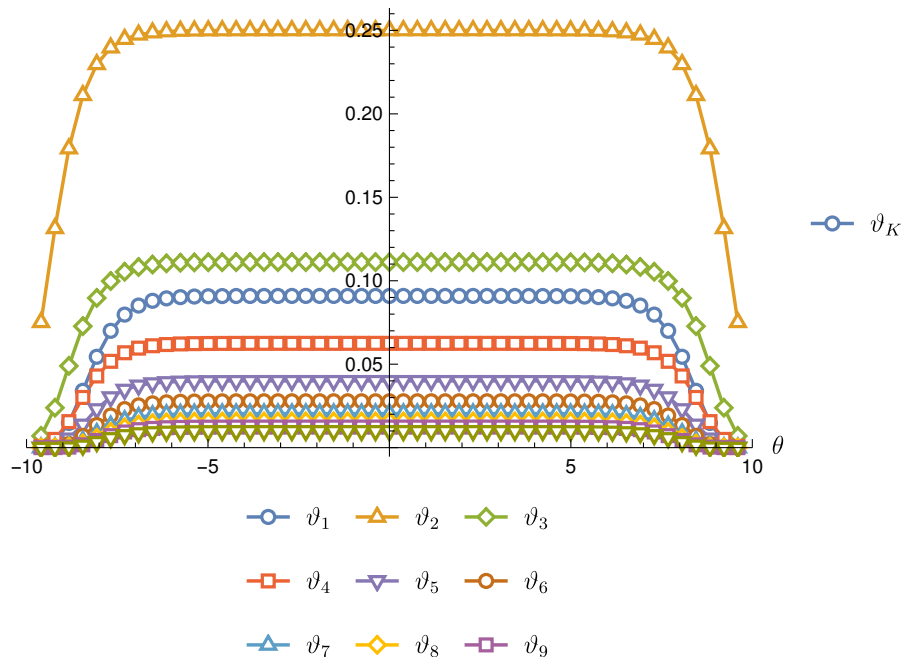


Fig. 3.3 Filling functions from the numerical solution of the TBA equations (3.39) and (3.40). Same parameters as Table 3.1.

Attractive regime and repulsive regimes

In the repulsive regime the TBA equations describing the thermodynamics of the Sine-Gordon model were derived in [186].

Atractive regime

In the attractive regime the TBA description is very recent and has been derived in [187]. We will not report the full expressions as we have not explored this regime, except at the reflectionless points where the TBA structure is diagonal.

3.2.2 Classical Sine-Gordon

The regime where semiclassical approximations apply is of significant importance, both for numerical validations and potential experimental uses, as we delve deeper into in the primary text. The precise thermodynamics associated with the classical sine-Gordon model was only recently formulated, as seen in Ref. [6]. We direct readers to this reference for an exhaustive discussion and merely present the core formulas and concepts here.

The semiclassical regime can be seen as a proper limiting case of the quantum model, more specifically one introduces an effective Planck constant $\hbar \rightarrow 0$ and simultaneously rescale the interaction $g_q^2 = \hbar g^2$ and temperature $\beta_q = \hbar \beta$, while keeping the fixed the product $\beta_q M_q = \beta M$. In this limit, one defines the continuum classical spectral parameter $\sigma \in [0, 1]$ through the correspondence $\sigma \leftrightarrow n\hbar/s_{\max}$ with

$$s_{\max} = \frac{8\pi}{cg^2} . \quad (3.41)$$

In the semiclassical limit, the number of breathers diverges and one replaces the discrete phase space of bound states with a continuum variable $\sigma \simeq hn$.

Then, one needs to scale the root densities and kink mass as

$$\left\{ \begin{array}{l} \rho_K = \lim_{\hbar \rightarrow 0} \rho_K^q(\theta) \\ \rho_s = \lim_{\hbar \rightarrow 0} \hbar^{-1} \rho_{n=s/\hbar}^q(\theta) \end{array} \right\} , \quad \left\{ \begin{array}{l} \rho_K^t = \lim_{\hbar \rightarrow 0} \hbar \rho_K^{qt}(\theta) \\ \rho_s^t = \lim_{\hbar \rightarrow 0} \hbar \rho_{n=s/\hbar}^q(\theta) \end{array} \right\} , \quad M = \lim_{\hbar \rightarrow 0} \hbar M_q \quad (3.42)$$

This ensures the correct scaling of the TBA. Notice that, in terms of the filling functions, the scaling is

$$\vartheta_{K,q}(\theta) \simeq \hbar \vartheta_K(\theta) \quad \vartheta_{n,q}(\theta) \simeq \hbar^2 \vartheta_s(\theta) \quad (3.43)$$

This scaling makes the limit of the statistical factors fairly simple. We define the classical energy of kinks as $\epsilon_K(\theta) = M \cosh \theta$ and analogously the energy of

antikinks, then the breather energy is $\epsilon_\sigma(\theta) = 2M \sin\left(\frac{\pi}{2} \frac{\sigma}{s_{\max}}\right)$, where one defines

$$M = \frac{8m}{g^2} . \quad (3.44)$$

In the subsequent discussions, we will confine our attention to classical quantities. Therefore, the tags "classical" and "quantum" are rendered redundant, implying a consistent reference to classical parameters.

In the shift to a semiclassical perspective, the reflective aspect of the kink-antikink scattering matrix diminishes, $S_R \rightarrow 0$ leading to purely transmissive scattering. This closely mirrors the equations touched upon in the previous segment. Nevertheless, distinctive differences emerge: the immediate semiclassical extension of the filling fractions becomes singular for diminishing σ . However, this anomaly is offset by the dressed momentum derivative, culminating in finite root densities giving rise to finite measurable observables in the semiclassical limit. To sidestep these deceptive singularities, it's prudent to redefine effective energies, dressings, and fillings appropriately. The dictionary follows closely Ref. [6]. For convenience, we present the results here, adapting the notations to fit our discussion. Utilizing a tilde, we introduce a nonsingular parametrization. The association of filling functions with effective energies manifests as:

$$\vartheta_K(\theta) = e^{-\epsilon_K(\theta)} \quad (3.45)$$

$$\vartheta_{\bar{K}}(\theta) = e^{-\epsilon_{\bar{K}}(\theta)} \quad (3.46)$$

$$\vartheta_\sigma(\theta) = e^{-\epsilon_\sigma(\theta)} . \quad (3.47)$$

The subsequent nonsingular fillings and conventional effective energies are introduced, manifesting as:

$$\tilde{\vartheta}_K(\theta) = e^{-\tilde{\epsilon}_K(\theta)} = \vartheta_K(\theta) \quad (3.48)$$

$$\tilde{\vartheta}_{\bar{K}}(\theta) = e^{-\tilde{\epsilon}_{\bar{K}}(\theta)} = \vartheta_{\bar{K}}(\theta) \quad (3.49)$$

$$\tilde{\vartheta}_\sigma = e^{-\sigma^2 \tilde{\epsilon}_\sigma(\theta)} = (s_{\max} \sigma)^2 \vartheta_\sigma(\theta) . \quad (3.50)$$

The integral equations determining the effective energy on thermal states best are expressed in the new parametrization as

$$\begin{aligned} \sigma \tilde{\varepsilon}_\sigma(\theta) &= -2 + \beta c^2 \frac{m_\sigma}{\sigma} \cosh \theta + \frac{1}{\sigma} \int \frac{d\theta'}{2\pi} \varphi_\sigma(\theta - \theta') (e^{-\tilde{\varepsilon}_K} + e^{-\tilde{\varepsilon}_{\bar{K}}}) \\ &\quad + \frac{1}{\sigma} \int \frac{d\theta'}{2\pi} \int_0^1 d\sigma' \varphi_{\sigma,\sigma'}(\theta - \theta') \frac{e^{-(\sigma')^2 \tilde{\varepsilon}_{\sigma'}(\theta')} - 1}{s_{\max}(\sigma')^2} \end{aligned} \quad (3.51)$$

$$\begin{aligned} \tilde{\varepsilon}_K(\theta) &= \log s_{\max} - 1 + \beta M c^2 \cosh \theta + \int \frac{d\theta'}{2\pi} \varphi(\theta - \theta') (e^{-\tilde{\varepsilon}_K} + e^{-\tilde{\varepsilon}_{\bar{K}}}) \\ &\quad + \int \frac{d\theta'}{2\pi} \int_0^1 d\sigma \varphi_\sigma(\theta - \theta') \frac{e^{-\sigma^2 \tilde{\varepsilon}_\sigma(\theta')} - 1}{s_{\max} \sigma^2} . \end{aligned} \quad (3.52)$$

Above, the classical breather-breather scattering shift is

$$\varphi_{\sigma,\sigma'}(\theta) = \frac{16}{c g^2} \log \left(\frac{[\cosh(\theta) - \cos((\sigma + \sigma')\pi/2)][\cosh(\theta) + \cos((\sigma - \sigma')\pi/2)]}{[\cosh(\theta) - \cos((\sigma - \sigma')\pi/2)][\cosh(\theta) + \cos((\sigma + \sigma')\pi/2)]} \right). \quad (3.53)$$

The remaining scattering shifts can be recovered as $\lim_{\sigma' \rightarrow 1} \varphi_{\sigma,\sigma'}(\theta) = 2\varphi_\sigma(\theta)$ and $\lim_{\sigma \rightarrow 1} \varphi_\sigma(\theta) = 2\varphi(\theta)$, where $\varphi_\sigma(\theta)$ is the breather-kink scattering shift. Consistently, also dressing equations should be conveniently redefined to remove the spurious singularities. To this end, we define a new dressing operation using bold labels $\{\tau_K, \tau_{\bar{K}}, \tau_\sigma\} \rightarrow \{\tau_K^{\mathbf{dr}}, \tau_{\bar{K}}^{\mathbf{dr}}, \tau_\sigma^{\mathbf{dr}}\}$ such that

$$\begin{aligned} \sigma \tau_\sigma^{\mathbf{dr}}(\theta) &= \frac{\tau_\sigma(\theta)}{\sigma} - \frac{1}{\sigma} \int \frac{d\theta'}{2\pi} \varphi_\sigma(\theta - \theta') [\tilde{\vartheta}_K(\theta') \tau_K^{\mathbf{dr}}(\theta') + \tilde{\vartheta}_{\bar{K}}(\theta') \tau_{\bar{K}}^{\mathbf{dr}}(\theta')] \\ &\quad - \frac{1}{\sigma} \int_0^1 \frac{d\sigma'}{s_{\max}} \int \frac{d\theta'}{2\pi} \varphi_{\sigma,\sigma'}(\theta - \theta') \tilde{\vartheta}_{\sigma'}(\theta') \tau_{\sigma'}^{\mathbf{dr}}(\theta'), \end{aligned} \quad (3.54)$$

$$\begin{aligned} \tau_K^{\mathbf{dr}}(\theta) &= \tau_K(\theta) - \int \frac{d\theta'}{2\pi} \varphi(\theta - \theta') [\tilde{\vartheta}_K(\theta') \tau_K^{\mathbf{dr}}(\theta') + \tilde{\vartheta}_{\bar{K}}(\theta') \tau_{\bar{K}}^{\mathbf{dr}}(\theta')] \\ &\quad - \int_0^1 \frac{d\sigma}{s_{\max}} \int \frac{d\theta'}{2\pi} \varphi_\sigma(\theta - \theta') \tilde{\vartheta}_{\sigma'}(\theta) \tau_{\sigma'}^{\mathbf{dr}}(\theta'). \end{aligned} \quad (3.55)$$

For the anti-kink the equation is identical. Passing from the standard dressing to the new parametrization, the following identities hold [6]: $\tau_K^{\mathbf{dr}}(\theta) = \tau_K^{\mathbf{dr}}(\theta)$, $\tau_{\bar{K}}^{\mathbf{dr}}(\theta) = \tau_{\bar{K}}^{\mathbf{dr}}(\theta)$, and $\tau_\sigma^{\mathbf{dr}}(\theta) = \sigma^2 \tau_\sigma^{\mathbf{dr}}(\theta)$.

3.2.3 Low and high temperature quantum thermodynamics

In the low and high temperature regimes TBA equations can be simplified. This is done in view of comparing predictions of BFT with known approaches. In the high temperature limit the Sine-Gordon field theory is described by a CFT and the fluctuations for the topological charge transport should take a universal form [140]. On the other hand, the low temperature limit allows comparison with Sachdev and Damle semiclassical theory to be introduced below.

3.3 Sachdev-Damle semi-classical theory

Drawing inspiration from earlier studies by Sachdev and Young [188, 189], Damle and Sachdev introduced a heuristic approach to compute phase fluctuations in sine-Gordon. Here, we outline their method and juxtapose it with our integrability-based exact results. While we summarize the essence of their derivation and results, the detailed computations can be referred to in the original paper. They base their method on several physical conjectures:

1. At reduced temperatures, the system behaves much like a sparse assembly of kinks and antikinks, that is the density is low. These are interpreted as a gas of classical solitons with Maxwell-Boltzmann statistics of the form $\sim e^{-\beta\epsilon_K(\theta)}$ where $\epsilon_K(\theta) = M \cosh \theta$. In the low-temperature regime, the relativistic dispersion is substituted with its low momentum counterpart, adopting a Galilean nature. For thermodynamic calculations, breather effects and excitation interactions are sidelined. Therefore, (anti-)kinks spread independently, and their count in an interval of size L follows Poisson statistics. Similarly, the velocities of these entities equate to the inherent velocity of relativistic particles given by $v_K = \tanh \theta$. Such insights establish the foundational conditions at $t = 0$ for this soliton "gas".
2. Only (anti-)kinks contribute to phase changes, causing shifts in multiples of 2π . Therefore, determining the phase disparity across a spatial segment $[0, x]$ is tantamount to counting the enclosed kinks and anti-kinks, expressed as $\phi(x) - \phi(0) = 2\pi(N_K - N_{\bar{K}})$
3. For the computation of unequal time correlations, the initial field configuration must evolve over time. Individual (anti)kinks advance as free entities with a velocity $\tanh \theta$. However, upon encounter, their scattering exhibits

complexities. Damle and Sachdev analyzed two potential scattering situations: initially, inspired by the typical low-energy scattering phenomena, they postulated an exclusively reflective mechanism. Subsequently, guided by the "reflectionless points" in quantum sine-Gordon, they proposed an entirely transmissive mechanism. It's plausible to extend this method to incorporate probabilistic outcomes during scattering events based on reflection and transmission magnitudes. Yet, this approach doesn't account for positional shifts due to interactions, which are often addressed in the context of soliton gases in several models. A thorough consideration of these spatial displacements, combined with the coherence emerging from scattering diagonalization, culminates in GHD.

Leveraging these hypotheses, Damle and Sachdev deduced the correlation function for the vertex operator $\mathcal{V}_\lambda = \langle e^{i\phi(x,t) - \phi(0,0)} \rangle$. Their findings are:

$$\mathcal{V}_\lambda(t, x)|_{\text{transmissive}} = C \exp \left[-2 \sin^2(\pi\lambda)(q_r + q_l) \right] \quad (3.56)$$

$$\mathcal{V}_\lambda(t, x)|_{\text{reflective}} = C e^{-q_r - q_l} \left[U_0(2iq_r\Theta, 2i\sqrt{q_l q_r}) + U_0(2iq_l\Theta, 2i\sqrt{q_l q_r}) \right] \quad (3.57)$$

$$- iU_1(2iq_r\Theta, 2i\sqrt{q_l q_r}) - iU_1(2iq_l\Theta, 2i\sqrt{q_l q_r}) - I_0(2\sqrt{q_l q_r}) \quad (3.58)$$

Where I_0 denotes the modified Bessel function, $U_{0,1}$ represents the Lommel functions, and the (relatively inconsequential) constant C is related to the expectation value of $\langle e^{i\lambda\phi(x,t)} \rangle$ on the state. We further defined $\Theta = \cos(2\pi\lambda)$ and

$$q_l = 2 \int_{\tanh\theta > x/t} \frac{d\theta}{2\pi} M \cosh\theta e^{-\beta\epsilon(\theta)} (t \tanh\theta - x), \quad (3.59)$$

$$q_r = 2 \int_{\tanh\theta < x/t} \frac{d\theta}{2\pi} M \cosh\theta e^{-\beta\epsilon(\theta)} (x - t \tanh\theta), \quad (3.60)$$

The large-time behaviors of these correlation functions vary considerably across the two conditions. In a purely transmissive scenario, kinks disperse uniformly without any disturbances from other excitations. This behavior is distinctly captured in the equation:

$$\mathcal{V}_\lambda(t, x)|_{\text{transmissive}} = C \exp \left[-2 \sin^2(\pi\lambda) \int \frac{d\theta}{2\pi} M \cosh\theta 2e^{-\beta\epsilon(\theta)} |x - t \tanh\theta| \right]. \quad (3.61)$$

3.4 Cumulants and Full Counting Statistics

For spacings obeying $|x/t| > 1$, the t -dependent part nullifies since it represents an odd function. This leads to the following representation:

$$\mathcal{V}_\lambda(t, x) = C e^{-2 \sin^2(\pi\lambda)n|x|} \quad |x/t| > 1 \quad (3.62)$$

where n is the overall kink density.

There is a light-cone phenomenon: outside this cone, the nature of collisions becomes irrelevant.

However, for time-like regions, the narrative is different. In the reflective case, kinks that move ballistically halt abruptly upon encountering an antikink. Essentially, in this perspective, at macro levels, (anti)kinks don't navigate uniformly but spread diffusively. In more complex scenarios, with both reflective and transmissive channels operational, one could speculate a combined evaluation wherein (anti)kinks are sporadically reflected or transmitted based on exact magnitudes derived from the precise two-body scattering matrices [49]. Adopting a rudimentary semiclassical view, it's tempting to perceive these scattering events as uncorrelated. In this view, diffusion becomes the overriding factor in the long run. Yet, our exact result, inspired by Ballistic Fluctuation Theory, always showcases a predominant ballistic element (with considerable effective velocity modifications) even in the presence of possible reflective scatterings. This behavior is attributed to the model's integrability ensuring ballistic transport and the recognition that scatterings aren't independent but display significant coherence.

3.4 Cumulants and Full Counting Statistics

Here we want to apply BFT to the calculation of the cumulants and the probability distribution of the phase differences in the classical Sine-Gordon model and compare it with microscopic numerical simulations. We also compute the cumulants in the quantum model at the reflectionless points and show that they go to their semiclassical limit in the proper scaling limit [6]. Of course, full analytical calculation is impossible due to the dressing equations. To evaluate the quantities numerically the starting point is (1.167) but the form of its last term is not very convenient and we have to manipulate it.

3.4.1 Expression for the SCGF: FCS and correlation functions

Let us consider for simplicity the case $x = \ell \sin(0) = 0$ (the extension to generic rays is trivial) and let us write

$$f_{\lambda, \alpha=0} = f_{\text{dyn}}(\lambda) \quad (3.63)$$

that is we factor out the dynamical part of the SCGF. We will do something similar in Chapter 4 when computing entanglement evolution after a quench. We can manipulate the last term of (1.167) as

$$\begin{aligned} \sum_j \int \frac{d\theta}{2\pi} \sum_{\kappa \in \{\pm\}} \sum_{v_j^{\text{eff}}(\theta, \bar{\lambda})=0} \kappa (F(\vartheta_j(\theta, \bar{\lambda})) - F(\vartheta_j(\theta, 0))) = \\ \sum_j \int \frac{d\theta}{2\pi} \sum_{v_j^{\text{eff}}(\theta, \bar{\lambda})=0} \frac{\partial_\lambda v_j^{\text{eff}}(\theta, \bar{\lambda})}{|\partial_\lambda v_j^{\text{eff}}(\theta, \bar{\lambda})|} (F(\vartheta_j(\theta, \bar{\lambda})) - F(\vartheta_j(\theta, 0))) = \\ \int d\lambda \sum_j \int \frac{d\theta}{2\pi} \delta(v_j^{\text{eff}}(\theta, \lambda)) \partial_\lambda v_j^{\text{eff}}(\theta, \lambda) (F(\vartheta_j(\theta, \lambda)) - F(\vartheta_j(\theta, 0))) \end{aligned} \quad (3.64)$$

where the sum over j in to account for the possibility of many particle spieces. In the Sine-Gordon case, in fact, there are bound states in addition to kinks and anti-kinks. We now wish to use the Dirac δ to integrate over the space of the rapidities. In this way, we will have a λ -dependent function that can be integrated on the fly while evolving the flux using (1.170) for the pseudo-energy or (1.171) for the filling.

First, we further simplify the delta. We recall that $v^{\text{eff}} = (\partial_\theta E)^{\text{dr}} / (\partial_\theta p)^{\text{dr}}$. The effective velocity is zero only if $(\partial_\theta E)^{\text{dr}} = 0$, hence

$$\delta(v^{\text{eff}}) = \delta[(\partial_\theta E)^{\text{dr}}] |(\partial_\theta p)^{\text{dr}}| \quad (3.65)$$

On the other hand, we can also notice that $\partial_\lambda v^{\text{eff}} = \frac{\partial_\lambda (\partial_\theta E)^{\text{dr}}}{(\partial_\theta p)^{\text{dr}}} - v^{\text{eff}} \frac{\partial_\lambda (\partial_\theta p)^{\text{dr}}}{(\partial_\theta p)^{\text{dr}}}$, but this must be evaluated on those points with $v^{\text{eff}} = 0$. Hence, in the end one gets (we assume $(\partial_\theta p)^{\text{dr}} > 0$, which is always the case)

$$\delta(v^{\text{eff}}) \partial_\lambda v^{\text{eff}} = \delta[(\partial_\theta E)^{\text{dr}}] \partial_\lambda [(\partial_\theta E)^{\text{dr}}] \quad (3.66)$$

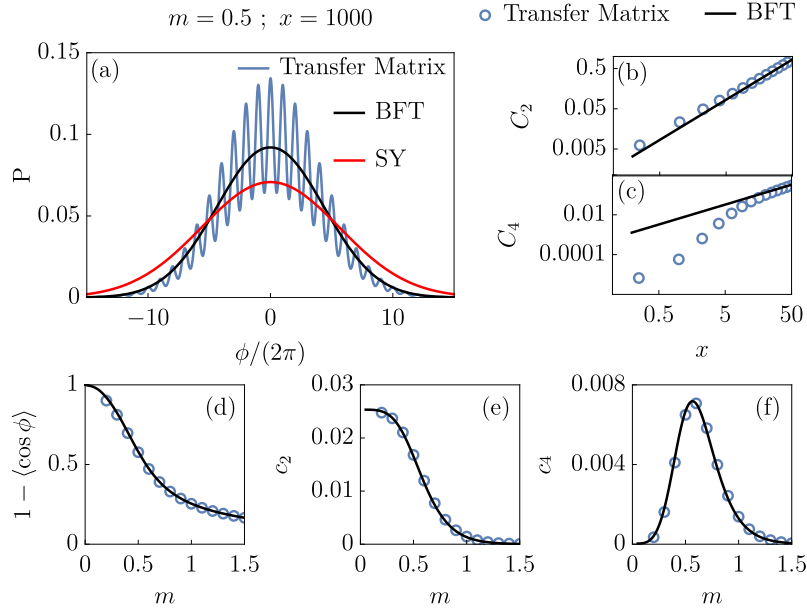


Fig. 3.4 Equal-time probability & cumulants.— We compare analytic predictions (BFT) [black line] in the classical regime of Sine-Gordon model with predictions from the SY picture [red line] and numerical results from Transfer Matrix [blue line and symbols]. The bare mass m is tuned while keeping $\beta = g = c = 1$. (a) The probability of phase differences is reported for a typical mass scale and distance, showing the convergence to the scaling behavior. (b-c) The convergence of cumulants upon increasing the relative distance is shown. (d-f) We scan different values of the bare mass: the vertex operator (d) helps to identify the strongly-interacting regimes away from the massless limit $\langle \cos \phi \rangle \simeq 1$ and the large-mass non-interacting regime $1 - \langle \cos \phi \rangle \simeq (4m)^{-1}$ [6]. (e-f) The large-distance scaling of the 2nd and 4th cumulants is shown, clearly non-Gaussian and in perfect agreement with numerics.

Hence we now reach the expression

$$\int d\lambda \sum_j \int \frac{d\theta}{2\pi} \delta[(\partial_\theta E)^{\text{dr}}] \partial_\lambda [(\partial_\theta E)^{\text{dr}}] (F(\vartheta_j(\theta, \lambda)) - F(\vartheta_j(\theta, 0))) \quad (3.67)$$

Finally, we use the δ to integrate in the space of rapidities

$$\int d\lambda \sum_j \frac{1}{2\pi} \left\{ \frac{\partial_\lambda [(\partial_\theta E)^{\text{dr}}]}{|\partial_\theta (\partial_\theta E)^{\text{dr}}|} (F(\vartheta_j(\theta, \lambda)) - F(\vartheta_j(\theta, 0))) \right\}_{(\partial_\theta E)^{\text{dr}}=0} \quad (3.68)$$

This is easier to handle than the original form, at least numerically. The quantity $\partial_\theta (\partial_\theta E)^{\text{dr}}$ can be easily computed by interpolations, while $\partial_\lambda [(\partial_\theta E)^{\text{dr}}]$ can be made explicit by using that we know how the filling changes thanks to the flow

equations (1.171). In order to compare with microscopic simulation of the classical Sine-Gordon equation we have to perform the semi-classical limit of the SCGF (1.167). Using the diagonal structure of the classical TBA we obtain

$$\begin{aligned}
f_{\text{dyn}}(\lambda) = & \int \frac{d\theta}{2\pi} \left\{ \partial_{\theta} E_K \left[\text{sign}(v_K^{\text{eff}}(\theta)) (\vartheta_K(\theta, \lambda) - \vartheta_K(\theta, 0)) \right] \right\} \\
& + \int \frac{d\theta}{2\pi} \left\{ \partial_{\theta} E_{\bar{K}} \left[\text{sign}(v_{\bar{K}}^{\text{eff}}(\theta)) (\vartheta_{\bar{K}}(\theta, \lambda) - \vartheta_{\bar{K}}(\theta, 0)) \right] \right\} \\
& + \int_0^{s_{\text{max}}} ds \int \frac{d\theta}{2\pi} \left\{ \partial_{\theta} E_s(\theta) \left[\text{sign}(v_s^{\text{eff}}(\theta)) (\vartheta_s(\theta, \lambda) - \vartheta_s(\theta, 0)) \right] \right\} \\
& - \int d\lambda \frac{1}{2\pi} \left\{ \partial_{\theta} E_K(\theta) \frac{\partial_{\lambda} [(\partial_{\theta} E_K)^{\text{dr}}]}{|\partial_{\theta} (\partial_{\theta} E_K)^{\text{dr}}|} (\vartheta_K(\theta, \lambda) - \vartheta_K(\theta, 0)) \right\}_{(\partial_{\theta} E)^{\text{dr}}=0} \\
& - \int d\lambda \frac{1}{2\pi} \left\{ \partial_{\theta} E_{\bar{K}}(\theta) \frac{\partial_{\lambda} [(\partial_{\theta} E_{\bar{K}})^{\text{dr}}]}{|\partial_{\theta} (\partial_{\theta} E_{\bar{K}})^{\text{dr}}|} (\vartheta_{\bar{K}}(\theta, \lambda) - \vartheta_{\bar{K}}(\theta, 0)) \right\}_{(\partial_{\theta} E_{\bar{K}})^{\text{dr}}=0} \\
& - \int_0^{s_{\text{max}}} ds \int d\lambda \frac{1}{2\pi} \left\{ \partial_{\theta} E_s(\theta) \frac{\partial_{\lambda} [(\partial_{\theta} E_s)^{\text{dr}}]}{|\partial_{\theta} (\partial_{\theta} E_s)^{\text{dr}}|} (\vartheta_s(\theta, \lambda) - \vartheta_s(\theta, 0)) \right\}_{(\partial_{\theta} E_s)^{\text{dr}}=0} \quad (3.69)
\end{aligned}$$

A similar analysis can be put forward for the static part of the SCGF

$$f_{\lambda, \alpha=\pi/2} = f_{\text{stat}}(\lambda) \quad . \quad (3.70)$$

Such quantity is easily obtained from the dynamic part with the substitutions

$$\text{sign}(v^{\text{eff}}) \rightarrow 1 \quad (3.71)$$

$$E \rightarrow p \quad (3.72)$$

something similar to crossing symmetry in relativistic field theories. This static part is what is used to plot the probability distribution in 3.4. One computes $f_{\text{stat}}(\lambda)$ and then performs a Legendre-Fenchel transform numerically.

The full SCGF can be manipulated in the same way starting from (1.167).

3.4.2 Cumulants

Since the SCGF is the generating function of (scaled) cumulants their exact expression in terms of TBA quantities can be obtained via differentiation. The derivations are tedious but straightforward. In the original paper [1, 2] the authors present the cumulants for the current fluctuations up to the fourth. Here we present the

cumulants for the random process

$$\Omega(x, t) = \int^{(x,t)} j(x, t) dt - q(x, t) dx \quad (3.73)$$

already introduced in (1.155) generalising in a natural way the result [1, 2]. The scaled even cumulants read (we consider only parity invariant states)

$$c_2 = \int d\theta \rho(\theta) |\sin \alpha - \cos \alpha v^{\text{eff}}| [h^{\text{dr}}(\theta)]^2 \quad (3.74)$$

$$\begin{aligned} c_4 = \int d\theta |\sin \alpha - \cos \alpha v^{\text{eff}}| g \rho(\theta) \{ & (h^{\text{dr}})^4 \hat{g} \tilde{g} + 3 [(sf(h^{\text{dr}})^2)^{\text{dr}}]^2 \\ & + 4 h^{\text{dr}} [g \tilde{g} (h^{\text{dr}})^3]^{\text{dr}} + 6 s \tilde{g} (h^{\text{dr}})^2 [sf(h^{\text{dr}})^2]^{\text{dr}} \\ & + 12 h^{\text{dr}} [sf h^{\text{dr}} (sf(h^{\text{dr}})^2)^{\text{dr}}]^{\text{dr}} \} \end{aligned} \quad (3.75)$$

where ρ is the root density. We recall that this has to be extracted from the TBA structure of the integrable model of interest, in this case the Sine-Gordon model. To compute it, one has to solve first (1.56) for ρ^t and then use its relation to the filling factor ϑ eq. (1.49). Moreover we have the definitions

$$\hat{g} = -\frac{d}{d\epsilon} \log(g \tilde{g}) - 3g \quad , \quad \tilde{g} = -\frac{d}{d\epsilon} \log(g) - 2g \quad (3.76)$$

that are statistical factors depending on $g(\vartheta)$ defined in (1.172) and

$$s = \text{sign}(\sin \alpha - \cos \alpha v^{\text{eff}}) \quad (3.77)$$

is a sign factor. All the quantities depend on the rapidity θ , the ray angle (different parametrisations are possible) α and the flow parameter λ . The calculation of the cumulants does not require the solution of the λ -flow once they are explicitly written in terms of TBA quantities. The first two even cumulants on generic space-time rays are written in (3.74) and (3.75). Besides standard TBA quantities they depend on various statistical factors. They are defined in (1.172) and (3.76). In the quantum sine-Gordon it is readily seen that as functions of the filling they are

$$g(\vartheta) = \begin{cases} 1 - \vartheta & \text{quantum} \\ 1 & \text{classical} \end{cases} \quad (3.78)$$

$$\tilde{g}(\vartheta) = \begin{cases} \vartheta - 2 & \text{quantum} \\ -2 & \text{classical} \end{cases} \quad (3.79)$$

$$\hat{g}(\vartheta) = \begin{cases} \frac{6\vartheta - 6 - \vartheta^2}{2 - \vartheta} & \text{quantum} \\ -3 & \text{classical} \end{cases} \quad (3.80)$$

from which the calculation of the cumulants becomes just a matter of matrix multiplication when discretising the rapidity integrals. In Fig. 3.4 (b)-(c) one can see the linear scaling with the size of the interval x of cumulants along the purely space direction while in (e)-(f) confirms the non-gaussianity of the distribution as function of the bare mass while all the other parameters are fixed. More interesting for the cumulants is Fig. 3.5 where we show two important things. In (a.1)-(b.1), the numerically computed cumulants from microscopic and montecarlo simulations of the classical Sine-Gordon equation are compared with cumulants obtained by solving the TBA equations (3.52) and (3.51) for the classical thermodynamics. The details of the montecarlo simulations can be found in [5] and in [6] but are now standard techniques in the context of out-of-equilibrium classical field theories. We have considered varying bare masses (this is equivalent to change the soliton mass) and the agreement with BFT is excellent. Secondly, in (a.2)-(b.2), it is shown that the cumulants of the quantum model at the reflectionless points approach the corresponding cumulants of the classical model in the appropriate scaling limit. The limit is done numerically in the following way. Below we reintroduce for a moment the notation for which the subscript q indicates a quantum quantity while no subscript means a classical quantity. We recall that $g_q = \hbar g$ and that the interaction is set as in (3.38). The number of breathers is N so that taking into account the scaling of the coupling with \hbar we have

$$(1 + N)^{-1} = \frac{\hbar g^2}{8\pi} \left(1 - \frac{\hbar g^2}{8\pi} \right)^{-1} \quad (3.81)$$

from which one sees that $N \gg 1$ corresponds to $\hbar \ll 1$. Recalling the soliton mass scaling $M_q = \hbar^{-1} M$ and the temperature scaling $\beta_q = \hbar \beta$ and further fixing $g = 1$ (always possible in a classical theory) and $\beta = 1$ for convenience we then tune N (number of breathers). We can see that even for a modest number of breathers $N = 10$ the quantum theory is not that far from the classical one. This is not trivial and such a semi-classical scaling was never analysed in such detail before. What we did in practice is to numerically solve the classical and quantum TBA equations (3.51)-(3.52) for the classical Sine-Gordon model. This is done in the

3.4 Cumulants and Full Counting Statistics

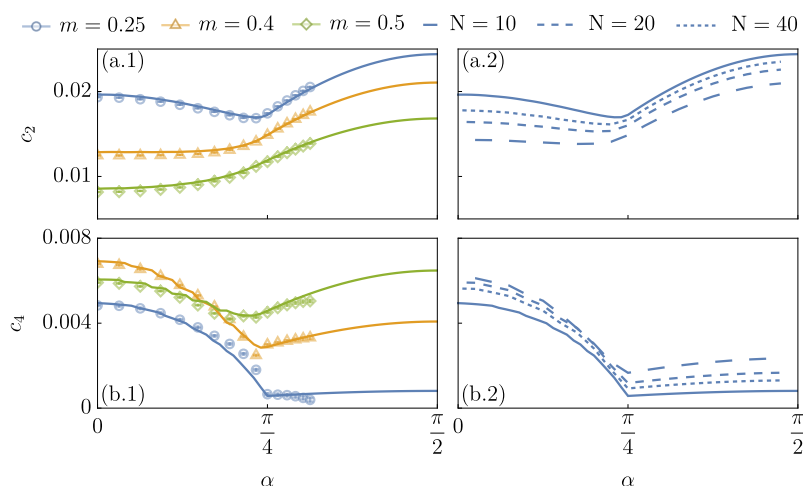


Fig. 3.5 Cumulants with space-time separation.— Scaling behavior of the second (a.1) and fourth (b.1) cumulant as function of the ray $x/t = \tan \alpha$ for representative choices of the mass scale m ($\beta = g = 1$) in the classical regime. Numerical values obtained with Monte Carlo (symbols) closely follow the analytic BFT prediction (solid lines). In Figure (a.2) and (b.2) we show the approach of the quantum prediction (dashed lines) to the classical limit (solid line) for the c_2 and c_4 , respectively. We take $m = 0.25$ and increase the number of breathers N , while tuning the quantum soliton mass according to the semiclassical limit [6].

usual way discretising integral operators and performing matrix operations. In Fig. 3.6 we show another comparison between spatial cumulants computed in the framework of BFT compared to numerical simulations. In panel (a), to emphasize the role of finite volume and periodic boundary conditions, we show the second cumulant $C_2(x)$ at equal times for two different volume realizations compared to (3.74). As an example, we choose $g = \beta = 1$ and $m = 0.25$. The second cumulant cannot grow forever and reaches a maximum peak in the center of the system: the linear growth predicted by BFT is realized at large distances compared with the microscopic correlation lengths, but much smaller than the system's size L . To reduce finite size effects within a fixed window $[0, \ell_{\max}]$ with ℓ_{\max} the maximum separation between the two points, we extract the scaling factors $c_n = C_n(x)/x$ by taking three system sizes of $L = 1024$, $L = 2048$ and $L = 4096$ respectively (the latter not shown in (a)) and extrapolate to infinite volume assuming corrections scale as $1/L$. The fourth cumulant is always much more challenging due to finite size effects. In (b)-(c) we show a typical example of the second and fourth cumulants for space-time separation, plotted as a function of time for different rays $\tan \alpha = x/t$ and already extrapolated to infinite size. As an example, we choose $g = \beta = 1$ and $m = 0.25$. The second cumulant (b) shows a clear linear growth

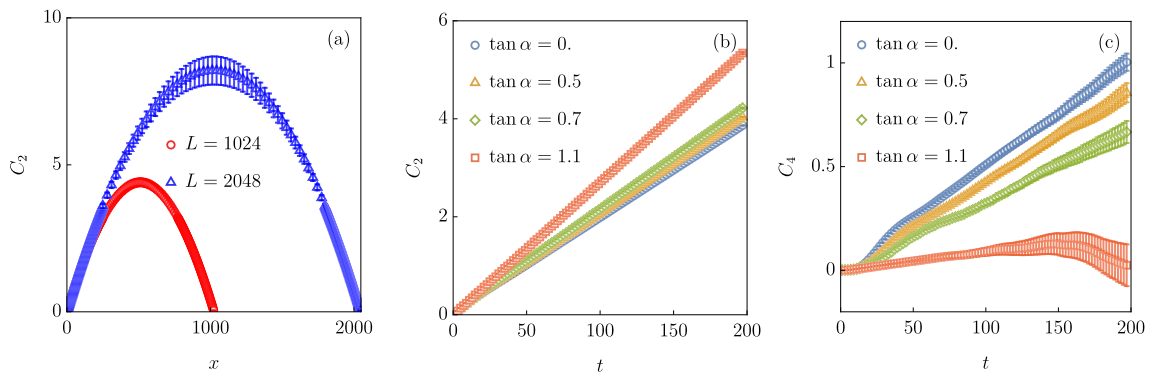


Fig. 3.6 **Further details on Monte Carlo data.**— (a) Role of periodic boundaries. (b)-(c) linear growth of cumulants along different rays.

with no appreciable corrections. The fourth cumulant C_4 (c) shows finite time corrections in the form of oscillations. C_4 is also more sensitive to finite-size corrections, as it is evident from the curve $\tanh \alpha = 1.1$: after an initial linear growth, suddenly bends downward with increased uncertainty: there, the extrapolation to infinite size fails and one can trust the curve $\tanh \alpha = 1.1$ up to $t \simeq 100$ at most. This issue could be solved by exploring even larger sizes, but the computational time needed for the Monte Carlo to reach convergence becomes prohibitively long.

We have gone a bit further than just this. We have also computed the second cumulant utilising experimentally realistic parameters. We have already mentioned that the Sine-Gordon model appears in the description of tunnel coupled quasi-condensates. Here we briefly explain the idea of how this experimental setup is realised. For a visual idea look at Fig. 3.7 (a). First, one realises quasi one dimensional condensates via laser confinement and then couples two of these tubes via a barrier which can be finely tuned thanks to atom chip technology. Such barrier induces weakly attractive interactions between the condensates and in the low energy sector, via bosonisation, in can be shown that the interference between the phases is described by the Sine-Gordon Hamiltonian.

Phase reconstruction measurement

In order to explain a bit how the experimental setup works we follow the SM of [5]. In the experimental setup, the phase is extracted from matter-wave interferometry measurements [176]. The two elongated condensates are suddenly released from the external three-dimensional trap keeping them in place, allowing the gas to expand. Because of the initial close confinement in the transverse direction, the

particle momentum following trap release is quite high. In order to reconstruct the position-dependent phase profile, one can proceed on the assumption that expansion occurs only in the transverse direction and that longitudinal evolution is frozen. The three-dimensional density profile is described by [190]

$$\begin{aligned}
 n_{3D}(x, \vec{r}, t) = & |f(\vec{r}, t)|^2 [\psi_1^\dagger(x)\psi_1(x) + \psi_2^\dagger(x)\psi_2(x) \\
 & + \psi_1^\dagger(x)\psi_2(x)e^{-i\vec{d}\cdot\vec{r}m/(\hbar t)} + \psi_2^\dagger(x)\psi_1(x)e^{i\vec{d}\cdot\vec{r}m/(\hbar t)}] \simeq \\
 & |f(\vec{r}, t)|^2 2n(x) \left[1 + \cos(\phi(x) - \vec{d}\cdot\vec{r}m/(\hbar t)) \right], \quad (3.82)
 \end{aligned}$$

where $\psi_i(x)$ are two complex fields describing the coupled condensates. In the last line one uses the density-phase approximation representation of the complex field. Above, x refers to the longitudinal spatial coordinate while \vec{r} is the radial direction (perpendicular to the direction of the tubes), \vec{d} is the relative distance of the two tubes. Finally, f is a Gaussian envelope coming from the expansion in plane waves of the transverse oscillator ground state function, the specific form is not needed for our purposes (see however Ref. [178], also for corrections beyond the weakly-interacting regime).

The three dimensional density is then projected in the plane containing the condensate by integrating in the orthogonal direction. Then the resulting two-dimensional pattern is sliced along the longitudinal direction x and the oscillating pattern in the remaining orthogonal direction is fitted with the oscillating function, extracting the phase shift $\phi(x)$. This procedure is equivalent to measure independently $n(x) \cos(\phi(x))$ and $n(x) \sin(\phi(x))$, as it is clearly seen by expanding the cosine (3.82) with the help of trigonometric identities $n(x) \cos(\phi(x) - \vec{d}\cdot\vec{r}m/(\hbar t)) = n(x) \cos(\phi(x)) \cos(\vec{d}\cdot\vec{r}m/(\hbar t)) + n(x) \sin(\phi(x)) \sin(\vec{d}\cdot\vec{r}m/(\hbar t))$

In theory, by combining these two numbers, the phase profile might be retrieved precisely; but, due to experimental constraints, such as the camera's finite resolution, it is not possible to resolve arbitrary tiny distances without causing coarse graining. Pixels in the longitudinal directions are equispaced on a grid $\{x_i\}_{i=1}^N$, with approximately $2\mu\text{m}$ spacing. The center of each pixel collects signals from its surrounding: in a good approximation, this imperfection can be mimicked

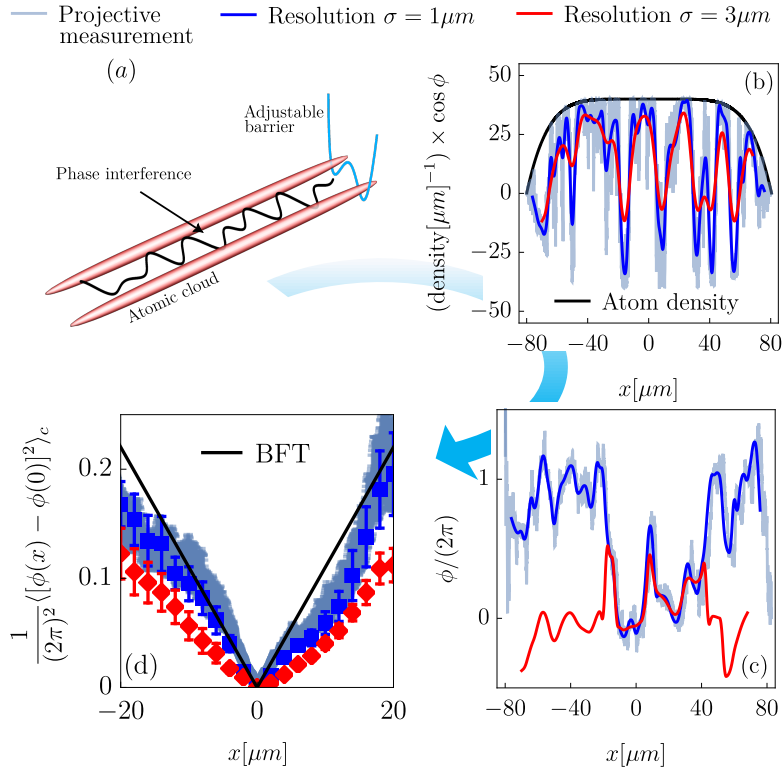


Fig. 3.7 (a) Experimental setup. (b-c) Phase-reconstruction protocol from the outcome of a single projective measurement for different pixel resolutions σ (see main text). (d) Statistics built on 100 samples already shows the scaling behavior of the equal-time second cumulant stemming from the center of the trap. The effect of a low resolution σ is to “miss” kinks (see also (c)) and underestimate phase fluctuations. A good quality measurement is already obtained with $\sigma = 1\mu\text{m}$. See main text for discussion of parameters, and the SM of [5] for further details and data. Credits to Dr. Alvise Bastianello for realising this picture.

by a convolution with a Gaussian with standard deviation σ [190]

$$[n(x_i) \sin(\phi(x_i))]_{\sigma} \equiv \int dy \frac{e^{-\frac{1}{2\sigma^2}(x_i-y)^2}}{\sigma\sqrt{2\pi}} n(y) \sin(\phi(y)) \quad (3.83)$$

$$[n(x_i) \cos(\phi(x_i))]_{\sigma} \equiv \int dy \frac{e^{-\frac{1}{2\sigma^2}(x_i-y)^2}}{\sigma\sqrt{2\pi}} n(y) \cos(\phi(y)). \quad (3.84)$$

We have simulated the projective measurement process on the phase allowing for a certain degree of error which is roughly speaking measured by σ and result are plotted in Fig. 3.7.

3.5 Comparison between semiclassics and BFT at low temperature

3.5.1 Semi-classical theory

In the spirit of the Sachdev and Damle semiclassical approach and based on what we said about the simplifications occurring in the low T limit, we can suppose there is a small density of kinks in the steady state. Since the density is small, kinks and anti-kinks are independently distributed according to a Poisson distribution of parameter μ . The distribution of the difference of independent Poisson variables is calculated in Appendix C.1.

Static fluctuations

Let us start simple and consider the case of purely spatial interval $[0, x]$. Let the average density of kinks and anti-kinks be $\mu = xd$ where d is the number of kinks per unit length. We have the charge

$$Q_x/(2\pi) = \int_0^x dy \partial_y \phi(y, 0) = \phi(x, 0) - \phi(0, 0) = (N_K - N_{\bar{K}}) \quad (3.85)$$

where N_K and $N_{\bar{K}}$ are the number of kinks and anti-kinks in the interval. The probability distribution of the charge is a Skellam distribution

$$P(Q_x/(2\pi) = x\delta) = e^{-2xd} I_{x\delta}(2xd) \quad (3.86)$$

where $I_n(z)$ is the Bessel function of order k . For large x follows a large deviation principle (see (C.24))

$$P(Q_x/(2\pi) = x\delta) \asymp e^{-xR(\delta, d)} \quad (3.87)$$

with $R(\delta, d)$ is calculated in Appendix C.2 and reads

$$R(\delta, d) = 2d + \delta \sinh^{-1} \left(\frac{\delta}{2d} \right) - \sqrt{(2d)^2 + \delta^2} \quad . \quad (3.88)$$

Space-time fluctuations

Let us consider the time evolution. In this case we have the difference of the fields at different times $\phi(0, 0) - \phi(x, t)$ and we want to know its distribution. As time goes solitons travel at speed $v(\theta)$ and if one soliton with rapidity θ was at $x = 0$ at time $t = 0$, it will be at $x' = v(\theta)t$ at time $t > 0$. This is true for every $\theta \in \mathbb{R}$ and

Sine-Gordon Field Theory

solitons with different rapidities are independent so their probability distribution factorises. This allows to work at fixed θ . The problem is simple because the field still jumps by $\pm 2\pi$. Due to the free dynamics of the solitons we will have $\phi(x, t) = \phi(x - v(\theta)t, 0)$

$$Q_x^\theta(t) = \phi(x_\theta, t) - \phi(0, 0) = \phi(x - v(\theta)t, 0) - \phi(0, 0) \quad , \quad (3.89)$$

and this means

$$Q_x(t) = \int d\theta Q_x^\theta(t) = 2\pi \int d\theta (N_K(\theta) - N_{\bar{K}}(\theta)) = \int d\theta Q_{x-v(\theta)t} \quad (3.90)$$

where now, $N_K(\theta)$ and $N_{\bar{K}}(\theta)$ are two Poisson variables with parameter

$$\mu(\theta) = \frac{1}{2\pi} (x - v(\theta)t) \vartheta(\theta) \quad (3.91)$$

where $\vartheta(\theta)$ is the fraction of solitons with rapidity θ . The full distribution is obtained as

$$\begin{aligned} P(Q_x(t)/(2\pi) = \Delta) &= \int \left(\prod_\theta dk_\theta \right) \delta \left(\int d\theta Q_x^\theta(t)/(2\pi) - \Delta \right) \prod_\theta P(Q_{x-v(\theta)t}/(2\pi) = k_\theta) \\ &= \int \left(\prod_\theta dk_\theta \right) \int \frac{ds}{2\pi} \prod_\theta e^{is(k_\theta - \Delta)} \prod_\theta P(Q_{x-v(\theta)t}/(2\pi) = k_\theta) \\ &= \int \frac{ds}{2\pi} e^{-is\Delta} \prod_\theta \int dk_\theta e^{isk_\theta} P(Q_{x-v(\theta)t}/(2\pi) = k_\theta) \\ &= \int \frac{ds}{2\pi} e^{-is\Delta} \prod_\theta \int dk_\theta e^{isk_\theta} e^{-2\mu(\theta)} I_{k_\theta}(2\mu(\theta)) \quad . \end{aligned} \quad (3.92)$$

The Fourier transform of the Bessel function with respect to its order is reported in Appendix C.3. Plugging eq. C.28 in the above formula, we obtain

$$\begin{aligned} P(Q_x(t)/(2\pi) = \Delta) &= \int_0^\pi \frac{ds}{2\pi} e^{-is\Delta} \prod_\theta \left[2\mu(\theta) \cos(s) e^{-2\mu(\theta)} \right] \\ &= \int_0^\pi \frac{ds}{2\pi} e^{-is\Delta} \exp \left\{ \int d\theta \log \left(2\mu(\theta) \cos(s) e^{-2\mu(\theta)} \right) \right\} \\ &= \int_0^\pi \frac{ds}{2\pi} e^{-is\Delta} \exp \left\{ \int d\theta \log (2\mu(\theta) \cos(s)) - 2 \int d\theta \mu(\theta) \right\} \quad . \end{aligned} \quad (3.93)$$

3.5 Comparison between semiclassics and BFT at low temperature

Now we use saddle-point method. To do this, we scale $\Delta \mapsto \ell\delta$, $x = \ell \sin \alpha$ and $t = \ell \cos \alpha$. In this way

$$\mu(\theta) \mapsto \ell\mu_\alpha(\theta) = \frac{\ell}{2\pi}(\sin \alpha - v(\theta) \cos \alpha)\vartheta(\theta) \quad (3.94)$$

and take $\ell \rightarrow +\infty$. This is the Euler scale limit. Noting that for $\ell \rightarrow +\infty$

$$\log(2 \cosh(\ell\mu_\alpha(\theta) \cos(s))) \sim 2\ell\mu_\alpha(\theta) \cos(s) \quad (3.95)$$

and defining momentarily

$$d_\alpha \equiv \int d\theta \mu_\alpha(\theta) \quad , \quad (3.96)$$

in this limit we are left with

$$P(Q_x(t)/(2\pi) = \ell\delta) = e^{-2d\ell} \int_0^\pi \frac{ds}{2\pi} e^{\ell f(s)} \quad , \quad (3.97)$$

with

$$f(s) = -\iota\delta s + 2d \cos(s) \quad . \quad (3.98)$$

which has to be evaluated by the saddle point method. In the Appendix C.4 we obtain

$$P(Q_x(t)/(2\pi) = \ell\delta) \asymp e^{-\ell R(\delta, d_\alpha)} \quad (3.99)$$

where again $R(\delta, d)$ is defined in (3.88). We take $\ell = \sqrt{t^2 + x^2}$.

3.5.2 BFT

Here we want to take the limit $\beta \rightarrow +\infty$ of the classical TBA equations (3.52) and (3.51), solve the flow equations to compute the SCGF, perform the Legendre-Fenchel transform and compare with Sachdev-Damle theory.

Low temperature classical TBA

In this limit the pseudo-energy of the kinks and anti-kinks in (3.45) is of order $\mathcal{O}(-\beta M)$ so that the filling $\vartheta_K = \mathcal{O}(e^{-\beta M})$ is small. Like-wise, the breathers filling is small, but in contrast, since their mass m_σ can be arbitrarily small, it can still be relevant with respect to the one of the kinks. In this regime the dressing equations *for the topological charge density* simplify. Indeed, the topological charge is $\tilde{Q} = Q/(2\pi) = \pm 1$ (recall we look at the rescaled charge, see (3.87)-(3.99) and Fig. 3.4) respectively for kinks and anti-kinks, while it's zero for breathers. Eq.

Sine-Gordon Field Theory

(3.54) gives zero to first order in the fillings for the breathers dressed topological charge density with $h_K(\theta)/(2\pi) = \tilde{h}_K = 1$ (we consider the kink for the moment). In turn, eq. (3.55) gives the bare one

$$h_K^{\text{dr}}(\theta) = h_K(\theta) \quad (3.100)$$

always in this regime of approximation, since kinks fillings are negligible and the contribution of the breathers is zero. Also, the pseudo-energy of breathers does not flow

$$\partial_\lambda \varepsilon_\sigma = 0 \quad (3.101)$$

and so do the breathers filling. Let us turn to the effective velocity of the kinks. Again, we neglect contributions to the dressing coming from the kinks fillings but this time we cannot neglect that from the background breathers because their dressed energy and momentum are not zero. For an illustration of this effect see Fig. 3.8. We have

$$(\partial_\theta E_K)^{\text{dr}}(\theta) = \partial_\theta E_K(\theta) - \int_0^1 \frac{d\sigma}{s_{\text{max}}} \int \frac{d\theta'}{2\pi} \varphi_\sigma(\theta - \theta') \vartheta(\theta', \sigma) (\partial_\theta E_\sigma)^{\text{dr}}(\theta') \quad , \quad (3.102a)$$

$$\sigma^2 (\partial_\theta E_\sigma)^{\text{dr}}(\theta) = - \int_0^1 \frac{d\sigma'}{s_{\text{max}}} \int \frac{d\theta'}{2\pi} \varphi_{\sigma, \sigma'}(\theta - \theta') \vartheta(\theta', \sigma') (\partial_\theta E_{\sigma'})^{\text{dr}}(\theta') \quad , \quad (3.102b)$$

and for the momentum

$$(\partial_\theta p_K)^{\text{dr}}(\theta) = \partial_\theta p_K(\theta) - \int_0^1 \frac{d\sigma}{s_{\text{max}}} \int \frac{d\theta'}{2\pi} \varphi_\sigma(\theta - \theta') \vartheta(\theta', \sigma) (\partial_\theta p_\sigma)^{\text{dr}}(\theta') \quad , \quad (3.103a)$$

$$\sigma^2 (\partial_\theta p_\sigma)^{\text{dr}}(\theta) = - \int_0^1 \frac{d\sigma'}{s_{\text{max}}} \int \frac{d\theta'}{2\pi} \varphi_{\sigma, \sigma'}(\theta - \theta') \vartheta(\theta', \sigma') (\partial_\theta p_{\sigma'})^{\text{dr}}(\theta') \quad . \quad (3.103b)$$

By virtue of (3.101), these equations give a non-zero effective velocity which is nevertheless independent of the flow parameter and the same for kinks and anti-kinks

$$v_K^{\text{eff}} = v_{\bar{K}}^{\text{eff}} \equiv v^{\text{eff}} \quad . \quad (3.104)$$

SCGF and Full counting statistics

We can immediately integrate the flow equation for the kinks and anti-kinks (with charge $Q/(2\pi)$)

$$\varepsilon_K(\theta, \lambda) = \text{sign}(\sin \alpha - v_K^{\text{eff}}(\theta) \cos \alpha) \tilde{h}_K \lambda + \varepsilon_K(\theta, 0) \quad , \quad (3.105a)$$

3.5 Comparison between semiclassics and BFT at low temperature

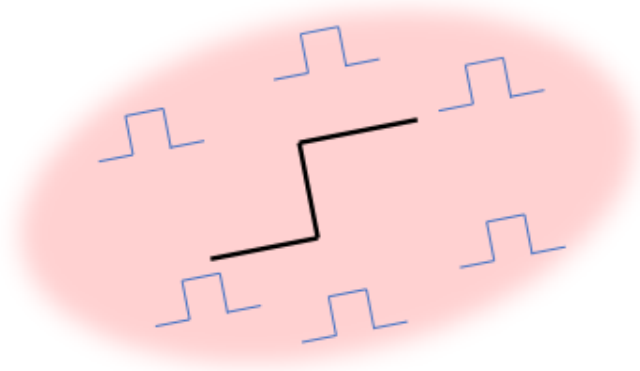


Fig. 3.8 Caricature of the low temperature breathers cloud (pink) renormalising the kink (blue bump) velocity (arrow). Of course the physics is one dimensional and both kinks and breathers lie on the same line but the analogy with the electron in a solid being renormalised by a photon cloud is powerful.

$$\epsilon_{\bar{K}}(\theta, \lambda) = \text{sign}(\sin \alpha - v_{\bar{K}}^{\text{eff}}(\theta) \cos \alpha) \tilde{h}_{\bar{K}} \lambda + \epsilon_{\bar{K}}(\theta, 0) \quad (3.105b)$$

with $\tilde{h}_K = 1 = -\tilde{h}_{\bar{K}}$. Taking into account the simplification of the TBA in the low temperature limit discussed above, from GHD we have

$$\begin{aligned} \langle j(0,0) \rangle_{\lambda'} &= \sum_{a=K,\bar{K}} \int \frac{d\theta}{2\pi} \partial_{\theta} E_a(\theta) v_a^{\text{eff}}(\theta) \vartheta_a(\theta, \lambda) \quad , \\ \langle q(0,0) \rangle_{\lambda'} &= \sum_{a=K,\bar{K}} \int \frac{d\theta}{2\pi} \partial_{\theta} P_a(\theta) \vartheta_a(\theta, \lambda) \quad , \end{aligned} \quad (3.106)$$

with $\vartheta_a = (1 + e^{\epsilon_a})^{-1}$ as usual for fermionic particles. By virtue of the solutions of the flow-equation above

$$\vartheta_{K,\bar{K}}(\theta, \lambda) = \vartheta(\theta, 0) e^{\pm \lambda} \quad . \quad (3.107)$$

Putting these results together we obtain

$$\begin{aligned} f_{\lambda, \alpha} &= 2(\cosh(\lambda) - 1) \int \frac{d\theta}{2\pi} |\sin \alpha - v^{\text{eff}}(\theta) \cos \alpha| \vartheta(\theta) \\ &= 2(\cosh(\lambda) - 1) d_{\alpha}^{\text{eff}} \end{aligned} \quad (3.108)$$

where in the last line we defined

$$d_{\alpha}^{\text{eff}} = \int \frac{d\theta}{2\pi} |\sin \alpha - v^{\text{eff}}(\theta) \cos \alpha| \vartheta(\theta) \quad (3.109)$$

which is the α -dependent integral above. The Legendre-Fenchel transform is easily done

$$\partial_\lambda f_{\lambda,\alpha} = 2d_\alpha^{\text{eff}} \sinh(\lambda) = \delta \implies \lambda = \sinh^{-1} \left(\frac{\delta}{2d_\alpha^{\text{eff}}} \right) \quad (3.110)$$

and so the rate function is

$$\begin{aligned} I(\delta, d_\alpha^{\text{eff}}) &= \lambda(\delta)\delta - f_{\lambda(\delta),\alpha} \\ &= \delta \sinh^{-1} \left(\frac{\delta}{2d_\alpha^{\text{eff}}} \right) - 2d_\alpha^{\text{eff}} \left[\sqrt{1 + \left(\frac{\delta}{2d_\alpha^{\text{eff}}} \right)^2} - 1 \right] = R(\delta, d_\alpha^{\text{eff}}) \quad . \end{aligned} \quad (3.111)$$

with $R(\delta, d)$ defined in (3.88).

3.5.3 Comment

We can compare the rate functions calculated from BFT (3.111) and that computed within the Sachdev-Damle semiclassical picture (3.88) for the classical Sine-Gordon model. While the shape of the rate function is unchanged, the difference lies in the parameter d_α . The semi-classical theory completely neglects the presence of the breathers which renormalise the effective velocity of the kinks non-trivially. Since the semi-classical picture is expected to apply in the low density limit only this is not a contradiction. It is a genuine prediction of BFT extending beyond the low density regime as it is basically able to account for the coherent superposition of excitations coming from the TBA structure. The low density limit can be viewed as a non-relativistic limit and in this case replacing relativistic bare energy and momentum with non-relativistic ones, the BFT prediction exactly recovers the semi-classical theory which is consistent with the findings of Ref. [71]. The difference between BFT and Sachdev and Damle semiclassical picture can be appreciated in Fig. 3.9.

3.6 Outlook

In this third chapter we have introduced and analysed some Euler scale physics of the Sine-Gordon model, especially in its classical regime. This was motivated by experimental applications on one side and on theoretical grounds on the other. In recent experiments on tunnel-coupled quasi-condensates, especially those realised by the Vienna group, they are in a parameters regime where the conditions for

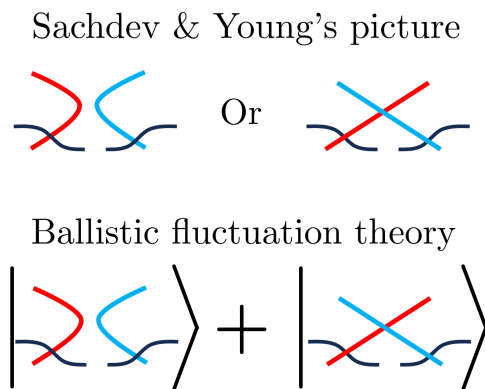


Fig. 3.9 Difference between Sachdev and Damle semiclassical picture accounting either for trasmission or reflection of quasi-particles and Ballistic Fluctuation Theory accounting for both at the same time.

the semi-classical limit of large number of breathers are reached. The classical Sine-Gordon model emerges. On this side, we were able to confirm with numerical experiments for this model our calculations are no difficult to perform and are comparable with realistic (in lab) experiments. On the other hand, we were motivated by comparisons with the more phenomenological approach of Sachdev and Damle. We have seen that in the low density limit the BFT predictions agree with that of Sachdev but otherwise the latter misses some coherent structure due to the stability of the quasi-particles. Since real experiments always have to deal with certain degree of inhomogeneity, it is important in the future to incorporate such effects in our description. Besides, high temperature (conformal) limits and more accurate analysis of the quantum regime are needed. This is especially true, as the quantum TBA for the attractive regime has now become available.

Chapter 4

Renyis and entanglement entropies from hydrodynamic

Goal of the chapter

This is the last chapter and it is dedicated to the important the application of BFT to the calculation of quantum information theoretical quantities: the Renyi entanglement entropies. It is based on the results of Ref. [4]. Such quantities characterise purely zero temperature quantum fluctuations. The phenomenology of the entanglement dynamics after a quantum quench is quickly reviewed and it is shown that the famous quasi-particle picture commonly utilised for the derivation of the entanglement growth can be derived from purely hydrodynamic principles. This constitutes the first ab-initio derivation of the quasi-particle picture as far as we are aware of.

4.1 Model and main results

4.1.1 Overview

The understanding of entanglement in quantum many-body systems received a considerable boost in the last decades, with the introduction and characterization of many different quantities which “measure” the amount of entanglement in a given quantum state [191–194]. An important set of such measures are the so-called entanglement Rényi entropies. Given a quantum system described by a density matrix ρ and a subsystem A of the total system, with \bar{A} denoting its complement, consider the associated reduced density matrix $\rho_A = \text{tr}_{\bar{A}}\rho$. Then, for

any $\alpha \in \mathbb{R}^+$, the α -Rényi entropy is defined as

$$S_\alpha = \frac{1}{1-\alpha} \log \text{tr} \rho_A^\alpha. \quad (4.1)$$

They are good entanglement measures for all pure quantum states, i.e. states of the form $\rho = |\Psi\rangle\langle\Psi|$. They fully characterise the entanglement spectrum, and an important property is that in the limit $\alpha \rightarrow 1$ they reduce to the famous entanglement Von Neumann entropy

$$S = -\text{tr}(\rho_A \log \rho_A). \quad (4.2)$$

In the context of one-dimensional systems, several exact results are available for such quantities. For example, at equilibrium, Rényi and entanglement entropies or their asymptotic behaviours can be obtained in the ground state states of critical [195], gapped [196] and more general integrable [197] field theories, as well as beyond integrability [198] (note that for free theories results were first obtained in [199]). In the case of critical systems described by a conformal field theory (CFT), such results are easily generalized to finite temperature states (i.e., Gibbs ensembles) [195], and also results for generic thermodynamic macrostates (i.e., generalized Gibbs ensembles [200]) have been obtained [201–203] in the context of integrable models relying on (thermodynamic) Bethe ansatz methods [204].

When moving to out-of-equilibrium scenarios, the situation is more complicated and available results are mainly qualitative or in the form of conjecture (an exception, however, is the exact result in [205]). For example, an imaginary time path-integral formulation, together with conformal invariance, has been used for a qualitative understanding of the ubiquitous linear growth of entanglement [206] observed after quantum quenches [207, 208]. Moreover, the dynamics of the entanglement entropy (4.2) for a generic integrable system was understood in terms of a semiclassical “quasiparticle picture” (whose original version was proposed in [206]), complemented with the Bethe ansatz knowledge of the stationary state attained at late times, as conjectured in [209] (see also [210]). These results have been extensively verified numerically (see, e.g., [210]). An important point to stress is that the quasi-particle picture *does not* admit a generalization for describing, for generic α , the growth of Rényi entropies [211, 212] (with the exception of free systems [201]).

4.1.2 Model and quench protocol

The model

The model considered here is a free fermion Hamiltonian on continuous space. Since we will be interested in a quench problem we introduce the pre-quench Hamiltonian

$$H_0 = \int d\theta E_0(\theta) a^\dagger(\theta) a(\theta) \quad (4.3)$$

and the post-quench one

$$H = \int d\theta E(\theta) \psi^\dagger(\theta) \psi(\theta) \quad . \quad (4.4)$$

We will always be interested in the time evolution of observables written in terms of the post-quench operators $\psi(x, t)$ which we take to be a complex field $\psi(x, t)$. Its Fourier modes are denoted $\psi(\theta, t)$ (with slight abuse of notation) and anti-commutation relation are $\{\psi(\theta)^\dagger, \psi(\theta')\} = \delta(\theta - \theta')$. Here θ represents the momentum, which we assume takes values in \mathbb{R} for simplicity (for quantum chains, this would be a bounded subset instead, but the general ideas are not affected). The same is valid for $a(x)$ and $a(\theta)$. We also denote the dispersion relation as $E(\theta)$ (and $E_0(\theta)$ of course), which we assume is strictly convex and symmetric $E(\theta) = E(-\theta)$. The field is written as

$$\psi(x, t) = \frac{1}{\sqrt{2\pi}} \int d\theta e^{i\theta x - iE(\theta)t} \psi(\theta). \quad (4.5)$$

As it is integrable, the model possesses an infinite number of conserved quantities as discussed in 1.1.1 and in particular it is $U(1)$ invariant. We recall that strictly speaking, the conserved charges $Q(\theta)$'s are not linearly extensive, but (for generic dispersion relation) any extensive conserved quantity can be obtained by a suitable "linear combination", or basis decomposition, $Q_i = \int d\theta h_i(\theta) Q(\theta)$. Here, $h_i(\theta)$ is again the one-particle eigenvalue of the extensive charge Q_i used multiple times in this thesis.

We then consider a spatial interval $A = [0, \ell x]$ and want to compute the Rényi entropies of ρ_A as in (4.1) after a quantum quench after time ℓt when $\ell \rightarrow \infty$. Both the evolution time and the length of the interval grow ballistically.

Quench protocol

A quantum quench is an initial value problem for the many-body system where the initial state is the ground state of a different Hamiltonian than that used for the time evolution. Typically, one imagines a sudden change of parameter. In integrable models, certain quenches are known to be of “integrable” type [213–215]. In these cases, the initial state can be written explicitly in terms of the scattering states (or Bethe ansatz states) of the post-quench, evolution Hamiltonian, as a so-called “squeezed state”:

$$|\Psi\rangle = \frac{1}{\mathcal{N}} \exp\left(\frac{1}{2} \int d\theta \mathcal{K}_{\theta,-\theta} \psi^\dagger(\theta) \psi^\dagger(-\theta)\right) |0\rangle \quad (4.6)$$

for some (θ -dependent) factor $\mathcal{K}_{\theta,-\theta}$, with \mathcal{N} denoting a normalization constant, and $|0\rangle$ being the ground state of the post-quench Hamiltonian. The squeezed state is generically a finite-density state, where the energy (of the post-quench Hamiltonian) is extensive with the system size. We will use later the fact that there is a Bogoliubov transformation of the fermionic mode operators

$$\psi(x, t) \leftrightarrow a(x, t) \quad (\text{Bogoliubov}) \quad (4.7)$$

defined as such that the squeezed state satisfies (is defined by)

$$a(x, t)|\Psi\rangle = 0. \quad (4.8)$$

This corresponds to changing the whole dispersion relation (not only a parameter as in typical quenches in the literature), see e.g. [112, 216]. The transformation is explicitly written as

$$\begin{pmatrix} a(\theta) \\ a^\dagger(-\theta) \end{pmatrix} = \begin{pmatrix} f(\theta) & g(\theta) \\ g^*(-\theta) & f^*(-\theta) \end{pmatrix} \begin{pmatrix} \psi(\theta) \\ \psi^\dagger(-\theta) \end{pmatrix}. \quad (4.9)$$

where the functions f and g are analytic functions of their arguments and depend on the particular dispersion relation. It is always possible to choose f and g real with f even and g odd. The schematic representation of the quench protocol is given in Fig. 4.1.

After a long time in a quench problem, the state locally approaches a GGE for what concerns local observables [217] (this is rigorous for spin chains with a maximal

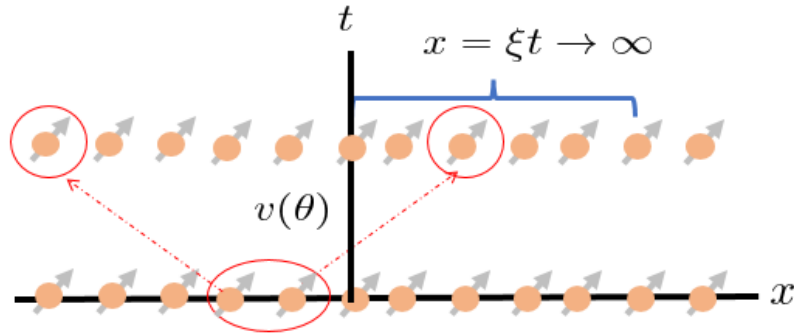


Fig. 4.1 Schematic picture of the scenario studied in this chapter. The initial state contains pairs of quasi-particles with opposite momenta that spread in opposite directions. At large time they reach different parts of the system. This quasi-particle picture phenomenological formula is derived from hydrodynamic principles in (4.15).

propagation velocity). In integrable quenches, there is a well-known relation between the squeezed-state representation of the initial state, and the long-time GGE (see e.g. [112]). The statement of convergence to a GGE pertains only to local operators, or operators supported on finite intervals (that do not grow with time):

$$\langle \Psi(t) | O(x) | \Psi(t) \rangle \rightarrow \langle O(x) \rangle_{\rho_w}, \quad t \rightarrow \infty. \quad (4.10)$$

where ρ_w is a GGE of the type (1) described by a function (1.55) as already used in Chapter 2 and $O(x)$ a local operator. The limit in (4.10) is expected to be valid everywhere in space. The relation between initial state and long-time GGE in free fermions can be worked out explicitly

$$e^{-w(\theta)} = |\mathcal{K}_{\theta, -\theta}|^2. \quad (4.11)$$

Namely, we see that the map from squeezed states to GGEs is in fact one-to-one.

4.1.3 Main result

Here we present the main results and discuss them, giving major emphasis on the physical principles underlying the derivations. We have obtained an exact relation between the growth of the Rényi entanglement entropies after a so-called integrable [213–215], pair-production quench, and static and dynamic “full counting statistics” in the final GGE. Define $N_{<, >} := \int_{|v(\theta)| <, > \xi/2} d\theta \psi^\dagger(\theta) \psi(\theta)$ the conserved quantity giving the total number of “slow” and “fast” fermionic modes

$\psi(\theta)$, with speeds $|v(\theta)| < \xi/2$ and $|v(\theta)| > \xi/2$, respectively, where $\xi = x/t$ is a space-time ray as usual and $v(\theta) = E'(\theta)$ is the group velocity of quasi-particles. In the notation of Chapter 2.1 this would be $N_{<} = Q|_{-\infty}^{2v(\theta)t}$ and $N_{>} = Q|_{v(\theta)t}^{\infty}$ where Q is the fermion number. In turn the SCGF will be written as

$$f(\lambda; \alpha) = - \int \frac{d\theta}{2\pi} |v(\theta)| \cos \alpha - \sin \alpha [F(w_\lambda(\theta; \alpha)) - F(w(\theta))] \quad (4.12)$$

where $\tan \alpha = x/t = \xi$ parametrised the ray direction in space-time as in previous chapters. Recall also that F is the free energy function in (1.51). Also, with slight change of notation compared to Chapter 2.1, we denote

$$f_{\text{dyn}}^{<,\xi}(\lambda) = \lim_{t \rightarrow \infty} t^{-1} \log \langle e^{\lambda J_{N_{<}}(t)} \rangle \quad (4.13)$$

the SCGF for the total current $J_{N_{<}}(t)$ of slow modes passing through a point in the time interval $[0, t]$ in the final GGE; and

$$f_{\text{stat}}^{>,\xi}(\lambda) = f = \lim_{x \rightarrow \infty} x^{-1} \log \langle e^{\lambda N_{>}(x)} \rangle \quad (4.14)$$

the SCGF for the total number $N_{>}(x)$ of fast modes lying on the spatial interval $[0, x]$ in the final GGE. Consider for simplicity α to be even. Then, as $x, t \rightarrow \infty$ with $x/t = \xi$ fixed, the Rényi entanglement entropy on the interval $[0, x]$, at time t after the quench, has asymptotic form:

$$S_\alpha(x, t) \sim \frac{1}{1 - \alpha} \left[2t \sum_{q=-\alpha/2+1}^{\alpha/2} f_{\text{dyn}}^{<,\xi}(ih_{2q-1}) + x \sum_{q=-\alpha/2+1}^{\alpha/2} f_{\text{stat}}^{>,\xi}(ih_{2q-1}) \right], \quad h_p = \frac{\pi p}{\alpha}. \quad (4.15)$$

This extends earlier observations of the connection between entanglement entropy and full counting statistics [218–220] to non-equilibrium quenches. This result directly provides a link between hydrodynamics, large deviation theory and entanglement growth which has not been noticed before.

The derivation is different and independent from the other exact result for the Ising model in [205], which was based instead on Toeplitz matrix representation. The presented method and ideas highlight how the structure of long-range correlations induced by particle pairs in integrable quenches allows one to describe both the growth and saturation of entanglement in a simple and universal way in terms of the long-time GGE, as this structure allows the separation of the contributions of fast and slow modes as per (4.15). The emphasis on the structure of long-range

correlations also gives a clear understanding as to why for quenches starting from more complicated states, for instance producing correlated groups of more than two particles, more information about the initial state is needed to describe the entanglement growth; in these case no simple formula exists (as showed for example in [221, 135]).

4.2 Twist Fields and replicas

Kadanoff-Cheva approach

Here we introduce a particular type of field operators encountered in many instances and that will be used throughout the chapter: twist fields. We have already mentioned and used twist fields in previous chapters: the Jordan-Wigner string (2.4). Twist fields, although they were not called this way, were introduced for the first time in the works [222, 223] and are reviewed in Ref. [224]. At the time, people were just about to discover the application of powerful methods of conformal field theory (CFT) [225]. Twist fields are also known as disorder operators as we will see in a moment. The easiest way to understand what these fields are is to think exactly like Kadanoff did: take the 2D Ising model,

$$H = - \sum_{\langle \underline{r}, \underline{r}' \rangle} J(\underline{r}, \underline{r}') \sigma(\underline{r}) \sigma(\underline{r}') \quad . \quad (4.16)$$

The spin variables take values in the binary alphabet $\{-1, 1\}$ and are placed on the vertices of a square lattice \mathbf{Z}_2 . Now one considers the dual lattice, that is the lattice whose vertices are placed at the center of each elementary plaquette of the original lattice. A plaquette in the square lattice is made by four spins connected by four links comprising a square. It is easy to see the the dual lattice of a square lattice is again a square lattice. We introduce a series of defects along a path Γ connecting two points in the dual lattice \underline{r} and \underline{r}' in the following way: for each link in the original lattice that is crossed by the path Γ we make the replacement $J \rightarrow -J$ in the Hamiltonian. Call $Z[K']$ the partition function obtained in the presence of the defects and $Z[K]$ the partition function without them where K denotes the whole set of couplings $-\beta J(\underline{r}, \underline{r}')$. The twist fields correlation function is defined by,

$$\langle \mathcal{T}(\underline{r}) \mathcal{T}(\underline{r}') \rangle = \frac{Z[K']}{Z[K]} = \exp(-\Delta F[\Gamma]) \quad , \quad (4.17)$$

where $\Delta F[\Gamma]$ is the free energy difference due to the presence of the defects line. It is easy to see that this definition does not depend on the path Γ but only on the end points. At infinite temperature $T = \infty$ we have $K = K' = 0$ so that,

$$\lim_{|\underline{r}-\underline{r}'|\rightarrow\infty} \langle \mathcal{T}(\underline{r})\mathcal{T}(\underline{r}') \rangle = \langle \mathcal{T}^2 \rangle = 1, \quad T > T_c. \quad (4.18)$$

At $T < T_c$ instead, the free energy cost of the dislocation is proportional to the length of the path (the proportionality being the surface tension t) so that,

$$\lim_{|\underline{r}-\underline{r}'|\rightarrow\infty} \langle \mathcal{T}(\underline{r})\mathcal{T}(\underline{r}') \rangle = \exp(-t|\underline{r}-\underline{r}'|), \quad T < T_c. \quad (4.19)$$

The twist field is called also disorder operator because it has a finite expectation value in the disordered phase while its two point function decays at large distances in the ordered phase. The field $\mathcal{T}(\underline{r})$ is thus dual to the order parameter (local magnetization) $\sigma(\underline{r})$. Now, note that nothing prevents us from considering the product of the disorder operator and the order operator, a composite field. Nevertheless, this definition is ambiguous because for each point in the dual lattice, there are two possible points \underline{r}_\pm in the original lattice, those at the extrema of the adjacent bonds (on the left for definiteness). If now one considers what happens when one composite field is transported around the other on a closed loop and soon realize that the correlator acquires a $-$ sign and so the field,

$$\psi_\pm(\underline{r}_\pm) \propto \sigma(\underline{r})\mathcal{T}(\underline{r}_\pm) \quad (4.20)$$

is a fermion. It turns out that this is the Majorana fermion discovered by Onsager in its exact solution of model [226]. An important example that we have already met is the $U(1)$ twist field in (1.157) for $\lambda \rightarrow i\lambda$. This is a twist field introducing a $U(1)$ shift acting as a multiplication by a phase λ reducing to \mathbf{Z}_2 in the case $\lambda \rightarrow i\pi\lambda$, which is exactly the Jordan-Wigner string. Let us now see how to define twist fields in general¹. Let Λ be a square lattice and $\tilde{\Lambda}$ its dual. Let Γ be a closed path on in the dual lattice and $g \in G$ with G a group. Also we denote with $R(g)$ a representation of g . Whenever Γ crosses an edge l in the original lattice we orient it calling l^+ its end point out of the loop and l^- that inside. Twist fields associated

¹The author learnt this from professor Denis Bernard during "Clean and Disordered Systems Out-of-Equilibrium", a summer school held at Institut d'Études Scientifique de Cargèse, Cargèse (9/2020).

to the group element g are defined by their correlation function as

$$\langle \mathcal{T}_g(\underline{x}) \mathcal{T}_g(\underline{y}) \rangle = \exp \left(\sum_{l \in \Gamma(\underline{x}, \underline{y})} H(\sigma_{l-}, \sigma_{l+}) - H(\sigma_{l-}, R(g) \sigma_{l+}) \right) \quad (4.21)$$

where $\Gamma(\underline{x}, \underline{y})$ is the path connecting the points \underline{x} and \underline{y} on the dual lattice. Importantly, note how the twist field depends on the space points and on the symmetry group element g but not on Γ if the symmetry group G is an internal symmetry of the Hamiltonian. This is easily seen in the example of the \mathbf{Z}_2 symmetry of the Ising model: everytime we cross two horizontal or two vertical bonds from the left and from the right the net contribution to the free energy difference is zero. It is clear that the definition given above is a generalization of the definition given by Kadanoff as it is just the exponential of (minus) the energy difference between the configuration before the group element acts and after. Another maybe simpler interpretation is to view the twist field as introducing a line of defects along the path Γ . In the end, twist fields are special fields associated to a given symmetry of the theory; they exist, in a many-body system, for every symmetry transformation.

Symmetries and exchange relations

Twist fields are very generic types of fields: they exist whenever there is an internal symmetry in the theory. Consider a unitary representation of a symmetry acting on a single point x

$$P_x = e^{i\lambda Q_x} \quad (4.22)$$

where Q_x is some Hermitian operator supported at x (it is ultra-local). Then we can define

$$\mathcal{T}(x, 0) = \prod_{y \geq x} P_y \quad (4.23)$$

and $\bar{\mathcal{T}}^\alpha(x, 0) = (\mathcal{T}^\alpha(x, 0))^\dagger$. If $O(x)$ is an observable of the theory under examination we have

$$P_x O(y) P_x^{-1} = \begin{cases} \sigma O(y) & y = x \\ O(y) & y \neq x \end{cases} \quad (4.24)$$

where σ is some representation of the symmetry on the space of observables. One can view \mathcal{T} as giving rise to a line of defects from x to ∞ such that if O is made going round x , the point where the field is, it gets transformed by the symmetry. The field is multivalued because of the presence of the cut introduced by the twist field.

The following equal-time exchange relations hold

$$\mathcal{T}(x, t)\psi(y, t) = \begin{cases} \sigma\psi(y, t)\mathcal{T}(x, t) & y \geq x \\ \mathcal{T}(x, t)\psi(y, t) & y < x \end{cases} \quad (4.25)$$

and

$$\bar{\mathcal{T}}(x, t)\psi(y, t) = \begin{cases} \sigma^{-1}\psi(y, t)\bar{\mathcal{T}}(x, t) & y \geq x \\ \bar{\mathcal{T}}(x, t)\psi(y, t) & y < x. \end{cases} \quad (4.26)$$

Twist fields and other concepts

Lastly, we mention that twist fields and their semilocality have been discussed extensively in various contexts, including: phase transitions in classical and quantum statistical models [223, 227, 47] (see the review [228]); vertex operators, Yangians, parafermions and orbifolds in conformal and integrable quantum field theory [229–233]; tau-functions and Painlevé equations [234–241]; and entanglement entropy in quantum field theory and in quantum spin chains [197, 242–244]. Twist fields have also been considered in higher dimensions [245]. In most works, the focus is on ultra-local “internal” symmetries, that strictly factorise in space, usually part of a symmetry group such as \mathbb{Z}_n , $U(1)$, $SU(n)$ like permutations.

4.2.1 Replica approach and branch point twist fields

Replicas

A common starting point for (most of) the results concerning the calculation of the entanglement entropy is the so-called replica approach extensively used in the context of disordered systems [246]. The trick is basically the following

$$\begin{aligned} - \lim_{\alpha \rightarrow 1^+} \frac{d}{d\alpha} \rho_A^\alpha &= - \lim_{\alpha \rightarrow 1^+} \frac{d}{d\alpha} \rho_A e^{(\alpha-1) \log \rho_A} \\ &= - \lim_{\alpha \rightarrow 1^+} e^{(\alpha-1) \log \rho_A} \rho_A \log \rho_A = -\rho_A \log \rho_A \quad , \end{aligned} \quad (4.27)$$

so that taking the expectation value and assuming it’s possible to commute the limit with it one obtains (4.2). It is also simple to see that in the same limit the Rényi entropies (4.1) give the same result. All boils down to computing the trace of the α power of the reduced density matrix [196]. It is important to stress that in principle α is an integers and the entanglement entropy can be recovered via analytic continuation which is not always difficult to perform.

In particular, within this approach, powerful tools are the so-called *branch point twist fields*, \mathcal{T}^α and its hermitian conjugate $\bar{\mathcal{T}}^\alpha$. The branch point twist fields are special kind of twist fields introduced above: as the replicated theory is invariant under permutations of the copies, $\mathcal{T}^\alpha, \bar{\mathcal{T}}^\alpha$ are the twist fields associated to the generator of cyclic permutations $i \mapsto i + 1 \pmod{\alpha}$ and its inverse, respectively. The quantities $\text{Tr} \rho_A^\alpha$ can be related to correlation functions of such twist fields, as first pointed out in quantum field theory in [197] clarifying ideas from [196], and as shown in quantum chains in [242]. We give here another way to see that these are the natural objects, based on the generalisation of Kadanoff idea presented above. The relevant quantity is

$$\text{Tr} \rho_A^\alpha = \text{Tr} \underbrace{\rho_A \cdots \rho_A}_{\alpha \text{ times}} \quad . \quad (4.28)$$

Now, each factor ρ_A is contracted with the next and the final trace simply contracts the last index of the last factor with the first index of the first factor: this is like going round a periodic structure and it is exactly like computing a partition function. The catch is that each factor is the reduced density matrix of the total one ρ so the indices corresponding to the subsystem A (the degrees of freedom) are not summed over and this is exactly like having a "defect". There is one such defect for each factor. In the case of a single interval the defect is a single line in space time along $t = 0$. Since these degrees of freedom are not summed over, the manifold over which the system whose (4.28) is the partition function of is continuous when we cross the defect. In the 2D Ising example, when we crossed the defect the bonds changed sign and the manifold was two dimensional space. Equivalently, the spin adjacent to the bond, either on the left or on the right depending on the chosen orientation, flips. In this case what happens when we cross the defect is that we "change" factor ρ_A in the α -fold product. In the summation over a complete set of states this means we jump from the index i to the index $i + 1$. The overall trace makes this periodic. It is then clear that the trace can be written as a ratio of partition functions

$$\text{Tr} \rho_A^\alpha = \frac{Z_\alpha(A)}{Z^\alpha(A)} \quad (4.29)$$

and this provides a definition of twist fields. $Z^\alpha(A)$ is the α power of the system without defects, with density matrix ρ while $Z_\alpha(A)$ is the partition function in the α -fold tensor product space. These arguments can be made even more explicit using permutation operators as in [242]. We can summarise as follows

: within the replica method, in order to compute entanglement entropies (cf. Eqs. (4.1)-(4.2)) in a given theory, one re-writes the quantity $\text{tr}\rho_A^\alpha$ in terms of an appropriate expectation value in the *replica model*. This is the model composed of α independent, commuting copies of the original model ($\alpha \in \mathbb{N}$). For a one-dimensional system in a state with density matrix ρ , and with the subsystem A being a single interval, e.g., $A = [x_1, x_2]$, it is a simple matter to show [197, 242] that $\text{tr}\rho_A^\alpha$ is exactly identified with the two-point function of *branch-point twist fields*,

$$\text{Tr}\rho_A^\alpha = \langle \mathcal{T}^\alpha(x_1, 0) \bar{\mathcal{T}}^\alpha(x_2, 0) \rangle_{\rho^{\otimes \alpha}}. \quad (4.30)$$

The expectation value on the r.h.s. is computed with the density matrix $\rho^{\otimes \alpha} = \otimes_{i=1}^\alpha \rho_i$, where ρ_i is the original density matrix, on copy i .

Branch point twist fields

Branch-point twist fields in the replica theory are twist fields associated to the symmetry under replica cyclic permutations of order α (which generate the group Z_α). They take the product form involving on-site copy-cyclic-permutation operators² [242]:

$$\mathcal{T}^\alpha(x, 0) = \prod_{y \geq x} P_y. \quad (4.31)$$

Here, denoting by $\psi_i(x)$ observables lying on (that is, acting nontrivially only on) copy $i \in \{1, 2, \dots, \alpha\}$ and position x , and identifying $\psi_{\alpha+1}(x) \equiv \psi_1(x)$ the equal-time exchange relations are

$$\mathcal{T}^\alpha(x, t) \psi_i(y, t) = \begin{cases} \psi_{i+1}(y, t) \mathcal{T}^\alpha(x, t) & y \geq x \\ \mathcal{T}^\alpha(x, t) \psi_i(y, t) & y < x \end{cases} \quad (4.32)$$

and an analogous one for $\bar{\mathcal{T}}^\alpha$. From Eq. (4.30), Rényi entanglement entropies can be simply obtained via Eqs. (4.1)-(4.2).

Equations (4.32), (4.26) were first introduced in the context of quantum field theories in Ref. [197], as a way of evaluating partition functions on branched surfaces, taking inspiration from [196].

We note that the action of branch-point twist fields can be diagonalized by going to the Fourier basis in the replica index (we choose anti-periodic boundary

²Here we omit any regularisation issue that may arise in models on a continuous space which do not affect exponential asymptotic behaviours.

conditions in replica space),

$$\psi_p(x, t) = \mathcal{F}_{j \rightarrow p}[\psi_j(x, t)] := \frac{1}{\sqrt{\alpha}} \sum_{j=0}^{\alpha-1} e^{ij\pi p/\alpha} \psi_j(x, t) \quad p \text{ odd} \quad (4.33)$$

which gives a diagonalised action

$$\mathcal{T}^\alpha(x, t)\psi_p(y, t) = \begin{cases} e^{-i\pi p/\alpha} \psi_p(y, t)\mathcal{T}^\alpha(x, t) & y \geq x \\ \psi_p(y, t)\mathcal{T}^\alpha(x, t) & y < x \end{cases} \quad (4.34)$$

and similarly for $\bar{\mathcal{T}}^\alpha(x, t)$.

The most general object we need to consider is the two-point correlation functions

$$\langle \mathcal{T}^\alpha(x_1, t_1) \bar{\mathcal{T}}^\alpha(x_2, t_2) \rangle_{\rho^{\otimes \alpha}} \quad (4.35)$$

at different spacetime points.

4.3 Application to Rényi entropies

4.3.1 Entropy of a single interval

A factorisation formula

Because of the quadratic nature of free fermion Hamiltonians, the Z_α symmetry of the replicated theory turns out to be embedded into the larger symmetry group $U(\alpha)$, which accounts for not only permutation of replicas, but also rotations amongst them. Indeed, say we have a lattice with N points and say the system Hamiltonian is $H = \vec{\psi}^\dagger A \vec{\psi}$ where $\vec{\psi}$ is the vector containing the field at each point and A a $N \times N$ hermitian matrix. Then the replicated theory has Hamiltonian $H = \sum_{\beta=1}^{\alpha} \vec{\psi}_\beta^\dagger A_\beta \vec{\psi}_\beta$ and it can also be written as

$$H = \vec{\Psi}^\dagger D_A \vec{\Psi} \quad (4.36)$$

where now

$$\vec{\Psi} = \begin{pmatrix} \vec{\psi}_1 \\ \vdots \\ \vec{\psi}_\alpha \end{pmatrix}, \quad D_A = \text{diag}(A_1, \dots, A_\alpha) \quad (4.37)$$

and this is manifestly invariant under complex rotations $U(N)$ ³. Thus, the branch-point twist field is a twist field associated to a particular symmetry transformation, part of a continuous symmetry group. The exchange relations translate simply to cyclic permutation matrices that can be diagonalised via Fourier transform. Imposing anti-periodic boundary conditions has the effect of fermionising the replica theory. Specifically, it is found [197]

$$\mathcal{T}^\alpha = \prod_{p \in I_\alpha} \tau_p^\alpha = \prod_{q=-\alpha/2+1}^{\alpha/2} \tau_{2q-1}^\alpha \quad (4.38)$$

with τ_p^α being a $U(1)$ twist field acting non-trivially only on ψ_p (as a phase),

$$\tau_p^\alpha(x, t) \psi_q(y, t) = \begin{cases} e^{-i\pi p/\alpha} \psi_q(y, t) \tau_p^\alpha(x, t) & y \geq x \text{ and } p = q \\ \psi_q(y, t) \tau_p^\alpha(x, t) & y < x \text{ or } p \neq q \end{cases} \quad (4.39)$$

(cf. (4.34)).

The decomposition (4.38) allows us to factorise the branch-point twist field two-point functions into products of $U(1)$ twist field two-point functions. This however only holds if the state can be likewise factorised. This is nontrivial: while factorisation in copy space is always true, a Fourier transform is likely to mix the components. Whenever the state is gaussian, that is it satisfies Wick's theorem, it is a simple matter to verify that $\rho^{\otimes \alpha}$ also factorises as a tensor product of states ρ in Fourier-copy space; this is because such states are completely determined by fermion two-point functions, which stay diagonal in Fourier-copy space. Therefore, we have, in Wick-theorem states ρ ,

$$\langle \mathcal{T}^\alpha(0, 0) \bar{\mathcal{T}}^\alpha(x, t) \rangle_{\rho^{\otimes \alpha}} = \prod_{q=-\alpha/2+1}^{\alpha/2} \langle \tau_{2q-1}^\alpha(0, 0) \bar{\tau}_{2q-1}^\alpha(x, t) \rangle_\rho. \quad (4.40)$$

Note how on the right-hand side, each factor is evaluated in the state ρ for the fermion ψ_{2q-1} .

To each of these correlation functions we can apply BFT. To do this we have to know the charge, the current and the one-particle eigenvalue. For any given p ,

³Notice that this would not be true for models whose fermionic representations contain superconducting terms like in Ising model. In such cases one need the so-called doubling trick [199, 197]

$\tau_p^\alpha(x, t)$ the charge is $U(1)$

$$Q_p = \frac{\pi p}{\alpha} \int dx \psi_p^\dagger(x) \psi_p(x) = \frac{\pi p}{\alpha} \int d\theta \psi_p(\theta)^\dagger \psi_p(\theta), \quad (4.41)$$

The explicit expressions as exponential of half-space integrals of charge densities is

$$\tau_p^\alpha(x, t) = \exp \left[i \int_x^\infty dx' q_p(x', t) \right], \quad q_p(x, t) = \frac{\pi p}{\alpha} \psi_p^\dagger(x, t) \psi_p(x, t). \quad (4.42)$$

Q_p acts on the single-particle basis as

$$Q_p |\theta, q\rangle = h_p \delta_{p,q} |\theta, q\rangle, \quad \text{with } h_p = \frac{\pi p}{\alpha} \quad (4.43)$$

(note that $\psi_p(x)$ has Q_p -charge $-h_p$, in agreement with (4.39)). With $Q = Q_p$, the twist field τ_p^α is identified with $\tau_p^\alpha = \mathcal{T}_{-i}$ in the notation of (1.157) (that is, with $\lambda = -i$), acting on the sector p . Recall that the action of the charge on the single-particle basis is all we need to know in order to apply the BFT.

Equilibrium Rényi entropy

We start by considering the α -Rényi entropy of a finite interval $A = [0, x]$ within a generic GGE ρ_w uniquely defined by the function $w(\theta)$. The relevant correlation function is

$$\langle T^\alpha(0, 0) \bar{T}^\alpha(x, 0) \rangle_{\rho_w^{\otimes \alpha}}. \quad (4.44)$$

From the BFT perspective, this is obtained by focusing on the *purely spatial direction*, namely, we consider an “horizontal path” by setting $\alpha = \pi/2$ in (4.12) (and we take $h(\theta) = h_p$). Each two-point function of $U(1)$ twist fields in (4.40) reads

$$\langle \tau_p^\alpha(0, 0) \bar{\tau}_p^\alpha(x, 0) \rangle_{\rho_w} \asymp \exp \{ x f(-i; p) \}, \quad f(-i; p) = \int \frac{d\theta}{2\pi} \log \left(\frac{1 + e^{ih_p - w(\theta)}}{1 + e^{-w(\theta)}} \right). \quad (4.45)$$

Then we consider the product in Eq. (4.40), which turns into a sum in the exponent, i.e.,

$$\langle T^\alpha(0, 0) \bar{T}^\alpha(x, 0) \rangle_{\rho_w^{\otimes \alpha}} \asymp \exp \{ x f(-i; \alpha) \}, \quad \text{with } f(-i; \alpha) = \sum_{q=-\alpha/2+1}^{\alpha/2} f(-i; 2q-1). \quad (4.46)$$

We may further evaluate those sums, by considering separately the part which depends and the part which does not depend on p (equivalently q, q' , Eq. (4.38)). The latter is trivial and simply gives a contribution to $f^\alpha(-i)$ which is $-\int d\theta/(2\pi)$ of

$$2 \sum_{q=1}^{\alpha/2} \log \left(1 + e^{-w(\theta)} \right) = \alpha \log \left(1 + e^{-w(\theta)} \right) . \quad (4.47)$$

For the remaining part, let us start by focusing on half of the sum, the terms from $q = 1$ to $\alpha/2$, in (4.46). By defining $z = \frac{2\pi i}{\alpha}$, $s = w + \frac{\pi i}{\alpha}$, we get

$$\sum_{q=1}^{\alpha/2} \log(1 + e^{zq-s}) = \sum_{r=1}^{\infty} \frac{(-1)^{r+1}}{r} e^{-r(s-z)} \left(\frac{1 - e^{rz\alpha/2}}{1 - e^{rz}} \right) \quad (4.48)$$

where we used the Taylor expansion $\log(1+x) = \sum_{r=1}^{\infty} (-1)^{r+1} x^r / r$ (which converges for $w > 0$), and we performed the sum over q . Next, we want to perform the sum in r in the r.h.s. of (4.48). To do that, we substitute the values of z and w first:

$$\sum_{r=1}^{\infty} \frac{(-1)^{r+1}}{r} e^{-r(w-\frac{\pi i}{\alpha})} \left(\frac{1 - e^{r\pi i}}{1 - e^{r\frac{2\pi i}{\alpha}}} \right) \quad (4.49)$$

where now we should consider separately three cases:

1. $r = \alpha m$ for integer m : in this case r is even (as α is even), and we have

$$\sum_{m=1}^{\infty} \frac{(-1)^{\alpha m+1}}{\alpha m} e^{-\alpha m w + m\pi i} \left(\frac{r\pi i}{2\pi i r / \alpha} \right) = \sum_{m=1}^{\infty} \frac{(-1)^{m+1}}{2m} e^{-\alpha m w} \quad (4.50)$$

$$= \frac{1}{2} \log \left(1 + e^{-\alpha w} \right) . \quad (4.51)$$

2. r even but $r \neq \alpha m$ for any integer m : in this case each term of the sum (4.49) is zero due to the vanishing of the numerator, i.e., $(1 - e^{r\pi i}) = 0$.
3. r odd: this gives

$$\sum_{r \text{ odd}} \frac{2}{r} e^{-rw} \left(\frac{e^{r\frac{\pi i}{\alpha}}}{1 - e^{r\frac{2\pi i}{\alpha}}} \right) = \sum_{r \text{ odd}} \frac{i}{r} \frac{e^{-rw}}{\sin \frac{\pi r}{\alpha}} . \quad (4.52)$$

4.4 Time dependence and long-range correlations

The sum of the terms for $q = -\alpha/2 + 1$ to 0 in (4.46) give exactly the complex conjugate of this result. Thus we get

$$\sum_{q=-\alpha/2+1}^{\alpha/2} \log(1 + e^{zq-s}) = \log(1 + e^{-\alpha w}) . \quad (4.53)$$

Putting everything together, $f^\alpha(-i)$ in (4.46) can be written as

$$f(-i; \alpha) = \int \frac{d\theta}{2\pi} \left[\log \left(1 + e^{-\alpha w(\theta)} \right) - \alpha \log \left(1 + e^{-w(\theta)} \right) \right] . \quad (4.54)$$

Finally, it is a matter of simple algebra to show that, in terms of the occupation function $\vartheta(\theta)$, we get

$$F(-i; \alpha) = \int \frac{d\theta}{2\pi} H^\alpha(\theta) \quad (4.55)$$

where we defined

$$H^\alpha(\theta) = \frac{1}{1-\alpha} \log [\vartheta(\theta)^\alpha + (1-\vartheta(\theta))^\alpha] . \quad (4.56)$$

The α -Rényi entropy is finally given by

$$S_\alpha(x) = \frac{1}{1-\alpha} \log \langle T^\alpha(x, 0) \bar{T}^\alpha(0, 0) \rangle_{\rho_w^{\otimes \alpha}} \sim x \int \frac{d\theta}{2\pi} H^\alpha(\theta) , \quad (4.57)$$

which coincides with the results obtained in [201, 203] (there in the more general context of interacting integrable models).

4.4 Time dependence and long-range correlations

4.4.1 Long range correlations and GGE

Before embarking in the calculation of the entanglement growth, it is important to recall the discussion at the end of Sec. 1.3.2 about long range correlations and the breaking of the large deviation principle behind BFT. This happens when cumulants do not have the correct scaling with the ballistic scale. We know that dynamic correlations of local observables at large times after quantum quenches is described quite generically by the same late-time GGE that describes static correlations as demonstrated in [217]. The proof of the authors assumes absence of long range interactions in the post-quench hamiltonian. What happens for the entanglement entropy?

This quantity is related to correlation functions of twist fields which are non-local with respect to the Hamiltonian as they depend on a semi-infinite part of the system. This should give an argument on why long range correlations can still be relevant in the context of entanglement and we will explicitly see this below. In particular, instead of having to analyse correlation functions of local observables, when dealing with twist fields we have to analyse *integrated* correlation functions. Such integrations are basically responsible for accumulating correlations. Let us see that is the case that large correlations develop after a quench of the type considered here.

Behavior of GGE correlations

Here we study in more detail the long range correlations of integrated densities and currents. Recall the definition of the generalised current as a line integral (1.155)

$$\Omega(x, t) = \int^{(x,t)} (j(x, t)dt - q(x, t)dx) \quad , \quad (4.58)$$

where $j(x, t)$ and $q(x, t)$ are the current and the density associated to the $U(1)$ conserved charge. It is not difficult to show that the associated current takes the form⁴⁵

$$j(x, t) = \frac{1}{2\pi} \int d\theta dk e^{ix(k-\theta)} \left(\frac{E(k) - E(\theta)}{k - \theta} \right) \psi^\dagger(\theta, t) \psi(k, t) \quad . \quad (4.59)$$

We now show that in a GGE, the connected correlation functions of densities decay fast enough in space, and the correlation functions of currents decay fast enough in time, in such a way that scaled cumulants are finite, thus making the BFT applicable. The former in fact is valid for all local observables, while the latter only hold for the currents. We focus on two-point functions for simplicity, higher order functions can be handled similarly via Wick theorem and multi-dimensional stationary phase methods.

⁴There is an x -independent integration constant that here is chosen in such a way that the result is a local observable. This in fact fixes the result up to an overall term proportional to the identity operator $\mathbf{1}$; indeed there are no x -independent homogeneous local operators, whose space-time translations are generated by the momentum and Hamiltonian, other than $\mathbf{1}$.

⁵Restricting the integration over momenta in $[-\pi, \pi]$ and taking $E(k) = \cos(k)$ one reproduces also the current on the lattice; but here we keep $\theta, k \in \mathbb{R}$ for simplicity.

4.4 Time dependence and long-range correlations

Let $\langle \cdot \rangle$ be a GGE. Let us assume that the occupation function $\vartheta(\theta)$ characterising the GGE is analytic in a neighbourhood of \mathbb{R} . From the basic fact

$$\langle \psi^\dagger(\theta)\psi(\theta') \rangle = \delta(\theta - \theta')\vartheta(\theta) \quad (4.60)$$

we have, on the one hand,

$$\langle \psi^\dagger(x)\psi(0) \rangle = \int \frac{d\theta}{2\pi} e^{-ix\theta} \vartheta(\theta) \quad (4.61)$$

For $x > 0$ (resp. $x < 0$), contour deformation can be performed as $\theta \mapsto \theta - i\gamma$ (resp. $\theta \mapsto \theta + i\gamma$) for $\gamma > 0$ small enough, and we see that the resulting integral decays exponentially as $|x| \rightarrow \infty$. This implies exponential decay of all two-point connected correlation functions of local observables formed out of sums of products of $\psi(x)$, $\psi^\dagger(x)$ and their derivatives, including $U(1)$ densities. It also implies linear scaling of cumulants; for instance this would mean

$$\begin{aligned} & \int_0^X dx \int_0^X dx' \langle \psi^\dagger(x)\psi(x') \rangle \\ &= \int_0^X dx \int_0^X dx' \int \frac{d\theta}{2\pi} e^{-i(x-x')\theta} \vartheta(\theta) \\ &\sim \int_0^X dx \int_0^X dx' e^{-\gamma|x-x'|} \sim X \end{aligned} \quad (4.62)$$

where in the last line we have shifted $\theta \mapsto \theta - i \operatorname{sign}(x - x')\gamma$ and used $\operatorname{sign}(x)x = |x|$. This is the correct ballistic growth of the cumulant.

On the other hand, we find

$$\langle \psi^\dagger(0, t)\psi(0, 0) \rangle = \int \frac{d\theta}{2\pi} e^{itE(\theta)} \vartheta(\theta). \quad (4.63)$$

This has a stationary phase at θ_* such that $E'(\theta_*) = 0$; this point is unique by our assumption of strict convexity (and $\theta_* = 0$ by symmetry, although we don't make use of this fact in this calculation), so a saddle point analysis gives

$$\langle \psi^\dagger(0, t)\psi(0, 0) \rangle \sim \frac{\sqrt{i} e^{itE(\theta_*)} \vartheta(\theta_*)}{\sqrt{2\pi t}}. \quad (4.64)$$

Therefore, correlation functions of generic local observables $O_1(x, t)$, $O_2(x, t)$ formed out of *bilinears of creation and annihilation operators* have algebraic decay

$$\langle O_1(0, t) O_2(0, 0) \rangle^c = \mathcal{O}\left(\frac{1}{t}\right) \quad (t \rightarrow \infty). \quad (4.65)$$

For such decay, cumulants of total time integrals do not grow linearly,

$$\left\langle \int_0^T dt O_1(0, t) \int_0^T dt' O_2(0, t') \right\rangle^c \gg T \quad (T \rightarrow \infty) \quad (4.66)$$

thus breaking the large-deviation principle at the basis of the BFT. However, an important remark is that this generic behaviour of fermion bilinears *does not hold in the case of currents*, $O_1(x, t) = O_2(x, t) = j(x, t)$. Indeed, using (4.59) with $x = 0$, we see that we must set $\theta = k = \theta_*$ for the long-time limit of the current two-point function. From

$$\frac{E(k) - E(\theta)}{k - \theta} = E'(k) + \mathcal{O}(k - \theta) \quad (4.67)$$

we realise that $\left. \frac{E(k) - E(\theta)}{k - \theta} \right|_{k=\theta=\theta_*} = 0$. Therefore, the current two-point function decays faster than $1/t$; in fact it decays as

$$\langle j(0, t) j(0, 0) \rangle^c = \mathcal{O}\left(\frac{1}{t^3}\right) \quad (t \rightarrow \infty). \quad (4.68)$$

This guarantees the correct scaling of cumulants

$$\left\langle \int_0^T dt j(0, t) \int_0^T dt' j(0, t') \right\rangle^c = \mathcal{O}(T) \quad (T \rightarrow \infty) \quad (4.69)$$

and thus the validity of the BFT. A similar argument shows can be done for the full $\Omega(x, t)$.

Approach to the GGE

We have seen that the behavior of integrated correlation functions on GGE states generically does not respect the large deviation principle assumptions but for the currents and the densities we are safe, at least in the fermionic theory. Here we want to discuss the approach to the GGE. This is relevant for the calculation of the entanglement growth after a quantum quench. Intuitively the presence of ballistically propagating quasi-particles in the initial state emitted with rapidities $\pm\theta$ causes correlations along space-time regions, depending where their trajectories lie with respect to the integration path in $\Omega(x, t)$. In order to apply the BFT we

4.4 Time dependence and long-range correlations

just repeat the usual arguments for the correlation function of $U(1)$ twist fields, this time, the one with one-particle eigenvalue (4.43). Here we analyse a bit more in detail how the GGE is approached in time to see whether we can arbitrarily choose this path exploiting the deformation invariance of the definition of twist fields.

Let $|\Psi\rangle$ be the initial state (4.6). We have

$$G_{\theta\theta'}^{\psi^\dagger\psi}(t,s) = \langle\Psi|\psi^\dagger(\theta)\psi(\theta')|\Psi\rangle = \langle\psi^\dagger(\theta)\psi(\theta')\rangle_{\rho_w} = \delta(\theta - \theta')\vartheta(\theta). \quad (4.70)$$

Since $|\Psi\rangle$ is gaussian, by Wick's theorem, the only difference between averages in $|\Psi\rangle$ and in $\langle\cdot\rangle_{\rho_w}$ come from the contraction

$$\langle\Psi|\psi(\theta)\psi(\theta')|\Psi\rangle \quad (4.71)$$

and its complex conjugate. Thus we evaluate $\langle\Psi|\psi(x,t)\psi(x',t')|\Psi\rangle$ in three main situations that are important for our analysis: $t = t'$, $x \neq x'$ (for the cumulants of space-integrated conserved densities), and $x = x'$, $t \neq t'$ (for the cumulants of time-integrated currents) and $x \neq x'$, $t \neq t'$ (for analysing the correlation between the spatially separated time-integrated currents).

In the first case, we have, using the bogoliubov transformation (4.7)

$$G_{xx'}^{\psi\psi}(t,t) = - \int \frac{d\theta}{2\pi} e^{i(x-x')\theta - 2itE(\theta)} f_{-\theta}^* g_{-\theta}. \quad (4.72)$$

Consider $t \rightarrow \infty$ with x, x' fixed. Then there is a stationary phase at $\theta_* : E'(\theta_*) = 0$, with a resulting integral $\propto \frac{1}{\sqrt{t}}$. Thus, this decays as $t \rightarrow \infty$: for every two-point functions on intervals that stay finite, the GGE is approached. We notice that as $g_{-\theta_*} = 0$ (recall that it can be chosen odd), for fermion two-point functions, the approach is proportional to $1/t^{3/2}$ instead of $1/\sqrt{t}$; and for multilinears of fermions, the approach is faster.

But we are interested in the scaling $x, x', t \propto \ell \rightarrow \infty$, $(x - x')/t = \xi$, for which the exponential has a stationary phase at $\theta_* = \theta_*(\xi) : E'(\theta_*) = \xi/2$, with a resulting integral $\propto 1/\sqrt{\ell}$. In charge-neutral fermion bilinears, such as those involved in densities and currents, two such contractions will be multiplied with each other. Thus we have, for instance,

$$\langle\Psi|q(x,t)q(x',t)|\Psi\rangle^c = \langle q(x,t)q(x',t) \rangle_{\rho_w}^c + C(\xi) (t\ell)^{-1} + \mathcal{O}(\ell^{-2}), \quad (4.73)$$

thus the correction is $O(1/\ell)$. Then, for the cumulant we have

$$\begin{aligned} \langle \Psi | \int_0^{\ell X} dx q(x, \ell t) \int_0^{\ell X} dx' q(x', \ell t) | \Psi \rangle^c &= \ell^2 \langle \Psi | \int_0^X dx q(\ell x, \ell t) \int_0^X dx' q(\ell x', \ell t) | \Psi \rangle^c \\ &\sim \langle \int_0^{\ell X} dx q(x, \ell t) \int_0^{\ell X} dx' q(x', \ell t) \rangle_{\rho_w}^c + \mathcal{O}(\ell) \end{aligned}$$

where the correction $O(\ell)$ is $\ell \int_{-X/t}^{X/t} d\zeta (X - 2\zeta t) C(\zeta)$. Therefore, the correction due to the quench changes the linearly scaling part of the cumulant, hence modifies the scaled cumulant from its GGE value (recall that the scaled cumulant is obtained by dividing by ℓX , and taking the large ℓ limit). Here it would be possible to evaluate explicitly this modification, however it is not necessary for our calculation. The modification due to the quench comes from pair productions – this will be made much clearer when we study the single-mode densities and currents below.

In fact, there is one limit where it is useful to evaluate this correction term: the limit $X/t \rightarrow 0$ of ℓX -scaled spatially-integrated densities as above. The result for the correction is explicitly

$$\lim_{X/t \rightarrow 0} \frac{t}{X} \int_{-X/t}^{X/t} d\zeta \left(\frac{X}{t} - 2\zeta \right) C(\zeta) = 0 \quad (4.74)$$

as $C(\zeta)$ is bounded. Thus, in this limit we recover the GGE result. This is in agreement with taking first the long-time limit of the finite-interval cumulant, then the limit of the scaled cumulant on a long interval (this means that the limit $X/t \rightarrow 0$ is in fact uniform in t).

In the second case, where we can set $x = x' = 0$, we find, with $E'(\theta_*) = 0$ and a saddle point analysis

$$G_{00}^{\psi\psi}(t, t') = - \int \frac{d\theta}{2\pi} e^{i(t+t')E(\theta)} f^*(-\theta) g(-\theta) \sim \frac{\sqrt{i} e^{i(t+t')E(\theta_*)} f(-\theta_*)^* g(-\theta_*)}{\sqrt{2\pi(t+t')}}. \quad (4.75)$$

As $E(\theta)$ is symmetric, this is $\theta_* = 0$, and then since $g(\theta_*) = 0$ the whole result vanishes. Therefore,

$$G_{00}^{\psi\psi}(t, t') = \mathcal{O}\left(\frac{1}{(t+t')^{3/2}}\right). \quad (4.76)$$

Hence, the corrections to cumulants of charge-neutral bilinears involve

$$\int_1^T dt \int_1^T dt' \frac{1}{(t+t')^2} = \mathcal{O}\left(\frac{1}{T^3}\right) \ll T \quad (T \rightarrow \infty) \quad (4.77)$$

4.4 Time dependence and long-range correlations

(where the lower boundary does not matter for the large- T analysis). This correction is sublinear, therefore the quench does not affect cumulants of equal-position time-integrated quantities: for these, the GGE is reached quickly enough. The lack of modification due to the quench comes from the lack of pairs of particles produced at equal (zero) momenta, due to the fermionic statistics.

We remark that if there were particles created at zero momentum (for instance, for bosonic systems), then, still by a calculation similar to that of Eqs. (4.67)-(4.69), the correction due to the quench would vanish for *cumulants of total currents*, which are in any case the objects of interest. Therefore, the fact that pairs of particles of zero momentum are not produced, is not an essential aspects of our calculation.

Finally, we may also analyse time-integrated currents at two different points in a similar way as above, finding:

$$\langle \Psi | \int_0^{\ell T} dt j(\ell x, t) \int_0^{\ell T} dt' j(\ell x', t') | \Psi \rangle^c \sim \langle \int_0^{\ell T} dt j(\ell x, t) \int_0^{\ell T} dt' j(\ell x', t') \rangle_{\rho_w}^c + \mathcal{O}(\ell).$$

This is important for the calculation of the Rényi entropy after the quench. With $\xi = (x - x')/(t + t')$, the saddle point leading to the $\mathcal{O}(\ell)$ correction is at θ_* : $E'(\theta_*) = \xi$. Thus, the correction due to the quench again changes the linearly scaling part of the two-point cumulant. Here, the limit $\xi \rightarrow \infty$ is interesting, and easy to evaluate: as $\xi \rightarrow \infty$, the saddle point will be at $\theta_* \rightarrow \infty$, and we only have to use the fact that $g_\theta \rightarrow 0$ as $|\theta| \rightarrow \infty$. Therefore, the correction vanishes as $\xi \rightarrow \infty$, and we may use the GGE result, where scaled cumulants of time-integrated currents become sums of cumulants at x and at x' in the GGE (which take the same values by translation invariance).

4.4.2 Time evolution of half-system entropy

In this case the relevant correlation function is

$$\langle \Psi^\alpha | T^\alpha(0, t) | \Psi^\alpha \rangle \tag{4.78}$$

and it is schematically depicted in 4.2 on the left. The twist field is inserted at $(0, t)$ and the cut goes from $(0, t) \rightarrow (\infty, t)$ along an horizontal path according to the definition (4.42). Along such path we have shown in (4.78) there long range correlations of time integrated currents modify the scaling of the cumulant and thus BFT breaks down. Nevertheless, using path independence of twist fields correlation functions, we can deform the path, between its initial and final points, in a way to avoid such correlations. Specifically, we choose the piece-wise linear

path joining the points $(0, t) \rightarrow (0, 0) \rightarrow (\infty, 0)$. We note that as the final point is at spatial infinity, it can be displaced to time 0 – this in fact implements the correct physics of the entanglement entropy due to the single boundary at $x = 0$. Then, we may represent the one-point function as

$$\langle \Psi^\alpha | T^\alpha(0, t) | \Psi^\alpha \rangle \asymp \langle \Psi^\alpha | T^\alpha(0, t) \bar{T}^\alpha(0, 0) T^\alpha(0^+, 0) | \Psi^\alpha \rangle \quad (4.79)$$

where the factors $T^\alpha(0, t) \bar{T}^\alpha(0, 0)$ represent the segment of path $(0, t) \rightarrow (0, 0)$, and the factor $T^\alpha(0^+, 0)$, the segment $(0, 0) \rightarrow (\infty, 0)$. This is valid as an asymptotic relation for large t , where the UV singularity due to the proximity of the fields $\bar{T}^\alpha(0, 0)$ and $T^\alpha(0^+, 0)$ (which occurs because of renormalisation effects) is neglected.

To simplify this we note that the segment of path $(0, 0) \rightarrow (\infty, 0)$ does not provide any contribution to the result. This is because we may re-write the branch-point twist field $T^\alpha(0^+, 0)$ as is done in Section 4.2, but *in the basis of the before-quench canonical free fermions of the replica theory* $a_i(x, 0)$. Once this is done, using the fact the $a(x, t)$ kills the initial state (according to (4.8)) we see it gives no contribution. We can now repeat the steps already done for the equilibrium entropy: using the factorisation formula (4.40) and setting $\alpha = 0$ in (4.12) and performing the sum one obtains the expected result

$$S_\alpha(t) = \frac{1}{1-\alpha} \log \langle T^\alpha(0, t) \bar{T}^\alpha(0, 0) \rangle_{\rho_w^{\otimes \alpha}} \sim t \int \frac{d\theta}{2\pi} |v(\theta)| H_\alpha(\theta). \quad (4.80)$$

obtained in the literature both from exact calculation in [205] and within the quasi-particle picture in [209, 210].

4.5 The case of ballistically growing interval

We have seen that long range correlations generically develop along paths in space-time. The trick to apply the BFT even in presence of the correlations has its roots in path independence of the twist fields. These can be deformed as in the case of the entropy of the half system in order to avoid dangerous correlations. One of the main results of [4] is the definition of new types of twist fields: they are a refined version of twist fields and are dubbed single-mode and pair-mode twist fields. They can be used to take into account the fact that if one wants to compute the entropy evolution of an interval at ballistic scales, the location in space-time

4.5 The case of ballistically growing interval

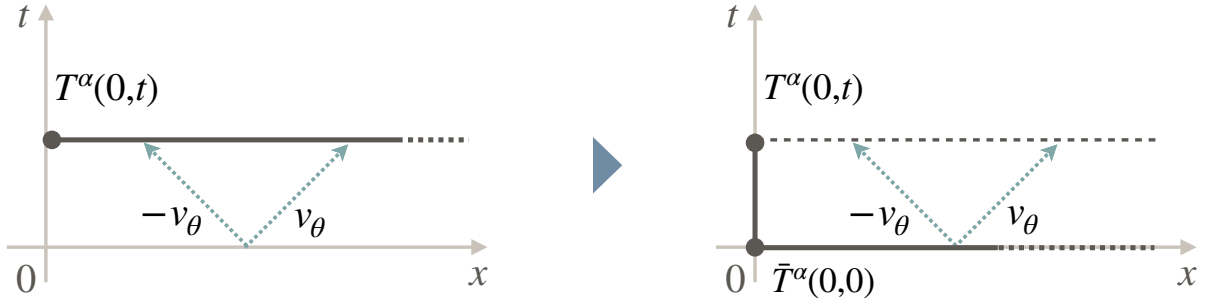


Fig. 4.2 Evolution of Rényi entropies of half system $A = [0, \infty]$ within BFT. Left: Initial integration path. Because of initially entangled pairs, points along this path at time t will be correlated, which prevents us from applying BFT directly. Right: Deformed integration path. Along this new path points are not correlated anymore. Moreover the only term contributing to the growth in time of entanglement is the vertical path from $(0, t)$ to $(0, 0)$.

where long range correlations develop generically depend both on the velocity of the quasi-particles and on the particular ray we are looking at. This is because of the saddle point equations governing the approach to a GGE of basic correlators are (see (4.72) and Fig. 4.3)

$$2v(\theta) = \zeta \quad . \quad (4.81)$$

The relevant correlation function in this case is

$$\langle \Psi^\alpha | T^\alpha(0, t) \bar{T}^\alpha(x, t) | \Psi^\alpha \rangle, \quad x = \zeta t, \quad t \rightarrow +\infty. \quad (4.82)$$

Looking at Fig. 4.3 it is easy to be convinced that the limits $\zeta \rightarrow \infty$ and $\zeta \rightarrow 0$ are relatively easy. In each of these cases it is enough to choose the path along which no correlations develop. This is the broken path on the left at short times ($x \gg t$) and that on the right at large times $x \ll t$. In this case the correlation function factors giving the predictions (4.57) and (4.80) in the two asymptotic limits

$$S_\alpha(x, t) = \frac{1}{1-\alpha} \log \langle T^\alpha(0, t) \bar{T}^\alpha(x, t) \rangle \sim \begin{cases} 2t \int \frac{d\theta}{2\pi} |v(\theta)| H_\alpha(\theta) & t \ll x \\ x \int \frac{d\theta}{2\pi} H_\alpha(\theta) & t \gg x. \end{cases} \quad (4.83)$$

Since we want a result that is valid all over space-time we next introduce the new type of twist fields.

4.5.1 Single-mode and pair-mode twist fields

Here we summarise the main construction of single-mode and pair-mode twist fields. These refined versions of twist fields allow to take into account the correlations along path. The basic idea is to write the conserved charge as a sum of charges in small rapidity shells such that the twist field factors $\mathcal{T} \sim \prod_{\theta} \mathcal{T}_{\theta}$. The BFT could be applied to every \mathcal{T}_{θ} and for each θ a smart choice of the path is made. This can be done because it's like one is working at fixed θ .

To construct the new conserved charges we note that a valid conserved charge Q is usually considered to be extensive, that is scale linearly with the volume (typically one requires $\langle Q^2 \rangle^c \propto L$ [247, 248]). Earlier we discussed the replica model with α copies, and the $U(1)$ charges Q_p , which are just the integration $Q_p = h_p \int d\theta Q_{\theta,p}$ (with $h_p = \frac{\pi p}{\alpha}$) over all momenta θ of the continuous basis $Q_{\theta,p} = \psi_{\theta,p}^{\dagger} \psi_{\theta,p}$ in the Fourier-copy p . There, we have also discussed the twist fields τ_p^{α} associated to these charges, which we could use in the computation of the Rényi entanglement entropies. A natural extension of these constructions is the twist fields associated to each conserved quantity $Q_{\theta,p}$. These charges Q_{θ} are not extensive. However, as they form a continuous basis, integrals on small θ -intervals are extensive; thus it is better to define, for $\epsilon > 0$ as small as desired the *single mode charges*

$$Q_{\theta} = \int_{\theta-\epsilon/2}^{\theta+\epsilon/2} d\theta' \psi(\theta')^{\dagger} \psi(\theta'). \quad (4.84)$$

These act as

$$Q_{\theta} |\theta'\rangle = \Theta(\epsilon/2 - |\theta' - \theta|) |\theta'\rangle \quad (4.85)$$

hence have one-particle eigenvalues

$$h_{\theta}(\theta') = \Theta(\epsilon/2 - |\theta' - \theta|) \quad , \quad (4.86)$$

where $\Theta(x)$ is the Heaviside theta function. Clearly each "regularised" (by ϵ) single-mode charge Q_{θ} is conserved, $[Q_{\theta}, H] = 0$ and in a GGE in a finite volume L , we have $\langle Q_{\theta}^2 \rangle^c \propto L$:

$$\langle Q_{\theta}^2 \rangle^c = \int_{\theta-\epsilon/2}^{\theta+\epsilon/2} d\theta' d\theta'' \delta(\theta' - \theta'')^2 n(\theta')(1 - n(\theta')) = \frac{L}{2\pi} \int_{\theta-\epsilon/2}^{\theta+\epsilon/2} d\theta' n(\theta')(1 - n(\theta')). \quad (4.87)$$

As mentioned, if we want to write a density in real space for each $b^{\dagger}(\theta)b(\theta)$, we will get something non local. However, Q_{θ} 's have quasi-local densities. We

seek a function $f_\theta(x, y)$ such that

$$\int dx dy b^\dagger(x) b(y) f_\theta(x - y) = Q_\theta. \quad (4.88)$$

Going to Fourier space, one can show that

$$f_\theta(z) = \frac{\sin(\frac{\epsilon z}{2})}{\pi z} e^{i\theta z}. \quad (4.89)$$

The corresponding regularised single-mode density, parametrised by the momentum, and one choice of the density (the only hermitian and PT symmetric one), is given by

$$q_\theta(x, t) = \int dz b^\dagger(x + z/2, t) b(x - z/2, t) f_\theta(z). \quad (4.90)$$

In terms of Fourier modes, this takes the form

$$q_\theta(x, t) = \int \frac{dk dk'}{2\pi} e^{ix(k'-k)} \Theta\left(\frac{\epsilon}{2} - \left|\frac{k+k'}{2} - \theta\right|\right) b_k^\dagger(t) b_{k'}(t). \quad (4.91)$$

As $[Q_\theta, H] = 0$, the density $q_\theta(x, t)$ has an associated current satisfying a continuity equation and by a calculation analogous to (4.59) one finds

$$j_\theta(x, t) = \int \frac{dk dk'}{2\pi} e^{ix(k'-k)} \left(\frac{E(k') - E(k)}{k' - k}\right) \Theta\left(\frac{\epsilon}{2} - \left|\frac{k+k'}{2} - \theta\right|\right) b_k^\dagger(t) b_{k'}(t). \quad (4.92)$$

Explicitly their associated densities and currents $q_\theta(x, t)$ and $j_\theta(x, t)$,

$$Q_\theta = \int dx q_\theta(x, t), \quad \partial_t q_\theta(x, t) + \partial_x j_\theta(x, t) = 0. \quad (4.93)$$

From this, one can immediately construct the associated *single mode* twist field

$$\tau_\theta(x, t) = \exp\left[i \int_x^{+\infty} dx' q_\theta(x', t)\right] \quad (4.94)$$

and, for its correlation functions, apply the corresponding BFT based on the one-particle eigenvalue (4.86). It is more useful the *pair mode* twist field

$$\tau_{|\theta|}(x, t) = \exp\left[i \int_x^{+\infty} dx' q_{|\theta|}(x', t)\right] \quad (4.95)$$

constructed from the *pair-mode charges* $Q_{|\theta|} = Q_\theta + Q_{-\theta}$ and the associated densities

$$q_{|\theta|}(x, t) = q_\theta(x, t) + q_{-\theta}(x, t). \quad (4.96)$$

Turning the attention to the squeezed state (4.6), it is clear that this state factorises into momentum intervals as follows:

$$|\Psi\rangle = \prod_{\theta \in (\mathbb{N} + \frac{1}{2})\epsilon} |\Psi_{|\theta|}\rangle \quad (4.97)$$

where

$$|\Psi_{|\theta|}\rangle = \frac{1}{\mathcal{N}_{|\theta|}} \exp\left(\int_{\theta-\epsilon/2}^{\theta+\epsilon/2} d\theta' \mathcal{K}_{\theta, -\theta} \psi^\dagger(\theta) \psi^\dagger(-\theta)\right) |0_{|\theta|}\rangle \quad (4.98)$$

and we write the ground state in a naturally factorised way as $|0\rangle = \prod_{\theta \in (\mathbb{N} + \frac{1}{2})\epsilon} |0_{|\theta|}\rangle$. Here $|0_{|\theta|}\rangle$ is the vacuum state of the operators $\psi_{|\theta|} = \psi_\theta + \psi_{-\theta}$. Both act trivially (as zero) on $|\Psi_{|\theta'|\rangle}$ if $\theta' \neq \theta$ ($\theta, \theta' \in (\mathbb{N} + \frac{1}{2})\epsilon$). The pair-mode twist field acts trivially (as the identity) on $|\Psi_{|\theta'|\rangle}$ if $\theta' \neq \theta$.

Pair-mode and single-mode twist fields are still $U(1)$ twist fields, for the sub- $U(1)$ symmetry acting on the tensor factor of modes within $[\theta - \epsilon/2, \theta + \epsilon/2]$. Note in particular that the global $U(1)$ twist field $\tau(x, t)$ associated to the total charge $Q = \int d\theta \psi_\theta^\dagger \psi_\theta = \int dx \psi^\dagger(x) \psi(x)$ can be factorised as

$$\tau(x, t) = \prod_{\theta \in (\mathbb{N} + \frac{1}{2})\epsilon} \tau_{|\theta|}(x, t) \quad (4.99)$$

and that, by factorisation of its action on the state, we have

$$\langle \Psi | \tau(x, t) \tau(x', t') | \Psi \rangle = \prod_{\theta \in (\mathbb{N} + \frac{1}{2})\epsilon} \langle \Psi_{|\theta|} | \tau_{|\theta|}(x, t) \tau_{|\theta|}(x', t') | \Psi_{|\theta|} \rangle. \quad (4.100)$$

Clearly, as the pair-mode twist fields act trivially on other tensor factors in the state, we may also write, more simply,

$$\langle \Psi | \tau(x, t) \tau(x', t') | \Psi \rangle = \prod_{\theta \in (\mathbb{N} + \frac{1}{2})\epsilon} \langle \Psi | \tau_{|\theta|}(x, t) \tau_{|\theta|}(x', t') | \Psi \rangle. \quad (4.101)$$

4.5.2 Hydrodynamic derivation of quasi-particle picture

Armed with single-mode and pair-mode twist fields (4.101), we re-write the correlation (4.82) factoring over replicas and over rapidity shells in the following

4.5 The case of ballistically growing interval

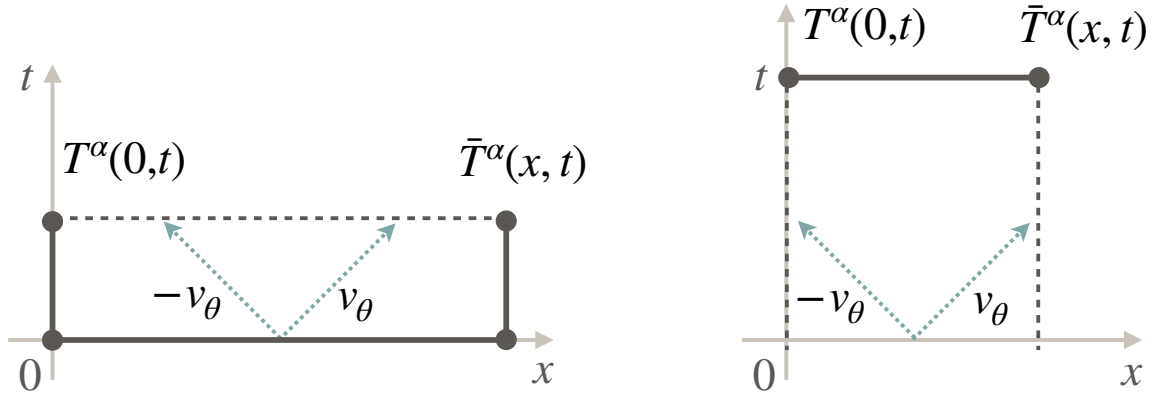


Fig. 4.3 Evolution of Rényi entropies of finite subsystem $A = [0, x]$ within BFT. The integration path that we need to choose (continuous dark-gray line) in order for BFT to apply is different at short (left) and long (right) times. The choice depends on which points in spacetime get correlated because of initially entangled pairs produced by the initial state.

way

$$\langle \Psi^\alpha | T^\alpha(0, t) \bar{T}^\alpha(x, t) | \Psi^\alpha \rangle = \prod_{\theta \in (\mathbb{N} + \frac{1}{2})\epsilon} \prod_{q = -\alpha/2 + 1}^{\alpha/2} \langle \Psi_{2q-1} | \tau_{|\theta|, 2q-1}^\alpha(0, t) \bar{\tau}_{|\theta|, 2q-1}^\alpha(x, t) | \Psi_{2q-1} \rangle. \quad (4.102)$$

Having made this re-writing, the analysis now follows that of the $\zeta \rightarrow \infty$ and $\zeta \rightarrow 0$ limits made above: there is an exact parallel for each individual two-point function

$$\langle \Psi_p | \tau_{|\theta|, p}^\alpha(0, 0) \bar{\tau}_{|\theta|, p}^\alpha(x, t) | \Psi_p \rangle \quad (p = 2q - 1),$$

with the only difference that *it is not necessary to take the asymptotic limit in ζ* . For each θ (and each p), the factor $|\Psi_{|\theta|, p}\rangle$ of the full state $|\Psi_p\rangle$, on which $\tau_{|\theta|, q}^\alpha$ act non-trivially, correlates points (x, t) , (x', t') only for

$$\frac{|x - x'|}{|t + t'|} \in [v(\theta - \epsilon/2), v(\theta + \epsilon/2)]$$

(recall that $\theta \in (\mathbb{N} + \frac{1}{2})\epsilon$). It is possible microscopically confirm this condition performing an analysis of cumulants for single-mode and pair-mode densities and currents, see [4] for details of the calculation.

Therefore, for $\zeta > 2v(\theta + \epsilon/2)$ correlations occur on the horizontal path $(0, t) \rightarrow (x, t)$, but no correlations occur on $(0, t) \rightarrow (0, 0) \rightarrow (x, 0) \rightarrow (x, t)$ (note that, again, the segment of path $(0, 0) \rightarrow (x, 0)$ does not contribute). Thus we

must choose the latter path (Fig. 4.3 (left)). On the contrary, $\xi < 2v(\theta - \epsilon/2)$, correlation occur between the segment of paths $(0, t) \rightarrow (0, 0)$ and $(x, 0) \rightarrow (x, t)$, but not on the horizontal path $(0, t) \rightarrow (x, t)$. Thus we must choose the latter (Fig. 4.3 (right)). In making these right choices, the correlation functions of pair-mode twist fields tend to their values in the long-time GGE,

$$\begin{aligned}
 & \langle \Psi_p | \tau_{|\theta|,p}^\alpha(0,0) \bar{\tau}_{|\theta|,p}^\alpha(x,t) | \Psi_p \rangle \\
 & \asymp \begin{cases} \langle \tau_{|\theta|,p}^\alpha(0,t) \bar{\tau}_{|\theta|,p}^\alpha(0,0) \tau_{|\theta|,p}^\alpha(x,0) \bar{\tau}_{|\theta|,p}^\alpha(x,t) \rangle_{\rho_w} & \xi > 2v(\theta + \epsilon/2) \\ \langle \tau_{|\theta|,p}^\alpha(0,0) \bar{\tau}_{|\theta|,p}^\alpha(x,0) \rangle_{\rho_w} & \xi < 2v(\theta - \epsilon/2) \end{cases} \\
 & \asymp \begin{cases} \left| \langle \tau_{|\theta|,p}^\alpha(0,t) \bar{\tau}_{|\theta|,p}^\alpha(0,0) \rangle_{\rho_w} \right|^2 & \xi > 2v(\theta + \epsilon/2) \\ \langle \tau_{|\theta|,p}^\alpha(0,0) \bar{\tau}_{|\theta|,p}^\alpha(x,0) \rangle_{\rho_w} & \xi < 2v(\theta - \epsilon/2) \end{cases} . \quad (4.103)
 \end{aligned}$$

At this point one uses the results already derived for the equilibrium entropy and for the time evolution after the quench for the half system in the two regions of space-time dictated by the velocity constraint. The only difference is that θ integrals are now restricted to a shell

$$\theta \in I_{\theta',\epsilon} := [\theta' - \epsilon/2, \theta' + \epsilon/2] \cup [-\theta' - \epsilon/2, -\theta' + \epsilon/2] \quad (4.104)$$

because of the restrictions imposed by the single-particle eigenvalue of the single-mode (actually of the pair-mode) twist field (4.86). The result is (taking the limit $\epsilon \rightarrow 0$)

$$S_\alpha(x,t) = \frac{1}{1-\alpha} \log \langle T^\alpha(0,t) \bar{T}^\alpha(x,t) \rangle \sim \int \frac{d\theta}{2\pi} \min(x, 2t|v(\theta)|) H_\alpha(\theta) . \quad (4.105)$$

This is in full agreement with the quasiparticle picture [209, 210]. This is the promised hydrodynamic origin of the entanglement growth and it is based on purely classical concepts. The fluctuations are encoded in the initial state and transported via the Euler equations: that is all we needed.

4.6 Outlook

In this last chapter we have discussed the application of BFT formalism to the calculation of the entanglement Renyi entropies. We have seen extensively how the presence of long range correlations might hinder the direct application of BFT to quench problems and presented a way to handle this complication. This is done

via the introduction of new types of fields, *single-mode* (and their pair relatives) twist fields. They are a refined version of twist fields. The research on long range correlations in the dynamics of many-body system is not well established and such concepts have not been appreciated too much in the recent literature, see [249] for an example. We would like to mention though that recently a space-time duality approach [212] has been proposed for the calculation of full counting statistics in many-body systems. This is consistent with our findings of course but they are able to deal with truly interacting systems. At present we have to further develop our theory to attach this situation. A comment is that a space-time duality is natural in a sense, at least from the point of view of transport equations. Indeed, in principle there space and time play the same role. Also, we have been able to give a fully hydrodynamic ab-initio derivation of the quasi-particle picture for Renyi entropies. The next natural step, is of course to understand how to generalise our construction in the presence of interactions. This is non-trivial as in that case the scattering matrix in replica space is not constant anymore. We will investigate these details in future works.

Conclusions

We have reached the end of this Thesis and at this point we hope that the reader enjoyed the journey and eventually learnt something new about the interplay between hydrodynamic principles and fluctuations in many-body systems. We hope to have been able to convey this central idea, which was the main conduction wire between all the chapters. We have started simply introducing the main ideas of integrability and hydrodynamics and later we moved to large deviations and probabilities in many-body quantum and classical systems. The Onsager fundamental idea that correlations and so fluctuations follow the same relaxation laws of macroscopic observables directly leads to the hydrodynamic theory of dynamical correlation functions. Hydrodynamic projections form the basis and the main tool to use in situations where the observables of interest have overlaps with conserved densities. When this fails, the decays of correlation functions, that means decorrelation and information loss, is faster than algebraic, typically exponential. Large deviations rule such exponential decays, probabilities that are extremely small. Such behavior can still be accessed knowing Euler scale hydrodynamics and equilibrium quantities via the Ballistic Fluctuation Theory. The by-product is that we have a powerful tool to compute a wide range of things: decay rates of correlations, counting statistics of certain internal charges to dynamics of certain measures of entanglement. At this point, it is worth mentioning a number of possible future possibilities and directions. First of all, the explicit calculation of counting statistics in spin models (even free) and bosonic systems has not been discussed in detail. In the literature there are a number of studies on this. The characterisation of generic oscillations [250] in correlation functions (or even one-point functions) is interesting and BFT potentially provides some of them together with saddle-point methods. Inhomogeneous scenarios like those of [251, 252] have remained excluded from our study but there exist already a large body of works, especially [136] allowing the repetition of what we have done for trapped systems. In interacting models, it is known that diffusion appears, especially in relation to thermalisation [253] and it is natural to ask what is the

fate of large deviations when looking at the finer diffusive scale. Recently third order dispersive hydrodynamics appeared [254] and the question of the analysis of dispersive structure in hydrodynamics is compelling. In soliton gas theories such phenomena have been known since the beginning [255] but the Witham theory does not offer a full solution [256]. Also, what is the fate of fluctuations at $T = 0$? Do hydrodynamic projections still occur when higher derivatives are included in the gradient expansion? Another more mathematical aspect related to this Thesis is the study of the asymptotic of Fredholm determinants [34]. All the present approaches to exactly calculable full counting statistics and dynamical correlation in spin chains make use of these tools. Is it possible to map back the operator of the determinant to some local hamiltonian and use hydrodynamic principles? All these questions pave the way for interesting future research and leave room for fundamental advances in understanding such a complicated topic as that of many-body systems out-of-equilibrium. There is one last thing that we would like to claim and that should appear relatively reasonable: equations describing large scale physics in the bulk of the system are classical. Indeed, besides finer and finer scales captured by higher orders in a derivative expansion of the response of the system with respect to the drives, the main contributions come from Euler and diffusive hydrodynamics (Navier-Stokes) which are two predominantly classical phenomena. The diffusion equation is not even relativistically invariant and depends on the reference frame. Of course the Planck's constant appears in the TBA equations via the scattering kernels related to the scattering matrix and so in the dressing equations and in the effective velocity so directly into the Euler equation already. Ref. [86] argues that, at least in free theories, high order corrections describe effects negligible far from the middle of the light-cone, only visible at the edges of the light-cone. In particular the third order spatial derivatives are proportional to \hbar^2 and become subleading. It looks like that as far as dynamics of the bulk is concerned the mechanisms responsible for the dynamics are the same as those of classical physics. Quantising the fluctuations around the classical theory [90] allows to reconstruct quantum fluctuations in the initial state: this is probably all that is needed, if one is interested in large scales only. Noise and dephasing make sure that classical physics emerges in the same way as commonly experienced electromagnetic fields are described by Maxwell's equations although the energy of a photon is quantised in units of \hbar . We have seen that even quantities that are believed to be purely characteristics of quantum systems, like the entanglement entropy, at large scales are captured by hydrodynamics. All that was needed was to take into account correctly the initial states. Although

there might be engineered protocols where signatures of quantum mechanics are visible macroscopically [257], in isolated systems with local interactions these mechanisms are non-generic and, at large scale, physics should be largely classical.

Appendix A

Jordan-Wigner strings

We consider the correlator $\langle \sigma_x^+(t) \sigma_0^-(0) \rangle$ and wish to establish formula (2.51). For simplicity, we concentrate on the expectation being taken in the odd-fermion sector, projected onto by P_- ; the argument is similar in the other sector. Then, according to the JW transformation (2.4), in $\langle \sigma_x^+(t) \sigma_0^-(0) \rangle$ we may set $\sigma_0^-(0) = a_0$ and

$$\sigma_x^+(t) = e^{iH_- t} a_x^\dagger \exp \left(i\pi \sum_{y=0}^{x-1} a_y^\dagger a_y \right) e^{-iH_+ t} = a_x^\dagger(t) \exp \left(i\pi \sum_{y=0}^{x-1} q(y, t) \right) e^{iH_- t} e^{-iH_+ t} \quad (\text{A.1})$$

where we use $q(x) = a_x^\dagger a_x$, and where the fermion time-evolution is with respect to H_- (see (2.10)).

We now show that, in the limit of an infinite chain $N \rightarrow \infty$, we have

$$e^{iH_- t} e^{-iH_+ t} = \exp \left(i\pi \int_0^t ds j(0, s) \right). \quad (\text{A.2})$$

For this purpose, let us denote by $H_\pm|_y^z$ the fermionic hamiltonians H_\pm where in (2.6) the sum is for x from y to $z - 1$. Then, one can check that for every $y \in \mathbb{N}$ and $z \gg y$,

$$e^{-iH_+|_{-y}^y t} = e^{i\pi Q|_0^z} e^{-iH_-|_{-y}^y t} e^{-i\pi Q|_0^z}. \quad (\text{A.3})$$

Therefore,

$$e^{iH_-|_{-y}^y t} e^{-iH_+|_{-y}^y t} = e^{i\pi Q|_0^z(t)} e^{-i\pi Q|_0^z} \quad (\text{A.4})$$

where $Q|_0^z(t)$ is evolved with respect to $H_-|_{-y}^y$. Note that $q(x)$ is still a conserved density for time evolution by $H_-|_{-y}^y$. Its associated current is the operator

$$j(x) = 2i(a_x^\dagger a_{x-1} - a_{x-1}^\dagger a_x) \quad (\text{A.5})$$

Jordan-Wigner strings

for time evolution by H_- for all $|x| \ll y$, but it is identically 0 for all $|x| \gg y$, because at these positions the evolution by $H_-|_{-y}^y$ is trivial. Therefore, using the conservation law (2.16) (for $H_-|_{-y}^y$), we have

$$Q|_0^z(t) = Q|_0^z + \int_0^t ds j(0, s). \quad (\text{A.6})$$

The limit $y \rightarrow \infty$ on the left-hand side of (A.4) exists, as $H_-|_{-y}^y - H_+|_{-y}^y$ is supported on the sites $-1, 0$, and thus by the Baker-Campbell-Hausdorff formula, the left-hand side becomes an operator supported with exponential accuracy around the position 0. Similarly, the limit $z \gg y \rightarrow \infty$ on the right-hand side of (A.4) also exists, using (A.6) and the fact that, by the Lieb-Robinson bound [258], the time-evolved current is supported on a finite number of site (at most proportional to t) with exponential accuracy. In this limit, $j(0, s)$ is now evolved with respect to H_- . We obtain

$$e^{iH_-t} e^{-iH_+t} = \exp\left(i\pi \int_0^t ds j(0, s) + i\pi Q^+\right) \exp(-i\pi Q^+). \quad (\text{A.7})$$

By contour deformation, we may rewrite

$$\int_0^t ds j(0, s) = \int_0^t ds j(z, s) + Q|_0^z(t) - Q|_0^z \quad (\text{A.8})$$

where $Q^+ = \lim_{z \rightarrow \infty} Q|_0^z$. By the Lieb-Robinson bound, the operator $I = \int_0^t ds j(z, s)$ is supported, with exponential accuracy, on $[z - vt, z + vt]$, where v is the Lieb-Robinson velocity. Therefore, the projection of I on negative positions is exponentially small as z is made large. As both H_- and $j(z)$ preserve fermion number, the operator I is also fermion-number-preserving. Therefore, for z large enough, all operators on the right-hand side of (A.8) are fermion-number-preserving and supported on non-negative positions. Hence they commute with Q^+ (with exponential accuracy). The Baker-Campbell-Hausdorff formula applied to (A.7) then gives (A.2), which is exact as the result is independent of z . Using (A.2) in expression (A.1), and similar arguments on the even-fermion sector (projector P_+) we obtain (2.52). We emphasise that this is an exact formula, and we expect that it be possible to make it rigorous with currently known theorems in the context of the algebraic formulation of quantum chains.

We now argue that the correct leading asymptotic behaviour at large x is (2.51). The argument is based on the idea that the commutator of local observables at

large distances in space-time tends to zero. This follows from the Lieb-Robinson bound if we understand local observables as those supported on finite number of sites, and if we take large space-like distances (again as determined by the Lieb-Robinson velocity). However, for our argument, we need to extend the concept of locality to “semi-local” observables, end-points of appropriate infinite strings (such as in the Jordan-Wigner transformation, or more generally twist fields), and to assume that vanishing also holds uniformly enough in time-like regions as well. We note that in time-like regions, the weaker statement of “almost-everywhere ergodicity” has been shown rigorously in thermal states for all quantum spin chains with short-range interactions [134, 259], based on exponential decay of correlations in space [260].

The observables

$$Q^+(x) := \sum_{y=x}^{\infty} q(y) \quad (\text{A.9})$$

are fermion-number-preserving, and commute with any fermion-number-preserving local operator supported at positions z far enough from x (this fact we have already used in our derivation above). Therefore, $Q^+(x)$ may be adjoined to the space of fermion-number-preserving local operators¹. This space also includes $j(x)$. Commutators of operators within this space vanish at large space-like separations. Assuming that vanishing also holds in time-like directions², it is then a simple matter to see that, by the Baker-Campbell-Hausdorff formula,

$$\begin{aligned} & \exp\left(i\pi \sum_{y=0}^{x-1} q(y, t)\right) \exp\left(i\pi \int_0^t ds j(0, s)\right) \\ &= \exp\left(i\pi Q^+(x, t) - i\pi Q^+(0, t)\right) \exp\left(i\pi \int_0^t ds j(0, s)\right) \\ &\asymp \exp\left(i\pi Q^+(x, t) - i\pi Q^+(0, t) + i\pi \int_0^t ds j(0, s)\right); \end{aligned} \quad (\text{A.10})$$

that is, the neglected commutators do not contribute to the leading long-time terms in the exponential. This gives (2.51).

¹It is shown in [261] that such observables are elements of the Gelfand-Naimark-Segal Hilbert space, and that they have good locality properties; this gives a partial justification of the present loose argument.

²The weaker statement of vanishing of correlations under long-time averaging, valid almost everywhere in space-time including time-like directions, is shown in [262], which serves to partially justify our present hypothesis.

Appendix B

Free fermionic techniques

B.1 Diagonalisation of quadratic fermionic Hamiltonians

There is a general recipe to diagonalise a generic quadratic fermionic Hamiltonian and it is discussed in [147]. The procedure is very simple and it is important in order to study correlation functions as well, especially for numerical approaches. Consider the generic quadratic Hamiltonian

$$H = \sum_{xy} a_x^\dagger M_{xy} a_y + \frac{1}{2} \sum_{xy} \left[a_x^\dagger B_{xy} a_y^\dagger + h.c. \right] \quad (\text{B.1})$$

where $h.c.$ stands for the hermitian conjugate. The matrix M is symmetric while the matrix B can always be chosen to be anti-symmetric and real. We want to find a canonical transformation to put the Hamiltonian in the form

$$H = \sum_k \Lambda_k \eta_k^\dagger \eta_k + C \quad (\text{B.2})$$

where C is a constant and η_k are normalised Majorana fermions satisfying ordinary anti-commutation relations. If this is possible then

$$[H, \eta_k] = -\Lambda_k \eta_k \quad (\text{B.3})$$

by definition. One defines the new fermions in the following way

$$\eta_k = \sum_x g_{kx} a_x + h_{kx} a_x^\dagger \quad (\text{B.4a})$$

Free fermionic techniques

$$\eta_k^\dagger = \sum_x g_{kx}^* a_x^\dagger + h_{kx}^* a_x \quad (\text{B.4b})$$

and substitutes in (B.3). One derives the following conditions

$$\Lambda_k g_{kx} = \sum_y [g_{ky} M_{yx} - h_{ky} B_{yx}] \quad (\text{B.5a})$$

$$\Lambda_k h_{kx} = \sum_y [g_{ky} B_{yx} - M_{ky} B_{yx}] \quad (\text{B.5b})$$

and introducing the linear combinations

$$\phi_{kx} = g_{kx} + h_{kx} \quad (\text{B.6a})$$

$$\psi_{kx} = g_{kx} - h_{kx} \quad (\text{B.6b})$$

one arrives at (in matrix notation)

$$\boldsymbol{\phi}_k (\mathbf{M} - \mathbf{B}) = \Lambda_k \boldsymbol{\psi}_k \quad (\text{B.7a})$$

$$\boldsymbol{\psi}_k (\mathbf{M} + \mathbf{B}) = \Lambda_k \boldsymbol{\phi}_k \quad (\text{B.7b})$$

which can easily be seen to give

$$\boldsymbol{\phi}_k (\mathbf{M} - \mathbf{B}) (\mathbf{M} + \mathbf{B}) = \Lambda_k^2 \boldsymbol{\phi}_k \quad (\text{B.8a})$$

$$\boldsymbol{\psi}_k (\mathbf{M} + \mathbf{B}) (\mathbf{M} - \mathbf{B}) = \Lambda_k^2 \boldsymbol{\psi}_k \quad (\text{B.8b})$$

Above $\boldsymbol{\phi}_k$ and $\boldsymbol{\psi}_k$ are the columns of the matrices $\boldsymbol{\phi}$ and $\boldsymbol{\psi}$. These two equations determine both the energy spectrum and the transformation to new non-interacting canonical fermions. Since $\mathbf{M} = \mathbf{M}^T$ and $\mathbf{B}^T = -\mathbf{B}$ we also have $(\mathbf{M} \pm \mathbf{B})^T = \mathbf{M} \mp \mathbf{B}$ and so both matrices $(\mathbf{M} \pm \mathbf{B})(\mathbf{M} \mp \mathbf{B})$ are symmetric and semi-positive definite. The eigenvalues Λ_k are real and the eigenvectors $\boldsymbol{\phi}_k$ and $\boldsymbol{\psi}_k$ are orthogonal and can be chosen to be real. This implies $\boldsymbol{\phi}\boldsymbol{\phi}^T = \mathbb{1}$ and $\boldsymbol{\psi}\boldsymbol{\psi}^T = \mathbb{1}$ which in turn means that the matrices \mathbf{g} and \mathbf{h} are real and they satisfy the relations

$$\mathbf{g}\mathbf{g}^T + \mathbf{h}\mathbf{h}^T = \mathbb{1} \quad (\text{B.9a})$$

$$\mathbf{g}\mathbf{h}^T + \mathbf{h}\mathbf{g}^T = 0 \quad (\text{B.9b})$$

This is proven by direct calculation from (B.6)

$$\boldsymbol{\phi}\boldsymbol{\phi}^T = \mathbf{g}\mathbf{g}^T + \mathbf{h}\mathbf{h}^T + \mathbf{g}\mathbf{h}^T + \mathbf{h}\mathbf{g}^T \quad (\text{B.10a})$$

B.1 Diagonalisation of quadratic fermionic Hamiltonians

$$\psi\psi^T = g g^T + h h^T - g h^T - h g^T \quad (\text{B.10b})$$

which after summing and subtracting gives (B.9). In the same way one proves that the η 's are canonical fermions. In matrix form we can write

$$\begin{pmatrix} \eta \\ \eta^\dagger \end{pmatrix} = \begin{pmatrix} g & h \\ h & g \end{pmatrix} \begin{pmatrix} a \\ a^\dagger \end{pmatrix} \quad (\text{B.11})$$

and by inspection one finds

$$\begin{pmatrix} a \\ a^\dagger \end{pmatrix} = \begin{pmatrix} g^T & h^T \\ h^T & g^T \end{pmatrix} \begin{pmatrix} \eta \\ \eta^\dagger \end{pmatrix} . \quad (\text{B.12})$$

These relations will prove very useful when computing correlation functions. It only remains to compute the constant C in the transformed Hamiltonian. This is done using the fact that the trace is invariant under canonical transformations. The proof of this fact is easier using a matrix notation. so that In a chain with N sites, on one side

$$\text{Tr } H = 2^{N-1} \text{Tr } A \quad (\text{B.13})$$

while on the other side

$$\text{Tr } H = 2^{N-1} \text{Tr } \Lambda + 2^N C . \quad (\text{B.14})$$

The factors $1/2$ come from the fact that $\text{Tr } a_x^\dagger a_x = 1/2$ because if the site at x is unoccupied that state does not contribute to the sum. This happens exactly ones in a fermionic trace. Overall we have found

$$H = \sum_k \Lambda_k \eta_k^\dagger \eta_k + \frac{1}{2} (\text{Tr } A - \text{Tr } \Lambda) . \quad (\text{B.15})$$

The results of this appendix are fundamental both for the analytical and the numerical study of correlation functions of spin chains that can be mapped to free fermionic theories.

B.2 Fermionic correlation functions

B.2.1 Determinants and Pfaffians

In this Appendix we provide details and proofs for some little known but useful results for Pfaffians and determinants.

Definition B.2.1 (Pfaffian). Given an anti-symmetric $2N \times 2N$ matrix A with complex coefficients, its pfaffian is defined as

$$\text{Pf } A = \frac{1}{2^N N!} \sum_{\sigma \in \mathcal{S}_{2N}} \epsilon_{\sigma} \prod_{i=1}^{2N-1} A_{\sigma(i), \sigma(i+1)} \quad . \quad (\text{B.16})$$

There are many redundant terms in this sum. The first redundancy comes from the fact that one can freely permute the factors $A_{\sigma(i), \sigma(i+1)}$ in the product. For instance, the permutation acting as $\sigma(1) = 2N - 1, \sigma(2) = 2N, \sigma(2N - 1) = 1, \sigma(2N) = 2$ and the identity permutation give the same contribution as only the order of the factors has changed. The number of ways to permute the factors is of course $N!$. The other redundancy comes from the anti-symmetry of A . Every time two permutations differ only by a swap of two labels, their signs differ by -1 which is compensated by the -1 coming from the anti-symmetry of the matrix. If they differ by more than one swap the same thing happens. Given a string of N pairs of indices, we can build a permutation differing by k swaps in $\binom{N}{k}$ different ways. Summing over we obtain $\sum_{k=1}^N \binom{N}{k} = 2^N$. In this way we can write

$$\text{Pf } A = \sum_{\substack{i_1 < \dots < i_N \\ j_1 < \dots < j_N}} A_{i_1 j_1} \dots A_{i_N j_N} \quad . \quad (\text{B.17})$$

There is one important theorem relating Pfaffians and determinants.

Theorem B.2.1. For a $2N \times 2N$ anti-symmetric matrix A we have

$$\det A = (\text{Pf } A)^2 \quad . \quad (\text{B.18})$$

An elementary proof using only properties of triangular matrices can be found in Ref. [263]. Pfaffians can be computed recursively. This can be seen as follows [264]: consider a fermion whose anti-commutation relations give a c -number

$$\{a_x, a_y\} = 2(x, y) \quad (\text{B.19})$$

where the symbol (xy) just means any c -number function of x and y , it is just notation. Consider also the following fermionic correlation function

$$\frac{1}{4} \text{Tr} a_1 \dots a_{2N} \equiv (1, \dots, 2N) \quad . \quad (\text{B.20})$$

This is a typical fermionic trace one would like to compute. Using the anti-commutation $2N$ times and rearranging we find

$$\text{Tr} a_1 \dots a_{2N} = \sum_k (-1)^k (1, k)(2, \dots, k-1, k+1, \dots, 2N) \quad (\text{B.21})$$

and iterating again we obtain

$$(1, \dots, 2N) = \sum_{i_1 < \dots < i_{2N}} (i_1, i_2) \dots (i_{2N-1}, i_{2N}) \quad . \quad (\text{B.22})$$

This holds at zero temperature $T = 0$. Comparing to (B.17) we can formulate the theorem

Theorem B.2.2. Given fermionic operators satisfying $\{a_x, a_y\} = 2(x, y)$ ¹ the trace of the product of $2N$ of them is given by

$$\text{Tr} a_1 \dots a_{2N} = 4 \text{Pf} C \quad (\text{B.23})$$

with the matrix C having elements

$$C_{xy} = (x, y) \quad x < y \quad x, y = 1, \dots, 2N \quad (\text{B.24a})$$

$$C_{xy} = -C_{yx} \quad . \quad (\text{B.24b})$$

It is possible to extend this result to finite temperature gaussian states following the method of Ref. [265]. A gaussian state is nothing but a state described by a density matrix of the form

$$\rho = \frac{1}{Z} e^{-\beta H} \quad (\text{B.25})$$

where the Hamiltonian H is quadratic. It is customary to call state also the expectation value with respect to ρ : $\langle \bullet \rangle_\rho = Z^{-1} \text{Tr} \rho \bullet$. This means that Wick's theorem [] holds. The generalisation of the above theorem reads

¹Note that these fermions are real, also called Majorana fermions.

Theorem B.2.3. Given a gaussian state ρ and fermionic operators satisfying $\{a_x, a_y\} = 2\delta_{xy}$, the following holds

$$\langle a_1 \dots a_{2N} \rangle_\rho = 4 \text{Pf} C \quad (\text{B.26})$$

with the matrix C having elements

$$C_{xy} = \langle a_x a_y \rangle_\rho \quad x < y \quad x, y = 1, \dots, 2N \quad (\text{B.27a})$$

$$C_{xy} = -C_{yx} \quad . \quad (\text{B.27b})$$

These are powerful results reducing the complexity of a multi-point correlation function to the calculation of Pfaffian. There are efficient algorithms for doing that and we will discuss them in the appropriate Appendix.

B.2.2 Correlation functions of quadratic Hamiltonians

Using the results of the the previous sections it is possible to write in a compact way a generic fermionic correlation function in a gaussian state. For simplicity we will take the state to be a GGE of the form

$$\rho = \frac{1}{Z} e^{-\sum_k W_k \eta_k^\dagger \eta_k} \quad (\text{B.28})$$

where η_k 's are canonical complex fermions. The density matrix is diagonal in the occupation number basis. This is true for quadratic theories [] and the function W_k completely characterised the state. With reference to the quadratic Hamiltonian (B.1) we introduce two independent sets of real Majorana fermions

$$A_x = a_x^\dagger + a_x \quad (\text{B.29a})$$

$$B_x = i(a_x^\dagger - a_x) \quad (\text{B.29b})$$

satisfying equal time anti-commutation relations

$$\{A_x, A_y\} = \{B_x, B_y\} = 2\delta_{xy} \quad (\text{B.30a})$$

$$\{A_x, B_y\} = 0 \quad . \quad (\text{B.30b})$$

B.2 Fermionic correlation functions

The state (B.28) remains quadratic under the transformation to Majorana fermions and Wick's theorem keeps holding true. In particular Theorem (B.2.3) is still valid. In particular, due to independence

$$\langle \prod_x A_x \prod_y B_y \rangle = \langle \prod_x A_x \rangle \langle \prod_y B_y \rangle \quad (\text{B.31})$$

The time evolution spoils such property because $\{A_x(t), B_y\} \neq 0$. We can compute this quantity in general using the transformation (B.12). In matrix form the commutation relations for the complex fermions can be written as

$$\{a, a^\dagger\} = a(a^\dagger)^T + a^\dagger a^T = \mathbb{1} \quad (\text{B.32a})$$

$$\{a, a\} = \{a^\dagger, a^\dagger\} = 0 \quad . \quad (\text{B.32b})$$

First of all we can compute the time evolution of the complex fermions a

$$\begin{aligned} a(t) &= e^{iHt} (\mathbf{g}^T \boldsymbol{\eta} + \mathbf{h}^T \boldsymbol{\eta}^\dagger) e^{-iHt} \\ &= \mathbf{g}^T e^{-i\Lambda t} \boldsymbol{\eta} + \mathbf{h}^T e^{i\Lambda t} \boldsymbol{\eta}^\dagger \end{aligned} \quad (\text{B.33})$$

and taking the hermitian conjugate

$$a^\dagger(t) = \mathbf{g}^T e^{i\Lambda t} \boldsymbol{\eta}^\dagger + \mathbf{h}^T e^{-i\Lambda t} \boldsymbol{\eta} \quad . \quad (\text{B.34})$$

With this result we get

$$\begin{aligned} A(t) &= a^\dagger(t) + a(t) \\ &= \boldsymbol{\phi}^T (e^{i\Lambda t} \boldsymbol{\eta}^\dagger + e^{-i\Lambda t} \boldsymbol{\eta}) \end{aligned} \quad (\text{B.35})$$

and in the same way

$$\begin{aligned} B(t) &= i(a^\dagger(t) - a(t)) \\ &= i\boldsymbol{\psi}^T (e^{i\Lambda t} \boldsymbol{\eta}^\dagger - e^{-i\Lambda t} \boldsymbol{\eta}) \end{aligned} \quad (\text{B.36})$$

Now we can compute the anti-commutator, which is simple but tedious. Taking into account the anti-commutation relations we have

$$\{A(t), B\} = 2\boldsymbol{\phi}^T \sin(\Lambda t) \boldsymbol{\psi}^T \quad (\text{B.37})$$

Free fermionic techniques

This is consistent with the fact that at $t = 0$ the Majorana fermions are independent. In the same way one computes all the other anti-commutators and verifies they are simple matrices so that Wick's theorem will continue to hold as well as the trace formula (B.2.3). The two point function correlation matrix on a GGE (B.28) is

$$\begin{aligned}\Gamma_{A(t)B} &= \langle A(t)B^T \rangle \\ &= \langle \boldsymbol{\phi}^T \left(e^{i\Lambda t} \boldsymbol{\eta}^\dagger + e^{-i\Lambda t} \boldsymbol{\eta} \right) i \left[\boldsymbol{\psi}^T \left(\boldsymbol{\eta}^\dagger - \boldsymbol{\eta} \right) \right]^T \rangle \\ &= i \boldsymbol{\phi}^T \left(-e^{i\Lambda t} \langle \boldsymbol{\eta}^\dagger \boldsymbol{\eta}^T \rangle + e^{-i\Lambda t} \langle \boldsymbol{\eta} (\boldsymbol{\eta}^\dagger)^T \rangle \right) \boldsymbol{\psi} \quad .\end{aligned}\tag{B.38}$$

Using

$$\langle \boldsymbol{\eta}^\dagger \boldsymbol{\eta}^T \rangle = (e^W + \mathbb{1})^{-1}\tag{B.39}$$

where W is the diagonal matrix associated to W_k defining the state in (B.28), it is a simple matter to establish

$$\Gamma_{A(t)B} = i \boldsymbol{\phi}^T \frac{\sinh(W/2 - i\Lambda t)}{\cosh(W/2)} \boldsymbol{\psi} \quad .\tag{B.40}$$

By the cyclicity of the trace

$$\Gamma_{AB(t)} = \Gamma_{A(-t)B} \quad .\tag{B.41}$$

The very same calculation, with minor modifications gives

$$\Gamma_{B(t)A} = -\boldsymbol{\psi}^T \frac{\sinh(W/2 - i\Lambda t)}{\cosh(W/2)} \boldsymbol{\phi} \quad .\tag{B.42}$$

$$\Gamma_{A(t)A} = \boldsymbol{\phi}^T \frac{\cosh(W/2 - i\Lambda t)}{\cosh(W/2)} \boldsymbol{\phi} \quad .\tag{B.43}$$

$$\Gamma_{B(t)B} = \boldsymbol{\psi}^T \frac{\cosh(W/2 - i\Lambda t)}{\cosh(W/2)} \boldsymbol{\psi} \tag{B.44}$$

These are the elementary contractions needed to compute any correlation function using the trace formula (B.2.3). We notice that such formulae can be used to study correlation functions not only of homogeneous fermionic Hamiltonian but are valid also in presence of disorder []. It is convenient to introduce the vector of fermions such that

$$\mathbf{U} = \begin{pmatrix} A \\ B \end{pmatrix}\tag{B.45}$$

with correlation matrix

$$\Gamma = \langle \mathbf{u} \mathbf{u}^T \rangle = \begin{pmatrix} \Gamma_{AA} & \Gamma_{AB} \\ \Gamma_{BA} & \Gamma_{BA} \end{pmatrix} \quad (\text{B.46})$$

such that a generic fermionic correlation function between operators A_x and B_x is obtained as a Pfaffian of a particular sub-matrix of (B.46). In general, given a matrix P such that $Z = PU$ we have

$$\langle \mathbf{Z} \mathbf{Z}^T \rangle = \text{Pf}(\mathbf{P} \Gamma \mathbf{P}^T) = \det P \text{Pf} \Gamma \quad . \quad (\text{B.47})$$

B.2.3 Application to XY spin chains

Consider the following correlation function

$$4 \langle s_y^1(t) s_{x+y}^2 \rangle = \langle A_1(t) B_1(t) \dots A_{y-1}(t) B_{y-1}(t) A_y(t) A_1 B_1 \dots A_{y+x-1} B_{y+x-1} A_{y+x} \rangle \quad (\text{B.48})$$

and it is of course a Pfaffian. The relevant matrix has dimension $2(y+x-1) \times 2(y+x-1)$ and its elements read for $i < j$

$$C_{2i-1, 2j-1} = \begin{cases} \langle A_i B_j \rangle & 1 \leq j \leq y-1 \\ \langle A_i A_y \rangle & j = y \\ \langle A_i(t) A_j \rangle & y+1 \leq j \leq y+x-2 \\ \langle A_i A_y \rangle & j = y+x \end{cases} \quad (\text{B.49a})$$

$$C_{2i-1, 2j} = \begin{cases} \langle A_i A_j \rangle & 1 \leq j \leq y-1 \\ \langle A_i(t) B_j \rangle & y+1 \leq j \leq y+x-1 \end{cases} \quad (\text{B.49b})$$

$$C_{2i, 2j-1} = \begin{cases} \langle A_i B_j \rangle & 1 \leq j \leq y-1 \\ \langle A_i A_y \rangle & j = y \\ \langle A_i(t) A_j \rangle & y+1 \leq j \leq y+x-2 \\ \langle A_i A_y \rangle & j = y+x \end{cases} \quad (\text{B.50})$$

$$C_{2i, 2j} = \begin{cases} \langle B_i A_j \rangle & 1 \leq j \leq y-1 \\ \langle A_i A_y \rangle & j = y \\ \langle A_i(t) A_j \rangle & y+1 \leq j \leq y+x-2 \\ \langle A_i A_y \rangle & j = y+x \end{cases} \quad (\text{B.51a})$$

$$C_{2i-1,2j} = \begin{cases} \langle A_i A_j \rangle & 1 \leq j \leq y-1 \\ \langle A_i(t) B_j \rangle & y+1 \leq j \leq y+x-1 \end{cases} \quad (\text{B.51b})$$

$$C_{2i,2j-1} = \begin{cases} \langle A_i B_j \rangle & 1 \leq j \leq y-1 \\ \langle A_i A_y \rangle & j = y \\ \langle A_i(t) A_j \rangle & y+1 \leq j \leq y+x-2 \\ \langle A_i A_y \rangle & j = y+x \end{cases} \quad (\text{B.52})$$

It is a simple matter to show that analogous formulae hold for all the other correlation functions between spin operators. For more details we refer to the Appendix of [3].

Appendix C

Asymptotic results

C.1 Skellam distribution

The Skellam distribution describes the difference of two Poissonian random variables. It can be derived in two ways, both easy. We use brute force here for the method using the generating function see the original paper [266]. Take now two independent Poisson variables with parameter μ_1 and μ_2 and distributions $Q(n; \mu_1)$ and $Q(n; \mu_2)$ respectively. The distribution $P(\Delta)$ of the difference is

$$\begin{aligned}
 P(\Delta; \mu_1, \mu_2) &= \sum_{n=-\infty}^{+\infty} \sum_{k=-\infty}^{+\infty} Q(n; \mu_1) Q(k; \mu_2) \delta_{n-k, \Delta} = \sum_{n=-\infty}^{+\infty} Q(n + \Delta; \mu_1) Q(n; \mu_2) \\
 &= e^{-(\mu_1 + \mu_2)} \sum_{n=-\infty}^{+\infty} \frac{\mu_1^{\Delta+n}}{(n + \Delta)!} \frac{\mu_2^n}{n!} = e^{-(\mu_1 + \mu_2)} \sum_{n=\max(0, -\Delta)}^{+\infty} \frac{\mu_1^{\Delta+n}}{(n + \Delta)!} \frac{\mu_2^n}{n!}
 \end{aligned} \tag{C.1}$$

where in the last line we used the fact the the factorial is divergent for negative values of the argument. If $0 > -\Delta$ we get

$$\sum_{n=0}^{+\infty} \frac{\mu_1^{\Delta+n}}{(n + \Delta)!} \frac{\mu_2^n}{n!} = \left(\frac{\mu_1}{\mu_2} \right)^{\frac{\Delta}{2}} \sum_{n=0}^{+\infty} \frac{1}{(n + \Delta)! n!} \left(2 \sqrt{\mu_1 \mu_2} \right)^{2n + \Delta} = \left(\frac{\mu_1}{\mu_2} \right)^{\frac{\Delta}{2}} I_{\Delta}(2 \sqrt{\mu_1 \mu_2}) \tag{C.2}$$

where I_n is the modified Bessel function of order n . On the other hand when $0 < -\Delta$

$$\sum_{n=-\Delta}^{+\infty} \frac{\mu_1^{\Delta+n}}{(n + \Delta)!} \frac{\mu_2^n}{n!} = \sum_{n=0}^{+\infty} \frac{\mu_1^n}{(n - \Delta)!} \frac{\mu_2^{n-\Delta}}{n!} \tag{C.3}$$

Asymptotic results

which is the same formula as before with $\mu_1 \leftrightarrow \mu_2$ and $\Delta \mapsto -\Delta$. Putting all together

$$P(\Delta; \mu_1, \mu_2) = e^{-(\mu_1 + \mu_2)} \left(\frac{\mu_1}{\mu_2} \right)^{\frac{\Delta}{2}} I_{|\Delta|}(2\sqrt{\mu_1 \mu_2}) \quad . \quad (\text{C.4})$$

In the special case $\mu_1 = \mu_2 = \mu$ we get

$$P(\Delta; \mu) = e^{-2\mu} I_{|\Delta|}(2\mu) \quad . \quad (\text{C.5})$$

C.2 Asymptotic of modified Bessel function of infinite order

Since we will have $\mu = xd$ and $\Delta = x\delta$ where d is the solitons density with $x \rightarrow +\infty$, in order to highlight a large deviation form of the distribution, we will have to analyze the asymptotic behavior of large order modified Bessel functions. This can be done exploiting integral representations and in combination with saddle point method but here we follow a WKB analysis. Consider a Schödinger equation for a particle of mass $m = 1/2$ in a potential $V(z)$

$$\psi''(z) = \frac{1}{\hbar^2} (V(z) - E) \psi(z) \quad (\text{C.6})$$

and assume a solution of the form

$$\psi(z) = e^{iS(z)} \quad . \quad (\text{C.7})$$

Substituting we obtain

$$S''(z) + (S'(z))^2 = \frac{1}{\hbar^2} (E - V(z)) \quad (\text{C.8})$$

and assuming $S''(z) \ll (S'(z))^2$ we obtain

$$S_0(z) = \frac{\pm 1}{\hbar} \int dz p(z) \quad , \quad p(z) = \sqrt{E - V(z)} \quad . \quad (\text{C.9})$$

where $p(z)$ is the classical local momentum. This is consistent as long as $\hbar \rightarrow 0$ because

$$\frac{S_0''(z)}{(S_0'(z))^2} \sim \hbar \quad . \quad (\text{C.10})$$

C.2 Asymptotic of modified Bessel function of infinite order

To proceed further one uses this solution as a 0-th order approximation to compute

$$S'_1(z) = \frac{\pm 1}{\hbar} \sqrt{(E - V(z)) - \hbar^2 S''_0(z)} \quad (\text{C.11})$$

and recalling that $\hbar^2 S''_0(z) \sim \hbar$, in the limit we can expand and get

$$S'_1(z) = \frac{\pm 1}{\hbar} p(z) \mp \frac{\hbar}{2p(z)} S''_0(z) + O(\hbar^2) \quad . \quad (\text{C.12})$$

Since $S''_0(z) = \frac{\pm 1}{\hbar} p'(z)$ we can integrate and obtain

$$S_1(z) = \frac{\pm 1}{\hbar} \int dz p(z) - \log \sqrt{|p(z)|} + O(\hbar^2) \quad (\text{C.13})$$

and we obtain the well known semi-classical approximation of the wave function

$$\psi(z) = \frac{1}{\sqrt{|p(z)|}} \left(A e^{\frac{i}{\hbar} \int dz p(z)} + B e^{-\frac{i}{\hbar} \int dz p(z)} \right) \quad . \quad (\text{C.14})$$

Now consider the modified Bessel equation of order $\nu \in \mathbb{R}$ and for $z \in \mathbb{R}$ as well

$$z^2 \psi''(z) + z \psi'(z) + (z^2 + \nu^2) \psi(z) = 0 \quad (\text{C.15})$$

and let us rescale $z \mapsto Nz$ and $\nu = N\delta$ with $\delta \in \mathbb{R}$.

$$z^2 \psi''(z) + z \psi'(z) + N^2(z^2 + \delta^2) \psi(z) = 0 \quad . \quad (\text{C.16})$$

To study the limit $N \rightarrow +\infty$ we assume in this limit the term $z \psi'(z) \ll z^2 \psi''(z)$ (we check the consistency later) so that the equation becomes

$$\psi''(z) = -N^2 \frac{z^2 + \delta^2}{z^2} \psi(z) \quad (\text{C.17})$$

and comparing to (C.6) we see that the role of \hbar is played by $1/N$ and we have bound state problem instead of a scattering one because $E = 0 < V(z) = \frac{z^2 + \delta^2}{z^2} \geq 0$. The wave function will be

$$\psi(z) = \frac{1}{\sqrt{|p(z)|}} \left(A e^{N \int dz q(z)} + B e^{-N \int dz q(z)} \right) \quad q(z) = \sqrt{V(z)} \quad . \quad (\text{C.18})$$

Note that $z^2 \psi''(z) / z \psi'(z) \sim N$ so as long as $N \rightarrow +\infty$ our approximation is good. We can directly extract the asymptotic behavior of large order modified Bessel

Asymptotic results

functions computing the rate function

$$J(\delta, z) = \int dz \sqrt{V(z)} = \sqrt{z^2 + \delta^2} - \delta \tanh^{-1} \left(\frac{\sqrt{z^2 + \delta^2}}{\delta} \right) \quad (\text{C.19})$$

so that

$$I_{N\delta}(Nz) \asymp e^{NJ(z,\delta)} \quad . \quad (\text{C.20})$$

Note that $\sqrt{\delta^2 + z^2} \geq \delta$ for all z and \tanh^{-1} develops an imaginary part but the exponential decay what matters is only the real part. In particular using $\tanh^{-1}(x) = \frac{1}{2} \log \left(\frac{1+x}{1-x} \right)$ one notes that the real parts of $\tanh^{-1}(1/x)$ and of $\tanh^{-1}(x)$ coincide. Further using the identity

$$\sinh(\tanh^{-1}(x)) = \frac{x}{\sqrt{1-x^2}} \quad (\text{C.21})$$

we can write

$$J(\delta, d) = -\delta \sinh^{-1} \left(\frac{\delta}{2d} \right) + \sqrt{(2d)^2 + \delta^2} \quad (\text{C.22})$$

and the sought asymptotic of the Skellam distribution eq. (C.5) with $\mu = 2xd$ and $\Delta = x\delta$ for $x \rightarrow +\infty$. We have

$$P(\Delta; \mu) \asymp e^{-xR(\delta,d)} \quad x \rightarrow \infty \quad (\text{C.23})$$

with rate function

$$R(\delta, d) = 2d - J(\delta, d) = 2d + \delta \sinh^{-1} \left(\frac{\delta}{2d} \right) - \sqrt{(2d)^2 + \delta^2} \quad . \quad (\text{C.24})$$

C.3 Fourier transform of Bessel function with respect to its order

We need to perform the Fourier transform of the Bessel function with respect to its order. This achieved with the help of the following integral representation [267]

$$I_\nu(z) = \frac{1}{\pi} \int_0^\pi d\theta e^{z \cos \theta} \cos(\nu\theta) - \frac{\sin(\nu\pi)}{\pi} \int_0^{+\infty} d\theta e^{-z \cosh(\theta) - \nu\theta} \quad . \quad (\text{C.25})$$

We have

$$\begin{aligned}\mathcal{F}[I_\nu(z)](k) &= \int \frac{d\nu}{\sqrt{2\pi}} e^{-\nu k} I_\nu(z) \\ &= \frac{1}{\pi} \int_0^\pi d\theta e^{z \cos \theta} \mathcal{F}[\cos(\nu\theta)](k) - \frac{1}{\pi} \int_0^{+\infty} d\theta e^{-z \cosh(\theta)} \mathcal{F}[e^{-\nu\theta} \sin(\nu\pi)](k)\end{aligned}\tag{C.26}$$

and using the results

$$\mathcal{F}[\cos \nu\theta](k) = \sqrt{\frac{\pi}{2}} (\delta(\theta - k) + \delta(\theta + k))\tag{C.27a}$$

$$\mathcal{F}[e^{-\nu\theta} \sin \nu\pi](k) = \iota \sqrt{\frac{\pi}{2}} (\delta(k + \pi - \iota\theta) + \delta(\iota\theta + \pi - k))\tag{C.27b}$$

we obtain

$$\mathcal{F}[I_\nu(z)](k) = \frac{2}{\sqrt{2\pi}} \cosh(z \cos k) H(k) H(\pi - k)\tag{C.28}$$

where $H(x) = 1$ for $x > 0$ and 0 otherwise.

C.4 Saddle point analysis of (3.97)

Let us write the integral as

$$I = \int_0^\pi \frac{ds}{2\pi} e^{\xi f(s)}\tag{C.29}$$

with

$$f(s) = -\iota\delta s + 2d \cos(s)\tag{C.30}$$

and since $f(s)$ is complex we have competition between the oscillatory phase and the increasing or decreasing modulus. The saddle point is

$$s^* = -\iota \sinh^{-1} \left(\frac{\delta}{2d} \right)\tag{C.31}$$

that is purely imaginary. Also

$$f''(s^*) = -\sqrt{4d^2 + \delta^2}\tag{C.32}$$

Defining $f''(s^*) = ae^{\iota\phi}$ and $s - s^* = r^2 e^{\iota\theta}$ we expand

$$f(s) - f(s^*) = \frac{1}{2} ar^2 e^{\iota(\phi+2\theta)} + O((s - s^*)^3)\tag{C.33}$$

Asymptotic results

so the steepest directions across the saddle point are

$$\theta^s = \frac{n\pi}{2} - \frac{\varphi_{\pm}}{2} \quad n = 0, 1 \quad (\text{C.34})$$

and the steepest *descent* directions are

$$\theta^d = \frac{(2n+1)\pi}{2} - \frac{\varphi_{\pm}}{2} \quad n = 0, 1 \quad . \quad (\text{C.35})$$

These directions will be needed soon. We now use Cauchy theorem to deform the contour such that we only follow steepest descent contours. Let us write $s = u + \iota v$ and

$$f(s) = \phi(u, v) + \iota\psi(u, v) \quad (\text{C.36})$$

with

$$\phi(u, v) = v\delta + 2d \cos u \cosh v \quad (\text{C.37a})$$

$$\psi(u, v) = -u\delta - 2d \sin u \sinh v \quad . \quad (\text{C.37b})$$

The steepest descent directions across the saddles points s^* are

$$\theta = \frac{\pi}{2}, \frac{3\pi}{2} \quad (\text{C.37c})$$

We deform the contour from 0 to π to the one going up $+\iota\infty$ passing through s^* and then going down from $+\iota\infty$ to $\pi/2$ along the curve determined by the equation $\psi(u, v) = -\frac{\pi}{2}\delta$. The main contribution is given by the saddle point so we conclude that

$$I \asymp e^{\xi f(s^*)} \quad (\text{C.38})$$

with

$$f(s^*) = \delta \sinh^{-1} \left(\frac{\delta}{2d} \right) - \sqrt{\delta^2 + 4d^2} \equiv -J(\delta, d) \quad . \quad (\text{C.39})$$

References

- [1] J. Myers, J. Bhaseen, R. J. Harris, and B. Doyon, "Transport fluctuations in integrable models out of equilibrium," *SciPost Physics*, vol. 8, Jan 2020.
- [2] J. Myers, J. Bhaseen, R. J. Harris, and B. Doyon, "Transport fluctuations in integrable models out of equilibrium," *SciPost Physics*, vol. 8, no. 1, p. 007, 2020.
- [3] G. D. V. Del Vecchio and B. Doyon, "The hydrodynamic theory of dynamical correlation functions in the XX chain," *Journal of Statistical Mechanics: Theory and Experiment*, vol. 2022, no. 5, p. 053102, 2022.
- [4] G. D. V. Del Vecchio, B. Doyon, and P. Ruggiero, "Entanglement Rényi entropies from ballistic fluctuation theory: the free fermionic case," *arXiv: 2301.02326*, 2023.
- [5] G. D. V. Del Vecchio, M. Kormos, B. Doyon, and A. Bastianello, "Exact large-scale fluctuations of the phase field in the sine-Gordon model," *arXiv: 2305.10495*, 2023.
- [6] R. Koch and A. Bastianello, "Exact thermodynamics and transport in the classical sine-Gordon model," *arXiv: 2303.16932*, 2023.
- [7] O. Castro-Alvaredo, Y. Chen, B. Doyon, and M. Hoogeveen, "Thermodynamic Bethe ansatz for non-equilibrium steady states: exact energy current and fluctuations in integrable QFT," *Journal of Statistical Mechanics: Theory and Experiment*, vol. 2014, p. P03011, mar 2014.
- [8] H. Goldstein, *Classical Mechanics*. Addison-Wesley, 1980.
- [9] M. Fagotti, "Local conservation laws in spin-xy chains with open boundary conditions," *Journal of Statistical Mechanics: Theory and Experiment*, vol. 2016, p. 063105, jun 2016.

References

- [10] M. Fagotti, “Charges and currents in quantum spin chains: late-time dynamics and spontaneous currents,” *Journal of Physics A: Mathematical and Theoretical*, vol. 50, p. 034005, dec 2016.
- [11] J.-S. Caux and F. H. L. Essler, “Time evolution of local observables after quenching to an integrable model,” *Phys. Rev. Lett.*, vol. 110, p. 257203, Jun 2013.
- [12] K. Huang, *Statistical Mechanics*. John Wiley & Sons, 2 ed., 1987.
- [13] E. T. Jaynes, “Information theory and statistical mechanics,” *Phys. Rev.*, vol. 106, pp. 620–630, May 1957.
- [14] E. T. Jaynes, “Information theory and statistical mechanics. ii,” *Phys. Rev.*, vol. 108, pp. 171–190, Oct 1957.
- [15] G. Mussardo, “Infinite-time average of local fields in an integrable quantum field theory after a quantum quench,” *Phys. Rev. Lett.*, vol. 111, p. 100401, Sep 2013.
- [16] A. N. Kolmogorov, “On conservation of conditionally periodic motions for a small change in Hamilton’s function,” *Dokl. Akad. Nauk SSSR*, vol. 98, pp. 527–530, 1954.
- [17] J. Möser, “On invariant curves of area-preserving mappings of an annulus,” *Nachr. Akad. Wiss. Göttingen, II*, pp. 1–20, 1962.
- [18] V. Arnold, “Proof of a theorem of an kolmogorov on the invariance of quasiperiodic motions under small perturbations of the hamiltonian,” *Uspekhi. Mat. Nauk*, vol. 18, pp. 13–41, 1965.
- [19] L. Chierchia, *Kolmogorov–Arnold–Moser (KAM) Theory*, pp. 5064–5091. New York, NY: Springer New York, 2009.
- [20] B. V. Chirikov, “A universal instability of many-dimensional oscillator systems,” *Physics Reports*, vol. 52, no. 5, pp. 263–379, 1979.
- [21] J.-C. Yoccoz, *An Introduction To Small Divisors Problems*, pp. 659–679. Berlin, Heidelberg: Springer Berlin Heidelberg, 1992.
- [22] E. Fermi, J. Pasta, S. Ulam, and M. Tsingou, “Studies of nonlinear problems,” *Los Alamos Report LA-1940*, 1955.

-
- [23] A. J. Lichtenberg and M. A. Leiberman, *Regular and chaotic dynamics*. Springer-Verlag, 1992.
- [24] J. Ford, "The Fermi-Pasta-Ulam problem: Paradox turns discovery," *Physics Reports*, vol. 213, no. 5, pp. 271–310, 1992.
- [25] G. Gallavotti, ed., *The Fermi-Pasta-Ulam Problem: A Status Report*. Springer, 2008.
- [26] N. J. Zabusky and M. D. Kruskal, "Interaction of "solitons" in a collisionless plasma and the recurrence of initial states," *Physical Review Letters*, vol. 15, no. 6, p. 240, 1965.
- [27] M. J. Ablowitz and H. Segur, *Solitons and the inverse scattering transform*. SIAM, 2003.
- [28] L. D. Faddeev and L. A. Takhtajan, *Hamiltonian methods in the theory of solitons*. Springer-Verlag, 1987.
- [29] M. J. Ablowitz and H. Segur, "The inverse scattering transform-fourier analysis for nonlinear problems," *Studies in Applied Mathematics*, vol. 53, no. 4, pp. 249–315, 1974.
- [30] C. S. Gardner, J. M. Greene, M. D. Kruskal, and R. M. Miura, "Method for solving the Korteweg-deVries equation," *Physical review letters*, vol. 19, no. 19, p. 1095, 1967.
- [31] A. D. Luca and G. Mussardo, "Equilibration properties of classical integrable field theories," *Journal of Statistical Mechanics: Theory and Experiment*, vol. 2016, p. 064011, jun 2016.
- [32] P. G. Drazin and R. S. Johnson, *Solitons: an introduction*. Cambridge University Press, 1989.
- [33] H. Bethe, "Zur theorie der metalle," *Zeitschrift für Physik*, vol. 71, pp. 205–226, Mar 1931.
- [34] V. E. Korepin, N. M. Bogoliubov, and A. Izergin, *Quantum Inverse Scattering Method and Correlation Functions*. Cambridge Monographs on Mathematical Physics, Cambridge University Press, 1993.
- [35] A. Luther, "Eigenvalue spectrum of interacting massive fermions in one dimension," *Phys. Rev. B*, vol. 14, pp. 2153–2159, Sep 1976.

References

- [36] F. Franchini, “An introduction to integrable techniques for one-dimensional quantum systems,” *Lecture Notes in Physics*, 2017.
- [37] G. Mussardo, *Statistical field theory: an introduction to exactly solved models in statistical physics*. Oxford University Press, 2010.
- [38] A. L. Retore, “Introduction to classical and quantum integrability,” *Journal of Physics A: Mathematical and Theoretical*, vol. 55, p. 173001, apr 2022.
- [39] P. Dorey, “Exact s-matrices,” *arXiv: hep-th/9810026*, 1998.
- [40] H. J. Schulz, “Fermi liquids and non-fermi liquids,” *arXiv: cond-mat/9503150*, 1995.
- [41] P. Coleman, *Introduction to Many-Body Physics*. Cambridge University Press, 2015.
- [42] L. D. Landau and E. M. Lifshitz, *Statistical Physics, Part 1*, vol. 5 of *Course of Theoretical Physics*. Oxford: Butterworth-Heinemann, 1980.
- [43] S. Parke, “Absence of particle production and factorization of the S-matrix in 1 + 1 dimensional models,” *Nuclear Physics B*, vol. 174, no. 1, pp. 166–182, 1980.
- [44] S. Coleman and J. Mandula, “All possible symmetries of the s matrix,” *Phys. Rev.*, vol. 159, pp. 1251–1256, Jul 1967.
- [45] B. Doyon, “Lecture notes on generalised hydrodynamics,” *SciPost Physics Lecture Notes*, 2020.
- [46] B. Doyon, “Generalized hydrodynamics of the classical Toda system,” *Journal of Mathematical Physics*, vol. 60, p. 073302, 07 2019.
- [47] B. Schroer and T. Truong, “The order/disorder quantum field operators associated with the two-dimensional Ising model in the continuum limit,” *Nuclear Physics B*, vol. 144, no. 1, pp. 80–122, 1978.
- [48] R. J. Baxter, *Exactly Solved Models in Statistical Mechanics*, pp. 5–63.
- [49] A. B. Zamolodchikov and A. B. Zamolodchikov, “Factorized S-matrices in two dimensions as the exact solutions of certain relativistic quantum field theory models,” *Annals of Physics*, vol. 120, no. 2, pp. 253–291, 1979.

-
- [50] A. B. Zamolodchikov, "Integrable field theory from conformal field theory," in *Integrable Sys Quantum Field Theory*, pp. 641–674, Elsevier, 1989.
- [51] A. E. Arinshtein, V. A. Fateev, and A. B. Zamolodchikov, "Quantum S-Matrix of the (1+1)-Dimensional Todd Chain," *Phys. Lett. B*, vol. 87, pp. 389–392, 1979.
- [52] P. Christe and G. Mussardo, "Elastic s-matrices in (1 + 1) dimensions and toda field theories," *International Journal of Modern Physics A*, vol. 05, no. 24, pp. 4581–4627, 1990.
- [53] L. D. Faddeev, "How algebraic Bethe ansatz works for integrable model," *arXiv : hep-th/9605187*, 1996.
- [54] G. Fehér and G. Takács, "Sine–Gordon form factors in finite volume," *Nuclear Physics B*, vol. 852, no. 2, pp. 441–467, 2011.
- [55] B. Bertini, L. Piroli, and M. Kormos, "Transport in the sine-Gordon field theory: From generalized hydrodynamics to semiclassics," *Phys. Rev. B*, vol. 100, p. 035108, Jul 2019.
- [56] B. Sutherland, *Beautiful Models*. World Scientific, 2004.
- [57] A. M. Gainutdinov, W. Hao, R. I. Nepomechie, and A. J. Sommes, "Counting solutions of the Bethe equations of the quantum group invariant open xxz chain at roots of unity," *Journal of Physics A: Mathematical and Theoretical*, vol. 48, p. 494003, nov 2015.
- [58] S. Belliard and A. Faribault, "Ground state solutions of inhomogeneous Bethe equations," *SciPost Phys.*, vol. 4, p. 030, 2018.
- [59] A. Faribault, O. El Araby, C. Sträter, and V. Gritsev, "Gaudin models solver based on the correspondence between Bethe ansatz and ordinary differential equations," *Phys. Rev. B*, vol. 83, p. 235124, Jun 2011.
- [60] J.-S. Caux and J. M. Maillet, "Computation of dynamical correlation functions of Heisenberg chains in a magnetic field," *Phys. Rev. Lett.*, vol. 95, p. 077201, Aug 2005.
- [61] J.-S. Caux, R. Hagemans, and J. M. Maillet, "Computation of dynamical correlation functions of Heisenberg chains: the gapless anisotropic regime," *Journal of Statistical Mechanics: Theory and Experiment*, vol. 2005, p. P09003, sep 2005.

References

- [62] W. Hao, R. I. Nepomechie, and A. J. Sommes, “Completeness of solutions of Bethe’s equations,” *Phys. Rev. E*, vol. 88, p. 052113, Nov 2013.
- [63] C. Marboe and D. Volin, “Fast analytic solver of rational Bethe equations,” *Journal of Physics A: Mathematical and Theoretical*, vol. 50, no. 20, p. 204002, 2017.
- [64] J.-S. Caux, “Correlation functions of integrable models: A description of the ABACUS algorithm,” *Journal of Mathematical Physics*, vol. 50, p. 095214, 09 2009.
- [65] M. Takahashi, *Thermodynamics of One-Dimensional Solvable Models*. Cambridge University Press, 1999.
- [66] E. H. Lieb and W. Liniger, “Exact analysis of an interacting Bose gas. i. the general solution and the ground state,” *Phys. Rev.*, vol. 130, pp. 1605–1616, May 1963.
- [67] E. H. Lieb, “Exact analysis of an interacting Bose gas. ii. the excitation spectrum,” *Phys. Rev.*, vol. 130, pp. 1616–1624, May 1963.
- [68] H. Bergknoff and H. B. Thacker, “Structure and solution of the massive Thirring model,” *Phys. Rev. D*, vol. 19, pp. 3666–3681, Jun 1979.
- [69] P. Zabreiko, “Integral equations—a reference text,” 1975.
- [70] F. Tricomi, *Integral Equations*. Pure and applied mathematics, Interscience Publishers, 1967.
- [71] B. Bertini, M. Collura, J. De Nardis, and M. Fagotti, “Transport in out-of-equilibrium $x \times z$ chains: Exact profiles of charges and currents,” *Physical review letters*, vol. 117, no. 20, p. 207201, 2016.
- [72] C. N. Yang and C. P. Yang, “Thermodynamics of a one-dimensional system of bosons with repulsive delta-function interaction,” *Journal of Mathematical Physics*, vol. 10, no. 7, pp. 1115–1122, 1969.
- [73] O. A. Castro-Alvaredo, B. Doyon, and T. Yoshimura, “Emergent hydrodynamics in integrable quantum systems out of equilibrium,” *Physical Review X*, vol. 6, p. 041065, Dec 2016.
- [74] T. Kinoshita, T. Wenger, and D. S. Weiss, “A quantum Newton’s cradle,” *Nature*, vol. 440, pp. 900–903, Apr 2006.

-
- [75] H. J. Schulz, "Interacting fermions in one dimension: from weak to strong correlation," *arXiv: cond-mat/9302006*, 1993.
- [76] D. C. Mattis, *The Many-Body Problem*. World Scientific, 1993.
- [77] M. A. Cazalilla, "Effect of suddenly turning on interactions in the Luttinger model," *Phys. Rev. Lett.*, vol. 97, p. 156403, Oct 2006.
- [78] H. Spohn, *Large scale dynamics of interacting particles*. Springer Science & Business Media, 2012.
- [79] G. A. El and A. M. Kamchatnov, "Kinetic equation for a dense soliton gas," *Phys. Rev. Lett.*, vol. 95, p. 204101, Nov 2005.
- [80] C. Boldrighini, R. L. Dobrushin, and Y. M. Sukhov, "One-dimensional hard rod caricature of hydrodynamics," *Journal of Statistical Physics*, vol. 31, pp. 577–616, Jun 1983.
- [81] V. B. Bulchandani, R. Vasseur, C. Karrasch, and J. E. Moore, "Bethe-Boltzmann hydrodynamics and spin transport in the xxz chain," *Phys. Rev. B*, vol. 97, p. 045407, Jan 2018.
- [82] M. Kardar, *Statistical Physics of Particles*. Cambridge University Press, 2007.
- [83] B. Doyon, H. Spohn, and T. Yoshimura, "A geometric viewpoint on generalized hydrodynamics," *Nuclear Physics B*, vol. 926, pp. 570–583, 2018.
- [84] B. Doyon, T. Yoshimura, and J.-S. Caux, "Soliton gases and generalized hydrodynamics," *Phys. Rev. Lett.*, vol. 120, p. 045301, Jan 2018.
- [85] B. Doyon, J. Dubail, R. Konik, and T. Yoshimura, "Large-scale description of interacting one-dimensional Bose gases: Generalized hydrodynamics supersedes conventional hydrodynamics," *Phys. Rev. Lett.*, vol. 119, p. 195301, Nov 2017.
- [86] M. Fagotti, "Locally quasi-stationary states in noninteracting spin chains," *SciPost Phys.*, vol. 8, p. 48, 2020.
- [87] H. Shi and W.-M. Zheng, "Critical temperature of a trapped interacting Bose-einstein gas in the local-density approximation," *Phys. Rev. A*, vol. 56, pp. 1046–1049, Jul 1997.

References

- [88] F. m. c. Riggio, Y. Brun, D. Karevski, A. Faribault, and J. Dubail, “Gradient corrections to the local-density approximation in the one-dimensional Bose gas,” *Phys. Rev. A*, vol. 106, p. 053309, Nov 2022.
- [89] P. Ruggiero, P. Calabrese, B. Doyon, and J. Dubail, “Quantum generalized hydrodynamics,” *Phys. Rev. Lett.*, vol. 124, p. 140603, Apr 2020.
- [90] P. Ruggiero, P. Calabrese, B. Doyon, and J. Dubail, “Quantum generalized hydrodynamics of the Tonks–Girardeau gas: density fluctuations and entanglement entropy,” *Journal of Physics A: Mathematical and Theoretical*, vol. 55, p. 024003, dec 2021.
- [91] F. Ares, S. Scopa, and S. Wald, “Entanglement dynamics of a hard-core quantum gas during a joule expansion,” *Journal of Physics A: Mathematical and Theoretical*, vol. 55, p. 375301, aug 2022.
- [92] S. Scopa, P. Calabrese, and J. Dubail, “Exact hydrodynamic solution of a double domain wall melting in the spin-1/2 XXZ model,” *SciPost Phys.*, vol. 12, p. 207, 2022.
- [93] C. W. Gardiner and P. Zoller, *Quantum Noise*. Springer, second ed., 2000.
- [94] W. B. Case, “Wigner functions and Weyl transforms for pedestrians,” *American Journal of Physics*, vol. 76, pp. 937–946, 10 2008.
- [95] L. C. Evans, *Partial differential equations*. Providence, R.I.: American Mathematical Society, 2010.
- [96] J. Dubail, J.-M. Stéphan, J. Viti, and P. Calabrese, “Conformal field theory for inhomogeneous one-dimensional quantum systems: the example of non-interacting Fermi gases,” *SciPost Phys.*, vol. 2, p. 002, 2017.
- [97] N. Malvania, Y. Zhang, Y. Le, J. Dubail, M. Rigol, and D. S. Weiss, “Generalized hydrodynamics in strongly interacting 1d Bose gases,” *Science*, vol. 373, pp. 1129–1133, sep 2021.
- [98] P. Ruggiero, Y. Brun, and J. Dubail, “Conformal field theory on top of a breathing one-dimensional gas of hard core bosons,” *SciPost Phys.*, vol. 6, p. 051, 2019.

-
- [99] S. Scopa, A. Krajenbrink, P. Calabrese, and J. Dubail, "Exact entanglement growth of a one-dimensional hard-core quantum gas during a free expansion," *Journal of Physics A: Mathematical and Theoretical*, vol. 54, p. 404002, sep 2021.
- [100] M. Fagotti, "Higher-order generalized hydrodynamics in one dimension: The noninteracting test," *Phys. Rev. B*, vol. 96, p. 220302, Dec 2017.
- [101] A. L. Kuzemsky, *Statistical Mechanics and the Physics of Many-Particle Model Systems*. World Scientific, 2017.
- [102] P. W. Anderson, "More is different," *Science*, vol. 177, no. 4047, pp. 393–396, 1972.
- [103] <https://dictionary.cambridge.org/dictionary/english/fluctuation>.
- [104] B. de Finetti, "Logical foundations and measurement of subjective probability," *Acta Psychologica*, vol. 34, pp. 129–145, 1970.
- [105] K. Jacobs, *Stochastic Processes for Physicists: Understanding Noisy Systems*. Cambridge University Press, 2010.
- [106] . Øksendal, B. K. (Bernt Karsten), *Stochastic differential equations : an introduction with applications*. Sixth edition. Berlin ; New York : Springer, [2003] ©2003, [2003].
- [107] E. Wigner, "On the quantum correction for thermodynamic equilibrium," *Phys. Rev.*, vol. 40, pp. 749–759, Jun 1932.
- [108] D. Bohm, "A suggested interpretation of the quantum theory in terms of "hidden" variables. i," *Phys. Rev.*, vol. 85, pp. 166–179, Jan 1952.
- [109] J. S. Bell, "On the impossible pilot wave," *Foundations of Physics*, vol. 12, pp. 989–999, Oct 1982.
- [110] M. Girardeau, "Relationship between Systems of Impenetrable Bosons and Fermions in One Dimension," *Journal of Mathematical Physics*, vol. 1, pp. 516–523, 12 2004.
- [111] M. Srednicki, *Quantum Field Theory*. Cambridge University Press, 2007.
- [112] F. H. L. Essler and M. Fagotti, "Quench dynamics and relaxation in isolated integrable quantum spin chains," *Journal of Statistical Mechanics: Theory and Experiment*, vol. 2016, p. 064002, jun 2016.

References

- [113] E. H. Lieb and D. W. Robinson, *The finite group velocity of quantum spin systems*. Springer, 2004.
- [114] H. Touchette, “The large deviation approach to statistical mechanics,” *Physics Reports*, vol. 478, pp. 1–69, jul 2009.
- [115] W. Feller, *An Introduction to Probability Theory and Its Applications*, vol. 1. Wiley, January 1968.
- [116] P. Billingsley, *Probability and Measure*. John Wiley & Sons, 1995.
- [117] B. Gnedenko, *The Theory of Probability*. Elsevier, 2015.
- [118] P. Hall and C. Heyde, “Martingale limit theory and its application,” *Probability and Mathematical Statistics*, 1980.
- [119] I. Ibragimov and Y. Linnik, *Independent and Stationary Sequences of Random Variables*. Wolters-Noordhoff Publishing, 1965.
- [120] C. Bender and S. Orszag, *Advanced Mathematical Methods for Scientists and Engineers I: Asymptotic Methods and Perturbation Theory*. Springer, illustrated ed., 1999.
- [121] C. Shannon, “A mathematical theory of communication,” *The Bell System Technical Journal*, vol. 27, no. 3, pp. 379–423, 1948.
- [122] A. Dembo and O. Zeitouni, *Large Deviations Techniques and Applications*. Springer, 1998.
- [123] S. R. S. Varadhan, “Asymptotic probabilities and differential equations,” *Communications on Pure and Applied Mathematics*, vol. 19, no. 3, pp. 261–286, 1966.
- [124] R. T. Rockafellar, *Convex analysis*. Princeton Mathematical Series, Princeton University Press, 1970.
- [125] R. K. P. Zia, E. F. Redish, and S. R. McKay, “Making sense of the Legendre transform,” *American Journal of Physics*, vol. 77, pp. 614–622, 07 2009.
- [126] H. Cramér, “Sur un nouveau théorème-limite de la théorie des probabilités,” 2018.
- [127] R. Ellis, *Entropy, Large Deviations, and Statistical Mechanics*. Classics in Mathematics, Springer, 2006.

-
- [128] J.-P. Bouchaud and A. Georges, “Anomalous diffusion in disordered media: Statistical mechanisms, models and physical applications,” *Physics Reports*, vol. 195, no. 4, pp. 127–293, 1990.
- [129] H. Lehmann, K. Symanzik, and W. Zimmermann, “Zur formulierung quantisierter feldtheorien,” *Il Nuovo Cimento (1955-1965)*, vol. 1, pp. 205–225, Jan 1955.
- [130] L. Onsager, “Reciprocal relations in irreversible processes. i.,” *Phys. Rev.*, vol. 37, pp. 405–426, Feb 1931.
- [131] J. P. Sethna, *Statistical Mechanics: Entropy, Order Parameters and Complexity*. Oxford University Press, first edition ed., 2006.
- [132] L. D. Landau and E. M. Lifshitz, *Fluid Mechanics, Second Edition: Volume 6 (Course of Theoretical Physics)*. Course of theoretical physics / by L. D. Landau and E. M. Lifshitz, Vol. 6, Butterworth-Heinemann, 2 ed., Jan. 1987.
- [133] B. Doyon, “Thermalization and pseudolocality in extended quantum systems,” *Communications in Mathematical Physics*, vol. 351, pp. 155–200, Apr 2017.
- [134] B. Doyon, “Hydrodynamic projections and the emergence of linearised Euler equations in one-dimensional isolated systems,” *Communications in Mathematical Physics*, vol. 391, pp. 293–356, Apr 2022.
- [135] A. Bastianello, B. Doyon, G. Watts, and T. Yoshimura, “Generalized hydrodynamics of classical integrable field theory: the sinh-Gordon model,” *SciPost Physics*, vol. 4, Jun 2018.
- [136] G. Perfetto and B. Doyon, “Euler-scale dynamical fluctuations in non-equilibrium interacting integrable systems,” *SciPost Physics*, vol. 10, no. 5, p. 116, 2021.
- [137] F. S. Møller, G. Perfetto, B. Doyon, and J. Schmiedmayer, “Euler-scale dynamical correlations in integrable systems with fluid motion,” *SciPost Physics Core*, vol. 3, dec 2020.
- [138] B. Doyon, “Exact large-scale correlations in integrable systems out of equilibrium,” *SciPost Phys.*, vol. 5, p. 054, 2018.

References

- [139] B. Doyon and J. Myers, “Fluctuations in ballistic transport from Euler hydrodynamics,” *arXiv: 1902.00320*, 2019.
- [140] D. Bernard and B. Doyon, “Conformal field theory out of equilibrium: a review,” *Journal of Statistical Mechanics: Theory and Experiment*, vol. 2016, p. 064005, jun 2016.
- [141] J. M. Lee, “Introduction to smooth manifolds,” 2000.
- [142] A. Its, A. Izergin, V. Korepin, and N. Slavnov, “Temperature correlations of quantum spins,” *Physical review letters*, vol. 70, no. 11, p. 1704, 1993.
- [143] J. D. Nardis, B. Doyon, M. Medenjak, and M. Panfil, “Correlation functions and transport coefficients in generalised hydrodynamics,” *arXiv: 2104.04462*, 2021.
- [144] B. Doyon and H. Spohn, “Drude weight for the Lieb-Liniger Bose gas,” *SciPost Physics*, vol. 3, Dec 2017.
- [145] B. Doyon, “Exact large-scale correlations in integrable systems out of equilibrium,” *SciPost Physics*, vol. 5, Nov 2018.
- [146] A. De Masi, P. A. Ferrari, and J. L. Lebowitz, “Reaction-diffusion equations for interacting particle systems,” *Journal of Statistical Physics*, vol. 44, pp. 589–644, Aug 1986.
- [147] E. Lieb, T. Schultz, and D. Mattis, “Two soluble models of an antiferromagnetic chain,” *Annals of Physics*, vol. 16, no. 3, pp. 407 – 466, 1961.
- [148] B. Doyon and J. Myers, “Fluctuations in ballistic transport from Euler hydrodynamics,” *Annales Henri Poincaré*, vol. 21, pp. 255–302, Jan 2020.
- [149] B. Bertini, M. Collura, J. De Nardis, and M. Fagotti, “Transport in out-of-equilibrium xxz chains: Exact profiles of charges and currents,” *Physical Review Letters*, vol. 117, Nov 2016.
- [150] M. Borsi, B. Pozsgay, and L. Pristyák, “Current operators in integrable models: a review,” *Journal of Statistical Mechanics: Theory and Experiment*, vol. 2021, p. 094001, sep 2021.
- [151] B. Pozsgay, “Algebraic construction of current operators in integrable spin chains,” *Phys. Rev. Lett.*, vol. 125, p. 070602, Aug 2020.

-
- [152] M. Borsi, B. Pozsgay, and L. Pristyák, “Current operators in Bethe ansatz and generalized hydrodynamics: An exact quantum-classical correspondence,” *Phys. Rev. X*, vol. 10, p. 011054, Mar 2020.
- [153] H. Spohn, “Collision rate ansatz for the classical toda lattice,” *Phys. Rev. E*, vol. 101, p. 060103, Jun 2020.
- [154] T. Yoshimura and H. Spohn, “Collision rate ansatz for quantum integrable systems,” *SciPost Phys.*, vol. 9, p. 040, 2020.
- [155] X. Jie, “The large time asymptotics of the temperature correlation functions of the XXO Heisenberg ferromagnetic: The reimann-hilbert approach,” *Ph.D. Thesis*, 1998.
- [156] J. B. Zuber and C. Itzykson, “Quantum field theory and the two-dimensional Ising model,” *Phys. Rev. D*, vol. 15, pp. 2875–2884, 1977.
- [157] B. Schroer and T. T. T., “The order/disorder quantum field operators associated with the two-dimensional Ising model in the continuum limit,” *Nucl. Phys. B*, vol. 144, pp. 80–122, 1978.
- [158] I. Klich, *An Elementary Derivation of Levitov’s Formula*, pp. 397–402. Dordrecht: Springer Netherlands, 2003.
- [159] I. Klich, “A note on the full counting statistics of paired fermions,” *Journal of Statistical Mechanics: Theory and Experiment*, vol. 2014, p. P11006, nov 2014.
- [160] M. J. Ablowitz and J. F. Ladik, “A nonlinear difference scheme and inverse scattering,” *Studies in Applied Mathematics*, vol. 55, no. 3, pp. 213–229, 1976.
- [161] P. Deift and X. Zhou, “A steepest descent method for oscillatory riemann–hilbert problems. asymptotics for the mkdv equation,” *Annals of Mathematics*, vol. 137, no. 2, pp. 295–368, 1993.
- [162] S. Sachdev, “Universal, finite-temperature, crossover functions of the quantum transition in the Ising chain in a transverse field,” *Nuclear Physics B*, vol. 464, p. 576–595, Apr 1996.
- [163] S. Sachdev and A. P. Young, “Low temperature relaxational dynamics of the Ising chain in a transverse field,” *Physical Review Letters*, vol. 78, p. 2220–2223, Mar 1997.

References

- [164] C. Buragohain and S. Sachdev, “Intermediate-temperature dynamics of one-dimensional Heisenberg antiferromagnets,” *Physical Review B*, vol. 59, p. 9285–9303, Apr 1999.
- [165] E. Granet, M. Fagotti, and F. H. L. Essler, “Finite temperature and quench dynamics in the Transverse Field Ising Model from form factor expansions,” *SciPost Phys.*, vol. 9, p. 33, 2020.
- [166] O. Gamayun, N. Iorgov, and Y. Zhuravlev, “Effective free-fermionic form factors and the XY spin chain,” *SciPost Phys.*, vol. 10, p. 70, 2021.
- [167] D. Chernowitz and O. Gamayun, “On the dynamics of free-fermionic tau-functions at finite temperature,” *arXiv: 2110.08194*, 2021.
- [168] D. Chernowitz and O. Gamayun, “On the dynamics of free-fermionic tau-functions at finite temperature,” *SciPost Phys. Core*, vol. 5, p. 006, 2022.
- [169] Y. Brun and J. Dubail, “One-particle density matrix of trapped one-dimensional impenetrable bosons from conformal invariance,” *SciPost Phys.*, vol. 2, p. 012, 2017.
- [170] S. Groha, F. H. L. Essler, and P. Calabrese, “Full counting statistics in the transverse field Ising chain,” *SciPost Phys.*, vol. 4, p. 043, 2018.
- [171] A. Lamacraft and P. Fendley, “Order parameter statistics in the critical quantum Ising chain,” *Phys. Rev. Lett.*, vol. 100, p. 165706, Apr 2008.
- [172] A. Bastianello, L. Piroli, and P. Calabrese, “Exact local correlations and full counting statistics for arbitrary states of the one-dimensional interacting Bose gas,” *Phys. Rev. Lett.*, vol. 120, p. 190601, May 2018.
- [173] D. A. Ivanov and A. G. Abanov, “Characterizing correlations with full counting statistics: Classical Ising and quantum xy spin chains,” *Phys. Rev. E*, vol. 87, p. 022114, Feb 2013.
- [174] V. Gritsev, E. Demler, M. Lukin, and A. Polkovnikov, “Spectroscopy of collective excitations in interacting low-dimensional many-body systems using quench dynamics,” *Phys. Rev. Lett.*, vol. 99, p. 200404, Nov 2007.
- [175] V. Gritsev, A. Polkovnikov, and E. Demler, “Linear response theory for a pair of coupled one-dimensional condensates of interacting atoms,” *Phys. Rev. B*, vol. 75, p. 174511, May 2007.

-
- [176] T. Schumm, S. Hofferberth, L. M. Andersson, S. Wildermuth, S. Groth, I. Bar-Joseph, J. Schmiedmayer, and P. Krüger, “Matter-wave interferometry in a double well on an atom chip,” *Nature Physics*, vol. 1, pp. 57–62, Oct 2005.
- [177] S. Hofferberth, I. Lesanovsky, B. Fischer, T. Schumm, and J. Schmiedmayer, “Non-equilibrium coherence dynamics in one-dimensional Bose gases,” *Nature*, vol. 449, pp. 324–327, Sep 2007.
- [178] Y. D. van Nieuwkerk, J. Schmiedmayer, and F. H. L. Essler, “Projective phase measurements in one-dimensional Bose gases,” *SciPost Phys.*, vol. 5, p. 046, 2018.
- [179] A. Bastianello, B. Doyon, G. Watts, and T. Yoshimura, “Generalized hydrodynamics of classical integrable field theory: the sinh-Gordon model,” *SciPost Phys.*, vol. 4, p. 45, 2018.
- [180] C. Rogers and W. Shadwick, *Bäcklund Transformations and Their Applications*. Conference Series / Institute of Mathematics and Its Applications, Academic Press, 1982.
- [181] A. M. Tselik, *Quantum Field Theory in Condensed Matter Physics*. Cambridge University Press, 1995.
- [182] T. Giamarchi, *Quantum physics in one dimension*, vol. 121. Clarendon press, 2003.
- [183] S. Coleman, “Quantum sine-Gordon equation as the massive Thirring model,” *Phys. Rev. D*, vol. 11, pp. 2088–2097, Apr 1975.
- [184] A. B. Zamolodchikov, “Mass scale in the sine-Gordon model and its reductions,” *International Journal of Modern Physics A*, vol. 10, no. 08, pp. 1125–1150, 1995.
- [185] W. E. Thirring, “A soluble relativistic field theory,” *Annals of Physics*, vol. 3, no. 1, pp. 91–112, 1958.
- [186] B. Bertini, L. Piroli, and M. Kormos, “Transport in the sine-Gordon field theory: From generalized hydrodynamics to semiclassics,” *Physical Review B*, vol. 100, Jul 2019.
- [187] B. C. Nagy, M. Kormos, and G. Takács, “Thermodynamics and fractal drude weights in the sine-Gordon model,” *arXiv: 2305.15474*, 2023.

References

- [188] K. Damle and S. Sachdev, “Universal relaxational dynamics of gapped one-dimensional models in the quantum sine-Gordon universality class,” *Phys. Rev. Lett.*, vol. 95, p. 187201, Oct 2005.
- [189] S. Sachdev and A. P. Young, “Low temperature relaxational dynamics of the Ising chain in a transverse field,” *Phys. Rev. Lett.*, vol. 78, pp. 2220–2223, Mar 1997.
- [190] M. Kuhnert, R. Geiger, T. Langen, M. Gring, B. Rauer, T. Kitagawa, E. Demler, D. Adu Smith, and J. Schmiedmayer, “Multimode dynamics and emergence of a characteristic length scale in a one-dimensional quantum system,” *Phys. Rev. Lett.*, vol. 110, p. 090405, Feb 2013.
- [191] L. Amico, R. Fazio, A. Osterloh, and V. Vedral, “Entanglement in many-body systems,” *Reviews of modern physics*, vol. 80, no. 2, p. 517, 2008.
- [192] P. Calabrese, J. Cardy, and B. Doyon, “Entanglement entropy in extended quantum systems,” *J. Phys. A*, vol. 42, no. 50, p. 500301, 2009.
- [193] J. Eisert, M. Cramer, and M. B. Plenio, “Colloquium: Area laws for the entanglement entropy,” *Reviews of modern physics*, vol. 82, no. 1, p. 277, 2010.
- [194] N. Laflorencie, “Quantum entanglement in condensed matter systems,” *Physics Reports*, vol. 646, pp. 1–59, 2016.
- [195] P. Calabrese and J. Cardy, “Entanglement entropy and conformal field theory,” *Journal of physics a: mathematical and theoretical*, vol. 42, no. 50, p. 504005, 2009.
- [196] P. Calabrese and J. Cardy, “Entanglement entropy and quantum field theory,” *Journal of statistical mechanics: theory and experiment*, vol. 2004, no. 06, p. P06002, 2004.
- [197] J. L. Cardy, O. A. Castro-Alvaredo, and B. Doyon, “Form factors of branch-point twist fields in quantum integrable models and entanglement entropy,” *Journal of Statistical Physics*, vol. 130, no. 1, pp. 129–168, 2008.
- [198] B. Doyon, “Bipartite entanglement entropy in massive two-dimensional quantum field theory,” *Phys. Rev. Lett.*, vol. 102, p. 031602, Jan 2009.
- [199] H. Casini, C. Fosco, and M. Huerta, “Entanglement and alpha entropies for a massive Dirac field in two dimensions,” *Journal of Statistical Mechanics: Theory and Experiment*, vol. 2005, no. 07, p. P07007, 2005.

-
- [200] M. Rigol, V. Dunjko, V. Yurovsky, and M. Olshanii, "Relaxation in a completely integrable many-body quantum system: an ab initio study of the dynamics of the highly excited states of 1d lattice hard-core bosons," *Physical review letters*, vol. 98, no. 5, p. 050405, 2007.
- [201] V. Alba and P. Calabrese, "Quench action and Rényi entropies in integrable systems," *Physical Review B*, vol. 96, no. 11, p. 115421, 2017.
- [202] V. Alba and P. Calabrese, "Rényi entropies after releasing the Néel state in the xxz spin-chain," *Journal of Statistical Mechanics: Theory and Experiment*, vol. 2017, no. 11, p. 113105, 2017.
- [203] M. Mestyán, V. Alba, and P. Calabrese, "Rényi entropies of generic thermodynamic macrostates in integrable systems," *Journal of Statistical Mechanics: Theory and Experiment*, vol. 2018, no. 8, p. 083104, 2018.
- [204] H. A. Bethe, "Zur Theorie der Metalle. i. Eigenwerte und Eigenfunktionen der linearen Atomkette," *Zeit. für Physik*, vol. 71, p. 205, 1931.
- [205] M. Fagotti and P. Calabrese, "Evolution of entanglement entropy following a quantum quench: Analytic results for the x y chain in a transverse magnetic field," *Physical Review A*, vol. 78, no. 1, p. 010306, 2008.
- [206] P. Calabrese and J. Cardy, "Evolution of entanglement entropy in one-dimensional systems," *Journal of Statistical Mechanics: Theory and Experiment*, vol. 2005, no. 04, p. P04010, 2005.
- [207] P. Calabrese and J. Cardy, "Quantum quenches in extended systems," *Journal of Statistical Mechanics: Theory and Experiment*, vol. 2007, no. 06, p. P06008, 2007.
- [208] P. Calabrese and J. Cardy, "Time dependence of correlation functions following a quantum quench," *Physical review letters*, vol. 96, no. 13, p. 136801, 2006.
- [209] V. Alba and P. Calabrese, "Entanglement and thermodynamics after a quantum quench in integrable systems," *Proceedings of the National Academy of Sciences*, vol. 114, no. 30, pp. 7947–7951, 2017.
- [210] V. Alba and P. Calabrese, "Entanglement dynamics after quantum quenches in generic integrable systems," *SciPost Physics*, vol. 4, no. 3, p. 017, 2018.

References

- [211] K. Klobas and B. Bertini, “Entanglement dynamics in rule 54: Exact results and quasiparticle picture,” *SciPost Physics*, vol. 11, no. 6, p. 107, 2021.
- [212] B. Bertini, K. Klobas, V. Alba, G. Lagnese, and P. Calabrese, “Growth of rényi entropies in interacting integrable models and the breakdown of the quasiparticle picture,” *Phys. Rev. X*, vol. 12, p. 031016, Jul 2022.
- [213] L. Piroli, B. Pozsgay, and E. Vernier, “What is an integrable quench?,” *Nuclear Physics B*, vol. 925, pp. 362–402, 2017.
- [214] G. Delfino, “Quantum quenches with integrable pre-quench dynamics,” *Journal of Physics A: Mathematical and Theoretical*, vol. 47, no. 40, p. 402001, 2014.
- [215] G. Delfino and J. Viti, “On the theory of quantum quenches in near-critical systems,” *Journal of Physics A: Mathematical and Theoretical*, vol. 50, no. 8, p. 084004, 2017.
- [216] A. Mitra, “Quantum quench dynamics,” *Annual Review of Condensed Matter Physics*, vol. 9, no. 1, pp. 245–259, 2018.
- [217] F. H. L. Essler, S. Evangelisti, and M. Fagotti, “Dynamical correlations after a quantum quench,” *Phys. Rev. Lett.*, vol. 109, p. 247206, Dec 2012.
- [218] I. Klich and L. Levitov, “Quantum noise as an entanglement meter,” *Phys. Rev. Lett.*, vol. 102, p. 100502, Mar 2009.
- [219] H. F. Song, S. Rachel, C. Flindt, I. Klich, N. Laflorencie, and K. Le Hur, “Bipartite fluctuations as a probe of many-body entanglement,” *Phys. Rev. B*, vol. 85, p. 035409, Jan 2012.
- [220] P. Calabrese, M. Mintchev, and E. Vicari, “Exact relations between particle fluctuations and entanglement in fermi gases,” *Europhysics Letters*, vol. 98, p. 20003, apr 2012.
- [221] B. Bertini, E. Tartaglia, and P. Calabrese, “Entanglement and diagonal entropies after a quench with no pair structure,” *Journal of Statistical Mechanics: Theory and Experiment*, vol. 2018, no. 6, p. 063104, 2018.
- [222] L. P. Kadanoff, “Operator algebra and the determination of critical indices,” *Phys. Rev. Lett.*, vol. 23, pp. 1430–1433, Dec 1969.

- [223] L. P. Kadanoff and H. Ceva, "Determination of an operator algebra for the two-dimensional Ising model," *Phys. Rev. B*, vol. 3, pp. 3918–3939, Jun 1971.
- [224] E. Fradkin, "Disorder operators and their descendants," *Journal of Statistical Physics*, vol. 167, p. 427–461, Feb 2017.
- [225] P. Di Francesco, P. Mathieu, and D. Senechal, *Conformal Field Theory*. Graduate Texts in Contemporary Physics, New York: Springer-Verlag, 1997.
- [226] L. Onsager, "Crystal statistics. i. a two-dimensional model with an order-disorder transition," *Phys. Rev.*, vol. 65, pp. 117–149, Feb 1944.
- [227] J. B. Zuber and C. Itzykson, "Quantum field theory and the two-dimensional Ising model," *Phys. Rev. D*, vol. 15, pp. 2875–2884, May 1977.
- [228] E. Fradkin, "Disorder operators and their descendants," *Journal of Statistical Physics*, vol. 167, no. 3, pp. 427–461, 2017.
- [229] R. Dijkgraaf, C. Vafa, E. Verlinde, and H. Verlinde, "The operator algebra of orbifold models," *Communications in Mathematical Physics*, vol. 123, no. 3, pp. 485 – 526, 1989.
- [230] F. Smirnov, *Form factors in completely integrable models of quantum field theory*. Adv. Series in Math. Phys. 14, World Scientific, Singapore, 1992.
- [231] D. Bernard and A. LeClair, "Quantum group symmetries and non-local currents in 2d QFT," *Communications in Mathematical Physics*, vol. 142, no. 1, pp. 99–138, 1991.
- [232] D. Bernard and A. LeClair, "The quantum double in integrable quantum field theory," *Nuclear Physics B*, vol. 399, no. 2, pp. 709–748, 1993.
- [233] D. Bernard and A. LeClair, "Differential equations for sine-Gordon correlation functions at the free fermion point," *Nuclear Physics B*, vol. 426, no. 3, pp. 534–558, 1994.
- [234] M. Sato, T. Miwa, and M. Jimbo, "Holonomic quantum fields I," *Publ. RIMS*, vol. 14, p. 223–267, 1979.
- [235] M. Sato, T. Miwa, and M. Jimbo, "Holonomic quantum fields II," *Publ. RIMS*, vol. 15, p. 201–278, 1979.

References

- [236] M. Sato, T. Miwa, and M. Jimbo, “Holonomic quantum fields III,” *Publ. RIMS*, vol. 15, pp. 577–629, 1979.
- [237] M. Sato, T. Miwa, and M. Jimbo, “Holonomic quantum fields IV,” *Publ. RIMS*, vol. 15, pp. 871–972, 1979.
- [238] M. Sato, T. Miwa, and M. Jimbo, “Holonomic quantum fields V,” *Publ. RIMS*, vol. 16, pp. 531–584, 1979.
- [239] J. Palmer, M. Beatty, and C. A. Tracy, “Tau functions for the Dirac operator on the Poincaré disk,” *Communications in Mathematical Physics*, vol. 165, no. 1, pp. 97–173, 1994.
- [240] B. Doyon, “Two-point correlation functions of scaling fields in the Dirac theory on the Poincaré disk,” *Nuclear Physics B*, vol. 675, no. 3, pp. 607–630, 2003.
- [241] O. Gamayun, N. Iorgov, and O. Lisovyy, “Conformal field theory of Painlevé VI,” *Journal of High Energy Physics*, vol. 2012, no. 10, p. 38, 2012.
- [242] O. A. Castro-Alvaredo and B. Doyon, “Permutation operators, entanglement entropy, and the XXZ spin chain in the limit $\Delta \rightarrow -1$,” *Journal of Statistical Mechanics: Theory and Experiment*, vol. 2011, no. 02, p. P02001, 2011.
- [243] P. Calabrese, J. Cardy, and E. Tonni, “Entanglement negativity in quantum field theory,” *Phys. Rev. Lett.*, vol. 109, p. 130502, Sep 2012.
- [244] M. Goldstein and E. Sela, “Symmetry-resolved entanglement in many-body systems,” *Phys. Rev. Lett.*, vol. 120, p. 200602, May 2018.
- [245] L.-Y. Hung, R. C. Myers, and M. Smolkin, “Twist operators in higher dimensions,” *Journal of High Energy Physics*, vol. 2014, no. 10, p. 178, 2014.
- [246] F. Morone, F. Caltagirone, E. Harrison, and G. Parisi, “Replica theory and spin glasses,” *arXiv : 1409.2722*, 2014.
- [247] E. Ilievski, M. Medenjak, T. Prosen, and L. Zadnik, “Quasilocal charges in integrable lattice systems,” *Journal of Statistical Mechanics: Theory and Experiment*, vol. 2016, no. 6, p. 064008, 2016.
- [248] B. Doyon, “Thermalization and pseudolocality in extended quantum systems,” *Communications in Mathematical Physics*, vol. 351, no. 1, pp. 155–200, 2017.

- [249] S. N. Santalla, G. Ramírez, S. S. Roy, G. Sierra, and J. Rodríguez-Laguna, “Entanglement links and the quasiparticle picture,” *Phys. Rev. B*, vol. 107, p. L121114, Mar 2023.
- [250] C. Flindt, C. Fricke, F. Hohls, T. Novotný, K. Netočný, T. Brandes, and R. J. Haug, “Universal oscillations in counting statistics,” *Proceedings of the National Academy of Sciences*, vol. 106, no. 25, pp. 10116–10119, 2009.
- [251] A. Komnik and A. O. Gogolin, “Full counting statistics for the Kondo dot,” *Phys. Rev. Lett.*, vol. 94, p. 216601, Jun 2005.
- [252] D. B. Gutman, Y. Gefen, and A. D. Mirlin, “Full counting statistics of a Luttinger liquid conductor,” *Phys. Rev. Lett.*, vol. 105, p. 256802, Dec 2010.
- [253] A. Bastianello, A. De Luca, B. Doyon, and J. De Nardis, “Thermalization of a trapped one-dimensional Bose gas via diffusion,” *Phys. Rev. Lett.*, vol. 125, p. 240604, Dec 2020.
- [254] J. D. Nardis and B. Doyon, “Hydrodynamic gauge fixing and higher order hydrodynamic expansion,” *Journal of Physics A: Mathematical and Theoretical*, vol. 56, p. 245001, may 2023.
- [255] G. El and M. Hoefer, “Dispersive shock waves and modulation theory,” *Physica D: Nonlinear Phenomena*, vol. 333, pp. 11–65, 2016.
- [256] F. Møller, P. Schüttelkopf, J. Schmiedmayer, and S. Erne, “The Whitham approach to generalized hydrodynamics,” *arXiv: 2304.10533*, 2023.
- [257] L. Zadnik, S. Bocini, K. Bidzhiev, and M. Fagotti, “Measurement catastrophe and ballistic spread of charge density with vanishing current,” *Journal of Physics A: Mathematical and Theoretical*, vol. 55, p. 474001, nov 2022.
- [258] E. H. Lieb and D. W. Robinson, “The finite group velocity of quantum spin systems,” *Communications in Mathematical Physics*, vol. 28, pp. 251–257, Sep 1972.
- [259] D. Ampelogiannis and B. Doyon, “Almost everywhere ergodicity in quantum lattice models,” *arXiv: 2112.12730*, 2022.
- [260] H. Araki, “Gibbs states of a one dimensional quantum lattice,” *Communications in Mathematical Physics*, vol. 14, no. 2, pp. 120 – 157, 1969.

References

- [261] B. Doyon and J. Myers, “Fluctuations in ballistic transport from Euler hydrodynamics,” in *Annales Henri Poincaré*, vol. 21, pp. 255–302, Springer, 2020.
- [262] D. Ampelogiannis and B. Doyon, “Ergodicity and hydrodynamic projections in quantum spin lattices at arbitrary frequency and wavenumber,” *To appear*, 2021.
- [263] W. Ledermann, “A note on skew-symmetric determinants,” *Proceedings of the Edinburgh Mathematical Society*, vol. 36, no. 2, p. 335–338, 1993.
- [264] E. R. Caianiello and S. Fubini, “On the algorithm of Dirac spurs,” *Il Nuovo Cimento (1943-1954)*, vol. 9, pp. 1218–1226, Dec 1952.
- [265] M. Gaudin, “Une démonstration simplifiée du théorème de wick en mécanique statistique,” *Nuclear Physics*, vol. 15, pp. 89–91, 1960.
- [266] J. O. Irwin, “The frequency distribution of the difference between two independent variates following the same poisson distribution,” *Journal of the Royal Statistical Society*, vol. 100, no. 3, pp. 415–416, 1937.
- [267] G. N. Watson, *A Treatise on the Theory of Bessel Functions*. Cambridge: Cambridge University Press, 1922.